

Old Dominion University

## ODU Digital Commons

---

Chemistry & Biochemistry Theses & Dissertations

Chemistry & Biochemistry

---

Summer 2021

# Improvement of Biochar Through Ozonization and Biosafety of Genetically Engineered Cyanobacteria

Oumar Sacko

*Old Dominion University*, [oumarius@gmail.com](mailto:oumarius@gmail.com)

Follow this and additional works at: [https://digitalcommons.odu.edu/chemistry\\_etds](https://digitalcommons.odu.edu/chemistry_etds)



Part of the [Biochemistry Commons](#), [Chemistry Commons](#), and the [Environmental Sciences Commons](#)

---

### Recommended Citation

Sacko, Oumar. "Improvement of Biochar Through Ozonization and Biosafety of Genetically Engineered Cyanobacteria" (2021). Doctor of Philosophy (PhD), Dissertation, Chemistry & Biochemistry, Old Dominion University, DOI: 10.25777/f83b-fy95

[https://digitalcommons.odu.edu/chemistry\\_etds/59](https://digitalcommons.odu.edu/chemistry_etds/59)

This Dissertation is brought to you for free and open access by the Chemistry & Biochemistry at ODU Digital Commons. It has been accepted for inclusion in Chemistry & Biochemistry Theses & Dissertations by an authorized administrator of ODU Digital Commons. For more information, please contact [digitalcommons@odu.edu](mailto:digitalcommons@odu.edu).

**IMPROVEMENT OF BIOCHAR THROUGH OZONIZATION AND BIOSAFETY OF  
GENETICALLY ENGINEERED CYANOBACTERIA**

by

Oumar Sacko

M.S. May 2020, Old Dominion University

B.S. May 2014, James Madison University

A Dissertation Submitted to the Faculty of  
Old Dominion University in Partial Fulfillment of the  
Requirements for the Degree of

DOCTOR OF PHILOSOPHY

CHEMISTRY

OLD DOMINION UNIVERSITY

August 2021

Approved by:

James. W. Lee (Director)

John R. Donat (Member)

Lesley H. Greene (Member)

Sandeep Kumar (Member)

## ABSTRACT

### IMPROVEMENT OF BIOCHAR THROUGH OZONIZATION AND BIOSAFETY OF GENETICALLY ENGINEERED CYANOBACTERIA

Oumar Sacko  
Old Dominion University, 2021  
Director: Dr. James W. Lee

Through the innovative technique of biochar post-production surface oxygenation by ozonization, we were able to improve certain properties of biochar. In project one, the incubation of an insoluble phosphate rock material (hydroxyapatite) with the wet ozonized pine 400 biochar and its filtrate resulted in a solubilization of 80 times more phosphate from hydroxyapatite ( $569.0 \text{ mg/L} \pm 6.4$ ) compared to the pure water-hydroxyapatite control ( $7.2 \text{ mg/L} \pm 0.3$ ). The ozonized biochar may provide a new possible way to unlock the phosphorus from insoluble phosphate mineral phases. The cation exchange capacity (CEC) is a key property of biochar when used as a soil amendment. In project two, using a high surface area biochar (rogue biochar), we were able to increase the CEC by a factor of almost 10 times upon ozone treatment; a biochar with an initial CEC of  $17.02 \text{ cmol/kg} \pm 0.63$  was increased to  $152.08 \text{ cmol/kg} \pm 4.06$  upon ozonization. The process of biochar ozonization generated large amount of dissolved organic carbon (DOC) in the filtrate/wash. Previously discarded as waste, here we showed that these DOC, even at low concentrations, may be useful for some applications such as unlocking phosphate from phosphate rock material. In project four, the bioassay of ozonized biochar substances was conducted on soil bacteria *Pseudomonas putida* and freshwater cyanobacteria *Synechococcus elongatus* PCC 7942. Results indicated that ozone treatment of certain biochars reduced their inhibiting effect on some microorganisms. The biocontainment of genetically

engineered (GE) cyanobacteria was recognized as a concern in case the latter was to break containment and escape into the environment. In project five, we tested the thermophilic nature of *Thermosynechococcus elongatus* BP1 as a biocontainment. A growth study in the greenhouse of Old Dominion University with genetically engineered (GE) *Thermosynechococcus elongatus* BP1-BY20 with biofuels producing genes showed that the GE *T. elongatus* BP1-BY20 did not actively grow in cool (15.44 °C to 25.30 °C) or warm season (31.42 °C to 36.27 °C) in the greenhouse. The thermophilic nature of *T. elongatus* BP1 may serve as a biosafety guarded mechanism during cool seasons but not so much during warmer seasons.

Copyright, 2021, by Oumar Sacko, All Rights Reserved.

I wholeheartedly dedicate this Ph.D. to my wonderful, exceptional, and deeply missed mother Didi Haidara who could not see this thesis complete. I would not be the person I am today without her unrelenting efforts, sacrifices, and love. The upbringing I received from her served as my blueprint to navigate throughout my life. At instances, when I thought of giving it all up, I remembered all the work she put into my life for me to succeed and that fueled me to keep going. Also, to my father Nazirou Sacko for guiding me all along, shaping my values, my way of seeing the world, supporting me, believing in me and immeasurably more. Finally, to my future children, hoping they will keep in mind that in life you can become whoever you want to become. When you find out what your true calling is, you must fight to get it. Nothing or no one can get between you and your dreams.

## ACKNOWLEDGEMENTS

I wish to thank my family and friends here and overseas, for being there when I needed it and for being my backbone. I could have not asked for a better support system. I would also like to thank my future kids for strengthening my purpose and giving me the motivation to go through this career.

I would like to express my sincere gratitude to my advisor, professor James W. Lee for all his help and for supporting me over the past 6 years. I have learned so much being in his research group, and I was given the wonderful opportunity to work on several projects. Dr. Lee has always been available no matter what day of the week. I would also like to thank my committee member Dr. Lesley Greene for her support throughout my Ph.D. I am very grateful for all the guidance provided by Dr. Greene who tirelessly, made sure I had everything I needed to succeed. Special thanks to Dr. Sandeep Kumar for his support, his guidance, and the wonderful opportunities of working in his lab in the Environmental Engineering Department. I would also like to thank Dr. John R. Donat for his support, guidance, and advice throughout my Ph.D.

I would like to give a special acknowledgment my lab partners Thu Nguyen, Cherrelle Barnes, Gyanendra Kharel, Andrea Zourou and Megan Hept for their support and friendship. Acknowledgments to previous lab members Dr. Matthew Huff, Dr. Haitham Said and Dr. Cameron Smith for welcoming me to the lab couple years ago and for their advice. Special thanks to the all the undergraduate students that I have had the privilege to mentor and to the Biotechnology Risk Assessment Grant Program competitive grant award no. 2016-33522-25624 from the U.S. Department of Agriculture for supporting me. I would like to also thank the

Department of Chemistry and Biochemistry at Old Dominion University. Very special thanks to Dr. Kumar lab and his Ph.D. students Kameron Adams, Anuj Thakkar, and others from the Department of Civil and Environmental Engineering for their support and friendship.

## NOMENCLATURE

<i>P300/ P400/ P500</i>	pine biochar made at 300 °C/ 400 °C/ 500 °C
<i>RBC</i>	rogue biochar
<i>P400 UN</i>	untreated (non-ozonized) pine 400 biochar
<i>P400 90W/ 90D</i>	90-minute wet/dry ozonized pine 400 biochar
<i>P400 UN-F</i>	filtrate from untreated (non-ozonized) pine 400
<i>P400 90W-F/ 90D-F</i>	filtrate from 90-min wet-/dry-ozonized pine 400
<i>RBC UN</i>	untreated (non-ozonized) rogue biochar
<i>RBC 90W/ 90D</i>	90-minute wet/dry ozonized rogue biochar
<i>RBC UN-F</i>	filtrate from non-ozonized rogue biochar
<i>RBC 90W-F/ 90D-F</i>	filtrate from 90-min wet-/dry-ozonized rogue biochar
<i>CEC</i>	cation exchange capacity
<i>DOC</i>	dissolved organic carbon
<i>-COOH/COO-</i>	carboxyl/carboxylate functional group
<i>ppm</i>	parts per million, here used for mg/L
<i>HA</i>	hydroxyapatite
<i>PCC 6803</i>	<i>Synechocystis</i> PCC 6803
<i>PCC 7942</i>	<i>Synechococcus elongatus</i> PCC7942
<i>WT</i>	wild-type
<i>BP1</i>	cyanobacteria <i>Thermosynechococcus elongatus</i> BP1
<i>GE-BY20</i>	genetically engineered <i>T. elongatus</i> BP1-BY20

## TABLE OF CONTENTS

	Page
LIST OF TABLES .....	xi
LIST OF FIGURES .....	xiv
Chapter	
I. INTRODUCTION .....	1
II. SOLUBILIZATION OF PHOSPHORUS FROM INSOLUBLE PHOSPHATE MATERIAL HYDROXYAPATITE WITH OZONIZED BIOCHAR .....	9
PREFACE .....	9
INTRODUCTION .....	9
MATERIALS AND METHODS .....	11
RESULTS AND DISCUSSION .....	18
CONCLUSION .....	35
III. COMPARATIVE STUDY OF BIOCHAR SURFACE OXYGENATION BY OZONIZATION FOR HIGH CATION EXCHANGE CAPACITY .....	37
PREFACE .....	37
INTRODUCTION .....	37
MATERIALS AND METHODS .....	39
RESULTS AND DISCUSSION .....	44
CONCLUSION .....	61
IV. WATER-SOLUBLE OZONIZED BIOCHAR MOLECULES TO UNLOCK PHOSPHORUS FROM INSOLUBLE PHOSPHATE MATERIAL .....	63
PREFACE .....	63
INTRODUCTION .....	63
MATERIALS AND METHODS .....	66
RESULTS AND DISCUSSION .....	71
CONCLUSION .....	93
V. OZONIZED BIOCHAR FILTRATE EFFECT ON THE GROWTH OF <i>PSEUDOMONAS PUTIDA</i> AND <i>SYNECHOCOCCUS ELONGATUS</i> PCC 7942 .....	95
PREFACE .....	95
INTRODUCTION .....	95
MATERIALS AND METHODS .....	97
RESULTS AND DISCUSSION .....	101
CONCLUSION .....	114

VI.	SURVIVABILITY AND COMPETITION STUDY OF WILD-TYPE AND GENETICALLY ENGINEERED CYANOBACTERIA .....	116
	PREFACE .....	116
	INTRODUCTION .....	116
	MATERIALS AND METHODS .....	118
	RESULTS AND DISCUSSION .....	123
	CONCLUSION .....	142
VII.	CONCLUSIONS AND DIRECTIONS FOR FUTURE WORK .....	143
	CONCLUSIONS .....	143
	DIRECTIONS FOR FUTURE WORK .....	145
	REFERENCES .....	148
	APPENDICES .....	157
	A. SUPPORTING INFORMATION FOR CHAPTER II .....	157
	B. SUPPORTING INFORMATION FOR CHAPTER III .....	158
	C. SUPPORTING INFORMATION FOR CHAPTER IV .....	160
	D. SUPPORTING INFORMATION FOR CHAPTER V .....	170
	E. SUPPORTING INFORMATION FOR CHAPTER VI .....	180
	F. RIGHTS AND PERMISSIONS .....	183
	VITA .....	189

## LIST OF TABLES

Table	Page
1. Hydroxyapatite preparation assay set-up .....	15
2. Experimental data on the concentration of phosphate and calcium from the hydroxyapatite and pH measurements for the hydroxyapatite assay .....	20
3. Cation Exchange Capacity and pH of the biochars and their respective filtrate .....	25
4. Experimental data on pH, calcium and phosphorus concentrations and the molar Ca/P ratio as measured in the incubation liquid at the end of the 14-day hydroxyapatite (HA) incubation experiment with wet-ozonized, dry-ozonized, and non-ozonized biochar .....	32
5. Biochar materials pine 300, pine 400, pine 500 and Rogue biochars (1 and 2) production source and methods .....	41
6. pH, CEC, and BET surface area of the ground biochar before and after ozonization .....	55
7. BET surface area of the ground pine 400 biochar (non-ozonized) and the ground rogue biochar (before and after ozonization) .....	56
8. BET surface area of the unground rogue biochar before and after ozonization .....	58
9. DOC material extracted from the non-ozonized control rogue biochar (RBC UN) and the dry-ozonized rogue biochar (RBC 90D) .....	59
10. Elemental analysis (oxygen and carbon) on the non-ozonized and dry-ozonized rogue biochar samples .....	61
11. Set-up of the hydroxyapatite solubilization assay at different DOC concentrations with filtrates from wet-ozonized pine 400 (P400 90W) and dry-ozonized rogue biochar (RBC 90D) .....	69
12. Set-up of milli-Q water controls at pH 2.6 and pH 3.0 incubation with hydroxyapatite .....	70
13. Calculated CEC (expressed in cmol of -COOH) in the filtrate of pine 400 and rogue biochar .....	77
14. Solubilized phosphate and pH data from the incubation of hydroxyapatite with water controls and filtrates from RBC 90D and P400 90W at low pH .....	88

Table	Page
15. Phosphorus and calcium concentration obtained from ICP-MS from the solubilization assay on day 8 of incubation .....	90
16. Concentration of phosphate, chloride, nitrate, and sulfate in filtrates/wash collected from the pine 400 wet-ozonized biochar (P400 90W) and the dry-ozonized rogue biochar (RBC 90D), as measured by ion chromatography .....	92
17. Set-up of bioassay multi-well plates .....	99
18. Concentration of phosphate, chloride, nitrate, and sulfate concentrations in the filtrate of the non-ozonized pine 400 (P400 UN), wet-ozonized pine 400 (P400 90W), non-ozonized rogue biochar (RBC UN) and dry-ozonized rogue biochar (RBC 90D) .....	112
19. Detection of potential bacterial inhibitory compounds (p-toluic acid and terephthalic acid) in the filtrate of non-ozonized pine 400 (P400 UN), wet-ozonized pine 400 (P400 UN), non-ozonized rogue biochar (RBC UN) and dry-ozonized rogue biochar (RBC 90D) .....	114
A1. Adsorption of calcium ( $\text{Ca}^{2+}$ ) by non-ozonized and dry-ozonized pine 400 biochar .....	157
B1. Ionic radius of divalent cations $\text{Cu}^{2+}$ , $\text{Ni}^{2+}$ , $\text{Mg}^{2+}$ , $\text{Zn}^{2+}$ , $\text{Cd}^{2+}$ , $\text{Pb}^{2+}$ and $\text{Fe}^{2+}$ in picometer .....	159
C1. DOC concentration from the 1 <sup>st</sup> 10-mL, 2 <sup>nd</sup> 25-mL wash and 3 <sup>rd</sup> 300-mL wash collected from biochar (mg/mL) and the total DOC extracted from biochar in mg DOC/g biochar .....	160
C2. Solubilized phosphate from hydroxyapatite incubation with the filtrates from RBC 90D and P400 90W at different DOC concentrations and pH conditions .....	162
C3. Solubilized phosphorus (mg P/L) from hydroxyapatite incubation with filtrate from RBC 90D and P400 90W at different DOC concentrations and pH conditions .....	163
C4. pH measurements of filtrates from the RBC 90D and P400 90W (no hydroxyapatite) at different DOC concentrations measured from day 0 to day 8 of the hydroxyapatite assay experiment .....	165
C5. mol ratio of solubilized calcium and phosphorus from the hydroxyapatite incubation assay samples collected on day 8 .....	166

Table	Page
C6. Measured concentrations (in mg/L) of some elements from the obtained from ICP-MS from the solubilization assay on day 8 of incubation of the filtrates from wet ozonized P400 (P400 90W) and dry-ozonized RBC biochar (RBC 90D) at DOC concentration of 600ppm (mg/L).....	166
E1. Daylength in Norfolk, Virginia during the cool season and warm season of the growth study.....	180
E2. Colony forming units from flask liquid cultures of GE <i>T. elongatus</i> BP1 BY20 (n=2), wild-type <i>T. elongatus</i> BP1 (n=2) and co-cultures GE <i>T. elongatus</i> BP1 BY20 + wild-type <i>T. elongatus</i> BP1 (n=3) .....	181

## LIST OF FIGURES

Figure	Page
1. Diagram of humic acid.....	6
2. Solubilized phosphate concentration as monitored in the incubation liquid of hydroxyapatite with wet-ozonized biochar and its filtrate, dry-ozonized biochar and its filtrate, or non-ozonized biochar and its filtrate (control) .....	19
3. <sup>31</sup> Phosphorus NMR of the filtrate from samples of the hydroxyapatite assay.....	23
4. Solubilized calcium concentration measured in the incubation liquid of hydroxyapatite with wet-ozonized, dry-ozonized, or non-ozonized biochar including each of their filtrates after incubating for 30 min (represented as day 0), 2 days and 14 days.....	27
5. pH measured in the incubation liquid of hydroxyapatite with wet-ozonized, dry-ozonized, or non-ozonized biochar including each of their filtrates after incubating for 30 min (represented as day 0), 2 days and 14 days.....	30
6. Milligram (mg) of calcium removed per gram of biochar; P400 UN for the non-ozonized pine 400 biochar and P400 90D for the dry-ozonized pine 400 biochar .....	33
7. Excitation emission matrix spectra of the filtrate from the non-ozonized control biochar (A) and the wet-ozonized biochar (B) .....	34
8. Adsorption of Cu <sup>2+</sup> , Ni <sup>2+</sup> , Mg <sup>2+</sup> , Zn <sup>2+</sup> , Pb <sup>2+</sup> and Fe <sup>2+</sup> from pine 400 non-ozonized biochar control, 30 min dry-ozonized, 60min dry-ozonized and 90min dry-ozonized in mg of metal (M <sup>2+</sup> ) per gram of biochar .....	47
9. pH measurements of the pine 300 (P300), pine 400 (P400), pine 500 (P500), rogue biochar 1 (RBC 1) and RBC 2 (50 μm) before ozone treatment and after ozone treatment .....	51
10. CEC measurements of the pine 300, pine 400, pine 500, rogue biochar 1 (106 μm) and rogue biochar 2 (50 μm) before ozone treatment and after ozone treatment.....	52
11. Photograph of the filtrate liquid from the non-ozonized control (A) and the dry-ozonized (B) rogue biochar samples .....	59
12. Total dissolved organic carbon (DOC) material extracted from the pine 400 biochar (P400) and rogue biochar (RBC) .....	73
13. Cation exchange capacity measurements of the dissolved organic carbon from the filtrates of Pine 400 and RBC biochar, expressed as cmol of carboxyl groups/mL filtrate .....	75

Figure	Page
14. Solubilized phosphate from hydroxyapatite by the filtrate/wash from the dry-ozonized rogue biochar (RBC 90D) at different DOC concentrations (10, 75, 300 and 600ppm) at the pH of the DOC measured every 2 days for up to 8 days .....	80
15. Solubilized phosphate from hydroxyapatite by the filtrate/wash from the wet-ozonized pine 400 biochar (P400 90W) at different DOC concentrations (10, 75, 300 and 600ppm) at the pH of the DOC measured every 2 days for up to 8 days.....	81
16. pH measurements of the filtrates from RBC 90D at different DOC concentrations incubated with hydroxyapatite at day 0, 2, 4, 6 and 8 .....	82
17. pH measurements of the filtrates from P400 90W at different DOC concentrations incubated with hydroxyapatite at day 0, 2, 4, 6 and 8 .....	84
18. Solubilized phosphate from hydroxyapatite by the filtrate/wash from the dry-ozonized rogue biochar (RBC 90D) at different DOC concentrations (10, 75, 300 and 600ppm).....	85
19. Solubilized phosphate from hydroxyapatite by the filtrate/wash from the wet-ozonized pine 400 biochar (P400 90W) at different DOC concentrations (10, 75, 300 and 600ppm).....	86
20. Total dissolved organic carbon measured in the filtrates of pine 300 (P300), pine 400 (P400), pine 500 (P500) and rogue biochar before and after wet/dry ozonization .....	102
21. Growth of <i>P. putida</i> in incubation with filtrates from wet-ozonized, dry-ozonized, and non-ozonized pine 400 biochar at different DOC concentrations .....	104
22. Growth of <i>P. putida</i> in incubation with filtrates from wet-ozonized, dry-ozonized, and non-ozonized rogue biochar at different DOC concentrations .....	106
23. Growth of <i>Synechococcus elongatus</i> PCC 7942 (7942) in incubation with filtrates from wet-ozonized, dry-ozonized, and non-ozonized pine 400 (P400) biochar at different DOC concentrations .....	108
24. Growth of <i>Synechococcus elongatus</i> PCC 7942 (7942) in incubation with filtrates from wet-ozonized, dry-ozonized, and non-ozonized rogue biochar (RBC) at different DOC concentrations .....	110
25. Gene map of the YFP-ST-R-Lipase construct visualized with CLC bio software .....	120
26. The greenhouse temperatures as recorded for the growth study during a period with cool temperatures ranging from 15.44 °C to 25.30 °C and warm temperatures ranging from 31.42°C to 36.27 °C .....	124

Figure	Page
27. Optical Density of wild-type and GE <i>T. elongatus</i> BP1 (BP1-BY20) cultures at $1 \times 10^7$ cells/mL during cool temperatures (15.44 °C to 25.30 °C) monitored weekly during a 4-week period in the greenhouse .....	125
28. Survivability assay for wild-type <i>T. elongatus</i> BP1, wild-type <i>Synechocystis</i> PCC 6803 and GE <i>T. elongatus</i> BP1-BY20 cultures at $1 \times 10^7$ cells/mL during cool temperatures (15.44 °C to 25.30 °C) in the greenhouse.....	127
29. Optical density ( $\lambda=730$ nm) of survivability assay for wild-type <i>T. elongatus</i> BP1, wild-type <i>Synechocystis</i> PCC6803 and GE <i>T. elongatus</i> BP1-BY20 cultures at $1 \times 10^7$ cells/mL during cool temperatures (15.44 °C to 25.30 °C) in greenhouse conditions.....	128
30. Colony-forming units (CFU) for the GE <i>T. elongatus</i> BP1-BY20 cultures during cool temperatures (15.44 °C to 25.30 °C) in greenhouse conditions (GH) and its associated control set for cultures incubated in the Percival incubator at 45 °C in (Percival).....	129
31. Optical Density of wild-type and GE <i>T. elongatus</i> BP1 (BP1- BY20) cultures at $1 \times 10^7$ cells/mL during warm temperatures (31.42°C to 36.27°C) monitored weekly during a 4-week period in the greenhouse .....	130
32. Survivability assay for wild-type <i>T. elongatus</i> BP1, wild-type <i>Synechocystis</i> PCC 6803 and GE <i>T. elongatus</i> BP1- BY20 cultures at $1 \times 10^7$ cells/mL during warm temperatures (31.42 °C to 36.27 °C) in the greenhouse.....	132
33. Optical density ( $\lambda=730$ nm) of survivability assay for wild-type <i>T. elongatus</i> BP1, wild-type <i>Synechocystis</i> PCC6803 and GE <i>T. elongatus</i> BP1- BY20 cultures at $1 \times 10^7$ cells/mL during warm temperatures (31.42 °C to 36.27 °C) in greenhouse conditions.....	133
34. Colony-forming units (CFU) for the GE <i>T. elongatus</i> BP1-BY20 cultures during warm temperatures (31.42 °C to 36.27 °C) in greenhouse conditions in (GH) and its associated control set for cultures incubated in the Percival incubator at 45 °C in (Percival).....	134
35. The relative percentage of cells in the coculture over a 4-week incubation in the greenhouse during the cool season (16-26°C) between the GE <i>T. elongatus</i> BP1 BY20 (BY20) and WT <i>Synechocystis</i> PCC 6803 in A and WT <i>T. elongatus</i> BP1 (WT BP1) and WT <i>Synechocystis</i> PCC 6803 in B .....	136
36. The relative percentage of cells in the coculture over a 4-week incubation in the greenhouse during the cool season (16-26°C) between the GE <i>Synechocystis</i> PCC 6803-YFP (6803-YFP) and WT <i>Synechococcus elongatus</i> PCC 7942 (WT 7942) in A; WT <i>Synechocystis</i> PCC 6803 (WT 6803) and WT <i>Synechococcus elongatus</i> PCC 7942 (WT 7942) in B .....	139

Figure	Page
37. The relative percentage of cells in the coculture over a 4-week incubation at room temperatures between the GE <i>Synechocystis</i> PCC 6803-YFP (6803-YFP) and WT <i>Synechococcus elongatus</i> PCC 7942 (WT 7942) in A; WT <i>Synechocystis</i> PCC 6803 (WT 6803) and WT <i>Synechococcus elongatus</i> PCC 7942 (WT 7942) in B.....	141
B1. Percent removal of Cu <sup>2+</sup> , Ni <sup>2+</sup> , Mg <sup>2+</sup> , Zn <sup>2+</sup> , Cd <sup>2+</sup> , Pb <sup>2+</sup> and Fe <sup>2+</sup> from pine 400 non-ozonized biochar control, 30 min dry-ozonized, 60min dry-ozonized and 90min dry-ozonized .....	158
C1. Conductivity signals of anions from the filtrate of the wet-ozonized pine 400 (P400 90W-F) biochar and the filtrate from the dry-ozonized rogue biochar (RBC 90D-F) at a DOC concentration of 300 ppm in A) and conductivity signals of standard acetate and oxalate in B).....	161
C2. pH measurements of the filtrates from the dry-ozonized rogue biochar (RBC 90D) at different DOC concentrations (10, 75, 300 and 600 ppm), used as the no-hydroxyapatite control .....	164
C3. pH measurements of the filtrates from the wet-ozonized pine 400 biochar (P400 90W) at different DOC concentrations (10, 75, 300 and 600 ppm), used as the no-hydroxyapatite control .....	164
C4. pH measurements of the filtrates from RBC 90D at neutralized pH at different DOC concentrations incubated with hydroxyapatite at day 0, 2, 4, 6 and 8 .....	167
C5. pH measurements of the filtrates from P400 90W at neutralized pH and different DOC concentrations incubated with hydroxyapatite at day 0, 2, 4, 6 and 8.....	168
C6. Conductivity signals of anions from the filtrate of the wet-ozonized pine 400 (P400 90W) biochar and the filtrate from the dry-ozonized rogue biochar (RBC 90D) at a DOC concentration of 300 ppm from the hydroxyapatite incubation assay on day 8 .....	169
D1. Photographs of the filtrates used as a control for the biochar filtrate toxicity assay .....	170
D2. Optical density (OD730) of the growth of <i>P. putida</i> in incubation with filtrates from non-ozonized pine 400 biochar at different DOC concentrations .....	171
D3. Optical density (OD730) of the growth of <i>P. putida</i> in incubation with filtrates from dry-ozonized pine 400 biochar at different DOC concentrations .....	171
D4. Optical density (OD730) of the growth of <i>P. putida</i> in incubation with filtrates from wet-ozonized pine 400 biochar at different DOC concentrations .....	172

Figure	Page
D5. Optical density (OD730) of the growth of <i>P. putida</i> in incubation with filtrates from non-ozonized rogue biochar (RBC) at different DOC concentrations.....	172
D6. Optical density (OD730) of the growth of <i>P. putida</i> in incubation with filtrates from wet-ozonized rogue biochar (RBC) at different DOC concentrations.....	173
D7. Optical density (OD730) of the growth of <i>P. putida</i> in incubation with filtrates from dry-ozonized rogue biochar (RBC) at different DOC concentrations .....	173
D8. Optical density (OD730) of the growth of <i>Synechococcus elongatus</i> PCC 7942 (7942) in incubation with filtrates from non-ozonized pine 400 biochar at different DOC concentrations.....	174
D9. Optical density (OD730) of the growth of <i>Synechococcus elongatus</i> PCC 7942 (7942) in incubation with filtrates from dry-ozonized pine 400 biochar at different DOC concentrations.....	174
D10. Optical density (OD730) of the growth of <i>Synechococcus elongatus</i> PCC 7942 (7942) in incubation with filtrates from wet-ozonized pine 400 biochar at different DOC concentrations.....	175
D11. Optical density (OD730) of the growth of <i>Synechococcus elongatus</i> PCC 7942 (7942) in incubation with filtrates from non-ozonized rogue biochar (RBC) at different DOC concentrations.....	175
D12. Optical density (OD730) of the growth of <i>Synechococcus elongatus</i> PCC 7942 (7942) in incubation with filtrates from dry-ozonized rogue biochar (RBC) at different DOC concentrations.....	176
D13. Optical density (OD730) of the growth of <i>Synechococcus elongatus</i> PCC 7942 (7942) in incubation with filtrates from wet-ozonized rogue biochar (RBC) at different DOC concentrations.....	176
D14. Conductivity signals of anions from pine 400 and rogue biochar (before and after ozonization) compared with standard acetic acid .....	177
D15. GC-MS spectra of p-toluic acid in pine 400 biochar filtrate.....	178
D16. GC-MS spectra of terephthalic acid in pine 400 biochar filtrate .....	179
E1. Weekly growth of GE <i>T. elongatus</i> BP1 BY20 (BY20), WT <i>T. elongatus</i> BP1 (WT BP1) and WT <i>Synechocystis</i> PCC 6803, used as control for the competition study conducted in the greenhouse during the cool season (16-26°C).....	180

Figure	Page
E2. Weekly growth of GE <i>Synechocystis</i> PCC 6803-YFP (6803-YFP) and WT <i>Synechococcus elongatus</i> PCC 7942 (WT 7942) and WT <i>Synechocystis</i> PCC 6803 (WT 6803), used as control for the competition study conducted in the greenhouse during the cool season (16-26°C).....	181
E3. Weekly growth of GE <i>Synechocystis</i> PCC 6803-YFP (6803-YFP) and WT <i>Synechococcus elongatus</i> PCC 7942 (WT 7942) and WT <i>Synechocystis</i> PCC 6803 (WT 6803), used as control for the competition study conducted at room temperatures .....	182

## CHAPTER I

### INTRODUCTION

Biochar is the carbon-rich material obtained from thermal decomposition of biomass. Sources of the biomass can vary from residues of plants and leaves, animal wastes such as manure and other carbon-containing wastes.<sup>1</sup> Thus, biochar has been made from many carbon-containing biomass materials coming from agricultural and forest residues<sup>2,3</sup>, municipal waste<sup>4</sup> and even industrial wastes<sup>5,6</sup>. The demographic growth paired with an increase in industrial and agricultural practices causes an increase in total biomass. In addition, forest residue accumulation has also been an issue since global warming is causing some forest trees to die off due to drought<sup>7</sup>. All this produced biomass urges the need for technologies to utilize them or to transform them. The transformation of biomass into biochar offers several practical uses. Biochar is mainly used as a soil amendment and carbon sequestration agent. It is also used to remediate contaminated soils and waters from toxic chemicals<sup>1-4</sup>. There are many ways of making biochar; low temperature processes, pyrolysis, gasification and combustion<sup>1,8</sup>. Low temperature processes, or torrefaction uses heating temperatures of 300 °C or below. Torrefaction has a great yield of solid biochar; however, the biochar is not stable over time as it can be degraded easily, therefore not a great carbon sequestration agent<sup>1,8</sup>. Gasification and combustion, on the other hand happen at high temperatures however, they have very low yield of biochar<sup>1,8</sup>.

The process of making biochar by pyrolysis has gained a particular interest due to its simplicity, applicability, and cost-effectiveness. Pyrolysis is the heating of biomass materials in the absence or low amount of oxygen; the end products are biochar, bio-oil, and syngas. Different techniques of pyrolysis are employed. Fast pyrolysis uses fast heating rates (around

180 °C s<sup>-1</sup>), employs high treatment temperatures (from about 400 °C to about 1300 °C) and short residence times<sup>9,10</sup>. Fast pyrolysis usually produces a biochar with great surface area, however the biochar yield and the oxygen functional groups are low<sup>1,8,9</sup>. Slow pyrolysis typically happens at relatively low treatment temperatures of 300-500°C, uses slow heating rate (around 0.5 °C s<sup>-1</sup>) and long residence time (10 min to couple hours or days)<sup>9,10</sup>. In addition to the pyrolysis conditions of the biomass, the characteristics of the biochar also depends on the type of biomass feedstock used, the ash composition of the biomass and the biomass pretreatment methods<sup>1,11</sup>. The transformation of biomass into biochar, converts the carbon into a more stable form that is not easily degraded and released back into the atmosphere. Among the various feedstock, particular interest is to be given to abundant sources of biomass in order to have a greater impact against global warming. Recently, an investigation into the mechanism of slow pyrolysis revealed some insights into the yield of biochar; biomass with high lignin content was found to yield higher mass of biochar whereas biomass with high cellulose content and higher treatment temperatures yielded a biochar with greater surface area,<sup>12</sup> an important feature that gives biochar a wide variety of applications. In addition, the mechanism of slow pyrolysis converts cellulose, hemicellulose and lignin into intermediates such as levoglucosan, furfural and aromatic compounds, respectively<sup>12</sup>. These intermediates then get further decomposed into a more aromatic structure; the heteroatoms (especially oxygen) are also lost in the process, thus giving a more porous structure to the biochar<sup>12</sup>.

There is an ambiguity between biochar, charcoal and activated carbon. They are all similar in that they can be made by similar techniques; they differ mainly in their uses. Charcoal is used for its calorific value, activated carbon is chemically or mechanically activated and it is used for industrial purposes. Biochar on the other hand, is made from biomass material and it is

mainly used for agricultural purposes and as a carbon sequestration agent <sup>1</sup>. Thus, the biochar with its high carbon content can be used to increase the soil carbon content, an important property for soil fertility. Carbonized biomass has been long used as a soil amendment, but the term “biochar” was only coined in 2005 by Peter Read <sup>8, 13</sup>. Its purpose as a soil amendment is to improve crop yield via its various properties such as alleviating the stress from nutrient deprivation <sup>14</sup>, increasing soil moisture and fertilizers retention with its cation exchange capacity <sup>1</sup>. The cation exchange capacity (CEC) refers to the ability of soil or biochar materials to retain and exchange positively charged ions ( $Mg^{2+}$ ,  $Ca^{2+}$ ,  $NH_4^+$  etc.). Thus, a soil with a high CEC value can retain more positively charged nutrients and provide them to the plant roots by exchanging them with other cations. The oxygen functional groups on the surface of biochar have an influence on its CEC <sup>1, 15, 16</sup>. Biochar is known to be highly aromatic, but its exact structure is not defined <sup>1</sup>. The temperature of biochar production influences its porosity and its functional groups. At lower pyrolysis temperature (less than 500 °C), there is a larger number of functional groups, and the biochar structure is more of a 3D network of benzene rings. As the pyrolysis temperature increases to 500-700 °C the biochar structure becomes more of a 2D network of fused rings and has greater porosity but lower functional groups. As the temperature further increases to more than 700 °C, the biochar has greater porosity, even less functional groups and a graphite microcrystalline structure<sup>17, 18</sup>. For biochars that have low functional groups on their surface, it is possible to increase the surface functional groups such as oxygen-containing functional groups by activating or treating the biochar with oxidizing agents; some oxidizing agents like hydrogen peroxide and acids such as hydrochloric acid, phosphoric acid and sulfuric acid were previously used for that matter <sup>19-23</sup>. Adding oxygen functional groups to biochar has gained much interest, however it is important to note that the installation of the

oxygen functional groups should be limited to just the surface of biochar; biochars with high oxygen contents in their bulk are unstable and degrade much quicker<sup>1</sup>. The use of some of these oxidizing agents for biochar treatment may cause problems in disposal or handling and/or may not be cost-efficient if we are considering large batches of biochar. Recently, our lab developed an innovative post-production surface oxygenation of biochar via ozonization<sup>24, 25</sup>. The technology ozonizes dry biochar material with a controlled flow of ozone, a mechanism that cleaves the olefinic groups; the treated biochar showed a doubling in cation exchange capacity compared to the control biochar due to the increase in carboxylic and oxygen groups as a result of the cleavage of the bonds<sup>24</sup>. Biochar with enriched oxygen functional groups on its surface has a multitude of uses including its participation in toxic metal removal; positively charged metals can form complexations with the negatively charged species on the biochar such as the oxygen groups<sup>2, 18, 19</sup>. In addition surface oxygenated biochar was also found to increase soil moisture due to its increased hydrophilicity<sup>26</sup>. These properties also give the surface oxygenated biochar the ability to retain nutrients such as those contained in fertilizers and thus reduce the need for frequent fertilizers applications.

Fertilizer's use has become very widespread globally; it is used daily to render the soil more fertile, and it facilitates the growth of crop during different seasons. Humans rely heavily on fertilizers to meet the demands especially with the growing population. Phosphorus fertilizers are mainly extracted from phosphate rocks. Manufacturing phosphate fertilizers often uses strong acids that are not very environmentally friendly, in that they can be hazardous to the health of the people handling them<sup>27-30</sup>. In chapter two, we report a new discovery regarding the application of ozonized biochar in solubilizing phosphorus from insoluble phosphate material (hydroxyapatite) without the use of any strong industrial acid. The use of this green chemistry

with ozonized biochar (which can be renewably made from waste biomass) may provide a new approach to solubilize phosphorus from mineral phosphate rock materials.

Terra Preta soils in the Amazonian area have been known for their great fertility. Part of their high fertility is due to the high cation exchange capacity (CEC) of these soils<sup>16,31</sup>. In the study reported in chapter three, using high surface area rogue biochar, we observed an increase in CEC by a factor of nearly ten times which resulted in a CEC well over 100 cmol/kg<sup>15</sup>, one of the highest reported CEC value for biochar reported in literature.

The CEC of biochar is a very important characteristic for soil amendment, its main proposed application. Users of biochar would typically apply up to 10% of biochar (w/w) to soil; biochar amount ranging from 0.1-5% also showed some beneficial effects when applied in the top 15-cm of soil layer<sup>32</sup>. Some compounds in the filtrate biochar were identified by our group to be humic-like substances<sup>33</sup>. Humic acids are known to be rich in carboxyl groups and hydroxyl groups as shown in Figure 1<sup>34</sup>. Therefore, the humic-like materials that may be contained in biochar filtrate may also carry some CEC which can further add more value to the biochar. Humic substances and humic-like materials have been shown to have some beneficial properties in crops whether in soil agricultural system or hydroponic<sup>35,36</sup>. In chapter four, we investigated into the characteristics of the filtrates from ozonized biochar.

Being in direct contact with soil bacteria and indirect contact with other microorganisms of the ecosystem, it is important that the applied biochar is safe to the microorganisms. In chapter five, we investigated the toxicity effect of the water extractable dissolved organic carbon (DOC) materials from the ozonized biochar on soil bacteria and cyanobacteria. Cyanobacteria is an autotrophic microorganism that is of particular interest of study due to its low requirements on carbon-based nutrients. In addition, cyanobacteria offer the versatility of being able to live

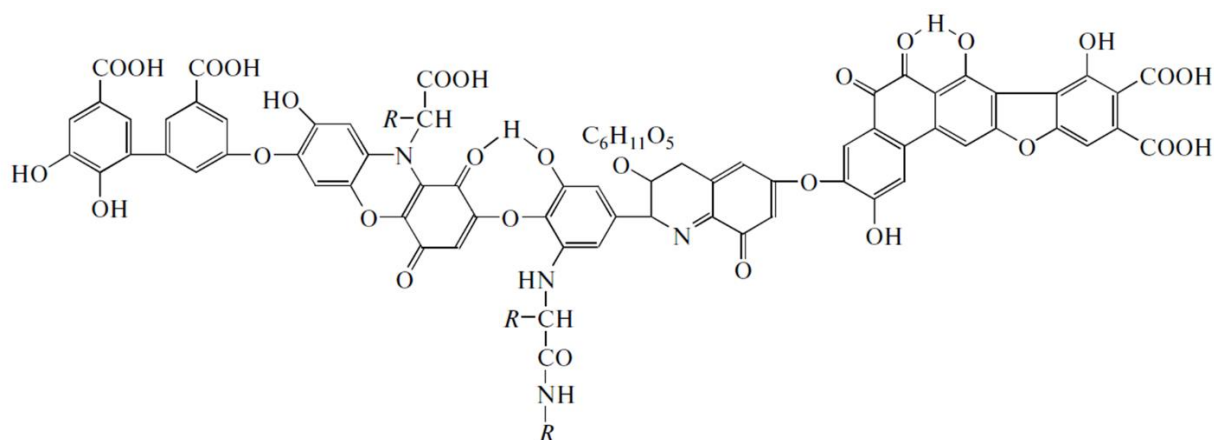


**Figure 1:** Diagram of humic acid. The represented diagram was proposed by Stevenson<sup>34</sup>. Reproduced with permission from Stevenson FJ. Humus chemistry: genesis, composition, reactions. John Wiley & Sons; 1994. License number 5039221441206. Permission is provided in Appendix F.

in many environments from fresh water, saltwater and even soils and rock surfaces<sup>37, 38</sup>.

Therefore, knowing how the application of the ozonized biochar and its filtrates in soil may impact the viability of cyanobacteria is of much importance. Furthermore, cyanobacteria have developed many metabolic pathways and they are easier to manipulate genetically compared to eukaryotic algae, thus making them quite desirable in the field of biotechnology.

Cyanobacteria can be used for biofuels production to help meet the energy demands; there are interests for its use as an alternative energy source to the limited and declining fossil fuels. The use of cyanobacteria as biofuels offers the advantage of not needing to grow in cultivable lands<sup>39</sup>. A common method employs the transformation of cyanobacteria biomass and its lipid content into biofuel<sup>39</sup>. Even though some cyanobacteria species such as *Synechococcus* UTEX 2973 are fast-growing photoautotrophic microorganism<sup>40</sup>, the biofuel energy they produced, and the cost of production are not very competitive to fossil fuels<sup>39</sup>. Renewable

energy via the use of genetically engineered microorganisms is referred to as a 4<sup>th</sup> generation biofuel production and provides a more promising and profitable avenue as an alternative source of energy. Cyanobacteria can be genetically engineered to not only photo-autotrophically produce more biofuels but also to produce some high value byproducts<sup>41-45</sup>, all that while keeping its advantage of not needing arable lands. However, a major biosafety concern arises with the use of GE cyanobacteria if the latter were to break physical containment and escape to the environment. Among the various biosafety techniques that sometimes involve additional genetic manipulations<sup>46,47</sup>, here we propose a simple natural biosafety-guarded mechanism. It consists in the use of a thermophilic cyanobacteria *Thermosynechococcus elongatus* BP1 that typically grows at 57 °C but can't grow at temperatures below 30°C<sup>48</sup>. The question that now emerges is whether the thermophilic nature of *T. elongatus* BP1 can be used as a biosafety guarded mechanism after being genetically engineered. In chapter six, the growth and survivability of GE *T. elongatus* BP1 was investigated under different natural temperature conditions and some biosafety parameters such as the competition between wild-type and GE cyanobacteria were also assessed.

The projects discussed in this dissertation are of much importance to the field of green chemistry and biosafety. The first three projects provide insights into the use of a sustainable technique of biochar surface oxygenation by ozonization for soil amendment purposes. The last projects take a slightly different turn with the assessment of the effect of the ozonized biochar on microorganisms and the evaluation of some biosafety features of genetically engineered cyanobacteria with biofuels-producing genes. Cyanobacteria were chosen as one of the microorganisms for these projects, mainly because of their ability to live in various environments

and their various applications. In chapter seven, the concluding remarks of this dissertation are presented as well as the opening into future routes of investigations.

## CHAPTER II

### SOLUBILIZATION OF PHOSPHORUS FROM INSOLUBLE PHOSPHATE MATERIAL HYDROXYAPATITE WITH OZONIZED BIOCHAR

#### PREFACE

The content of this chapter has been published in 2020 in ACS Sustainable Chemistry and Engineering. Full citation of the manuscript is provided below. Reported here, is a modified version of the published work reprinted with permission from publisher. Permission is provided in Appendix F.

Sacko, O.; Whiteman, R.; Kharel, G.; Kumar, S.; Lee, J. W., Sustainable Chemistry: Solubilization of Phosphorus from Insoluble Phosphate Material Hydroxyapatite with Ozonized Biochar. *ACS Sustainable Chemistry & Engineering* **2020**, 8 (18), 7068-7077.

#### INTRODUCTION

The use of phosphorus in agriculture is very crucial to civilization and cannot be replaced by other elements. Famous science writer Isaac Asimov said that phosphorus is “life’s bottleneck” and once stated: “We may be able to substitute nuclear power for coal, and plastics for wood, and yeast for meat, and friendliness for isolation—but for phosphorus there is neither substitute nor replacement”<sup>49</sup>. There is large amount of phosphorus (P) already present in the soil; the total level of phosphorus in soils has an average of about 600 mg P/kg soil with a minimum of 200 mg P/kg soil to a maximum of 5000 mg P/kg soil<sup>50</sup>. However, only a small amount of that soil total phosphorus (P) is available for plants to use. The Olsen-P is a measure

of that available phosphorus in soil. For example, a study conducted with a variety of soils found that the minimum Olsen-P to generate optimal crop production was 20 mg P/kg<sup>51</sup> but it is typical for soils to have an Olsen-P around 10 mg P/kg soil<sup>51,52</sup> which is much less than the total level of phosphorus in soil. Phosphate is readily usable by plants when it is in orthophosphate form such as  $\text{H}_2\text{PO}_4^-$  or  $\text{HPO}_4^{2-}$ , depending on soil pH. Thus, a major challenge consists in increasing the availability of soil phosphorus, in its usable orthophosphate form so that plants can use it. One of the reasons contributing to the low amount of usable phosphate is because the inorganic phosphate forms complexes with aluminum, calcium and iron and becomes insoluble and plants can't use it<sup>53,54</sup>. To compensate for the low amount of usable phosphate, large amount of phosphate fertilizers is applied on soil.

Phosphate fertilizers are mainly generated from phosphate rock reserves. Some studies predict that the expected global peak in phosphorus production could occur as early as 2030<sup>55,56</sup>, particularly for countries like the US that have quite limited phosphate rock reserves with 1 million tons compared to 50 million tons in Morocco and Western Sahara, and 3.2 million tons in China<sup>57,58</sup>. Application of large amounts of phosphate fertilizers in soil can cause ground water pollution and its runoff can cause eutrophication of surface water of aquatic ecosystems<sup>59</sup>. Therefore, another main challenge consists in developing technologies that can make farming system use less amount of phosphorus fertilizers, while ensuring there is enough phosphorus for plants. Being a limited and highly needed resource, it is very important to find efficient ways to generate and utilize the phosphorus.

Here, we propose an improvement of the utilization of phosphorus using ozonized biochar. This green technology could result in an increase in soluble phosphate availability in soil while being less compromising to the environment. Furthermore, the ozonized biochar with

its enriched functional groups and increased nutrient retention capabilities would help reduce the runoff of fertilizers nutrients, another desirable trait of the application of ozonized biochar.

## **MATERIALS AND METHODS**

### **Production of biochar**

Loblolly pine wood biomass (*Pinus taeda*) was collected from the campus of Old Dominion University, in Norfolk Virginia. The biochar was made in a slightly modified manner as reported by Huff et al (2018)<sup>24</sup>. Briefly, the pine woods were cut into pieces with dimensions of 1 cm by 3 cm on average and the bark was removed. The wood pieces were then dried in an electrical Heratherm oven (OGS 100) overnight at 105 °C. Using a hastelloy parr 0.5 L reactor, the chamber was loaded with 50.0 g of the pine wood biomass. An outlet was made to prevent autogenic pressure build up. The reaction chamber was purged with nitrogen for 5 min and the biomass was slowly heated to 400 °C while collecting the bio-oil via the outlet. It was maintained at 400 °C for 30 min before slowly cooling it down using the internal water coil cooling system. The biochar was collected and named as “pine 400” or P400. For this study, a total of eight batches of pine 400 biochar were made. The average heating rate was  $6.88 \pm 1.87$  °C/min. The average yield of biochar produced was 36.78% ( $\pm 1.16\%$ ) and the average yield of bio-oil and water collected was 38.21% ( $\pm 1.79\%$ ). The collected biochar was ground and sieved through a 106- $\mu\text{m}$  screen. Portions of 5 g of biochar were then washed with milli-Q water (100 mL of milli-Q water for every gram of biochar). The biochar was dried in the oven overnight at 105°C and was used as the stock biochar in the experiment.

### **Wet ozone treatment of biochar**

The biochar was treated with ozone under wet conditions in the following manner. Here,

1.5 g of the dried biochar was mixed with 35 mL of milli-Q water (4% biochar and 96% liquid). The mixture was placed in a specialized reactor glass vessel and treated with an ozone-containing gas stream produced from oxygen through a Welsbach T series ozone generator for 90 min. The ozone-containing gas flow was set to 3.0 L/min with an oxygen gas pressure set to 8 psi and the voltage of ozone generator set to 116 V. After the 90 minutes treatment time, the wet-ozonized mixture was then filtered through a Buchner funnel filtration system using a Fisherbrand P8 filter paper (catalog number 09-795B). The filtrate liquid was collected and referred to as “wet-ozonized biochar filtrate” or P400 90W-F. The wet-ozonized pine 400 biochar (P400 90W) was then washed with an additional 300 mL of milli-Q water through filtration to remove any water-extractable organic and residual ash components. Subsequently, the treated biochar (P400 90W) was dried in the Heratherm oven (OGS 100) at 105 °C and the filtrate was stored in a refrigerator at 4°C for later use.

### **Dry ozone treatment of biochar**

For the dry ozonization treatment, 1.5 g of the dried biochar was treated with ozone generated from a Welsbach T series ozone generator for 90 min. The experimental conditions here were similar to that of the wet ozonization treatment described earlier except that the dry ozonization treatment was done in the absence of any liquid water. The reactor glass vessel was hand shaken every 15 min to ensure proper mixing for the ozonization reaction with biochar particles during the 90-min ozonization treatment. The dry-ozonized biochar was then washed with 35 mL of milli-Q water and the wash liquid was collected by vacuum filtration and was referred to as “dry-ozonized biochar filtrate” or P400 90D-F. The dry-ozonized biochar was further washed with an additional 300 mL of milli-Q water through filtration to remove any

water-extractable organic and residual ash components. The treated biochar (P400 90D) was then dried in the oven at 105 °C. The filtrate/wash was stored in a refrigerator at 4 °C for later use.

### **Biochar control sample (non-ozonized biochar)**

For the non-ozonized control biochar preparation, 1.5 g of the dried biochar was washed with 35 mL of milli-Q water. The wash liquid was collected by vacuum filtration and was referred to as “non-ozonized biochar filtrate” (P400 UN-F). The biochar was further washed with an additional 300 mL of milli-Q and filtered to remove any water-extractable organic and residual ash components. The biochar (P400 UN) was then dried in the oven at 105 °C and the filtrate of the wash was stored in a refrigerator at 4°C.

### **pH Measurement**

For each of the biochar treatment types (non-ozonized control, dry-ozonized, and wet-ozonized biochar), 1.0 g of the biochar was mixed with 10.0 mL of Millipore water and shaken at 100 RPM on an Innova 2300 Platform Shaker for 1 hour. The pH of the slurry was then measured with the pH meter (Beckman Coulter model number pHi570) and a Thermoscientific pH probe. The pH for each biochar treatment type was measured in duplicate.

### **Cation Exchange Capacity measurement**

The biochar cation exchange capacity (CEC) was measured using the barium acetate or Ba(OAc)<sub>2</sub>-based method as reported by Rippey and Nelson<sup>60</sup>. Briefly, 0.5 g of biochar was mixed with 50 mL of 0.5M HCl. The mixture was shaken for 2 hours at 100 rpm using the platform shaker Innova 2300. The biochar was washed with about 3 L of milli-Q water using vacuum filtration through a Buchner funnel filtration system using a Fisherbrand P8 filter paper. Another 100 mL of milli-Q water was used to wash the biochar and the resulting filtrate was tested with

silver nitrate ( $\text{AgNO}_3$ ) until there was no precipitate formed or biochar was further washed with milli-Q water. The biochar was then placed in another flask containing 50 mL of 0.5 M barium acetate  $\text{Ba}(\text{OAc})_2$  and the mixture was shaken at 100 rpm for 1 hr. The mixture was then filtered and further washed with 300 mL of milli-Q water. The resulting 350 mL of the collected filtrate was titrated with 0.1 M NaOH solution until the end point ( $\text{pH} = 8.2$ ) was reached. The CEC was then calculated with the same approach as done in a previous study using the following equation<sup>61</sup>.

$$\frac{\text{cmol}}{\text{Kg biochar}} = \frac{\text{mL NaOH} \times \text{molarity NaOH} \times 100}{\text{gram sample}} \quad (1)$$

The CEC measurements for each biochar sample treatment were done in 6 replicates.

### **Hydroxyapatite Assay preparation**

Reagent grade Hydroxyapatite ( $\text{Ca}_5(\text{PO}_4)_3(\text{OH})$ ) was purchased from Sigma Aldrich (289396-25G). Using 50-mL polypropylene tubes, each of the assay treatments shown in Table 1 was done in triplicate. Briefly, 0.5 g of biochar material and 12 mL of liquid was used in order to maintain the 4% of biochar and 96% liquid as used during the wet ozone treatment. Several controls were included where the hydroxyapatite material was omitted; a control with water and biochar was used to determine the amount of phosphorus and calcium from the biochars; biochar filtrate was used to determine the amount of phosphorus and calcium from the biochar filtrates.

The liquid incubational treatment samples totaled to 51 tubes. The tubes were incubated by placing them at room temperature on an Innova 2300 Platform Shaker at 100 rpm. After 30 min of shaking (Day 0), the pH was measured in each tube using the pH probe. The samples were centrifuged at 4500 rpm using Beckman Coulter centrifuge with a JS-5.3 swinging-bucket rotor. 1 mL of the supernatant was collected from each sample and was stored in the freezer. The

tubes were placed back on the shaker for further incubation. The procedure was repeated at day 2 and day 14.

**Table 1: Hydroxyapatite preparation assay set-up.**

	<b>Blank</b>	<b>P400 UN</b>	<b>P400 90W</b>	<b>P400 90D</b>
12 mL Milli-Q + 0.5g biochar	milli-Q	milli-Q + biochar	milli-Q + biochar	milli-Q + biochar
Water + 0.25g hydroxyapatite (HA) + 0.5g biochar	milli-Q + HA	milli-Q + HA + biochar	milli-Q + HA + biochar	milli-Q + HA + biochar
12 mL biochar filtrate	N/A	P400 UN-F	P400 90W-F	P400 90D-F
12 mL biochar filtrate + 0.25g hydroxyapatite (HA)	N/A	P400 UN-F + HA	P400 90W-F + HA	P400 90D-F + HA
12 mL biochar filtrate + 0.25g hydroxyapatite (HA) + 0.5g biochar	N/A	P400 UN-F + HA + biochar	P400 90W-F + HA + biochar	P400 90D-F + HA + biochar

### Calcium Concentration Measurement

The samples collected from the hydroxyapatite liquid incubation assay were stored in the freezer and were subsequently analyzed for their calcium content. Half of the 1 mL that was stored for each sample was used and diluted to a concentration within the detection limit of the instrument. A standard calibration calcium curve was prepared using a standard solution of

calcium sulfate  $\frac{1}{2}$  hydrate. The calcium concentration was determined using a Shimadzu Flame Atomic Absorbance Spectrophotometer ASC-7000.

### **Phosphate Concentration Measurement**

The remaining half of the collected samples from the hydroxyapatite liquid incubation assay was analyzed for its phosphate content. A standard calibration curve was prepared using Dionex 7 Anion Standard II purchased from Thermo Scientific (057590). The phosphate concentration of the samples was measured using the AS40 Automated ICS-5000 Dionex Ion Chromatography System. The eluent used was 4.5 mM  $\text{Na}_2\text{CO}_3$  and 0.8 mM  $\text{NaHCO}_3$ . The data was analyzed using the Chromeleon software.

### **$^{31}\text{P}$ Phosphorus NMR Spectroscopy**

$^{31}\text{P}$ Phosphorus nuclear magnetic resonance (NMR) was conducted on a set of filtrates sampled from the hydroxyapatite assay after the 14 days of incubation. The liquid sample from the assay was filtered through a 0.2 $\mu\text{m}$  polytetrafluoroethylene (PTFE) filter (Millex-FG SLFG025LS). The filtrate was suspended in  $\text{DMSO-d}_6$ ; 90 $\mu\text{L}$  of filtrate was added to 500 $\mu\text{L}$  of  $\text{DMSO-d}_6$ . Using phosphoric acid (85% in  $\text{DMSO-d}_6$ ) as a reference, NMR was conducted using a 400 MHz Bruker Avance III HD NMR spectrometer.

### **Excitation Emission Matrix Spectroscopy**

The filtrate/wash isolated from the wet-ozonized biochar was analyzed with excitation emission matrix spectroscopy (EEMS) using a Thermo Scientific Lumina Fluorescence Spectrometer. The wash of the non-ozonized control biochar was also analyzed. The samples were analyzed with Luminous Software 3D Scan: the EEMS contour map was obtained by pairing an Excitation with an Emission wavelength.

### Calcium Adsorption Assay

The capacity of ozonized biochar (P400 90D) and control (P400 UN) samples in adsorbing calcium was measured. For each sample, 0.050 g of biochar was incubated with 30.0 mL of calcium ( $\text{Ca}^{2+}$ ) at 6 mg/L (0.150 mM  $\text{Ca}^{2+}$ ) prepared from calcium chloride dihydrate (Sigma C7902). The incubation was done in 50-mL polypropylene tubes. As a control, to determine the amount of calcium originally present in the biochar, the biochars were also incubated with pure water (Milli-Q). Every sample was prepared in triplicate. In order to limit the precipitation of calcium due to high pH, and to ensure that the pH is above the pKa of the carboxylic acid functional groups of the biochar (~4.5), every sample was adjusted to a pH of  $6.0 \pm 0.5$  using 1.0 M of HCl and NaOH. After the 72 hours of incubation, the pH was re-measured and readjusted pH  $6.0 \pm 0.5$  if needed. The liquid samples were then centrifuged at 4500 RPM for 15 minutes using the Avanti J-26 XP centrifuge with a bucket swing rotor (JS 5.3). 2 mL of the supernatant of each sample was collected for calcium measurement using the Shimadzu Flame Atomic Absorbance Spectrophotometer ASC-7000.

The concentration of calcium and/or possible interfering ions detected in the control samples (biochar + 30 mL Milli-Q) was subtracted from the concentration measured in test samples (biochar + 30 mL of 6 mg/L  $\text{Ca}^{2+}$ ). The amount of calcium (mg) removed per g of biochar (g) was then calculated in the same way as of Arami-Niya et al., (2012)<sup>62</sup> using the following equation:

$$Q_e = [(C_o - C_e)V]/W \quad (2)$$

where  $Q_e$  is the amount of calcium (mg) removed at equilibrium per every gram of biochar,  $C_o$  is the initial concentration of calcium in the mixture (here 6 mg/L),  $C_e$  is the calcium concentration at equilibrium (expressed in mg/L), after 72 hours of incubation,  $V$  is the volume

of the mixture (here 0.030 L) and W is the weight of biochar (here 0.050 g). The percent removal of calcium was also calculated with the following equation:

$$\% \text{ removed} = ((C_o - C_e) / C_o) \times 100 \quad (3)$$

## RESULTS AND DISCUSSION

### Phosphate of hydroxyapatite assay

In the incubation assays of hydroxyapatite, we observed significant differences among the different biochar treatments. Among the different experimental setups, the use of wet-ozonized biochar and its filtrate resulted in a maximum solubilized phosphate concentration of  $569.9 \text{ mg/L} \pm 6.4$  after 2 days of incubation with hydroxyapatite which is more than 80 times greater than the phosphate solubilization from the water control ( $7.17 \text{ mg/L} \pm 0.26$ ) as shown in Figure 2 and Table 2. The use of dry-ozonized biochar plus its filtrate also showed an increase in hydroxyapatite solubilization activity and resulted in a solubilized phosphate concentration of  $165.9 \text{ mg/L} \pm 16.9$  (Figure 2 and Table 2).

Upon the removal of the biochar filtrate, that is when the clean (washed) biochar was incubated with hydroxyapatite and water, we also observed a significant solubilization of phosphate. The dry-ozonized biochar was able to solubilize about 8 times more phosphate from hydroxyapatite compared to the non-ozonized biochar: for example, after 2 days of incubation the dry-ozonized biochar solubilized  $78.31 \text{ mg/L} \pm 2.25$  and the non-ozonized control biochar solubilized  $10.90 \text{ mg/L} \pm 2.77$  (Table 2). Note that the dry ozonized biochar and its filtrate solubilized twice as much phosphate compared to that of clean (washed) dry-ozonized biochar alone (when the liquid from washing the dry-ozonized biochar was removed and replaced with pure water) as seen in Table 2.

Similarly, after 2 days of incubation, the wet-ozonized biochar (washed) was able to solubilize 10 times more phosphate ( $103.0 \text{ mg/L} \pm 4.2$ ) than the washed non-ozonized control biochar ( $10.90 \text{ mg/L} \pm 2.77$ , Table 2). Interestingly, the non-ozonized biochar on the other hand was far less potent in solubilizing phosphate upon addition of its wash filtrate and resulted in a solubilized phosphate concentration of only  $0.14 \text{ mg/L} \pm 0.25$  after 2 days of incubation, which was even lower than that of the water and hydroxyapatite control  $7.17 \text{ mg/L} \pm 0.26$  (Table 2).

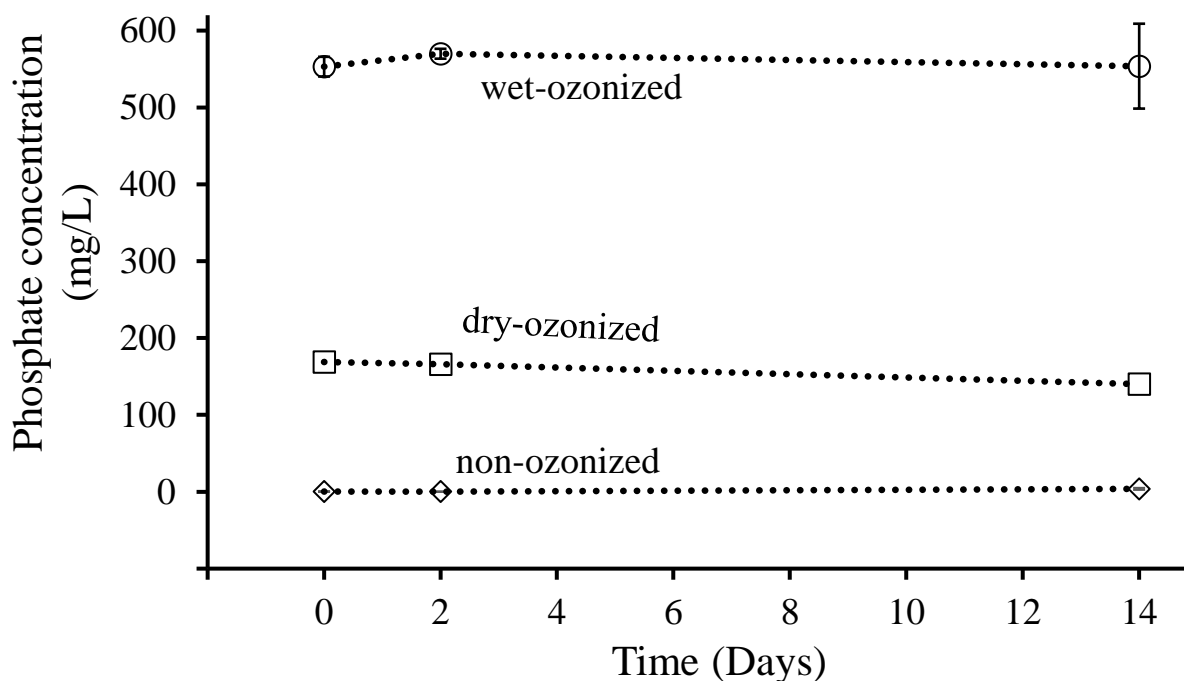


**Figure 2:** Solubilized phosphate concentration as monitored in the incubation liquid of hydroxyapatite with wet-ozonized biochar and its filtrate, dry-ozonized biochar and its filtrate, or non-ozonized biochar and its filtrate (control). The graph shows the data after incubating for 30 min (represented as day 0), 2 days and 14 days. The set-up of the treatments is shown in 5<sup>th</sup> row of Table 1. The concentrations of solubilized phosphate from hydroxyapatite presented here are the corrected concentration values (the phosphates that came from the biochar and its filtrate was subtracted; therefore, the values shown are solely from the hydroxyapatite). The values shown are means  $\pm$  SD (n=3).

**Table 2: Experimental data on the concentration of phosphate and calcium from the hydroxyapatite and pH measurements for the hydroxyapatite assay. The data is shown for 30min, 2 days and 14 days of incubation. Set-up shown in rows 2, 4 and 5 of Table 1. The data shown here are the corrected data and were obtained by subtracting the phosphate and calcium that resulted from biochar and/or its filtrate from the total phosphate and calcium upon addition of hydroxyapatite. Each measurement is the average of 3 replicates  $\pm$  SD (n=3).**

	Phosphate concentration from Hydroxyapatite		
	30 min	2 days	14 days
	Concentration (mg/L)	Concentration (mg/L)	Concentration (mg/L)
P400 UN + water + HA	7.21 $\pm$ 0.51	10.90 $\pm$ 2.77	9.61 $\pm$ 0.61
P400 90W + water + HA	73.73 $\pm$ 5.14	103.0 $\pm$ 4.2	89.73 $\pm$ 11.46
P400 90D + water + HA	59.04 $\pm$ 2.00	78.31 $\pm$ 2.25	80.52 $\pm$ 2.09
Water + HA (no biochar control)	4.68 $\pm$ 0.31	7.18 $\pm$ 0.26	6.90 $\pm$ 1.96
P400 UN + P400 UN-F + HA	0.29 $\pm$ 0.26	0.14 $\pm$ 0.25	3.77 $\pm$ 1.34
P400 90W + P400 90W-F + HA	553.1 $\pm$ 12.8	569.9 $\pm$ 6.4	553.7 $\pm$ 55.2
P400 90D + P400 90D-F + HA	168.8 $\pm$ 10.8	165.9 $\pm$ 16.9	140.0 $\pm$ 39.2
P400 UN-F + HA	3.70 $\pm$ 0.92	0.60 $\pm$ 1.04	6.19 $\pm$ 0.57
P400 90W-F + HA	524.0 $\pm$ 7.0	529.9 $\pm$ 5.2	466.2 $\pm$ 58.3
P400 90D-F + HA	135.8 $\pm$ 2.7	101.2 $\pm$ 22.6	78.49 $\pm$ 44.08

Table 2 Continued

	<b>Calcium concentration from Hydroxyapatite</b>		
	30 min	2 days	14 days
	Concentration (mg/L)	Concentration (mg/L)	Concentration (mg/L)
P400 UN + water + HA	1.92 ± 0.37	1.59 ± 1.78	0.72 ± 0.90
P400 90W + water + HA	14.39 ± 0.35	20.27 ± 0.78	12.64 ± 3.39
P400 90D + water + HA	9.70 ± 1.12	8.51 ± 1.05	10.97 ± 0.43
Water + HA (no biochar control)	2.92 ± 0.97	1.20 ± 1.09	3.15 ± 0.65
P400 UN + P400 UN-F + HA	0	0.45 ± 0.78	0.34 ± 0.14
P400 90W + P400 90W-F + HA	58.84 ± 5.26	66.02 ± 4.16	33.50 ± 7.10
P400 90D + P400 90D-F + HA	0	8.45 ± 4.82	6.28 ± 8.00
P400 UN-F + HA	0	0	1.053 ± 0.188
P400 90W-F + HA	59.63 ± 7.22	91.80 ± 6.02	51.66 ± 3.50
P400 90D-F + HA	53.71 ± 1.53	15.00 ± 2.93	6.80 ± 8.11
	<b>pH</b>		
	30 min	2 days	14 days
	pH	pH	pH
P400 UN + water + HA	5.91 ± 0.06	5.64 ± 0.13	6.67 ± 0.05
P400 90W + water + HA	5.04 ± 0.01	3.96 ± 0.01	5.71 ± 0.04
P400 90D + water + HA	5.05 ± 0.21	4.19 ± 0.01	5.90 ± 0.00
Water + HA (no biochar control)	5.88 ± 0.08	4.77 ± 0.03	6.68 ± 0.03

**Table 2 Continued**

P400 UN + P400 UN-F + HA	$5.98 \pm 0.02$	$5.81 \pm 0.01$	$6.79 \pm 0.05$
P400 90W + P400 90W-F + HA	$3.97 \pm 0.00$	$4.28 \pm 0.00$	$5.72 \pm 0.01$
P400 90D + P400 90D-F + HA	$4.63 \pm 0.03$	$4.83 \pm 0.01$	$6.17 \pm 0.01$
P400 UN-F + HA	$6.48 \pm 0.08$	$6.33 \pm 0.03$	$6.90 \pm 0.02$
P400 90W-F + HA	$3.98 \pm 0.01$	$4.27 \pm 0.01$	$6.15 \pm 0.09$
P400 90D-F + HA	$4.68 \pm 0.02$	$4.98 \pm 0.01$	$6.36 \pm 0.03$

The potency of ozonized biochar filtrate liquid in helping phosphorus solubilization from the insoluble phosphate rock material was demonstrated also by incubation of hydroxyapatite with the filtrates without the solid biochar material. As shown in Table 2, when hydroxyapatite was incubated with the filtrates without the biochars, on day 2 it resulted in the solubilized phosphate concentrations of  $529.9 \text{ mg/L} \pm 5.2$  and  $101.2 \text{ mg/L} \pm 22.6$  for the hydroxyapatite incubation treatments with the filtrates from the wet-ozonized biochar and dry-ozonized biochar, respectively. The filtrate from non-ozonized biochar on the other hand solubilized very negligible amount of phosphate on day 2 ( $0.60 \text{ mg/L} \pm 1.03$ ). These results suggest that the filtrates isolated from the ozonized biochars are sufficient in solubilizing phosphorus from hydroxyapatite.

We also analyzed the liquid samples resulting from the incubation of hydroxyapatite with biochar and its filtrate by  $^{31}\text{P}$ Phosphorus nuclear magnetic resonance (NMR). The goal was to see the nature of the solubilized phosphorus in the mixture and compare the amount of solubilized

phosphate among the different samples. The NMR results showed a peak for the mono-protonated phosphate ( $\text{HPO}_4^{2-}$ ) that is the dominant form of phosphate in the mixtures. In addition, the NMR results also showed a relatively stronger signal for the liquid sample isolated from incubation of the hydroxyapatite and the wet-ozonized biochar and its filtrate compared to the mixture of hydroxyapatite and the non-ozonized (control) biochar and its filtrate (Figure 3). This finding is well consistent with the results from the ion chromatography measurements.

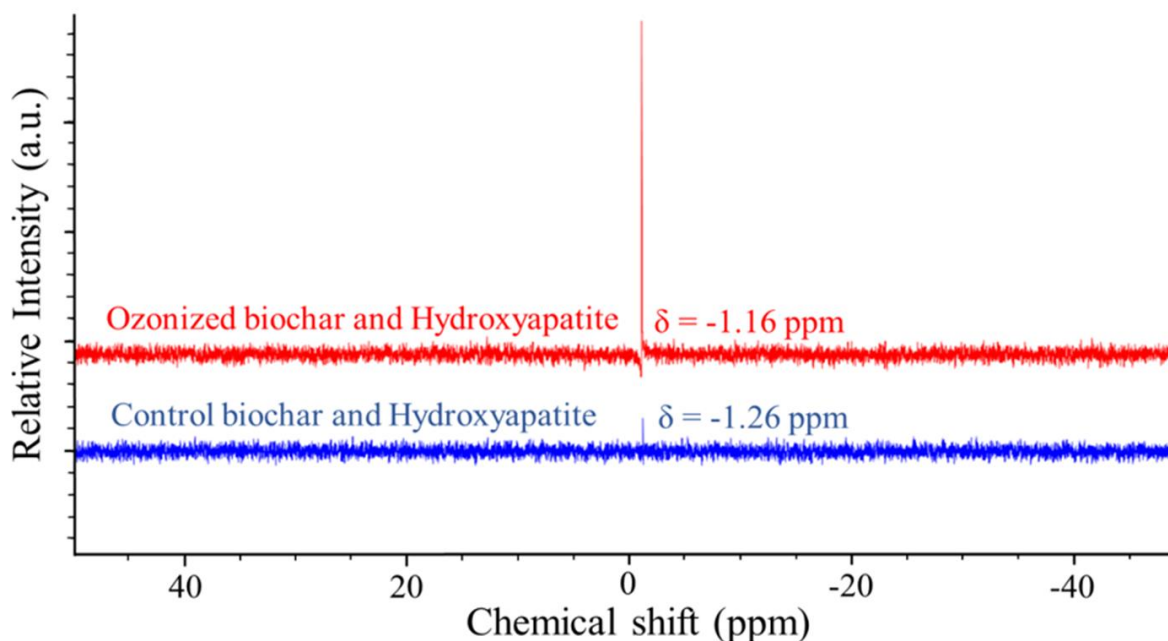


**Figure 3:**  $^{31}\text{P}$  Phosphorus NMR of the filtrate from samples of the hydroxyapatite assay. The signals shown are from the ozonized biochar and hydroxyapatite (-1.16 ppm) and the control biochar and hydroxyapatite (-1.26 ppm).

### Calcium of hydroxyapatite assay

The measurement of calcium solubilized from hydroxyapatite through incubation with control (non-ozonized) biochar and water showed only very little solubilization ( $1.59 \text{ mg Ca}^{2+}/\text{L} \pm 1.78$ ), as expected (Table 2). Similarly, very little calcium solubilization was observed for the water control (incubation of hydroxyapatite with water only):  $1.20 \text{ mg Ca}^{2+}/\text{L} \pm 1.09$ . On the other hand, the 2-day liquid incubation of hydroxyapatite with the wet ozonized biochar and the dry ozonized biochar resulted in a significant increase (8 to 10 times more than the non-ozonized biochar) in solubilized calcium concentration in the incubation liquid:  $20.27 \text{ mg Ca}^{2+}/\text{L} \pm 0.78$  and  $8.51 \text{ mg Ca}^{2+}/\text{L} \pm 1.05$ , respectively (Table 2). These results further support the claim that the ozonized biochar may enable solubilization of more calcium from hydroxyapatite than the non-ozonized biochar.

We hypothesized that the calcium solubilized from the hydroxyapatite was stabilized by the oxygen-functional groups on the surface of the biochar. In this experiment, the measurement of the cation exchange capacity (CEC), which is a key property for biochar when used as a soil amendment, showed a significant increase when the biochar was treated with ozone under wet and dry conditions. The CEC increased from  $10.4 \text{ cmol/kg}$  (non-ozonized control biochar) to  $13.2 \text{ cmol/kg}$  (dry-ozonized biochar); the greatest increase was seen for the wet-ozonized biochar with  $14.4 \text{ cmol/kg}$  as shown in Table 3. Here, we demonstrated for the first time that wet-ozone treatment of biochar is an efficient way to increasing its CEC. Previously, in our group we employed dry ozone treatment of biochar. However, ozone treatment of biochar is a highly exothermic reaction<sup>24</sup> and therefore poses a fire hazard risk if large amount of biochar is to be treated with ozone. Wet-ozone treatment on the other hand has very little to no fire hazard risks associated with it as the reaction happens in water. This technique is more desirable for large

scale industrial applications.

The increase in CEC post-ozone-treatment observed here, by a factor of 1.5 also showed the efficiency of ozone treatment in creating more oxygen-functional groups on biochar surface. This understanding is also consistent with the results from our separate study where the analysis of an ozonized biochar by x-ray photoelectron spectroscopy (XPS) showed an increase in oxygen functional groups (for example carboxylic acid groups) by a factor of 2 when compared with the non-ozonized biochar <sup>15</sup>. The oxygen-functional groups following ozonization are now believed to include carboxylic groups as well as some phenolic groups <sup>15, 61</sup>.

**Table 3: Cation Exchange Capacity and pH of the biochars and their respective filtrate. The CEC was measured for all types of biochar and the recorded values are the averages for the 6 replicates done for each biochar type  $\pm$  SD (n=6). The wet-ozonized biochar had the highest CEC ( $14.4 \pm 1.5$  cmol/kg). The pH was measured in duplicate for all types of biochar  $\pm$  SD (n=2). The pH results revealed that the wet-ozonized biochar was the most acidic ( $3.60 \pm 0.01$ ). The pH of the biochar filtrates was also measured in duplicate  $\pm$  SD (n=2).**

	Non-ozone treated biochar	Wet-ozone treated biochar	Dry-ozone treated biochar
Cation Exchange Capacity (cmol/kg)	10.4 ( $\pm 1.2$ )	14.4 ( $\pm 1.5$ )	13.2 ( $\pm 0.9$ )
pH of the biochar	5.64 ( $\pm 0.02$ )	3.60 ( $\pm 0.01$ )	3.96 ( $\pm 0.01$ )
pH of the filtrate from the biochar	6.49 ( $\pm 0.05$ )	2.53 ( $\pm 0.01$ )	3.00 ( $\pm 0.04$ )

In addition to CEC measurement, the pH of the biochars were also measured to better understand their properties and mode of action. A pH of  $5.64 \pm 0.02$  was measured for the non-ozonized control biochar (Table 3). Data showed a more acidic pH of  $3.60 \pm 0.01$  and  $3.96 \pm 0.01$  for the wet-ozonized and dry-ozonized biochars, respectively. This pH observation also supports the understanding that biochar ozonization can enrich the formation of oxygen-functional groups such as carboxylic acid groups on biochar surface (Biochar-COOH)<sup>15, 61</sup>. This may explain why the ozonized biochars with their low pH due to the oxygen functional groups on their surface are able to achieve a greater solubilization of hydroxyapatite.

We investigated whether the addition of the biochar filtrates would influence the solubilization of calcium from hydroxyapatite. As shown in Table 2, upon the addition of the filtrates from the ozonized biochars, the calcium solubilization was significantly increased for the ozonized biochars samples. The wet-ozonized biochar and its filtrate reached its peak calcium solubilization on day 2 ( $66.02 \text{ mg Ca}^{2+}/\text{L} \pm 4.16$ ) (Figure 4, Table 2); that is three times more solubilized calcium compared to the incubation of wet-ozonized biochar (washed) with hydroxyapatite (Table 2). Note that the calcium concentration dropped on day 14 to  $33.50 \text{ mg Ca}^{2+}/\text{L} \pm 7.10$ ; we suspected that some calcium was being adsorbed on the biochar, thus causing a reduction in the solubilized calcium in the liquid medium. The dry-ozonized biochar and its filtrate solubilized much less calcium from the hydroxyapatite (HA) compared to the wet ozonized biochar and its filtrate. On day 2, the dry-ozonized biochar and its filtrate only solubilized  $8.452 \text{ mg Ca}^{2+}/\text{L} \pm 4.819$  (Figure 4, Table 2). The non-ozonized biochar and its filtrate on the other hand did not solubilize any  $\text{Ca}^{2+}$  on day 0, and solubilized negligible amounts on day 2 ( $0.448 \text{ mg Ca}^{2+}/\text{L}$ ) and 14 ( $0.339 \text{ mg Ca}^{2+}/\text{L}$ ) as shown in Table 2 and Figure 4. Note that the liquid from the wash of the non-ozonized biochar had a pH of  $6.49 \pm 0.05$  which

is much less acidic compared to the filtrates of the ozonized samples (Table 3), the higher pH of the non-ozonized biochar filtrate may reduce the solubilization of calcium from hydroxyapatite.

The removal of biochar and the incubation of hydroxyapatite with the filtrates only, also resulted in large amount of solubilized calcium (Table 2). In fact, the measured soluble calcium in the incubation of HA with the ozonized biochar filtrates only, was greater than when the ozonized biochar was present. For example, the wet-ozonized biochar and its filtrate solubilized

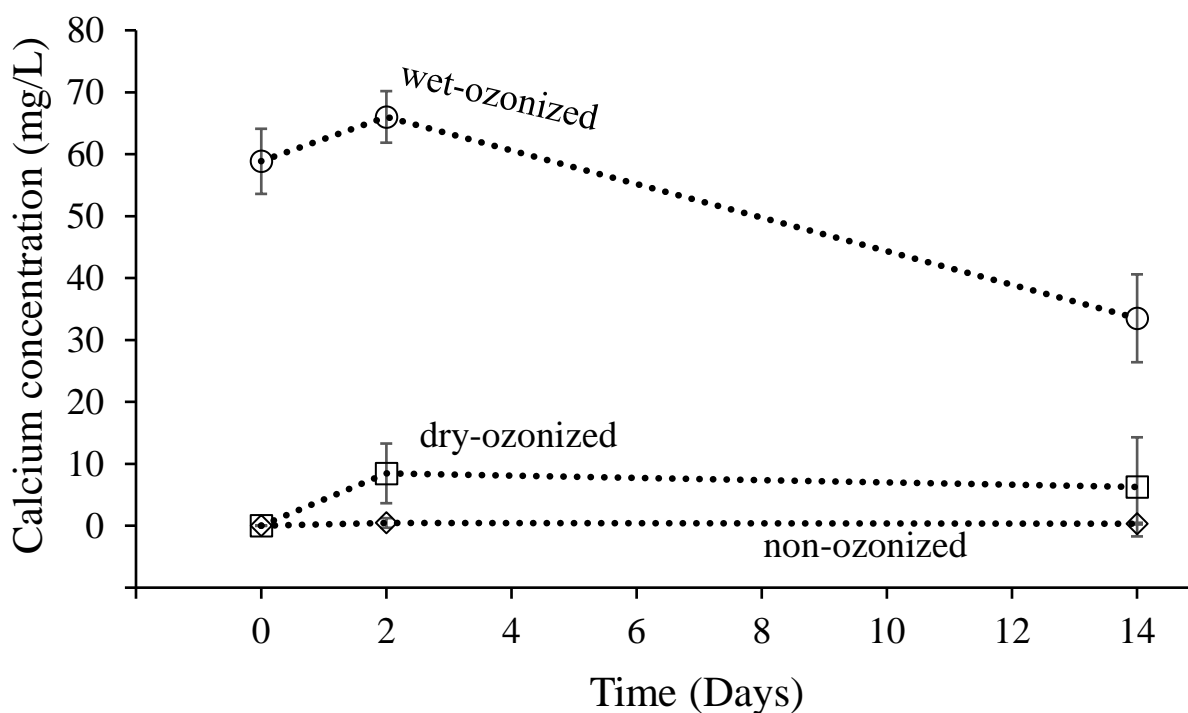


**Figure 4:** Solubilized calcium concentration measured in the incubation liquid of hydroxyapatite with wet-ozonized, dry-ozonized, or non-ozonized biochar including each of their filtrates after incubating for 30 min (represented as day 0), 2 days and 14 days. The concentrations of solubilized calcium from hydroxyapatite presented here are the corrected concentration values (the calcium that came from the biochars were subtracted, therefore the values shown are solely from the hydroxyapatite.) The values shown are means  $\pm$  SD (n=3).

66.02 mg Ca<sup>2+</sup>/L ± 4.16 on day 2, whereas the filtrate only from the wet ozonized biochar solubilized 91.80 mg Ca<sup>2+</sup>/L ± 6.02 on day 2 (Table 2). These results suggest that the ozonized biochar-derived organic matters that can be measured as dissolved organic carbons (DOC)<sup>15</sup> from the filtrate of the wet ozonized biochar appear to be more potent in solubilizing calcium than the wet-ozonized biochar solid material itself. The lower concentration of calcium in the incubation with the wet-ozonized biochar may be partly due to the adsorption of the calcium on the ozonized biochar surface.

Interestingly, we also noticed that even in the absence of biochar, the Ca<sup>2+</sup> concentration in the incubation of HA with the wet-ozonized biochar filtrate only, dropped from 91.8 mg/L on day 2 to 51.7 mg/L on day 14 (Table 2). This type of decrease in calcium concentration was observed also for hydroxyapatite incubation treatment with the dry-ozonized biochar whether the filtrate was present or not (Table 2). This drop may be due to the return of calcium to the solid hydroxyapatite, a process also observed by other researchers<sup>63</sup>. Furthermore, other research groups found that hydroxyapatite has high adsorptive properties in removing heavy metals and some radionuclides in liquid solution,<sup>64,65</sup> thus corroborating with the possible mechanism for the return of the calcium to the solid hydroxyapatite. In the phosphorus solubilization from hydroxyapatite, we also observed that the solubilized phosphate concentration dropped somewhat as measured on day 14 (Table 2, Figure 2). The decrease of solubilized phosphate concentration can be attributed to the return of phosphate to the solid hydroxyapatite which already had an excess positive charge due to the return of the calcium as noticed also in a previous study<sup>63</sup>.

### **pH of hydroxyapatite assay**

During the hydroxyapatite solubilization assay, the pH of the incubation liquid was monitored after incubating for 30 min (day 0), 2 days and 14 days as shown in Figure 5 and Table 2. As measured at the first 30 min (day 0) of the solubilization assay, the incubation liquid pH of hydroxyapatite with dry-ozonized biochar including its filtrate was measured to be  $4.68 \pm 0.02$ , which was lower than the pH ( $6.48 \pm 0.08$ ) of the incubation liquid of hydroxyapatite with the non-ozonized control biochar (including its filtrate). Furthermore, a more acidic pH value of  $3.98 \pm 0.01$  was observed in the incubation liquid of hydroxyapatite with the wet-ozonized biochar including its filtrate which appeared to be the most acidic incubation liquid demonstrated in the experiment (Figure 5, Table 2). For all the incubation liquid samples, over time the pH became less acidic; for example, a 1.5 pH unit increase was observed for the wet-ozonized and dry ozonized assays from 0 to 14 days (Figure 5, Table 2), probably indicating the progression and equilibration of the hydroxyapatite solubilization processes. Overall, the incubation liquid of hydroxyapatite with wet-ozonized biochar (including its filtrate) had the most acidic pH over the entire 14-day experiment (Table 2, Figure 5) and resulted in the highest concentration of solubilized phosphate from hydroxyapatite (Table 2 and Figure 2). This result indicated that the protonic effect from the ozonized biochar material very likely played a significant role in helping solubilize phosphorus from the insoluble calcium phosphate material hydroxyapatite.

In the incubation of hydroxyapatite with clean biochars, there was a slight increase in pH from 30 min to 2 days and from 2 days to 14 days (Table 2) but not as much as when the biochar filtrates were present. The increase in pH can be due to a combination of factors: release of  $\text{CO}_2$  from the liquid into the air, the release of certain residual ash components from the biochar, and the consumption of protons in the hydroxyapatite solubilization reaction process.

In the presence of ozonized biochar filtrates without the biochars, there was also a 1.5 pH unit increase in the incubation liquid with hydroxyapatite from 2 days to 14 days (Table 2). Since the consumption of protons in solubilizing hydroxyapatite is probably a significant factor responsible for the increase in pH, this also suggests that ozonized biochar filtrate alone is also sufficient to enhance the solubilization reaction of hydroxyapatite.

### Mechanisms of phosphorus solubilization from hydroxyapatite revealed by the Ca to P molar ratio

In the hydroxyapatite  $\text{Ca}_5(\text{PO}_4)_3(\text{OH})$  solid material, the molar ratio of calcium (Ca) to phosphorus (P) is 1.67:1. During the hydroxyapatite solubilization assay, we also

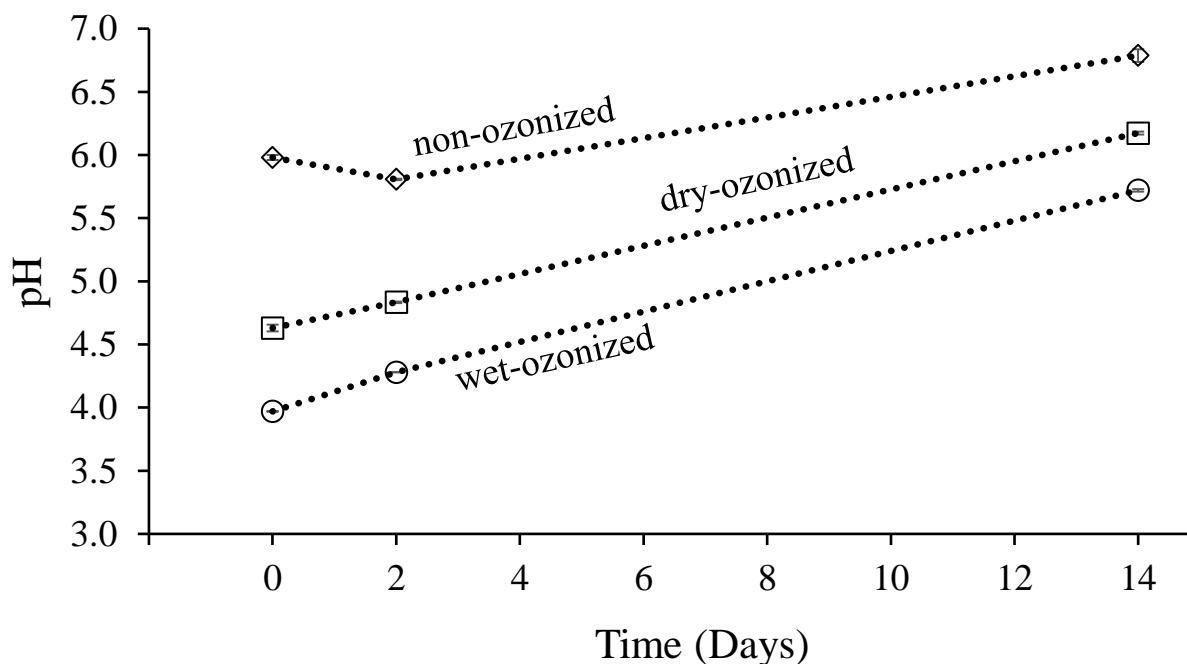


**Figure 5:** pH measured in the incubation liquid of hydroxyapatite with wet-ozonized, dry-ozonized, or non-ozonized biochar including each of their filtrates after incubating for 30 min (represented as day 0), 2 days and 14 days. The values shown are means  $\pm$  SD (n=3).

determined the experimental molar ratio of calcium to phosphorus (Ca / P) in the incubation liquid solution (Table 4). The mass concentrations of calcium and phosphorus were converted to molarity in calculating the molar Ca/P ratios.

The calcium and phosphorus solubilized in the liquid medium from the mixture of hydroxyapatite with water showed the highest molar Ca:P ratio (1.084:1), which was somewhat close to the theoretical molar ratio of 1.67:1 for hydroxyapatite. The calcium and phosphorus solubilized from the mixture of the hydroxyapatite with the non-ozonized biochar filtrate had molar Ca:P ratio of 0.403:1. When incubated with the non-ozonized biochar and its filtrate, the molar Ca:P ratio decreased to 0.213:1. In the presence of non-ozonized biochar only (without its filtrate) in the hydroxyapatite incubation liquid, the molar Ca:P ratio further decreased to 0.177:1. When incubated with dry-ozonized biochar and its filtrate, the molar Ca:P ratio was 0.106:1, which was the lowest observed of all. When incubated with wet-ozonized biochar and its filtrate, the molar Ca:P ratio was 0.143:1, which is much smaller than the molar Ca:P ratio of 1.67:1; it resulted in the highest solubilized P concentration of  $180.6 \text{ mg/L} \pm 18.0$  (Table 4). The observed low molar Ca:P ratio (e.g., 0.143:1) showed that protonic effect may not be the only mechanism here; there may also be a possible effect of calcium cation exchange including the effect of calcium complexation with the deprotonated biochar carboxylate groups on biochar surfaces and/or biochar molecular carboxyl groups such as the ozonized biochar derived organic matters and dissolved organic acids that takes calcium away and thus thermodynamically favors the release of phosphate from the insoluble phosphate materials. In order to verify that mechanism, a calcium removal assay was conducted to determine the adsorptive properties of biochar.

**Table 4: Experimental data on pH, calcium and phosphorus concentrations and the molar Ca/P ratio as measured in the incubation liquid at the end of the 14-day hydroxyapatite (HA) incubation experiment with wet-ozonized, dry-ozonized, and non-ozonized biochar. The data includes each of the biochar type and their filtrates. The data also includes the water + HA only (no biochar) control. Values are the means of triplicates  $\pm$  SD (n=3).**

	pH	Ca (mg/L)	P (mg/L)	Ca:P mol ratio
P400 UN +water + HA	6.67 $\pm$ 0.05	0.72 $\pm$ 0.89	3.13 $\pm$ 0.20	0.177
P400 90W + water + HA	5.71 $\pm$ 0.04	12.64 $\pm$ 3.39	29.26 $\pm$ 3.73	0.334
P400 90D + water + HA	5.90 $\pm$ 0.00	10.97 $\pm$ 0.43	26.26 $\pm$ 0.68	0.323
water + HA (no biochar)	6.68 $\pm$ 0.03	3.15 $\pm$ 0.65	2.25 $\pm$ 0.64	1.084
P400 UN + P400 UN-F + HA	6.79 $\pm$ 0.05	0.34 $\pm$ 0.14	1.23 $\pm$ 0.43	0.213
P400 90W + P400 90W-F + HA	5.72 $\pm$ 0.01	33.50 $\pm$ 7.10	180.6 $\pm$ 18.0	0.143
P400 90D + P400 90D-F + HA	6.17 $\pm$ 0.01	6.28 $\pm$ 8.00	45.70 $\pm$ 12.77	0.106
P400 UN-F + HA	6.90 $\pm$ 0.02	1.05 $\pm$ 0.19	2.02 $\pm$ 0.19	0.403
P400 90W-F + HA	6.15 $\pm$ 0.09	51.66 $\pm$ 3.50	152.0 $\pm$ 19.0	0.263
P400 90D-F + HA	6.36 $\pm$ 0.03	6.80 $\pm$ 8.11	25.60 $\pm$ 14.38	0.205

The calcium adsorption assay showed that the non-ozonized pine 400 and the dry-ozonized pine 400 biochars removed 3.53 mg Ca<sup>2+</sup>/g biochar  $\pm$  0.02 and 3.56 mg Ca<sup>2+</sup>/g biochar  $\pm$  0.01, respectively (Figure 6, Table A1); P400 UN and the P400 90D are indeed able to adsorb calcium. That may be one of the reasons for the observed decrease in calcium concentration at day 14 in the hydroxyapatite assay (Table 2, Figure 4). In addition, the observed calcium

removal supports one of the proposed mechanisms (i.e., calcium complexation with carboxylate group on the surface of biochar) in solubilizing phosphate from hydroxyapatite.

We noticed, the incubation of hydroxyapatite with wet-ozonized biochar filtrate alone also resulted in a very high solubilized P concentration of  $152.0 \text{ mg/L} \pm 19.0$ , and the molar Ca:P ratio was 0.263:1. The wet-ozonized biochar filtrate contains significant amounts of ozonized biochar derived organic matters including dissolved organic carbon materials. In an effort to characterize the molecular compositions of the wet-ozonized biochar filtrates, we analyzed the samples by excitation emission matrix spectroscopy (EEMS). The data here showed that the filtrate from the non-ozonized biochar had one major group of humic-like molecular compounds displaying as high intensity contours (Figure 7).

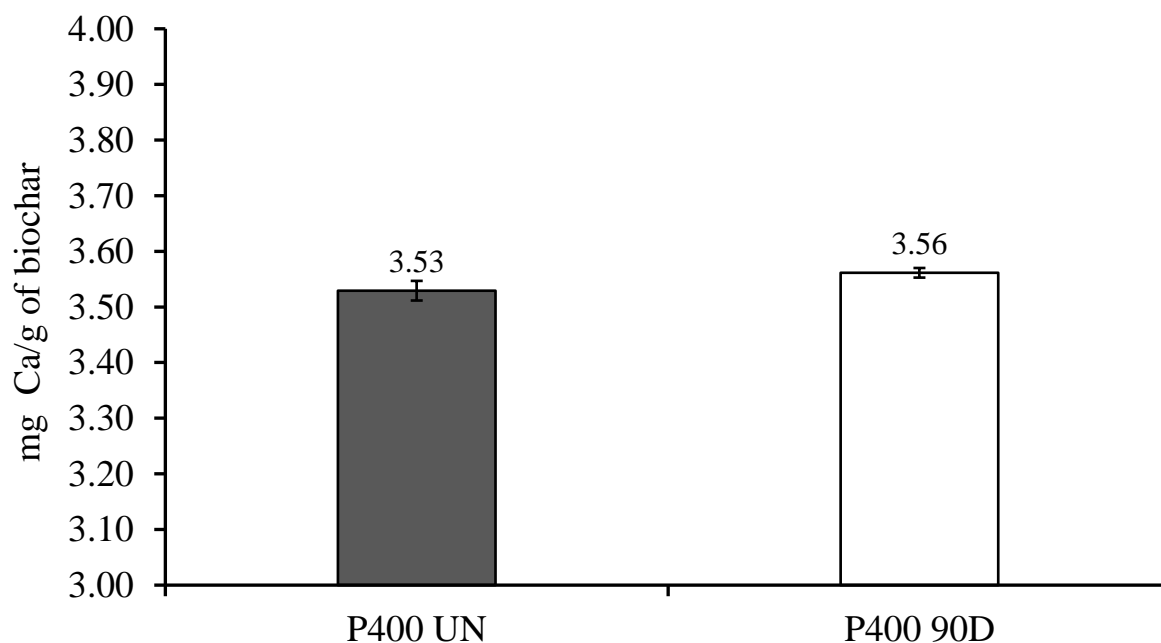


**Figure 6:** Milligram (mg) of calcium removed per gram of biochar; P400 UN for the non-ozonized pine 400 biochar and P400 90D for the dry-ozonized pine 400 biochar. The values shown are means  $\pm$  SD (n=3).

In contrast, the filtrate from the wet-ozonized biochar contained at least 3 additional groups of humic-like molecular compounds generated by ozonization as shown by the contour plots (Figure 7). Even though, the amount of fluorescing DOC molecules may be small compared to the total amount of DOC in the biochar filtrate/wash this finding is very important; it suggests that the process of ozonization of biochar may be used to generate humic-like materials, a desirable carbon material in soil system.

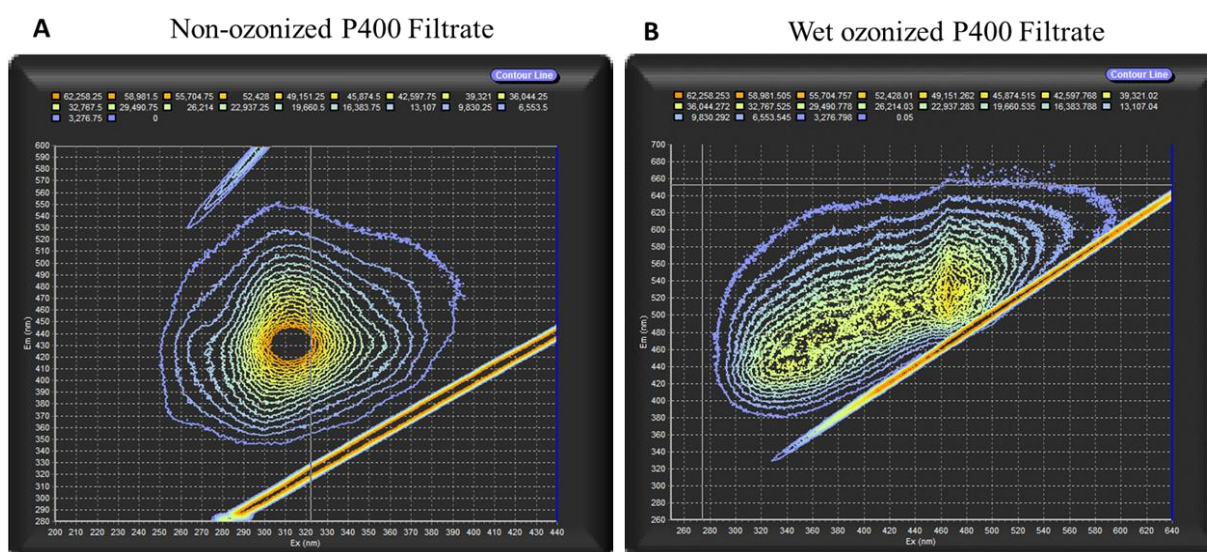


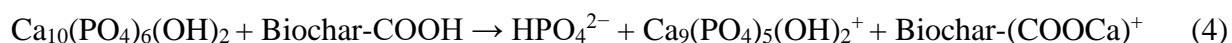
**Figure 7:** Excitation emission matrix spectra of the filtrate from the non-ozonized control biochar (A) and the wet-ozonized biochar (B).

Earlier, in Table 3 we noted that the pH of the filtrate from ozonized biochar is particularly acidic. We know that ozone treatment creates oxygen groups on the surface of biochar such as carboxyl groups (-COOH). Therefore, we also propose that anion exchange

including the effect of anions such as the deprotonated biochar molecular carboxylate groups and its associated dissolved organic acids in exchange with the phosphate (anion) of the insoluble phosphate materials may also thermodynamically favor the solubilization of hydroxyapatite. It is also important to note that excess phosphate in the soil can be undesired. A future study may further investigate the anion exchange properties of ozonized biochar as a possible way in the reverse direction to remove negatively charged molecular species such as phosphate as well.

## CONCLUSION

This experimental study showed that liquid incubation of ozonized biochar with insoluble phosphate materials in the form of solid hydroxyapatite particles,  $\text{Ca}_{10}(\text{PO}_4)_6(\text{OH})_2$ , can significantly increase the solubilization of phosphate into the liquid solution. This indicated that ozonized biochar with enriched oxygen-functional groups such as carboxylic acid groups on biochar surface ( $\text{Biochar-COOH}$ )<sup>15</sup> may be used to help solubilize phosphate from “insoluble” phosphate rock materials such as hydroxyapatite through a phosphorous solubilization reaction such as:



Based on this study, phosphorous solubilization may be accomplished through at least one of the following molecular mechanisms: a) Protonic effect; b) Cation; c) Anion exchange; and d) combinations thereof.

The green chemistry of phosphorus solubilization with ozonized biochar as exemplified in Eq. 4 reported above may have practical implications to develop a new type of P fertilizer without requiring strong industrial acids. In addition, the biochar and its functional groups could serve as

a tool to retain the phosphate and other nutrients in fertilizers from runoffs, thus limiting the need of large application of fertilizers.

## CHAPTER III

### COMPARATIVE STUDY OF BIOCHAR SURFACE OXYGENATION BY OZONIZATION FOR HIGH CATION EXCHANGE CAPACITY

#### PREFACE

Part of the content of this chapter has been published in 2019 in ACS Sustainable Chemistry and Engineering. Full citation of the manuscript is provided below. Reported here, is a modified version of the published work reprinted with permission from publisher. Permission is provided in Appendix F.

Kharel, G.; Sacko, O.; Feng, X.; Morris, J. R.; Phillips, C. L.; Trippe, K.; Kumar, S.; Lee, J. W., Biochar Surface Oxygenation by Ozonization for Super High Cation Exchange Capacity. *ACS Sustainable Chemistry & Engineering* **2019**, 7 (19), 16410-16418.

#### INTRODUCTION

The cation exchange capacity (CEC) is an important property of biochar and soil. Biochars reported in the literature typically have a CEC around 15 cmol/kg<sup>66-68</sup> and a review by Spokas et al (2012) found that about only half of biochars published in literature were shown to increase crop yield<sup>69</sup>. The low yield may partially be due to the low CEC of biochar. Furthermore, a biochar with high CEC also provides the soil with a larger buffering capacity<sup>70</sup>. Therefore, it is very important to develop technologies that can improve the CEC of biochar to make it better as a soil amendment agent<sup>71-74</sup>. The application of biochar with high CEC may

also help reduce the fertilizers runoff by retaining nutrients in the soil. In a previous study using pine wood biochar, we performed an ozonization process and observed an increase in CEC by a factor of 1.5 to 2<sup>33</sup>. While the improvement was significant, those CEC were still in the range of some pristine biochars reported in literature<sup>66-68,75</sup>. Therefore, more optimization is needed to further improve the CEC upon ozonization. In this chapter via the dry-ozonization of rogue biochar, we were able to increase the CEC by a factor of almost 10 with values well over 100 cmol/kg. We believe the CEC is correlated with oxygen functional groups such as carboxylates that can serve as retention and exchange sites for cations in fertilizers. Our preliminary understanding<sup>24</sup> of the ozone treatment mechanisms is showed in the Eq. 5 below.



From this equation, we believe the ozone cleaves the C=C (carbon-carbon double bonds) of olefinic groups exposed on the edge of the carbon crystal lattice. One of the many applications of biochar involves its use as a remediation for heavy metals<sup>76,77</sup>. Via the surface oxygenized biochar by ozonization, we hypothesized that the ozonized biochar would be more efficient at removing heavy metals. In part of this chapter, to understand a little more on the effect of ozone treatment on biochar, a heavy metal removal assay was conducted with ozonized biochar. Further understanding on the process of biochar ozonization is important in order to use it to maximize the cation exchange capacity of the biochar and other properties. Additionally, our previous findings showed that ozone treatment on biochar under dry conditions is an exothermic reaction<sup>24</sup> and can pose a risk if conducted on a larger scale. In this project we also tested the applications and efficiency of biochar ozone treatment under wet conditions, which is a much safer approach.

## MATERIALS AND METHODS

### Heavy metals removal assay with ozonized pine 400 biochar

#### *Source of biochar*

The pine 400 biochar was prepared in a similar fashion as described in chapter two<sup>33</sup>. After grinding and sieving the biochar through 106 $\mu$ m sieve, the biochar was washed with 100mL portions of milli-Q for every 1g of biochar and it was dried in the oven at 105°C.

#### *Dry-ozonized P400 biochar*

In order to see the effect of ozone treatment and its efficiency here, the ozone treatment was done for 30 min, 60 min or 90 min as previously performed by Huff et al (2018)<sup>24</sup>. The amount of biochar used for the ozone treatment was 1.0 g. After ozone treatment, each biochar was then thoroughly washed with 300 mL of milli-Q water and dried in the oven.

#### *Non-ozonized P400 biochar control*

The control non-ozonized pine 400 biochar preparation consisted in washing 1.0 g of non-ozonized biochar with 300 mL of milli-Q water prior to its drying in the oven.

#### *Metal removal assay with Zinc, Copper, Nickel, Magnesium, Lead, and Iron*

Liquid solutions of 2 mg/L of Zn<sup>2+</sup>, 7 mg./L of Cu<sup>2+</sup>, 20 mg/L of Ni<sup>2+</sup>, 1 mg/L of Mg<sup>2+</sup>, 35 mg/L of Pb<sup>2+</sup>, and 15mg/L of Fe<sup>2+</sup> were prepared for the assay. In 50 mL polypropylene tubes, 0.0500g  $\pm$ 0.0010g of biochar was mixed with 30.0 mL of each of the metal solutions. Each tube sampling was done in triplicate. To account for the background and competing ions control assay samples were also prepared: they consisted in the suspension of each type of biochar in 30.0 mL of milli-Q water.

The remaining portion of the metal removal assay followed a similar protocol as done for the calcium removal assay in chapter two<sup>33</sup> with some slight changes. Here, the initial pH was

adjusted to  $5.0 \pm 0.5$  with 0.5M HCl/0.1M NaOH. After shaking at 110 rpm for 24hrs and 48hrs the pH was remeasured and readjusted if needed. After 48hrs, the metal concentration was measured using the Flame Atomic Absorption Spectroscopy.

Note: The metal concentration in the liquid and the mass of biochar were chosen so that each of the metal % removal would not exceed 95%, otherwise if a total metal removal (i.e., 100%) is achieved in the liquid incubation, a comparison cannot be made to assess the effect of each ozone treatment.

### **Effect of ozone treatment on the CEC of pine 300, pine 400, pine 500 and rogue biochar**

The experiment consisted in a comparative study between five different types of biochar: Pine 300 (P300), Pine 400 (P400), Pine 500 (P500), Rogue biochar 1 (RBC 1), and Rogue biochar 2 (RBC 2) as shown in Table 5.

#### *Preparation of Pine 300, Pine 400, and Pine 500 (lab-made)*

The preparation method of the pine biochars (P300, P400 and P500) below is slightly different from that of the pine 400 used previously for the metal removal assay and in chapter two. Here, two changes were applied in the pre-pyrolysis step. The effect of milling of biomass before pyrolysis was shown to reduce the activation energy of the cellulose by disrupting its crystallinity.<sup>78</sup> Therefore to ensure a more complete reaction and transformation of the biomass, here the pine biomass was further chopped into 5 mm diameter pieces. 50 grams of dried and chopped pine was then washed with 300 mL of water before the pyrolysis to remove ashes. Reduction in the content of ash in the biomass, was shown to be effectively done by water washing the biomass prior to pyrolysis<sup>79, 80</sup> Low-ash content biomass results in biochar with high solid density, as well as low ash-content biochar<sup>1</sup>. For the pyrolysis, the parameters of the reactor were similar to that described earlier in chapter two. Except that here, the highest

treatment temperature was 300 °C (for pine 300), 400 °C (for pine 400) and 500 °C (for pine 500). Each biochar type was made in duplicate. The biochar yield of P300 was 40.98 %  $\pm$  1.44, P400 was 28.36 %  $\pm$  0.28 and P500 was 25.10 %  $\pm$  1.30 (Table 5). Here, after the grinding and sieving through 106- $\mu$ m, the washing of the biochar with milli-Q was omitted. The biochar was then dried in the electric oven.

**Table 5: Biochar materials pine 300, pine 400, pine 500 and Rogue biochars (1 and 2) production source and methods.**

	Pine 300 (106 $\mu$ m)	Pine 400 (106 $\mu$ m)	Pine 500 (106 $\mu$ m)	Rogue biochar 1 (106 $\mu$ m)	Rogue biochar 2 (50 $\mu$ m)
Temperature of Production	300 °C	400 °C	500 °C	~700 °C	~700 °C
Method of production	Slow pyrolysis	Slow pyrolysis	Slow pyrolysis	Company's intellectual property	Company's intellectual property
Biochar yield	40.98 % $\pm$ 1.44	28.36 % $\pm$ 0.28	25.10 % $\pm$ 1.30	N/A	N/A
Source of production	In lab	In lab	In lab	Oregon Biochar Solutions	Oregon Biochar Solutions

*Rogue Biochar 1 and Rogue Biochar 2 (from Oregon Biochar Solutions)*

The Rogue biochars 1 and 2 (RBC 1 and RBC 2) were obtained from Oregon Biochar

Solutions. Rogue biochar is characterized as a high surface area biochar<sup>15</sup> made from softwood tree materials such as sugar pine, Douglas fir etc. The exact method of production was not revealed by the company. In short, the biomass was wetted with humid air and was heated to a temperature of 700 °C. Upon reception of the biochar material, it was dried in the Heratherm electric oven at 105 °C for at least 24 hrs. Rogue biochar 1 was received as small chips (~5mm diameter); the biochar was then ground and sieved through 106 µm. Rogue biochar 2 was directly received as powder (50 µm diameter) from the company.

#### *Dry and wet ozone treatment of biochar and filtrate collection*

The biochars were all oven-dried prior to the ozone treatment. Each type of biochar was dry-ozonized or wet-ozonized in a similar fashion as described in chapter two but with a slight change. Here, for the wet-ozone treatment 1.5 g of biochar was mixed with 10 mL of milli-Q prior to the ozone treatment. For each type of biochar, the filtrate collection was done with a first 10 mL wash, a second 25 mL wash and a final 300 mL wash. All filtrates collected were filtered through a 0.2 µm filter and stored at 4 °C for later use. The washed biochar was then placed in the oven at 105 °C for drying. A non-ozonized biochar control was also prepared, and its filtrate washes were collected.

Note: For an isolated study reported in this chapter, the filtrate collection following the dry ozone treatment of the 1.5 g rogue biochar was done with a first wash of 25 mL and a second wash of 300 mL. The 10 mL was omitted. The DOC data these filtrates is presented in Table 9<sup>15</sup>.

#### *pH and CEC measurements of biochar*

The pH was performed in triplicate for each biochar type, in a similar manner as described earlier in chapter two. The CEC was also done as described in chapter two except that

here, the biochars were washed with 4-5 L of milli-Q before the silver nitrate test and, the NaOH used for the final titration was made at a concentration of 0.025 mol/L.

### **Dissolved organic carbon (DOC) measurement**

The dissolved organic carbon (DOC) concentration of the filtrates collected from the rogue biochar 1 was measured using a TOC-Analyzer (Shimadzu TOC-V CPH). The total amount of DOC in mg, extracted from the 1st, 2<sup>nd</sup> and 3rd wash were combined and divided by the mass of biochar sample in order to get the mg of DOC per gram of biochar. Prior to the measurement, in order to exclude the non-dissolved organic materials, the solutions were filtered through a hydrophobic Polytetrafluoroethylene (PTFE) 0.2 µm filter (Millex-FG SLFG025LS). The samples were then diluted at two different concentrations and the DOC was measured.

### **Surface area measurement with BET**

The surface area was measured for the pine 400 and rogue biochar 1 samples before and after ozonization by using the Brunauer–Emmett–Teller (BET) nova 2000e series instrument. The biochar was weighted (about 0.1-0.3 g) and inserted into the sample cell. The biochar was then vacuum degassed for 4 hours at 150 °C. Helium at 10 psi was used for the backfill. The mass of the degassed biochar was then measured. For the analysis portion, the biochar samples were bathed on liquid nitrogen at 77 K and the nitrogen pressure was set to 10 psi. The multi-point BET technique was then used to obtain the surface area of the biochar samples. The surface area was measured for both the ground and sieved biochar samples (RBC UN and RBC 90D) as well as the unground biochar samples (RBC UN and RBC 90D) before and after ozonization. The surface area was also measured for a non-ozonized ground and sieved P400 biochar. The same procedure as done for the RBC UN and RBC 90D was used for measuring the surface area of the P400 except that the backfill was done with the adsorbate (here nitrogen) instead of

helium. The reason for the change in the backfill gas was because the P400 being microporous the method using helium as a backfill resulted in the inability of the nitrogen gas to adsorb and desorb on the surface, thus resulting in no measurable BET surface area. This may be due to possible entrapment of helium in the micropores of the biochar. To circumvent that limitation, nitrogen gas was used as backfill instead of helium.

### **Elemental Analysis**

The ground and sieved non-ozonized control biochar (RBC UN) and the dry-ozonized biochar (RBC 90D) samples had their carbon and oxygen contents measured by Elemental Analysis. It was performed using a FLASH 2000 Organic Elemental Analyzer to determine the oxygen and carbon contents of the biochar samples. In the elemental analysis, the measured mass percentages of oxygen and carbon were converted to molar percentages by dividing the weight percent of each element with its molar mass. The molar O/C ratio was determined by dividing the molar percentages of O with that of C.

## **RESULTS AND DISCUSSION**

### **Adsorption of divalent cations with ozonized pine 400 biochar**

The purpose of this assay was to understand the efficiency of ozonization on biochar by testing its adsorptive properties for divalent cations and certain heavy metals. Our goal was not to remove the maximum amount of metals from the solution but rather to assess the relationship between ozone treatment time and divalent cations adsorption. In the literature, the functional groups presented on biochar surface were shown to adsorb certain heavy metals<sup>81</sup>. Here, we expected to see an increase in metal removal after ozone treatment due to the increased oxygen functional groups on the biochar such as carboxylic groups that would form electrostatic

complexation with the metals. In chapter two, the adsorption of calcium by pine 400 biochar was tested and showed that both the non-ozonized P400 and the dry-ozonized P400 were able to remove some calcium<sup>33</sup>. However, the adsorption achieved in that model was close to 100% for both biochars, therefore the efficiency due to ozone treatment could not be assessed. Here, we assessed the adsorption by the pine 400 biochar before and after ozone treatment on a series of different divalent cations.

In Figure 8, we observed that ozone treatment increased the capacity of biochar to adsorb certain metals. The adsorption assay of copper showed that as the biochar ozone treatment time increased from 0 to 60 minutes, its capacity to adsorb copper also increased; the amounts of copper removed were  $1.17 \text{ mg Cu}^{2+}/\text{g biochar} \pm 0.08$ ,  $1.47 \text{ mg Cu}^{2+}/\text{g biochar} \pm 0.04$ ,  $1.73 \text{ mg Cu}^{2+}/\text{g biochar} \pm 0.08$  for the non-ozonized biochar, the 30 minutes ozonized biochar and the 60 minutes ozonized biochar, respectively. A similar pattern was also observed for nickel and magnesium. Surprisingly, the 90 minutes ozone treatment resulted in a decrease in the adsorption of copper with  $1.17 \text{ mg Cu}^{2+}/\text{g biochar} \pm 0.08$  compared to the 60 minutes ozonized biochar with  $1.73 \text{ mg Cu}^{2+}/\text{g biochar} \pm 0.08$ . That same drop was also observed for the adsorption of the magnesium with the 90 minutes ozonized P400 with  $0.011 \text{ mg Mg}^{2+}/\text{g biochar} \pm 0.005$  compared to the 60 minutes ozonized P400 with  $0.06 \text{ mg Mg}^{2+}/\text{g biochar} \pm 0.01$ . Among the metals tested, the removal of zinc ( $\text{Zn}^{2+}$ ) was the only one that was strongly correlated with the biochar ozone treatment time (from 0 min to 90 min): the mg of  $\text{Zn}^{2+}$  removed for each gram of biochar were  $0.093 \pm 0.02$ ,  $0.162 \pm 0.01$ ,  $0.206 \pm 0.02$  and  $0.243 \pm 0.02$  for the non-ozonized P400, the 30 min ozonized P400, the 60 min ozonized P400 and the 90 min ozonized P400, respectively (Figure 8). This led us to think that the optimum ozone treatment time for removal of magnesium, copper and nickel was 60 minutes. Even though this is contradictory to our expectation of that longer

ozone treatment would increase the adsorption properties of metals, these results are very important in understanding the effect of ozone on biochar properties. It is possible that the 90 minutes ozone treatment time caused the destruction of some of the pores which then resulted in a decreased adsorption of the metals. However, that is unlikely because, if that was true the 90 minutes ozonized biochar would have a lower CEC than the 60 minutes and the 30 minutes ozonized biochar. A previous work in our lab by Huff et al (2018) showed that the non-ozonized P400, the 30-minute ozonized P400, the 60-minute ozonized P400 and the 90-minute ozonized P400 had CEC values of  $15.39 \pm 1.59$  (cmol/kg),  $30.26 \pm 3.23$  (cmol/kg),  $31.03 \pm 2.44$  (cmol/kg) and  $32.69 \pm 2.51$  (cmol/kg), respectively<sup>24</sup>. Another possibility is that the increased ozone treatment time may have further changed the overall physicochemical properties of the biochar, thus making it have a weaker electrostatic interaction with certain metals but not others.

As shown in Figure 8, the non-ozonized P400 removed  $16.1 \text{ mg Pb}^{2+}/\text{g biochar} \pm 1.2$  and after undergoing ozone treatment the adsorption of lead decreased to  $12.8 \text{ mg Pb}^{2+}/\text{g biochar} \pm 0.6$  and  $13.1 \text{ mg Pb}^{2+}/\text{g biochar} \pm 0.5$  for the 30-minute ozonized and 60-minute ozonized biochar, respectively. A similar pattern was also observed for iron  $\text{Fe}^{2+}$  (Figure 8). Unlike the other metals (Cu, Zn, Mg and Ni), ozone treatment for 60 minutes caused a drop in the affinity of lead and iron. Another observation important to note is that the 90-minute ozone treatment resulted in an increase in lead and iron adsorption compared to the 60-minute ozone treatment, which also was the opposite of what was observed for the other metals (Cu, Zn, Mg and Ni). The shift in the affinity for the adsorption for these metals, from 60 minutes to 90 minutes of ozone treatment, led us to believe that instead of having a destruction of pores by prolonged ozone treatment as we initially thought, the biochar may just have gone through a shift in base saturation. For example, the 60 minutes ozone treatment may increase the affinity of biochar for

metals like copper or magnesium and reduce the biochar affinity for metals like lead or iron. A longer ozone treatment to 90 minutes, may have then changed the base saturation level of the biochar to have it favor metals like lead or iron and reduced the affinity for copper and magnesium.

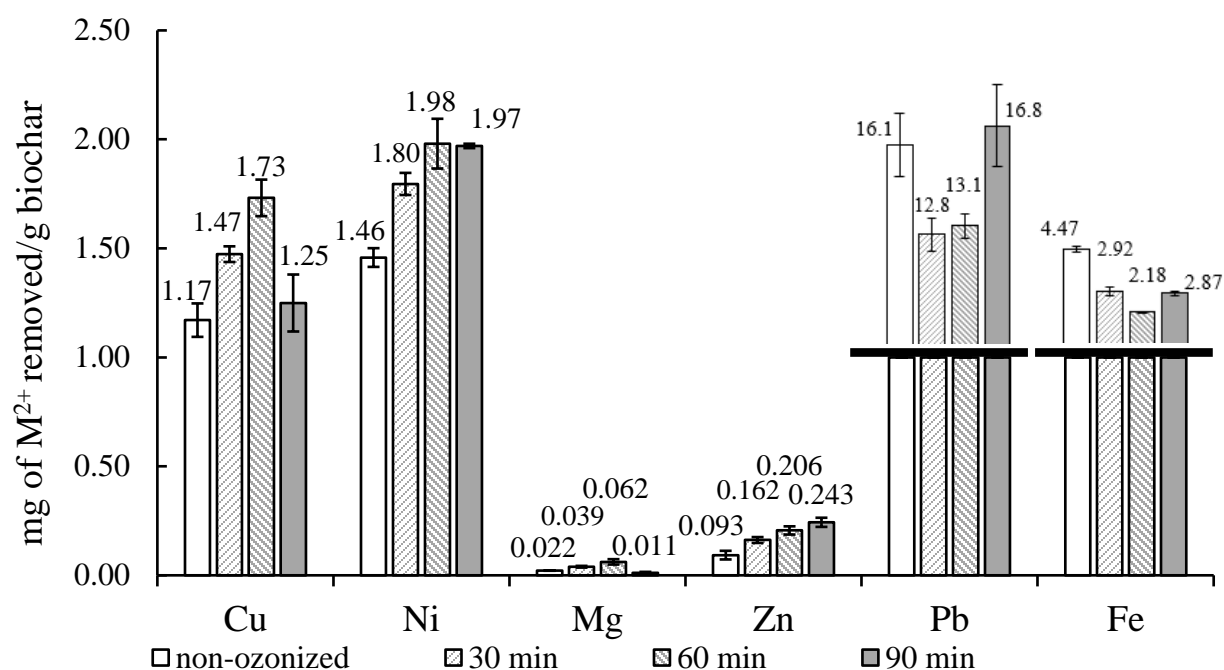


**Figure 8:** Adsorption of  $\text{Cu}^{2+}$ ,  $\text{Ni}^{2+}$ ,  $\text{Mg}^{2+}$ ,  $\text{Zn}^{2+}$ ,  $\text{Pb}^{2+}$  and  $\text{Fe}^{2+}$  from pine 400 non-ozonized biochar control, 30 min dry-ozonized, 60min dry-ozonized and 90min dry-ozonized in mg of Metal ( $\text{M}^{2+}$ ) per gram of biochar. The error bars denote standard deviation for 3 replicates ( $n=3$ ). Note that the  $\text{Pb}^{2+}$  and  $\text{Fe}^{2+}$  were rescaled.

The metal removal data showed that dry-ozone treatment of biochar enhanced the adsorptive properties of P400 biochar in adsorbing certain types but not others. Ozone treatment

of biochar increased the biochar affinity for certain metals, but that may have occurred at the expense of decreasing its affinity for other metals. Only  $Zn^{2+}$  adsorption significantly increased as the ozone treatment time of biochar increased from 0-30min, 30-60min and 60-90min. Among the metals tested here zinc has the second smallest electronegativity constant (1.65) after magnesium (1.31) as shown in Table B1<sup>82</sup>. Therefore, zinc would be less attracted to the negative carboxylate groups on biochar compared to the other heavy metals; the amount of magnesium (mg/g biochar) and zinc (mg/g biochar) adsorbed by the biochar were indeed much smaller than that of the other metals (Figure 8); the overall percentage of magnesium and zinc removed was also smaller than that of the other metals (Figure B1) which is consistent with their lower electronegativity constant. However, that does not explain why the 90-minute ozonized biochar (i.e. more carboxylate  $COO^-$  groups) adsorbed more than the 60 minutes ozonized biochar for the zinc but not the others. Another factor such as the size of the ions may also impact metals adsorption on the surface of the ozonized biochars.  $Zn^{2+}$  is smaller than  $Pb^{2+}$  and  $Fe^{2+}$ , however it is larger than  $Cu^{2+}$ ,  $Mg^{2+}$  and  $Ni^{2+}$  (Table A2)<sup>82</sup>. The adsorption of copper, magnesium and nickel decreased from the 60-minute ozonized biochar to the 90-minute ozonized biochar. The prolonged ozone treatment (i.e., 90-minute ozone treatment) may have led to the obstruction of smaller pores on the surface of biochar, which caused a decrease in the adsorption of metals having an affinity for the functional groups present in those micropores. Therefore, we believe that ozone treatment first reacts with the macropores (30-minute ozone treatment), then the mesopores (60-minute ozone treatment) and finally the microporous (90-minute ozone treatment) structure of biochar. Overall, the 90-minute biochar ozone treatment appeared to be more efficient than the 60-minute and 30-minute biochar ozone treatment as they removed more milligram of the combined  $M^{2+}$  ( $Cu^{2+}$ ,  $Ni^{2+}$ ,  $Mg^{2+}$ ,  $Zn^{2+}$ ,  $Pb^{2+}$  and  $Fe^{2+}$  combined) for every gram

of biochar.

It is also important to note that electrostatic interaction is not the only acting force for the removal of metals with biochar, nor the major one. As reported in literature,  $\pi/M^{2+}$  is also another acting force in the removal of metals, as well as precipitation caused by minerals coming from the biochars (for example  $PO_4^{3-}$ ,  $CO_3^{2-}$  etc.)<sup>76, 77</sup>. Literature also reports ion exchange as another mechanism that could also play a part in heavy metal removal<sup>77</sup>.

In the second part of this chapter, all the biochars were treated with ozone for 90 minutes, to allow a more thorough reaction.

### **Comparative study of the effect of wet and dry ozone treatment on different biochars**

Earlier, we noted that dry-ozone treatment has a fire hazard concern. Dry-ozone treatment of biochar releases lot of heat. In fact, when treating large biochar samples (10g or above) we sometimes observed smoke in the reaction vessel. That raises a major concern in the scalability of the dry ozone treatment of biochar and calls for some engineering designs to reduce the fire risks of such procedures. Furthermore, dry ozone treatment results in loss of material as there is a release of volatile materials during the treatment. Lastly, dry-ozone treatment requires constant mixing of biochar in order to allow reaction of ozone with the surface of the maximum amount of biochar. Due to the abovementioned limitations of dry-ozone treatments we conducted a comparative study between dry-ozone treatment of biochar and wet-ozone treatment, which is a much safer approach and does not require stirring due to the bubbling of ozone gas in the liquid mixture.

In this study, 5 different biochars were used: pine 300, pine 400, pine 500, rogue biochar at 106 $\mu$ m diameter (RBC 1) and rogue biochar at 50 $\mu$ m diameter (RBC 2). Each biochar was ozonized under wet conditions and dry conditions for 90 minutes.

### *pH of Biochars*

The pH measurements of the biochars showed that the temperature of pyrolysis had an impact on the pH of the biochar. The low temperature biochar (pine 300) had the smallest initial pH ( $3.98 \pm 0.03$ ) as seen in Figure 9. The pH increased with the increase in pyrolysis temperature: the pine 400 had a pH of  $4.78 \pm 0.12$  and the pine 500 had a pH of  $7.55 \pm 0.09$  (Figure 9). The rogue biochar which was made industrially at a temperature of 700 °C, had the highest pH of  $7.97 \pm 0.04$  (RBC 1). Rogue biochar 2 had a particle size of 50  $\mu$ m (RBC 2) versus 106  $\mu$ m for RBC 1. The initial pH of RBC 2 was  $8.99 \pm 0.08$  (Figure 9) which is higher than RBC 1. The dry-ozone treatment caused a significant drop in the pH for both rogue biochars; the recorded pH was  $3.08 \pm 0.08$  and  $4.35 \pm 0.06$  for the RBC 1 90D and RBC 2 90D, respectively. Among the pine biochars, dry-ozonization had a greater effect on the pH of pine 500 where it dropped from  $7.55 \pm 0.09$  (P500 UN) to  $5.14 \pm 0.03$  (P500 90D); dry-ozonization had little effect on the pH of pine 300 (Figure 9). Wet-ozonization of pine biochars made them more acidic than dry-ozonization did (Figure 9).

The pH drop observed for the wet and dry ozonized biochars is a first indication of the presence of more oxygen functional groups on those biochars compared to the non-ozonized control. The reason why the difference in pH was not significant between the control rogue biochar and the wet-ozonized rogue biochar may be because of their high initial pH. In liquid medium, higher pH reduces the stability of ozone and decreases its lifetime<sup>83</sup>. Here, with both rogue biochars having an initial pH of 8-9 (Figure 9), the liquid solution consisting of the

mixture of biochar and water for the ozone treatment was basic. That basic solution made the ozone reaction with the biochar less efficient.

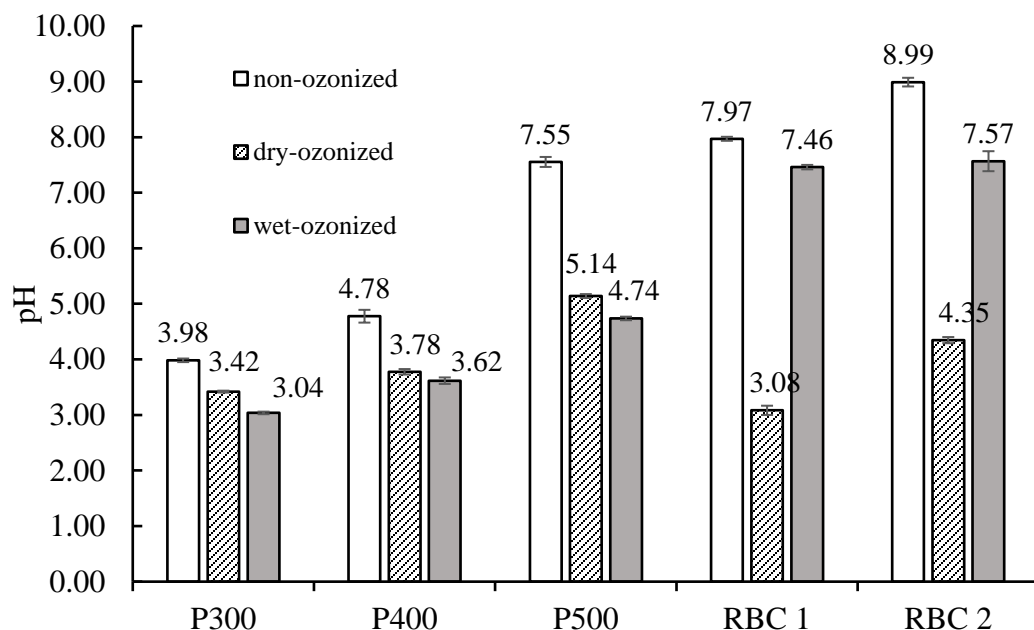


**Figure 9:** pH measurements of the pine 300 (P300), pine 400 (P400), pine 500 (P500), rogue biochar 1 (RBC 1) and RBC 2 (50  $\mu$ m) before ozone treatment and after ozone treatment. The data represent the average of 3 replicates (n=3) with the standard deviation.

### *CEC of Biochars*

The cation exchange capacity (CEC) was measured. We observed that the CEC of the control biochars decreased as the temperature of pyrolysis increased; the P300 non-ozonized biochar (P300 UN) had a CEC of 48.90 cmol/kg  $\pm$  0.98, the P400 UN had a CEC of 32.74 cmol/kg  $\pm$  0.79 and the P500 had a CEC of 17.18 cmol/kg  $\pm$  0.20 (Figure 10). This was expected

because higher pyrolysis temperatures cause the release of more volatile matter and the rearrangement into aromatic sheets which is accompanied by the loss of functional groups <sup>1</sup>. However, compared to our previous CEC values for the P400 non-ozonized biochar, here we observed higher CEC values for the P400 UN; previously we reported CEC values of  $10.4 \text{ cmol/kg} \pm 1.2$  <sup>33</sup> to  $15.39 \text{ cmol/kg} \pm 1.59$  <sup>24</sup> for the non-ozonized P400 biochar. Note that here, the CEC of non-ozonized pine 400 was  $32.74 \text{ cmol/kg} \pm 0.79$  (Figure 10) which is much higher than our previous results; this may be due to the changes (i.e., grinding of pine biomass and water-washing pretreatment for ash removal) performed in the pre-pyrolysis step.

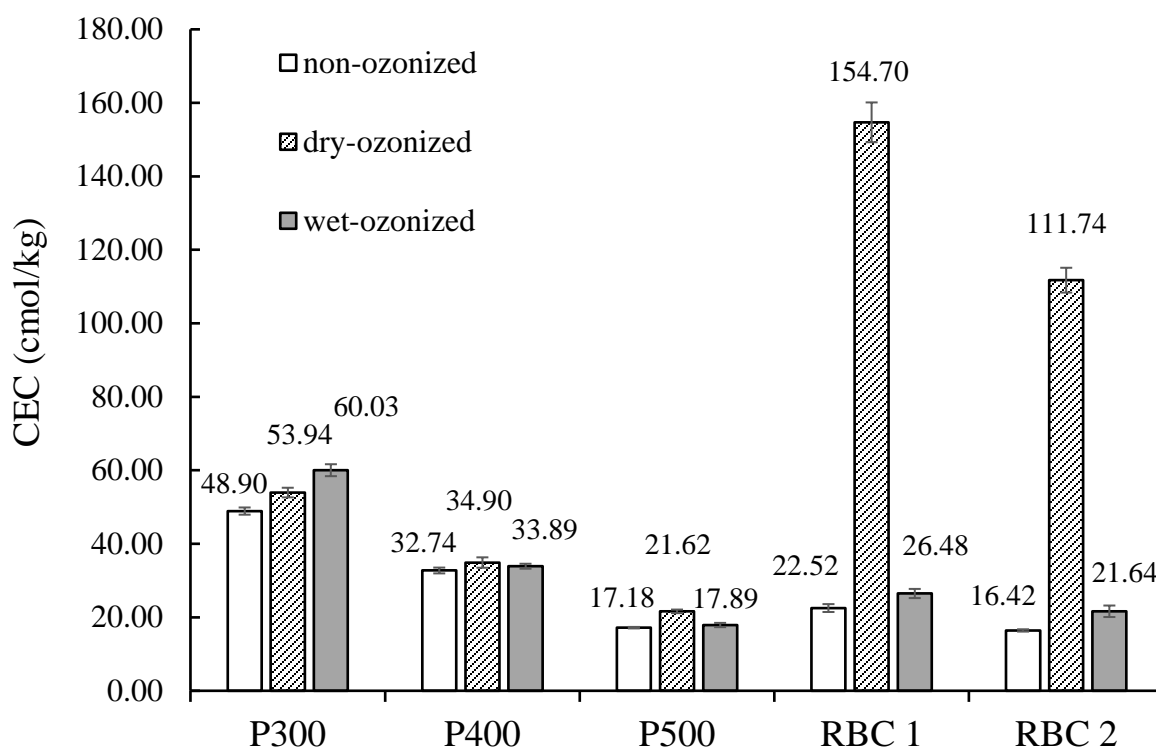


**Figure 10:** CEC measurements of the pine 300, pine 400, pine 500, rogue biochar 1 (106  $\mu\text{m}$ ) and rogue biochar 2 (50  $\mu\text{m}$ ) before ozone treatment and after ozone treatment. The data represent the average of 3 replicates ( $n=3$ ) with the standard deviation.

Contrary to the rogue biochar, the wet-ozone treatment was effective for the pine biochars; pine 300 biochar had the highest CEC after being wet-ozonized ( $60.03 \text{ cmol/kg} \pm 1.63$ ) which may be due to the lower initial pH of pine 300 biochar as discussed earlier. Dry-ozone treatment slightly increased the CEC of pine 500; dry-ozone treatment did not significantly increase the CEC of pine 400 which contradicts our previously reported data where the CEC was increased by a factor of 1.5 to 2<sup>24</sup>. The reason for that low increase in CEC observed upon ozone treatment, may be due to the loss of large quantities of the oxygenated biochar molecular fragments during the extensive wash (4-5 L) performed in the CEC measurement. This, then led us to think that the biochar filtrates collected from the washes may contain a lot of oxygenated biochar molecular fragments in its DOC, an investigation that is discussed in chapter four.

The CEC was measured for the dry-ozonized rogue biochars. The data showed that dry-ozonized RBC 1 biochar had the highest CEC value of  $154.70 \text{ cmol/kg} \pm 5.41$  (Figure 10) which is much higher than most biochars' CEC reported in literature. Here, the non-ozonized RBC 1 had a CEC of  $22.52 \text{ cmol/kg} \pm 1.07$ , which is 7 times smaller than the dry-ozonized RBC 1. The CEC of the non-ozonized RBC 2 was lower ( $16.42 \text{ cmol/kg} \pm 0.31$ ) but showed an increase by a factor of 7 as well upon being dry-ozonized ( $111.74 \text{ cmol/kg} \pm 3.38$ ) (Figure 10). As expected, wet-ozonization showed very slight increase in CEC compared to the non-ozonized controls for both the RBC 1 ( $26.48 \text{ cmol/kg} \pm 1.25$ ) and RBC 2 ( $21.61 \text{ cmol/kg} \pm 1.56$ ) as shown in Figure 10. This was expected because the pH of the wet-ozonized rogue biochars (RBC 1 90W and RBC 2 90W) were not much different from that of the non-ozonized rogue biochar controls (RBC 1 UN and RBC 2 UN) as shown in Figure 9. As mentioned earlier, ozone may have not reacted thoroughly with the biochars in high pH liquid medium due to its instability in basic solutions<sup>83</sup>. The CEC of the dry-ozonized rogue biochar 1 was much higher than that of the dry-

ozonized rogue biochar 2 (Figure 10). The RBC 1 is different from RBC 2 in that its particles' sizes are bigger; 106  $\mu\text{m}$  (for RBC 1) versus 50  $\mu\text{m}$  (for RBC 2). It's possible that the particles of RBC 2 were too fine, therefore leading to destruction of pores during ozone treatment. Given that the ozone treatment was more efficient on RBC 1, the latter will be discussed for the remainder of this study.

Biochar cation exchange capacity (CEC) is important and may help in reducing fertilizer runoff by retaining nutrients or increasing the water holding capacity. In order to further verify the increased CEC of the RBC 1 biochar after ozone treatment, several independent CEC measurements were conducted. CEC measurements were reconducted in lab, independently and the results were consistent (Table 6)<sup>15</sup>. Another independent measurement of CEC even used a different CEC measurement technique; the CEC was measured by  $\text{NH}_4\text{-OAc}$  method by one of our collaborators at a USDA laboratory and also showed an increase by a factor of 7 upon ozone treatment (Table 6). The present experimental study showed that the biochar ozonization can increase the biochar CEC value by a factor of 7-9 to reach CEC values anywhere between 109.02  $\text{cmol/kg} \pm 6.33$  to 152.08  $\text{cmol/kg} \pm 4.06$  (Table 6), one of the highest biochar CEC reported values in literature to the best of our knowledge. This is a significant result since the improvement on biochar CEC value by ozonization is now far much more than that of our previous study<sup>24, 33</sup> where we demonstrated the increase in the CEC value of biochars by a factor of 1.5-2 through ozonization of a pinewood-derived biochar produced by slow pyrolysis at 400  $^\circ\text{C}$  (P400).

In an effort to understand the greater efficiency of ozone treatment on rogue biochar, compared to pine biochars several other analyses were performed. The rogue biochar is known to have a high surface area. In order to further understand the high increase in cation exchange

capacity following ozonization, the surface area was measured on the rogue biochar in comparison with that of the P400 biochar.

**Table 6: pH, CEC, and BET surface area of the ground biochar before and after ozonization. The values are means  $\pm$  SD from duplicates (n=2) of measurements for pH, 6 replicates (n=6) for CEC measured by Ba(OAc)<sub>2</sub>, triplicates (n=3) for the CEC measured by NH<sub>4</sub>-OAc, and 5 replicates (n=5) for the BET surface area measured with N<sub>2</sub> after a backfill with helium.**

<b>Parameters</b>	<b>Non-ozonized Biochar (RBC UN) (means <math>\pm</math> SD)</b>	<b>Dry-ozonized Biochar (RBC 90D) (means <math>\pm</math> SD)</b>
CEC (cmol/kg) measured by Ba(OAc) <sub>2</sub> method * <sup>1</sup>	17.02 $\pm$ 0.63	152.08 $\pm$ 4.06
CEC (cmol/kg) measured by NH <sub>4</sub> -OAc method * <sup>2</sup>	14.57 $\pm$ 1.62	109.02 $\pm$ 6.33
BET Surface area (m <sup>2</sup> /g)	418.3 $\pm$ 17.7	229.2 $\pm$ 6.9

\*<sup>1</sup> was performed in 6 replicates where 3 replicates were from G. Kharel and 3 replicates from O. Sacko; \*<sup>2</sup> CEC independent measurements performed by Claire L. Phillips and Kristin Trippe at USDA.

### **BET surface area measurement of biochar**

The ground and sieved rogue biochar samples before ozone treatment (RBC UN) had a surface area of 418.3 m<sup>2</sup>/g  $\pm$  17.7 as reported in Table 6. Compared to the P400 with a measured surface area of only 2.05 m<sup>2</sup>/g  $\pm$  0.42 as shown in Table 7, the rogue biochar presented a very large surface area; rogue biochar surface area is 200 times greater than P400 (Table 6,7). We

believe that the high surface area of the rogue biochar may make the latter more favorable to interact with ozone molecules. Therefore, a major difference on biochar CEC improvement between our present and previous studies<sup>24</sup> may be attributed to the difference in BET surface area between the P400 and the rogue biochar.

Upon being ozonized, the ground and sieved rogue biochar decreased in surface area to  $229.2 \text{ m}^2/\text{g} \pm 6.9$  as shown in Table 6. Even the surface area measurement that consisted in the use of nitrogen as the backfill showed that the ozonized rogue biochar ( $240.5 \text{ m}^2/\text{g} \pm 6.1$ ) had lower surface area than the non-ozonized ( $389.9 \text{ m}^2/\text{g} \pm 10.3$ ) as shown in Table 7.

**Table 7: BET surface area of the ground pine 400 biochar (non-ozonized) and the ground rogue biochar (before and after ozonization.) Nitrogen was used as backfill following the evacuation procedure. Values are means  $\pm$  SD from triplicates (n=3).**

Biochar sample	BET surface area ( $\text{m}^2/\text{g}$ ) $\pm$ SD
Pine 400 non-ozonized biochar	2.05 ( $\pm 0.42$ )
Rogue biochar non-ozonized	389.9 ( $\pm 10.3$ )
Rogue biochar dry-ozonized	240.5 ( $\pm 6.1$ )

The drop in the measured surface area upon being ozonized may be due to two factors:

- 1) It is possible that the ozone is causing the destruction of the pores of the biochar as suspected earlier.
- 2) It is also possible that such a drop in surface area measurement may be because of the

oxygen-rich functional groups created in the micro/nanometer pores of the ozonized biochar. The method of BET surface area measurement uses non-polar nitrogen gas as the adsorbate. Therefore, these non-polar gases may be inadequate in terms of giving a true surface area when polar oxygen groups are obtruding the pores and/or coating the surface of the biochar<sup>84</sup>.

We also tested the effect of grinding and sieving on biochar. The surface area was measured before and after ozonization from the unground biochar materials. The unground non-ozonized biochar had a BET surface area of  $377.4 \text{ m}^2/\text{g} \pm 22.2$  (Table 8) which is somewhat less than the ground non-ozonized biochar control which had  $418.3 \text{ m}^2/\text{g} \pm 17.7$  (Table 6). This was expected because grinding biochar is a process used to increase its surface area<sup>1</sup>. After ozonization, the measured BET surface area of the unground biochar was  $332.1 \text{ m}^2/\text{g} \pm 17.8$  (Table 8); the unground biochar samples also showed a slight drop in the measured surface area after ozonization. However, with the unground biochar samples, the decrease in the surface area (after ozonization) was not as significant as the decrease in surface area that was observed with the ozonization of the ground biochar samples (Table 6). This may be because the process of ozonization have occurred more thoroughly, over a larger surface on the ground biochar sample compared to the unground biochar sample.

### **Dissolved organic carbon (DOC) measurement of biochar filtrates**

Ozone treatment resulted in a low biochar pH as reported in Figure 9. We think that the process of ozonization caused the breaking of C=C double bonds on the biochar material (Huff et al. 2018)<sup>24</sup>. We believe that bond cleavage creates oxygen groups in the form of -COOH on the biochar; this was verified by XPS analysis conducted by our collaborator; an increase in -COOH groups was observed on rogue biochar after ozonization<sup>15</sup> (data not shown.) Therefore, the other

**Table 8: BET surface area of the unground rogue biochar before and after ozonization. Helium was used as backfill following the evacuation procedure. Values are means  $\pm$  SD from triplicates (n=3).**

Biochar sample	BET surface area (m <sup>2</sup> /g) $\pm$ SD
Rogue biochar non-ozonized	377.4 $\pm$ 22.2
Rogue biochar dry-ozonized	332.1 $\pm$ 17.8

biochar molecular fragments from the ozone cleavage, could be extracted in the biochar filtrate. To further test the efficiency of ozone treatment on our biochar, and to verify the formation of those “Biochar-COOH” fragments, the filtrate of the wash of the biochar was collected before and after ozonization for dissolved organic carbon concentration measurement. The effect of ozonization on the biochar was seen on the color of the filtrate extracted from the biochar. The filtrate from the non-ozonized biochar (RBC UN) appeared clear while the filtrate of the dry-ozonized biochar (RBC 90D) appeared dark brown thus indicating more presence of organic carbon fragments (Figure 11). The total extracted DOC from the dry-ozonized rogue biochar was 10.98 mg DOC/g biochar  $\pm$  1.00 whereas the non-ozonized rogue biochar control only resulted in 2.10 mg DOC/g biochar  $\pm$  0.23 as observed in Table 9. Ozonization leads to a high amount of dissolved organic carbon in its filtrate which is a result of the ozone cleavage of the C=C double bonds. This result demonstrated that biochar ozonization can also produce certain amount of soluble biochar molecular fragments, which may also contain some oxygen groups; thus the

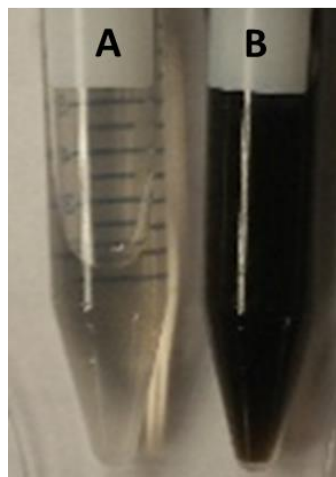


**Figure 11:** Photograph of the filtrate liquid from the non-ozonized control (A) and the dry-ozonized (B) rogue biochar samples.

DOC from these soluble biochar molecular fragments can be used for certain special applications such as to help unlocking phosphorous from insoluble phosphate materials in soils as discussed in chapter one.<sup>33, 85</sup> A more comprehensive study on the use of DOC to solubilize phosphorus from hydroxyapatite material is discussed in chapter four.

**Table 9: DOC material extracted from the non-ozonized control rogue biochar (RBC UN) and the dry-ozonized rogue biochar (RBC 90D). The values are means  $\pm$  SD (n =2).**

Biochar Sample	DOC from biochar (mg DOC/g biochar)
Non-ozonized biochar control RBC UN	2.10 $\pm$ 0.23
Dry-ozonized biochar RBC 90D	10.98 $\pm$ 1.00

## Elemental Analysis

In an attempt to have a characterization of the elemental atomic content of the rogue biochar before and after ozonization, elemental analysis was performed. Prior to ozonization, the biochar had a high content of carbon (87.02 mol % C  $\pm$ 5.68) as reported in Table 10. Following ozonization, the carbon content dropped to 72.23 mol %  $\pm$ 0.91 (Table 10). In addition, following ozonization, there was a significant increase in oxygen content; the non-ozonized control had 6.67 mol %  $\pm$ 1.30 of oxygen whereas the ozonized sample had 13.93 mol %  $\pm$ 1.59 of oxygen (Table 10). The mole percentages of carbon and oxygen were used to calculate the molar O: C. The ozonization process increased the molar O:C ratio by a factor of 2.5; the non-ozonized control had a molar O:C ratio of 0.077 whereas the dry-ozonized sample had a molar O:C ratio of 0.193 (Table 10). Ozone treatment changed the molar percentages of oxygen and carbon in the rogue biochar. In our model we believe that ozonization mostly happened on the surface of the biochar, therefore we didn't expect the bulk properties of the biochar to be affected by ozone treatment. Those results suggested that dry-ozone treatment may have altered the overall oxygen content of the biochar. We then compared the changes in bulk properties before and after ozonization of this high surface area biochar (rogue biochar) with that of a lower surface area biochar. Previously in our lab using P400 biochar, Huff et al. (2018) demonstrated that the bulk properties of the biochar didn't vary as much following ozonization; the carbon content and the oxygen content measured by elemental analysis were quite similar before and after ozonization of P400<sup>24</sup>. Therefore, here we attributed this large change in O:C mol ratio of the rogue biochar to the ozonization of a much greater surface area. As reported earlier, P400 is a low-surface-area biochar with only 2.05 m<sup>2</sup>/g  $\pm$ 0.42 compared to the rogue biochar with 389.9 m<sup>2</sup>/g  $\pm$ 10.3 (Table 7); P400 has a surface area 200 times smaller than that of rogue biochar. Therefore, we believe

that the oxygen groups that are installed on the surface of the rogue biochar (by ozonization) cover a very large area; the combined mass of all the surface-created oxygen groups has then an impact on the biochar total mass.

**Table 10: Elemental analysis (oxygen and carbon) on the non-ozonized and dry-ozonized rogue biochar samples. The values are moles average percentages from 6 replicates  $\pm$  SD. The weight percent of each element was converted to mole percent by using the respective molar mass of each element. The O:C mol ratio was calculated from the averages of moles percentages of O and C.**

	Non-ozonized Biochar (RBC UN)	Dry-ozonized Biochar (RBC 90D)
Oxygen mol % ( $\pm$ SD)	6.67 ( $\pm$ 1.30)	13.93 ( $\pm$ 1.59)
Carbon mol % ( $\pm$ SD)	87.02 ( $\pm$ 5.68)	72.23 ( $\pm$ 0.91)
O:C mol ratio	0.077:1	0.193:1

## CONCLUSION

The metal adsorption assay showed that moderate ozone treatment time (30-60 min) increased the adsorption of most metals tested (copper II, nickel II, magnesium II, and zinc II) but decreased the adsorption of lead II and iron II. The data suggest that biochar ozonization may increase or decrease its affinity for certain metals, depending on the biochar ozone treatment time. We suspect that long ozone treatment time of biochar may obstruct some micropores, thus reducing the affinity of smaller metals.

In this study we have demonstrated that wet-ozone treatment of pine biochars may be used as a safer approach to increase the CEC of the biochars produced at lower temperatures.

Wet-ozone treatment of pine 300 biochar (P300) showed a greater improvement in the CEC compared to wet-ozone treatment of pine 400, pine 500 and rogue biochar. The effect of dry-ozonization was better at improving the CEC of higher temperature biochars. The breakthrough increase in CEC was demonstrated via the dry-ozonization of rogue biochar. The CEC of the non-ozonized control rogue biochar was  $17.02 \text{ cmol/kg} \pm 0.63$  and upon being dry ozonized for 90 minutes, the CEC increased to  $152.08 \text{ cmol/kg} \pm 4.06$  comparable to certain humic substances. Additionally, we observed a drop in the biochar pH after being ozonized. Non-ozonized rogue biochar had a pH  $7.97 \pm 0.04$  and after being ozonized the pH was  $3.08 \pm 0.08$ ; this indicates the formation of oxygen-functional groups mainly in the form of carboxylic acid groups. The elemental analysis data of the rogue biochar showed an increase in O:C molar ratio following ozonization; which is more likely due to the installation of oxygen groups over the large surface area of the rogue biochar.

## CHAPTER IV

### WATER-SOLUBLE OZONIZED BIOCHAR MOLECULES TO UNLOCK PHOSPHORUS FROM INSOLUBLE PHOSPHATE MATERIAL

#### PREFACE

The content of this chapter has not been published. The manuscript was submitted in 2021.

Sacko, O.; Feng, X.; Morris, J. R.; Council-Troche, R.M.; Kumar, S.; Lee, J. W., Water-Soluble Ozonized Biochar Molecules to Unlock Phosphorus from Insoluble Phosphate Material.

Manuscript submitted for publication 2021.

#### INTRODUCTION

The use of biochar as a soil amendment has gained lots of interest. The transformation of biomass into biochar converts the carbon into a more stable form that is not easily degraded <sup>1</sup>, thus making biochar a great candidate for soil amendment purposes. Research efforts were made to maximize the efficiency of biochar as a soil amendment through surface oxygenation methods which in turn would improve the cation exchange capacity of the biochar <sup>1, 15, 18, 86</sup>. Thus, with a higher capacity to retain ions, biochars can better retain fertilizers. In addition, biochars contain some nutrients including their ash components which may comprise certain residual amount of ammonium, nitrate, phosphorus and potassium that may be released over time after application in soils <sup>87, 88</sup>.

It is common that some soils have phosphorus as the limiting element<sup>89,90</sup>. Plants can only take phosphorus in its orthophosphate form ( $\text{HPO}_4^{2-}$ ,  $\text{H}_2\text{PO}_4^-$ )<sup>91</sup>. Certain bacteria are able to solubilize insoluble phosphate and make it available to plants<sup>92</sup>. Some researchers have used a combination of both biochar and bacteria as an inoculant in soil and have showed an increase in soil available phosphorus as well as increased soil carbon content<sup>93</sup>. There is a need to develop more strategies to transform the insoluble phosphate into a soluble, more usable form for the plants to uptake.

While the use of biochar as a soil amendment offers many benefits, some concerns regarding its mass application in soil were raised. Biochar is a strong adsorbent. A study compared the nutrient adsorption properties of several biochars and found that some biochars can adsorb large amount of nitrate, ammonium and phosphate from soil while others showed no effect<sup>94</sup>. This has long been a desired trait of biochar as it indicates its capacity to retain fertilizers<sup>95</sup> which would increase the level of soil bioavailable nutrients. Additionally, some research also showed that biochar can reduce the bioavailability of soil toxic metals<sup>96</sup>. Reducing bioavailable heavy metals in contaminated soils is highly desirable, but it raises the question of whether certain biochars would also reduce the bioavailability of important nutrients like ammonium, nitrate, phosphate etc. Little information is available on determining the conditions when biochars with high adsorption capacity can reduce the bioavailability of those important nutrients for plants. Another concern about mass application of biochar (typically tons per hectare) on soil is that it reduces surface albedo<sup>97</sup> which can cause a temperature rise, thus a concern for global warming. To address those possible drawbacks associated with the application of biochar in soil, here we propose the use of a green chemistry with water-soluble ozonized biochar molecules with ppm concentration levels to achieve functions to improve soil fertility,

which would reduce the required dose to just a few kg per hectare in a stark contrast to the conventional biochar application that typically uses tons of biochar materials per hectare.

Our recent study<sup>33</sup> showed that the ozonized biochar powders (particle size about 100 micrometers) and liquid paste containing humic-like molecules were both quite potent to help solubilize phosphate from insoluble phosphate rock material<sup>33</sup>. A fraction of the dissolved organic materials obtained by water extraction and filtration (using the P8 filter with pore size of 20  $\mu\text{m}$  micrometers) from the ozonized biochar substances was shown to be resembling humic-like materials<sup>33</sup>. Humic acids contain some carboxylic groups which give them some cation exchange properties<sup>98,99</sup>. Humic substances such as fulvic acids (FA) were shown to increase soil fertility by increasing phosphorus availability and soil CEC<sup>100</sup>. Thus, humic substances are an important contributor to a healthy fertile soil. In the literature, several technologies were developed to generate humic-like substances. A group of scientists showed the generation of humic-like materials from coal following oxidation<sup>101</sup>. Any technique that uses green chemistry to generate some organic fragments with humic-like properties is highly desirable.

The innovative use of ozonized biochar substances that contain humic-like molecules can potentially be a promising avenue to new approaches such as application of the functionalized biochar molecules through the irrigation systems into soils within the plant root zone. Such application at the plant root zone, would enable the unlocking of P from insoluble phosphate materials in soils for crop uptake without requiring the use of any physical biochar particles in the fields. Before realizing this long-term vision, it is important to better the fundamental understanding on the chemistry of biochar ozonization to synthesize functionalized biochar substance containing humic-like molecules in relation to the capability of unlocking P from the insoluble phosphate mineral phases. Therefore, this article reports our latest experimental results

on the efficiency of ozonization in generating water-soluble functionalized biochar substance containing humic-like molecules that can pass through a membrane with 200 nanometer pore size and be measured as DOC. It also reports the test results on the efficiency of the water-soluble functionalized biochar substance containing humic-like molecules and organic acids in solubilizing phosphorus from the model insoluble phosphate material, hydroxyapatite ( $\text{Ca}_{10}(\text{PO}_4)_6(\text{OH})_2$ ), under different conditions.

## **MATERIALS AND METHODS**

### **Measurement of dissolved organic carbon from biochar filtrates**

Pine 400 biochar (dry-ozonized, wet-ozonized, and non-ozonized control) and rogue biochar (dry-ozonized, wet-ozonized, and non-ozonized control) were used in this study. The filtrate collection was previously done for these two biochars before and after ozonization as described in chapter three. Briefly, several washes of milli-Q water aliquots were used to extract DOC from the biochars: a first 10-mL wash, a second 25-mL, and a final 300-mL wash. Next, the filtrates were filtered through 0.2 $\mu\text{m}$  filter (Millex-FG SLFG025LS) to remove non-dissolved biochar fragments. The DOC concentration was determined for all these washes and the total extracted DOC in mg was calculated for each gram of biochar to have a normalized comparison between the biochar species.

### **Quantification of oxygen functional groups of biochar filtrates**

A fraction of the organic molecular fragments extracted from the biochar showed the presence of some fragments previously identified as humic-like materials<sup>33</sup>. Some of these organic fragments can be measured as dissolved organic carbon. In this study, the cation

exchange capacity of the soluble biochar molecular fragments in the filtrates was quantified by measuring the carboxyl groups contained in the 10 mL filtrate, using a modified approach as done by Khil'ko et al (2011)<sup>99</sup> with a potentiometric titration of the filtrates.

The method employed consisted in mixing 1.00- or 2.00-mL filtrate of known DOC concentration in 40.00 mL of 0.025 M NaOH. The mixture was stirred continuously with a stir bar until the pH was stabilized. The mixture was then titrated with 0.025 M HCl while recording the pH. A blank titration was also performed consisting of only 40.00 mL of 0.025 M NaOH without any filtrate. After each addition of titrant, the pH meter was read after stabilizing; wait-time varied between 15 seconds to 5 min. A total of 3 replicates were performed for each treatment including the blank. The equation below (Eq. 6) was used to quantify the -COOH groups:

$$-COOH \text{ (cmol/mL filtrate)} = [ ((V3-V1)/1000) \times M \text{ HCl} \times 100 ] \div VF \quad (6)$$

where V3 is the equivalence point for the titration of NaOH only (in mL), V1 is the equivalence point for titration of biochar filtrate (in mL), M HCl is the molarity of HCl, and VF is the volume of filtrate used (in mL). The equivalence point for each titration was determined by using the first derivative method.

Note: the cmol of -COOH were calculated from the first 10-mL filtrate regardless of the DOC concentration. To understand the nature of the fragments in the DOC, the cmol of -COOH for every mg of DOC was also calculated.

## **Phosphorus solubilization assay at different DOC concentrations and pH**

### *Experimental setup*

The solubilization assay of phosphorus from hydroxyapatite was performed with the wet-ozonized pine 400 biochar filtrate (P400 90W-F) and the dry-ozonized rogue biochar (RBC 90D-

F) filtrate at several DOC concentrations of the water-soluble ozonized biochar molecules: 10 ppm, 75 ppm, 300 ppm and 600 ppm (with “ppm” being mg/L). The mixture liquid incubation was done in a 50 mL polypropylene conical tube. The total liquid volume in each tube was 15.0 mL; 0.20 g of hydroxyapatite (HA) was added to each tube. Controls of filtrates samples without the hydroxyapatite were also made. Another control using milli-Q water (0 ppm of DOC) was done with and without hydroxyapatite. In order to further understand the mechanism of the phosphorus solubilization, a separate assay was performed where the filtrates were neutralized with NaOH to a pH of  $7.0 \pm 0.5$ . Every sample incubation was done in three replicates ( $n=3$ ). The setup of the hydroxyapatite assay is shown below in Table 11. The tubes were all placed on an Innova 2300 platform shaker operating at 100 rpm at room temperature.

#### *Liquid incubation assay pH measurements*

The pH in the incubation assay liquid was measured for each triplicate tube on day 0 (30 min), day 2, day 4, day 6 and day 8 of incubation. For the samples incubated at neutralized pH ( $7.0 \pm 0.5$ ), the pH was adjusted with NaOH/HCl after 30 minutes of liquid incubation assay if it was not within the range. Since the hydroxyapatite also has an effect on the pH of the liquid, the pH adjustment was done as follows; only the pH for of the controls filtrates without HA was measured and if it wasn't within the range it was adjusted with NaOH/HCl; the same amounts of NaOH/HCl that were added to the control filtrates were also directly added to the samples with HA.

**Table 11: Set-up of the hydroxyapatite solubilization assay using different DOC (water-soluble ozonized biochar molecules) concentrations (ppm) of the filtrates from wet-ozonized pine 400 (P400 90W-F) and the filtrates from dry-ozonized rogue biochar (RBC 90D-F). Each sample treatment was made in triplicate (n=3).**

Samples without hydroxyapatite (HA) (15.0 mL of liquid samples)	Samples with hydroxyapatite (HA) (15.0 mL of liquid samples + 0.20 g of HA)
Milli-Q water only	Milli-Q water + HA
P400 90W-F 10ppm	P400 90W-F 10ppm + HA
P400 90W-F 75ppm	P400 90W-F 75ppm + HA
P400 90W-F 300ppm	P400 90W-F 300ppm + HA
P400 90W-F 600ppm	P400 90W-F 600ppm + HA
P400 90W-F pH 7 10ppm	P400 90W-F pH 7 10ppm + HA
P400 90W-F pH 7 75ppm	P400 90W-F pH 7 75ppm + HA
P400 90W-F pH 7 300ppm	P400 90W-F pH 7 300ppm + HA
P400 90W-F pH 7 300ppm	P400 90W-F pH 7 300ppm + HA
RBC 90D-F 10ppm	RBC 90D-F 10ppm + HA
RBC 90D-F 75ppm	RBC 90D-F 75ppm + HA
RBC 90D-F 300ppm	RBC 90D-F 300ppm + HA
RBC 90D-F 600ppm	RBC 90D-F 600ppm + HA
RBC 90D-F PH 7 10ppm	RBC 90D-F PH 7 10ppm + HA
RBC 90D-F PH 7 75ppm	RBC 90D-F PH 7 75ppm + HA
RBC 90D-F PH 7 300ppm	RBC 90D-F PH 7 300ppm + HA
RBC 90D-F PH 7 600ppm	RBC 90D-F PH 7 600ppm + HA
Milli-Q water pH 7	Milli-Q water pH 7 + HA

*Sample collection for phosphate concentration measurement*

A liquid sample was collected from each liquid incubation tube, in a similar approach as done previously<sup>33</sup>. Briefly, the tubes containing the incubation assay liquid were centrifuged at 4500 rpm for 15 min and 1.0 mL of the supernatant was collected.

Here, the collection of 1 mL from the supernatant was done at:

Day 0 (30 min): 90 samples (=30 treatments × 3 replicates)

Day 2: 90 samples (=30 treatments × 3 replicates)

Day 4: 90 samples (=30 treatments × 3 replicates)

Day 6: 90 samples (=30 treatments × 3 replicates)

Day 8: 90 samples (=30 treatments × 3 replicates)

*Water controls at low pH*

To quantify the amount of phosphate solubilized due to the protonic effect only, water controls at pH 2.6 and pH 3.0 were also made and incubated with hydroxyapatite as shown in Table 12 below. These controls were only incubated for 4 days.

**Table 12: Set-up of milli-Q water controls at pH 2.6 and pH 3.0 for incubation with and without hydroxyapatite**

Milli-Q water pH 2.6 (3 replicates)	Milli-Q water pH 2.6 + HA (3 replicates)
Milli-Q water pH 3.0 (3 replicates)	Milli-Q water pH 3.0 + HA (3 replicates)

### *Measurement of phosphate concentration with Ion Chromatography*

For the phosphate concentration measurement, the samples were diluted by a factor of 10. A Thermo Scientific Dionex 7 Anion standard solution was used (057590). The samples were loaded onto a Dionex AS 40 autosampler. The phosphate concentration was measured using a Dionex 5000 Ion chromatography instrument, packed with AG23/AS23 column of 0.4 x 250 mm. A 4.5 mM Na<sub>2</sub>CO<sub>3</sub>/0.8 mM NaHCO<sub>3</sub> was used as mobile phase eluents. The signals were detected with a conductivity detector. The data collection time of the ion chromatography was set to 30 minutes. Certified grade potassium oxalate was purchased from Fisher Scientific, and sodium acetate from Baker Analyzed Reagent; they were used as reference for conductivity signals using the ion chromatography.

To characterize the different anions in the P400 90W filtrate and the RBC 90D filtrate, the concentration of several anions (nitrate, sulfate, and chloride) was also measured. For this analysis, the filtrate collected from the 2<sup>nd</sup> wash (25mL wash) was used and was diluted by a factor of 5. Each sample type was measured in triplicate.

### *Elemental composition measurements with ICP-MS*

Samples after the 8<sup>th</sup> day of hydroxyapatite incubation were collected and sent to Virginia Tech (Blacksburg, VA) where an independent phosphorus concentration measurement was done. The concentration of several other elements was also measured.

## **RESULTS AND DISCUSSION**

### **DOC and pH measurements of biochar filtrates**

After ozone treatment, the pH of the pine 400 biochar and the rogue biochar decreased, thus indicating the installment of more oxygen-functional groups on the biochar molecular

fragments<sup>15</sup> (Figure 9). The dry biochar ozonization resulted in a dramatic reduction of the RBC pH from 7.97 to 3.08 while it resulted in a reduction of the P400 pH from 4.78 to 3.78. In contrast, the wet-ozonization showed only a relatively minor pH change for the RBC pH to 7.97 to 7.46 while it reduced the P400 pH from 4.78 to 3.62 (Figure 9).

To quantify the generated biochar organic molecular fragments by ozonization, the amount of dissolved organic carbon from the biochar filtrate was measured as DOC. The non-ozonized P400 filtrate had a total of 1.96 mg DOC/g biochar  $\pm$  0.31, and the non-ozonized rogue biochar released 2.37 mg DOC/g biochar  $\pm$ 0.14 (Figure 12, Table C1). Dry-ozone treatment of P400 led to a release of more DOC materials in the biochar filtrate (9.32 mg DOC/g biochar  $\pm$  1.72) which is more than three times greater than that of the non-ozonized P400 biochar. Wet ozone treatment was even more efficient at generating DOC from P400 biochar; the filtrate from the P400 90W (P400 90W-F) had a value of 23.49 mg DOC/g biochar  $\pm$  1.70 which twelve times more than the non-ozonized control (Figure 12, Table C1).

Previously we reported that dry-ozonization of rogue biochar increased its CEC by a factor of 7-9<sup>15</sup>; we therefore expected the filtrate of the dry-ozonized rogue biochar to contain high amount of DOC materials because of the cleavage due to ozone. The results matched our expectations; the dry-ozonized rogue biochar filtrate (RBC 90D-F) had the most DOC (34.50 mg DOC/g  $\pm$ 1.00) in its filtrate, an increase by a factor of fifteen compared to that of the non-ozonized rogue biochar (Figure 12, Table C1).

We previously demonstrated that water-soluble ozonized biochar molecules containing -COOH groups are produced as a result of ozone cleavage of graphite/graphene types of biochar carbon<sup>15, 24</sup>. The larger amount of DOC generated<sup>15</sup> by ozone-treated biochar observed here, is an indication that oxidation cleavage occurred; we observed more water-soluble biochar molecular

fragments (molecules) in the form of DOC released from the ozonized biochar compared to the non-ozonized biochar. However, if there is such a release of DOC material from biochar particles that would also indicate that there is an oxygenation/conversion of carbon material from the biochar particles to water-soluble organic molecules following ozonization. Thus, the CEC of the biochar solid particle material may not be complete as it does not take into account the CEC of the water-soluble biochar molecular fragments that may have been released from biochar particles during the ozonization and measurement processes. Consequently, substantial amounts of ozonized biochar molecular fragments (oxygenated biochar organic molecules) containing CEC values may be now contained in the filtrate.

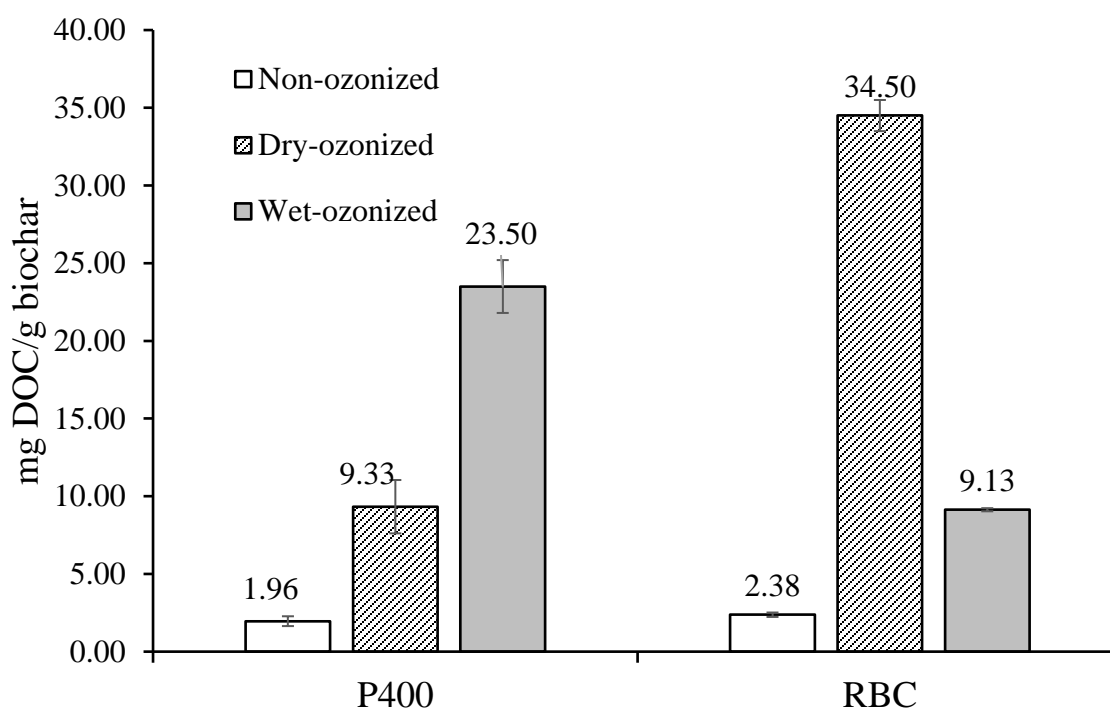


**Figure 12:** Total dissolved organic carbon (DOC) material extracted from the pine 400 biochar (P400) and rogue biochar (RBC). The DOC was measured from the filtrate/wash of the control non-ozonized biochar filtrate  $\square$ , the dry-ozonized biochar filtrate  $\square$  and the wet-ozonized biochar  $\square$ . The error bars denote standard deviation of 3 replicate (n=3) measurements.

The highest extractable DOC was obtained from the dry-ozonized rogue biochar (RBC 90D) and the wet-ozonized pine 400 biochar (P400 90W). The mechanism of ozonization on these two biochars may be different. Given their higher yield in DOC, they were used for the next experiments that involved the measurement of the CEC in one part and the solubilization of phosphorus in another part.

### **Cation exchange capacity of soluble biochar molecular fragments**

The cation exchange capacity of the filtrates is expressed here in cmol of carboxyl groups (-COOH). Here, we measured the soluble molecular biochar-COOH content in the filtrates that pass through the membrane filter with 0.2 micrometer pore size.

The filtrate of the non-ozonized P400 (P400 UN-F) had a CEC value of  $0.0102 \text{ cmol/mL} \pm 0.0019$  compared to  $0.0084 \text{ cmol/mL} \pm 0.003$  for the non-ozonized rogue biochar filtrate (RBC UN-F) (Figure 13). The dry-ozonized pine 400 biochar filtrate contained  $0.0167 \text{ cmol -COOH/mL} \pm 0.0016$  and the wet ozonized pine 400 filtrate had the most -COOH groups ( $0.0236 \text{ cmol/mL} \pm 0.0020$ ). The filtrate from the dry-ozonized rogue biochar also contained significantly more -COOH groups ( $0.0204 \text{ cmol/mL} \pm 0.0018$ ) compared to the filtrate ( $0.0084 \text{ cmol/mL} \pm 0.003$ ) of the non-ozonized RBC (Figure 13). The dry-ozonization of rogue biochar generated more DOC materials than the wet-ozonization of P400 (Figure 12). Therefore, we expected the filtrate from the dry-ozonized rogue biochar (RBC 90D-F) to have more -COOH groups than the filtrate from the wet-ozonized pine 400 (P400 90W-F). However, data showed the opposite; the P400 wet-ozonized biochar filtrate contained slightly more -COOH groups than the RBC 90D filtrate.

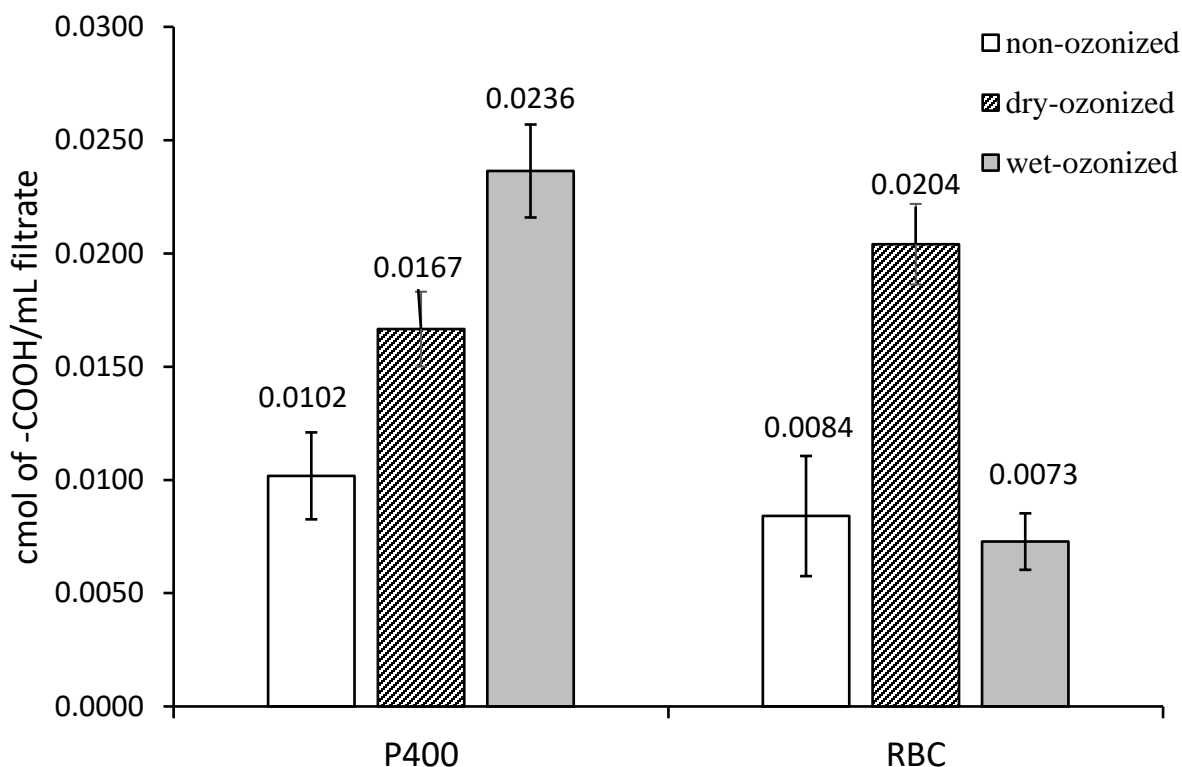


**Figure 13:** Cation exchange capacity measurements of the dissolved organic carbon from the filtrates of Pine 400 and RBC biochar, expressed as cmol of carboxyl groups/mL filtrate. The data is shown for the non-ozonized control biochar filtrate  $\square$ , the dry-ozonized biochar filtrate  $\text{▨}$  and the wet-ozonized biochar filtrate  $\blacksquare$ . The error bars represent the standard deviation of triplicate measurements.

To further understand the relationship between the -COOH groups and the DOC, the cmol of -COOH groups was calculated per mg of DOC. The DOC that is present in the filtrate of pine 400 non-ozonized biochar showed more -COOH per mg DOC (0.1862 cmol -COOH/mg DOC  $\pm$  0.0351) than the filtrate from the dry ozonized pine 400 (0.0340 cmol -COOH/mg DOC  $\pm$  0.0034) (Table 13). The P400 90W-F showed even much less -COOH groups, with 0.0100 cmol -COOH/ mg DOC  $\pm$  0.0001. These results were quite surprising, not as what one would expect. The filtrate from the ozonized pine 400 biochar contained more DOC than the filtrate

from the non-ozonized pine 400 biochar (Figure 12, Table C1) but the generated DOC fragments did not contain more -COOH groups than the DOC molecules released from the non-ozonized biochar. The DOC of the dry-ozonized rogue biochar filtrate also contained much less -COOH ( $0.0063 \text{ cmol -COOH/mg DOC} \pm 0.0001$ ) than that of the non-ozonized rogue biochar ( $0.0907 \text{ cmol -COOH/mg DOC} \pm 0.0286$ ) and the wet-ozonized rogue biochar ( $0.0624 \text{ cmol -COOH/mg DOC} \pm 0.0107$ ) (Table 13). Given that there is more DOC released from the RBC 90D biochar than the RBC UN biochar, the total -COOH released from 1g biochar were comparable; RBC UN released about  $0.2154 \text{ cmol -COOH/g biochar} \pm 0.0680$  and the RBC 90D leached  $0.2181 \text{ cmol -COOH/g biochar} \pm 0.0190$  (Table 13). Interestingly, the RBC 90W biochar released more -COOH ( $0.5706 \text{ cmol -COOH/g} \pm 0.0977$ ) than the non-ozonized rogue biochar ( $0.2154 \text{ cmol -COOH/g} \pm 0.0680$ ) and the dry-ozonized rogue biochar ( $0.2181 \text{ cmol -COOH/g} \pm 0.0190$ ) (Table 13). That is, wet ozonization of rogue biochar resulted in twice more -COOH ( $0.5706 \text{ cmol -COOH/g} \pm 0.0977$ ) in the filtrate than in that ( $0.2154 \text{ cmol -COOH/g} \pm 0.0680$ ) of the non-ozonized rogue biochar.

As discussed earlier, ozonization caused an increase in DOC (dissolved organic carbon) biochar molecular fragments. We previously identified some of those molecular fragments to be humic-like substances<sup>33</sup>. In addition, the low pH of the filtrate from the ozonized biochar also led us to think that they may be rich in carboxyl functional groups. Here, the investigation on the CEC properties of the filtrates from P400 and RBC biochar showed that there is an overall increase in -COOH groups in the filtrate of the ozonized biochars compared to the non-ozonized biochar; however, our results indicate that the total DOC molecules that were generated by the ozonized biochars did not have more -COOH groups per mg DOC than the DOC molecules released from the non-ozonized biochar. This may be due to several factors. The prolonged

biochar ozone treatment of 90 minutes may have led to the degradation of the biochar molecular fragments into smaller fragments that are more soluble in water. Ozone was shown to degrade

**Table 13: Calculated CEC (expressed in cmol of -COOH) in filtrates from pine 400 and rogue biochar. The table also shows the CEC in each of the filtrates that was calculated per gram of biochar. The values shown are averages of 3 replicates (n=3).**

	cmol of -COOH/ mL filtrate	cmol -COOH/mg DOC	Total -COOH-DOC in 1g biochar (cmol -COOH/g biochar)
P400 UN	0.0102 ± 0.0019	0.1862 ± 0.0351	0.3649 ± 0.0688
P400 90D	0.0167 ± 0.0016	0.0340 ± 0.0034	0.3174 ± 0.0315
P400 90W	0.0236 ± 0.0020	0.0100 ± 0.0001	0.2350 ± 0.0204
RBC UN	0.0084 ± 0.0026	0.0907 ± 0.0286	0.2154 ± 0.0680
RBC 90D	0.0204 ± 0.0018	0.0063 ± 0.0001	0.2181 ± 0.0190
RBC 90W	0.0073 ± 0.0012	0.0624 ± 0.0107	0.5706 ± 0.0977

humic substance into small organic acids such as formic acid, acetic acid, and oxalic acid <sup>102, 103</sup>.

The ion chromatography data showed the presence of anions, that were generated by the wet-ozonization of pine 400 and the dry-ozonization of rogue biochar (Figure C1); they were labeled “a”, “b” and “c”. We suspect some of those compounds to be monocarboxylated organic anions <sup>104</sup>; the signals of standard acetate displayed a conductivity signal that is within the range of one of the anion “a” (Figure C1); We also suspect some dicarboxylated anions shown by the

strong signal marked “b” and “c” (Figure C1)<sup>104</sup>; the conductivity signals of standard oxalate (Figure C1) were not within the range of the anions “b” and “c” thus indicating that oxalate may have not been generated. More characterization of those organic acids is needed to fully identify them. The non-ozonized biochar may contain larger biochar molecular fragments such as graphite/graphene types of carbon substances that are mostly insoluble. The ozone treatment may cause the breaking of those molecular fragments into smaller acidic compounds that are more water-soluble; this may explain the larger amount of DOC released from the ozonized biochar. While some of the DOC from the ozonized biochar filtrate may belong to the humic-like groups<sup>33</sup>, the majority may be in the form of smaller organic acids. The ozone treatment time used here was 90 minutes. Maybe decreasing the ozone treatment time would yield more biochar molecular fragments without degrading them into smaller organic acids. Regarding the RBC 90W-F, we observed that it had more water-soluble biochar-COOH product ( $0.0624 \pm 0.0107$  cmol -COOH/mg DOC) than the RBC 90D-F ( $0.0063$  cmol -COOH/mg DOC  $\pm 0.0001$ ). We observed that the wet ozonization of rogue biochar was not as efficient as the dry ozonization as shown by the pH (Figure 9) and CEC data (Figure 10). The low reactivity of ozone in the wet-ozonization of RBC somehow made some biochar molecular fragments more soluble (Figure 12). However, the ozone was not reactive enough to cleave those released fragments into smaller organic acids.

We expect that these -COOH groups in the filtration may play an important role in solubilization of phosphorus from insoluble phosphate materials.

### **Solubilization of Phosphorus from hydroxyapatite**

The hydroxyapatite assay was conducted with DOC at different concentrations from the

filtrates of the dry-ozonized rogue biochar (RBC 90D-F) and the filtrates of the wet-ozonized pine 400 (P400 90W-F).

*Solubilized phosphate from hydroxyapatite at different DOC concentrations*

The solubilized phosphate concentration was measured with ion chromatography. The RBC 90D-F solubilized phosphate ( $5.6 \pm 0.7$  mg/L) after only 30 minutes of incubation with hydroxyapatite at a DOC concentration of 10 ppm (Figure 14, Table C2-C3). The highest solubilized phosphate from the treatment of hydroxyapatite with 10 ppm RBC 90D-F was  $8.0 \pm 0.8$  mg/L after 4 days of incubation. The treatment with 10 ppm DOC of P400 90W-F also showed a similar pattern in elevating the solubilized phosphate concentration to  $7.5 \pm 2.0$  mg/L at day 4 (Figure 15, Table C2-C3). Both filtrates from the P400 90W and the RBC 90D showed more solubilization of P than the water control which had its highest solubilization on day 2 with  $4.8 \pm 1.4$  mg/L. These results showed that at low DOC concentration, the filtrate from the ozonized biochars can solubilize phosphate from insoluble hydroxyapatite material.

Increasing the RBC 90D-F DOC concentration from 10 to 75 ppm resulted in 4-5 times increase in solubilized phosphate with the highest solubilized phosphate ( $35.9 \pm 1.8$  mg/L) achieved on day 6 of incubation. The hydroxyapatite (HA) incubation with RBC 90D-F at 300 ppm, resulted in 4 times more solubilized phosphate (max of  $150.2 \pm 6.6$  mg/L on day 4) compared to the HA incubation with RBC 90D-F at 75ppm (max of  $35.9 \pm 1.8$  mg/L on day 6) as shown in Figure 14 and Table C2-C3. The RBC 90D-F at 600ppm further increased the solubilization of phosphate by another factor of 2 (max of  $339.6$  mg/L  $\pm 8.5$  on day 6) compared to the incubation with RBC 90D-F at 300ppm.

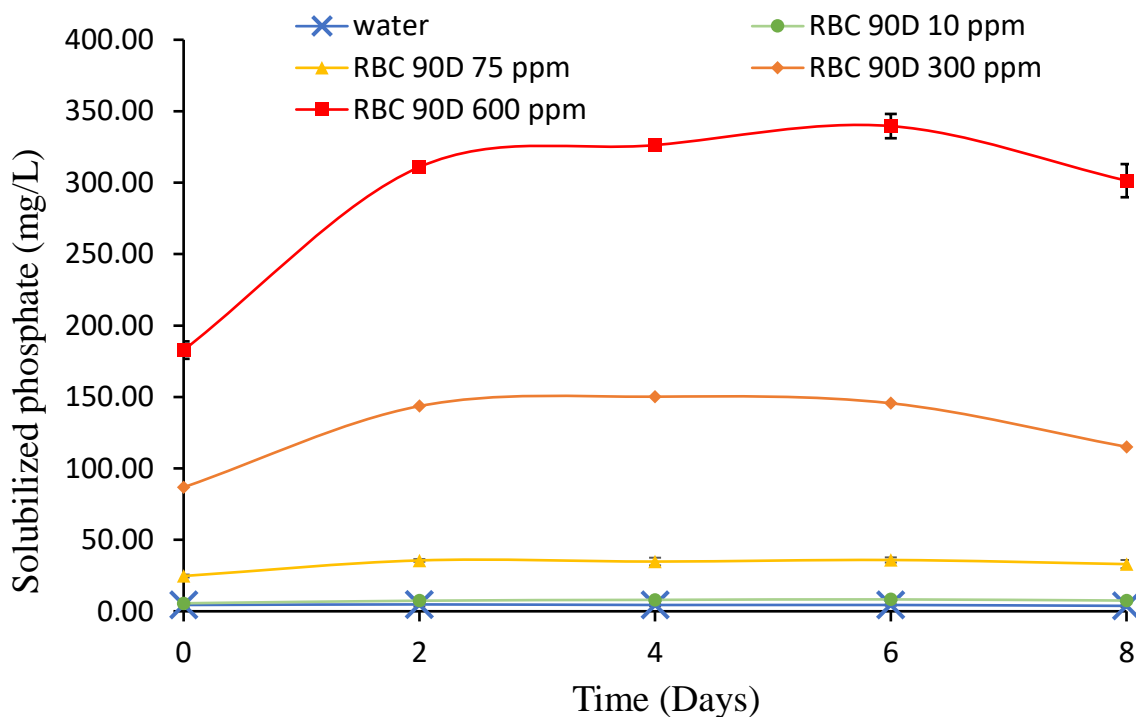


**Figure 14:** Solubilized phosphate from hydroxyapatite by the filtrate/wash from the dry-ozonized rogue biochar (RBC 90D) at different DOC concentrations (10, 75, 300 and 600ppm) at the pH of the DOC measured every 2 days for up to 8 days. The error bars denote standard deviation of 3 replicates (n=3).

The filtrate from the wet-ozonized pine 400 (P400 90W-F) also showed a similar pattern; as the DOC concentration increased, the solubilized phosphate increased (Figure 15, Table C2-C3).

These results suggest a positive correlation between the DOC concentration and the solubilized phosphate from HA. The pH of the samples was also measured throughout the incubation assay.

The incubation of HA with RBC 90D-F at 10 ppm had an initial pH of  $6.18 \pm 0.02$  (Figure 16).

Over the course of the 8-day incubation period, the pH had a gradual increase and attained a final value of  $7.02 \pm 0.08$  on day 8 (Figure 16).

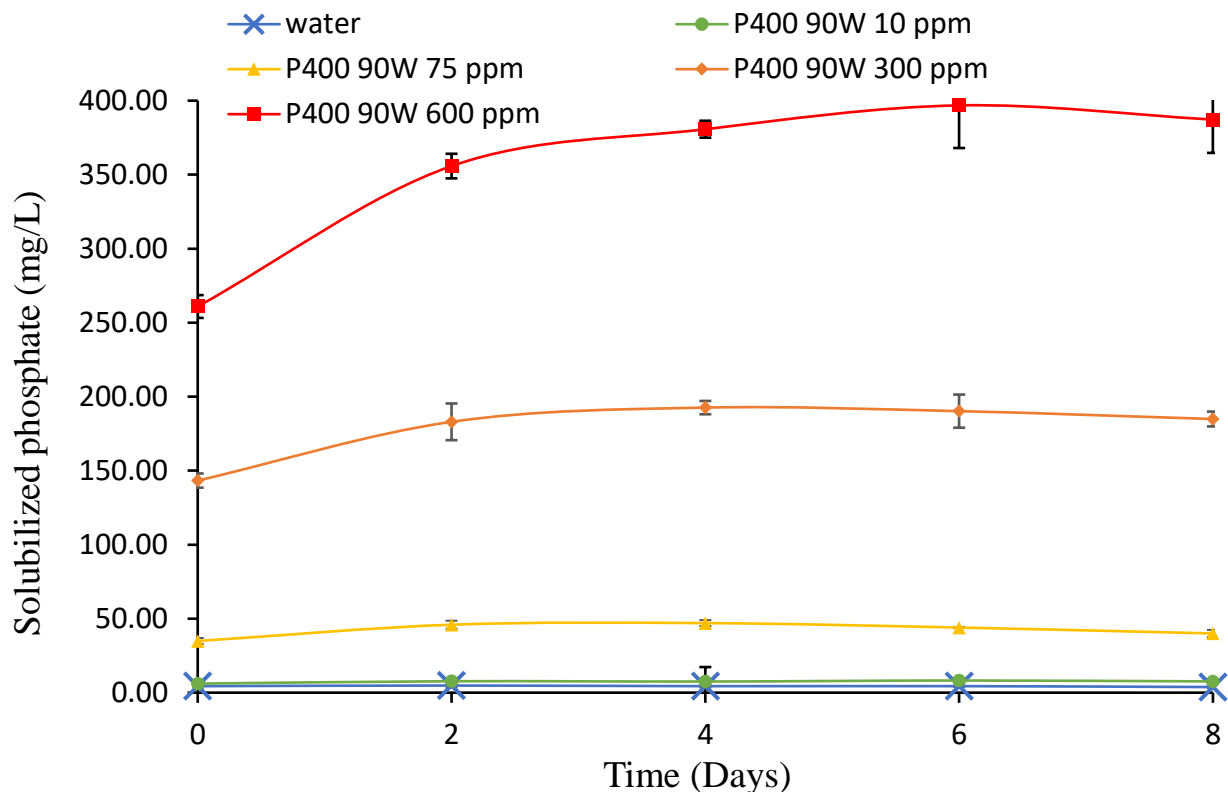


**Figure 15:** Solubilized phosphate from hydroxyapatite by the filtrate/wash from the wet-ozonized pine 400 biochar (P400 90W) at different DOC concentrations (10, 75, 300 and 600ppm) at the pH of the DOC measured every 2 days for up to 8 days. The error bars denote standard deviation of 3 replicates (n=3).

The incubation of hydroxyapatite with RBC 90D-F at 75 ppm, 300 ppm and 600 ppm DOC also showed a similar pattern (Figure 16). The pine 400 90W-F incubation with hydroxyapatite showed a slightly lower initial pH for the 10 ppm DOC ( $5.97 \pm 0.08$ ) (Figure 17). Similarly, the incubation of the 10 ppm P400 90W-F with HA experienced a gradual increase in pH over the 8 day-incubation. The P400 90W-F at 75, 300 and 600 ppm also showed an increase in pH over time (Figure 17). One major difference in the pH measurements is that on day 8 of incubation of hydroxyapatite with P400 90W-F (Figure 17), the measured pH's were in the range of  $6.63 \pm 0.13$ ,  $6.87 \pm 0.09$ ,  $6.63 \pm 0.06$  and  $6.47 \pm 0.08$  for the 10, 75, 300 and 600 ppm samples,

respectively. These values were much smaller than the pH measurements of the incubation liquid of the HA with RBC 90W-F on day 8; the measured pH data for HA with RBC 90D-F were  $7.02 \pm 0.08$ ,  $7.22 \pm 0.03$ ,  $7.65 \pm 0.19$  and  $7.77 \pm 0.25$  for the 10, 75, 300 and 600 ppm respectively (Figure 16). The pH of the filtrate without HA (control sample) was also measured over the 8-day period (Table C4).

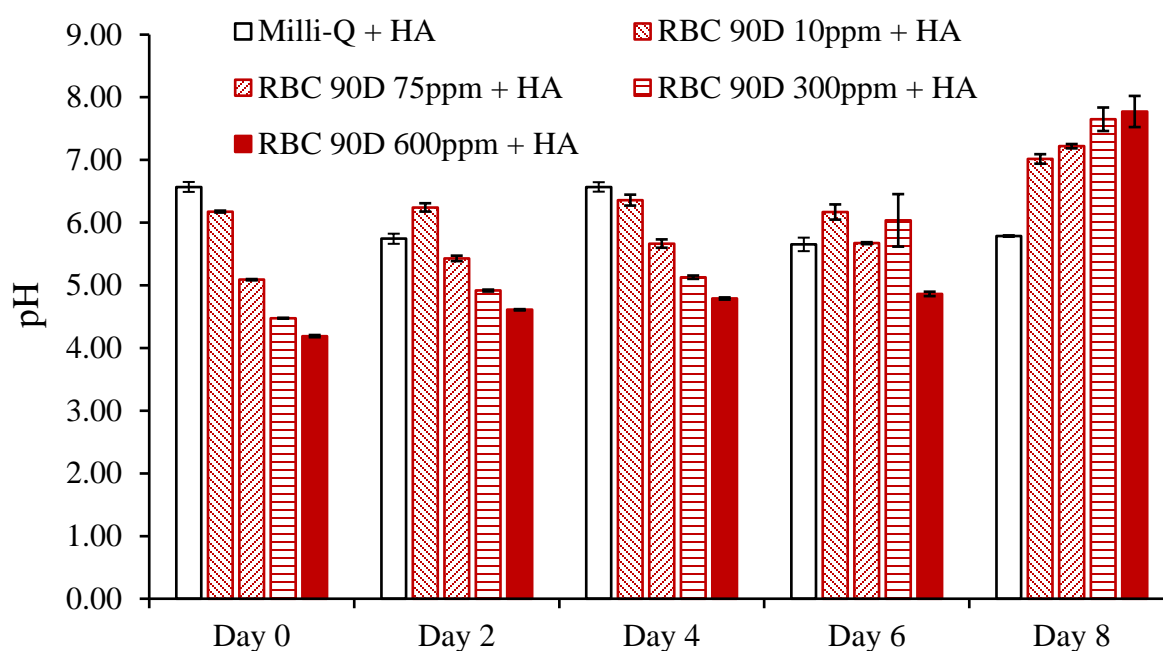


**Figure 16:** pH measurements of the filtrates from RBC 90D at different DOC concentrations incubated with hydroxyapatite at day 0, 2, 4, 6 and 8. The data shown are the average of 3 replicates ( $n=3$ ) for the water control (□), the 10 ppm DOC (▨), the 75 ppm DOC (▩), the 300 ppm DOC (▧) and the 600 ppm DOC (■).

Given that protons are consumed because of hydroxyapatite solubilization, the large change in pH for the RBC 90D from day 6 to day 8 (Figure 16) would have indicated more

solubilized phosphate; but that was not observed. Instead, from day 6 to day 8, the solubilized phosphate decreased significantly when HA was incubated with the RBC 90D-F at 300 ppm DOC and RBC 90D-F at 600 ppm DOC (Figure 14). It's possible that some phosphate may have precipitated back into its non-soluble form. Furthermore, we noted that at a similar DOC concentration, the P400 90W-F solubilized more phosphate from HA than the RBC 90D-F (Table C2-C3, Figure 14,15). We suspected that this may be due to a combination of several factors:

- 1-The filtrate from the P400 90W (P400 90W-F) had more carboxylic groups than the RBC 90D-F as discussed earlier (Figure 13, Table 13). Those carboxylic groups may lead to form complexations with the calcium released from the HA, thus favoring the solubilization of phosphate.

- 2- The pH protonic effect. The protonic effect is a major driving force in solubilizing HA<sup>33, 63</sup>. The RBC 90D-F (Figure C2) are less acidic than the P400 90W-F (Figure C3) at any given DOC concentration. The more acidic P400 90W-F may favor more solubilization via the protonic effect.

- 3- The filtrate of the P400 90W may contain some other compounds that enhance the solubilization of hydroxyapatite.

- 4-The filtrate of the RBC 90D may contain some other compounds that do not favor the solubilization of HA.

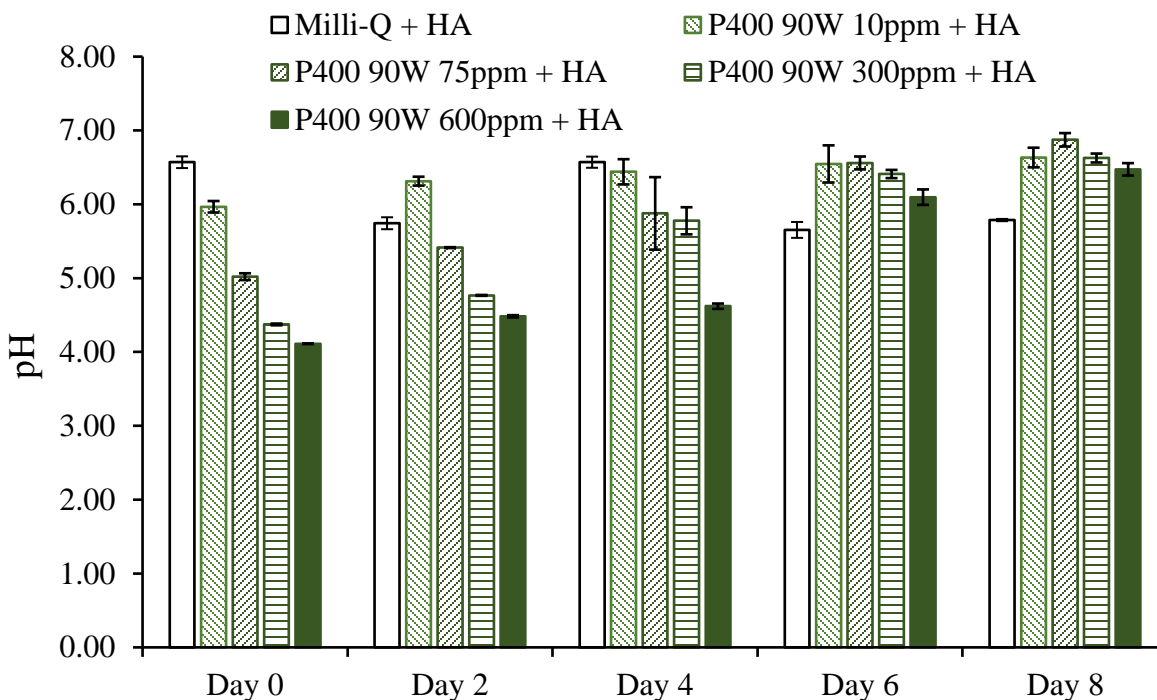


**Figure 17:** pH measurements of the filtrates from P400 90W at different DOC concentrations incubated with hydroxyapatite at day 0, 2, 4, 6 and 8. The data shown are the average of 3 replicates (n=3) for the water control (□), the 10 ppm DOC (▨), the 75 ppm DOC (▩), the 300 ppm DOC (▧) and the 600 ppm DOC (■).

#### *Solubilized phosphate from hydroxyapatite at different pH*

Here, the RBC 90D-F and the P400 90W-F were neutralized (pH 7) before use in the liquid incubation assay with hydroxyapatite. The filtrates that were pre-neutralized to pH 7 showed a much smaller amount of solubilized phosphate from HA. The 10 ppm-RBC 90D-F (pH 7) solubilized 2.0 mg/L  $\pm$ 1.0 within the first 30 min on day 0; the solubilized phosphate then increased to reach its maximum on day 2 before reaching an equilibrium value of around 4 mg/L on day 4, 6 and 8 (Figure 18, Table C2). The RBC 90D-F at 75 ppm DOC also showed a slight similar pattern. The RBC 90D-F at a DOC concentration of 300 ppm solubilized less phosphate.

At a higher DOC concentration (600 ppm), the RBC 90D-F solubilized little to no phosphate (Figure 18, Table C2). Even the control water at pH 7 solubilized slightly more phosphate than the RBC 90D-F 600 ppm at pH 7 (Figure 18, Table C2).

We noticed that the incubation of the filtrates (P400 90W-F and RBC 90D-F) with hydroxyapatite showed no overall pH change over time (Figure C4, Figure C5) thus indicating that there is no major consumption of proton. The P400 90W-F at 10 ppm DOC and at a pH 7 solubilized little amount of phosphate; the maximum solubilized phosphate was reached on day 6 with  $3.2 \text{ mg/L} \pm 0.7$  (Figure 19, Table C2). Unlike the pH-neutralized RBC 90D-F, here the pH-neutralized pine 400 90W-F solubilized more phosphate at higher DOC concentrations.

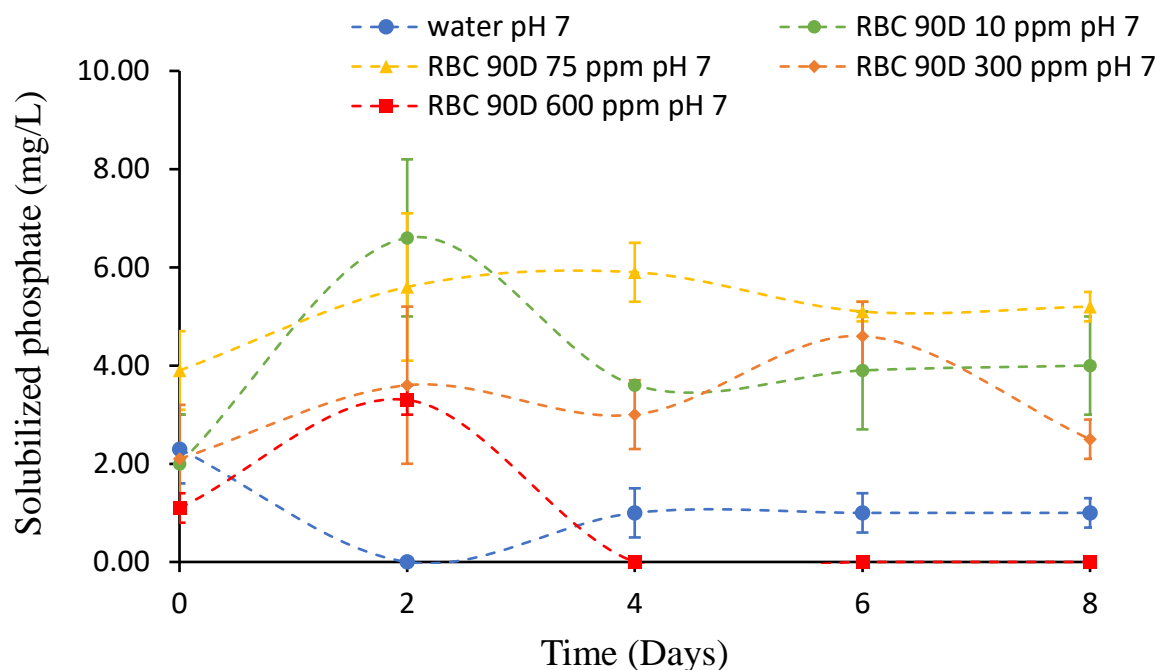


**Figure 18:** Solubilized phosphate from hydroxyapatite by the filtrate/wash from the dry-ozonized rogue biochar (RBC 90D) at different DOC concentrations (10, 75, 300 and 600ppm). All filtrate wash, including the water control were neutralized with NaOH to obtain a pH of 7. The error bars denote standard deviation of 3 replicates (n=3).

Overall, the data showed that the pH-neutralized DOC from the P400 90W-F and the pH-neutralized DOC from the RBC 90D-F solubilized very little phosphate, compared to the non-neutralized filtrate. In the literature, biochar application to alkaline soil was also shown to not significantly increase phosphorus availability<sup>88</sup>. Even though the solubilized phosphate from HA by the P400 90W-F and RBC 90D-F at pH 7 is much smaller than that of the non-pH-neutralized biochar filtrates, it is important to note that they are all (except RBC 90D-F at 600 ppm) 2 to 9 times more efficient than neutralized water (Table C2-C3).

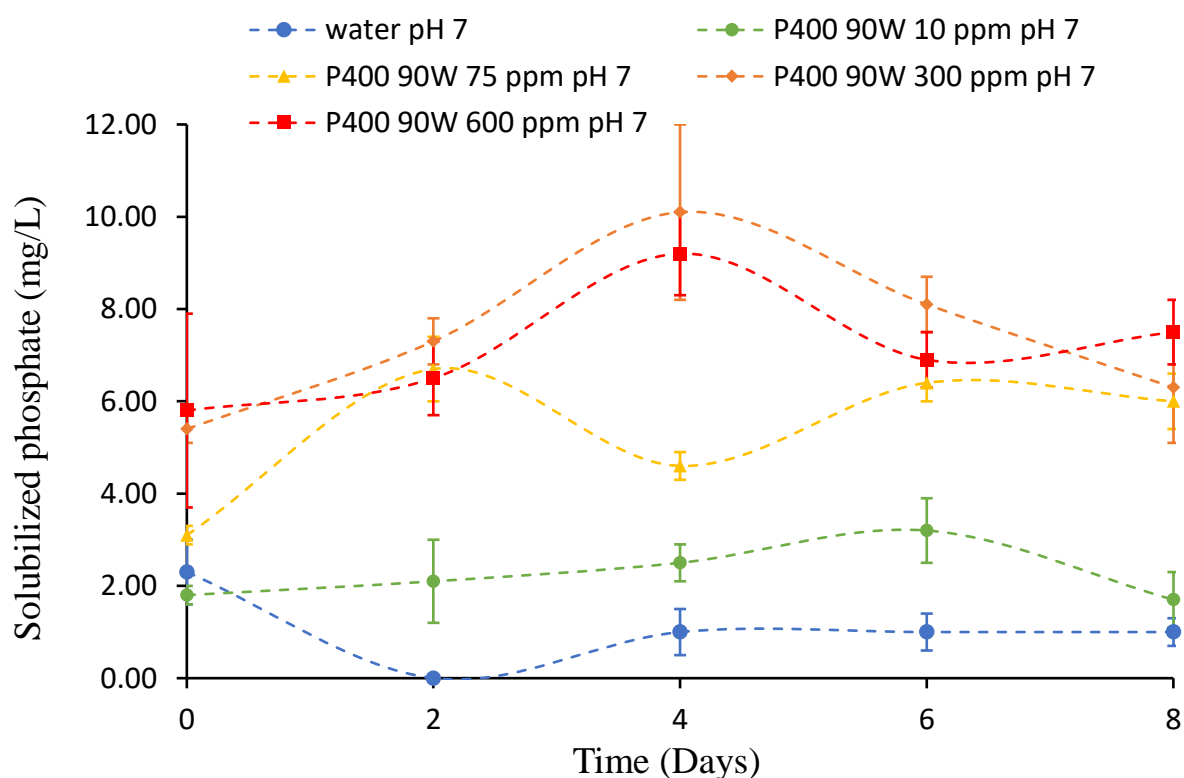


**Figure 19:** Solubilized phosphate from hydroxyapatite by the filtrate/wash from the wet-ozonized pine 400 biochar (P400 90W) at different DOC concentrations (10, 75, 300 and 600ppm). All filtrate wash, including the water control were neutralized with NaOH to obtain a pH of 7. The error bars denote standard deviation of 3 replicates (n=3).

These data supported the importance of the protonic effect in the solubilization of HA. However, as we noted in our previous work<sup>33</sup> we believe that cation effect, anion exchange and other mechanisms also play an important role. In the experiment here, being at pH 7 may have altered the contribution of other factors in solubilizing the phosphate. To understand and quantify the phosphorus solubilizing due solely to the protonic effect, another control was conducted where HA was incubated with water at low pH's. The highest solubilization observed with the RBC 90D-F and P400 90W-F was at a DOC of 600 ppm when the pH was unaltered (i.e., not neutralized) (Figure 14, 15 and Table C2-C3). The pH of the RBC 90D-F at 600 ppm DOC without HA was in the range of 3.0-3.2 and the pH of P400 90W-F at 600ppm was in the range of 3.0-3.2 as shown in Figures C1, C2. The water controls were then made at those pH's (3.0 and 2.6) and incubated with HA. Water at pH 3.0 solubilized  $24.96 \text{ mg/L} \pm 1.78$  of phosphate (Table 14) which is much less than the phosphate solubilized by RBC 90D-F at pH 3.0 ( $326.30 \text{ mg/L} \pm 3.70$ ) (Table 14). Even the RBC 90D-F at pH of 3.2 solubilized more phosphate ( $150.20 \text{ mg/L} \pm 6.60$ ) than water at pH 3.0 (Table 14). Similarly, the P400 90W-F at pH 2.6 solubilized four times more phosphate ( $380.70 \text{ mg/L} \pm 5.70$ ) than the water control at pH 2.6 ( $97.23 \text{ mg/L} \pm 3.69$ ). The P400 90W-F at pH 2.8 solubilized two times more phosphate than the water at pH 2.6 (Table 14).

The incubation of HA with water at pH 3.0 showed an increased in pH to  $5.87 \pm 0.07$  after only 30 min (Day 0), but the pH did not vary much from 30 min to day 4 ( $5.94 \pm 0.02$ ) (Table 14). Upon addition of HA to the RBC 90D-F at pH 3, the pH increased to  $4.48 \pm 0.01$  after 30 min; from 30 min to day 4 (pH  $5.13 \pm 0.03$ ) the pH changed by about 0.5 unit. From time 0 min to 30 min, the pH-change in the incubation of HA with water at pH 3 is greater than the pH-change of the RBC 90D-F with HA at pH 3; from 30 min to day 4 the opposite occurred. The

same pattern was observed for the P400 90W-F at pH 2.6 versus water at pH 2.6. This indicated that the solubilization of HA by the RBC 90D-F and P400 90W-F is a slower process than the solubilization caused by just water and hydrochloric acid. This pH control data also showed that at the same pH, the organic acids present in the filtrate of the ozonized biochar are more efficient than hydrochloric acid at solubilizing phosphate.

**Table 14: Solubilized phosphate and pH data from the incubation of hydroxyapatite with water controls and filtrates from RBC 90D and P400 90W at low pH.**

	pH Day 0	pH Day 4	Solubilized phosphate (mg/L) Day 4
Milli-Q pH 2.6 + HA	5.39 ± 0.06	5.38 ± 0.04	97.23 ± 3.69
P400 90W-F pH 2.6 (600 ppm DOC) + HA	4.11 ± 0	4.62 ± 0.04	380.70 ± 5.70
P400 90W-F at pH 2.8 (300 ppm DOC) + HA	4.37 ± 0.01	5.78 ± 0.18	192.60 ± 4.50
Milli-Q pH 3.0 + HA	5.87 ± 0.07	5.94 ± 0.02	24.96 ± 1.78
RBC 90D-F pH 3.0 (600 ppm DOC) + HA	4.48 ± 0.01	5.13 ± 0.03	326.30 ± 3.70
RBC 90D-F pH 3.2 (300 ppm DOC) + HA	4.19 ± 0.02	4.79 ± 0.02	150.20 ± 6.60

*ICP-MS of the solubilization assay of phosphorus from hydroxyapatite*

The ICP-MS was run on the samples collected from the last day of the incubation assay (day 8) at Virginia Tech by our collaborators. The independent measurements of the solubilized phosphate concentrations showed that here also, the P400 90W-F at 600 ppm DOC solubilized the most phosphate (98.131 mg phosphorus /L, equivalent to 304.08 mg  $\text{HPO}_4^{2-}$ /L) among all the samples (Table 15). As the DOC concentration of P400 90W-F decreased, the solubilized phosphorus from HA also decreased; here, the 10 ppm DOC did not show any major effect on the solubilization of phosphate as it was close to that of water control (Table 15). The ICP-MS data are consistent with the ion chromatography data.

Note that the phosphorus values from the ICP-MS are in mg of phosphorus/mL, whereas the values from ion chromatography are reported in mg of phosphate ions ( $\text{HPO}_4^{2-}$ ).

The ICP-MS data also showed that at pH 7, there is only a small amount of phosphorus that is being solubilized; at pH 7 the highest amount of phosphorus was solubilized by the P400 90W-F at 75 ppm DOC (4.846 mg/L equivalent to 15.02 mg  $\text{HPO}_4^{2-}$ /L). The RBC 90D-F (pH 7) solubilized even less phosphorus; the highest amount of phosphorus solubilized by RBC 90D-F was at 10 ppm (2.352 mg/L equivalent to 7.288 mg  $\text{HPO}_4^{2-}$ /L) (Table 15). This is the same pattern that was observed with the ion chromatography data.

The P400 90W-F and the RBC 90D-F at a DOC concentration of 10 ppm were able to solubilize small amount of calcium (Table 15). Here also, the concentration of solubilized calcium increased as the DOC concentration increased (Table 15). Interestingly at pH 7, the filtrates that had a concentration of 75 ppm DOC achieved the greatest solubilization of calcium; the concentration of solubilized calcium then decreased as the filtrate DOC concentration increased to 300 ppm and 600 ppm (Table 15). The Ca:P mol ratio was calculated as shown in

Table C5. We observed that the highest Ca: P mol ratio is achieved when the DOC is at a concentration of 75 ppm, for both the P400 90W-F (1.308) and the RBC 90D-F (1.035) as seen in Table C5. Even at neutralized pH, the highest Ca: P mol ratio was seen in the HA incubation with filtrates at a DOC concentration of 75 ppm (Table C5). The incubation of HA with the pH-neutralized RBC 90D-F at a DOC concentration of 600 ppm had the smallest Ca: P mol ratio (0.145) (Table C5); this sample was also previously shown to have the smallest amount of solubilized phosphate and calcium (Table 15).

**Table 15: Phosphorus and calcium concentration obtained from ICP-MS from the solubilization assay on day 8 of incubation. The data shown here are solubilized phosphate (in mg of phosphorus/L) from hydroxyapatite, that is the phosphate from the biochar filtrate prior to the addition of HA was subtracted.**

DOC concentration in filtrate (mg/L)	Solubilized $^{31}\text{P}/^{44}\text{Ca}$ from HA with P400 90W filtrate in mg/L		Solubilized $^{31}\text{P}/^{44}\text{Ca}$ from HA with RBC 90D filtrate in mg/L	
	DOC pH	pH 7	DOC pH	pH 7
10	<b>3.825</b> /5.989	<b>2.327</b> /1.809	<b>3.554</b> /4.308	<b>2.352</b> /2.664
75	<b>15.388</b> /26.047	<b>4.846</b> /6.490	<b>11.675</b> /13.997	<b>2.176</b> /3.346
300	<b>57.014</b> /81.848	<b>4.257</b> /4.246	<b>38.356</b> /39.609	<b>1.561</b> /1.748
600	<b>98.131</b> /133.252	<b>4.328</b> /2.991	<b>79.772</b> /50.988	<b>1.623</b> /0.305
Water control (pH not neutralized)	P= 4.085 mg/L and Ca=7.544 mg/L			

*P400 90W VS RBC 90D in solubilizing hydroxyapatite*

At a similar DOC concentration, the P400 90W-F was significantly better than the RBC 90D-F at solubilizing phosphate. Understanding the greater efficiency of P400 90W-F in solubilizing hydroxyapatite would also help in creating a biochar with better phosphate rock solubilization capacity.

To further understand the difference between these two filtrates, the concentration of several anions was measured. Unlike the P400 90W-F, the RBC 90D-F already contained a significant amount of phosphate ( $25.94 \text{ mg HPO}_4^{2-}/\text{L} \pm 1.18$ ), sulfate and chloride prior to the introduction of hydroxyapatite (Table 16). The levels of phosphate and other anions (chloride, nitrate, and sulfate) released from the 25-mL filtrate/wash of the P400 90W biochar were not quantifiable (Table 16). It's possible that phosphate already being present in high concentration in the RBC 90D-F didn't favor the reaction to move forward and solubilize more phosphate from hydroxyapatite. In addition to phosphate, RBC 90D-F also contained some chloride, nitrate, and sulfate, whereas the P400 90W-F did not show them in detectable amounts (Table 16). The conductivity signals of the incubation assay were also recorded before and after hydroxyapatite (HA) addition, as shown in Figure C6. The signals "a", "b" and "c" previously suspected to be the organic acids generated by ozonization, disappeared after the addition of hydroxyapatite (Figure C6 B); this indicated their use in the solubilization of HA, possibly in stabilizing the metals by complexation. To further understand the difference between P400 90W-F and RBC 90D-F the concentration of certain elements was measured prior to hydroxyapatite addition and after hydroxyapatite addition. The data are presented in Table C6. The RBC 90D-F contained 20.608 ppm of magnesium (Mg) compared to the P400 90W-F that contained only 2.534 ppm (Table C6).

**Table 16: Concentration of phosphate, chloride, nitrate, and sulfate in filtrates/wash collected from the pine 400 wet-ozonized biochar (P400 90W) and the dry-ozonized rogue biochar (RBC 90D), as measured by ion chromatography. The error bars denote standard deviation of 3 replicates (n=3).**

	Phosphate (mg/L)	Chloride (mg/L)	Nitrate (mg/L)	Sulfate (mg/L)
P400 90W	NQ	NQ	NQ	NQ
RBC 90D	25.94 ±1.18	3.74 ±0.49	21.49 ±0.24	20.30 ±0.28

Calcium (Ca), zinc (Zn), potassium (K), manganese (Mn), and copper (Cu) also appeared in greater amount in RBC 90D-F than they appeared in P400 90W-F (Table C6). However, molybdenum (Mo) was more prevalent in P400 90W-F compared to the RBC 90D-F; P400 90W-F had 0.040 mg/L of Mo versus 0.003 mg/L in RBC 90D-F; (Table C6). Overall, the RBC 90D-F contained much more metals than the P400 90W-F. It's possible that a large concentration of those metals in the RBC 90D filtrate impede the solubilization of hydroxyapatite by not favoring the release of  $\text{Ca}^{2+}$ , especially at high DOC concentrations.

Furthermore, upon incubation with hydroxyapatite there is a large decrease in the concentration of Mn, Mo, Zn, Cu, Fe, K and Mg; this was not observed in the samples where the pH was neutralized prior to HA addition (Table C6). The drop in their concentration may be due to them being used in the hydroxyapatite complexation. At pH 7, there is little effect in the concentration of most metals after the HA is added, indicating that most metals may not participate in complexation at pH 7. At pH 7, manganese and zinc were the only metals where the concentration dropped significantly after the addition of hydroxyapatite; that drop was much

bigger in the incubation of HA with P400 90W-F (pH 7) than the incubation of HA with RBC 90D-F (pH 7) (Table C6). As discussed earlier, at pH 7 the P400 90W-F was able to solubilize much more phosphate than RBC 90D-F as shown previously. At pH 7, zinc and manganese may participate more in complexation than most of the other metals.

The phosphate solubilization assay showed that pH-neutralized filtrates are not as efficient at solubilizing HA. Neutralizing the pH reduced the efficiency of both P400-90W-F and especially the RBC 90D-F at solubilizing phosphate from HA. Prior to HA addition, RBC 90D-F contained large quantities of phosphate and calcium as well as other metals and anions, whereas the P400 90W-F only had them in little to negligible amount. Metals may aid the solubilization by forming complexation but too much of them could impede the solubilization process.

## CONCLUSION

Previously, we showed that the process of biochar ozonization increased the oxygen-functional groups on the biochar surfaces<sup>15, 24, 33</sup>. Here, we showed that biochar ozonization also results in an increase in the carbon-based acidic groups (likely -COOH groups) in the filtrates/washes of the biochar substances. The ozone treatment of biochar cleaves the biochar into molecular fragments; 90-minute biochar ozone treatment yielded large amounts of biochar organic acids that were shown here to dramatically increase the solubilization of hydroxyapatite even at a low DOC concentration (10 ppm). The main mechanism of the P solubilization appears to be the protonic effect. We postulate the presence of small carboxylated organic acids such as acetate as well. These small organic acids were shown in literature to be products of the degradation of humic substance by ozone<sup>102, 103</sup>. Recently, oxalic acid was shown to be more efficient than sulfuric acid at solubilizing rock phosphate<sup>105</sup>. Metals in the filtrate of ozonized biochar

substances may also help in stabilizing the released phosphate via complexation, thus favoring the solubilization of hydroxyapatite.

Further future investigation into the properties of the water-soluble ozonized biochar substances containing humic-like molecules for their potential utilization in agroecosystems would be very useful such as to unlock P from the insoluble/recalcitrant phosphate mineral phases in soils for crop plants to uptake; this approach may offer a multitude of applications that may be potentially transformative to reduce input costs such as phosphorus fertilizers and increase crop productivity, fostering economic development in rural America and across the world. Another potential application involves the possible new opportunities of utilizing ozonized biochar substances containing humic-like molecules in hydroponic farming, an ancient technique that consists in the growing and harvesting of crops without soil, using just nutrient rich liquid water.

## CHAPTER V

### OZONIZED BIOCHAR FILTRATE EFFECT ON THE GROWTH OF *PSEUDOMONAS PUTIDA* AND CYANOBACTERIA *SYNECHOCOCCUS ELONGATUS* PCC 7942

#### PREFACE

The content of this chapter has not been published. The manuscript was submitted in 2021.

Sacko, O.; Engle, N.L.; Tschaplinski, T.J.; Kumar, S.; Lee, J. W., Ozonized biochar filtrate effect on the growth of *Pseudomonas putida* and cyanobacteria *Synechococcus elongatus* PCC 7942.

Manuscript submitted for publication **2021**.

#### INTRODUCTION

The pyrolysis of biomass to biochar may produce some chemical compounds such as polyaromatic hydrocarbons (PAH's), furans, and dioxins that may be toxic to microorganisms<sup>106</sup>. The use of biochar was proposed for the remediation of soil and waste waters<sup>76,77</sup>. To be applied to soils, the toxicity effect of biochar on microorganisms needs to be investigated. Several factors including the feedstock used for pyrolysis, the temperature of pyrolysis, and the age of biochar may affect its toxic effect<sup>1,107</sup>. Smith et al (2016) showed that the water-soluble organic compounds from biochars made at high temperatures exhibit less toxicity on cyanobacteria<sup>108</sup>.

The effect of ozonization was shown to create some oxygen groups on the biochar surface, which resulted in an increase in cation exchange capacity (CEC),<sup>24,33</sup> a key property for fertilizer retention in soil; we recently showed the biochar CEC increased by up to almost 10

times upon ozonization <sup>15</sup>. Given that the innovative technique of ozone treated biochar for improved cation exchange capacity may be a scalable technique, it is important to see what possible impacts the latter would have on microorganisms in soils. *P. putida* is a common bacterium found in the plant rhizosphere, and their presence was shown to promote plant growth <sup>109, 110</sup>. Recently, there has been particular interest in the inoculation of biochar with bacteria prior to its introduction to soils and plant roots <sup>111</sup>. Some bacteria-inoculated biochars were shown to improve the soil microbial community and plant growth <sup>112-114</sup>. Our ozonized biochar may be a potential candidate for the development of bacteria-inoculated biochars; given the increased oxygen functional groups on its surface <sup>15,33</sup>, we would expect it to immobilize nutrients that can be used by soil bacteria. In addition, our ozonized biochar was shown to unlock phosphate from insoluble hydroxyapatite material <sup>33</sup>, which would enable plant roots to have easier access to usable phosphate. However, before considering the application of ozonized biochar as a bacterial inoculant, it is important to test whether the latter would be toxic or not to microbial growth. To the best of our knowledge, there is no study that has shown the effect of ozone-treated biochar on microorganisms. In this study, the effect of ozonized biochar water extractable dissolved organic carbon was tested on the growth of *Pseudomonas putida*, which is a soil environmental bacterium.

Freshwater on the land surface is an essential part of the water cycle. Allochthonous organic matter can gain access to the watershed via soil leaching. If ozonized biochar were to be applied to soil systems, the leaching from soil to freshwater would bring some ozonized biochar molecular fragments, such as the dissolved organic carbon materials, into the freshwater. Therefore, it is also important to know what effect the ozonized biochar would have on microorganisms of a freshwater ecosystem. In addition, contamination of freshwater by toxic

metals has also posed serious concerns<sup>115</sup>. Therefore, for the application of ozonized biochar as a remediation of toxic metals in freshwater to be considered, it is important to determine its effects on freshwater microorganisms. Cyanobacteria are commonly found in freshwater. In this study, we also investigated the effect of ozonized biochar water soluble organic materials on *Synechococcus elongatus* PCC 7942, a freshwater cyanobacteria. Lastly, we tested for the potential differences between the filtrate of ozonized biochars and non-ozonized biochar.

## **MATERIALS AND METHODS**

### **Biochar materials and dissolved organic carbon measurements**

For this study, three types of pine biochar materials were used (P300, P400, P500). Their production was previously reported in chapter 3. Additionally, rogue biochar (RBC)<sup>15</sup> from Oregon Biochar Solutions, was also used. All biochars were ground and sieved through a 106- $\mu\text{m}$  screen and stored in an oven at 105°C.

Each biochar was ozone treated under wet or dry conditions and their water extractable organic carbon was then collected through washing with water and filtered through a 0.2- $\mu\text{m}$  pore-size filter. The concentration of the dissolved organic carbon in the filtrate was measured in a similar manner, as described in our previous work<sup>33</sup>.

### **Toxicity Assay of biochar filtrate on *Pseudomonas putida* and *Synechococcus elongatus* PCC 7942**

Wild-type cyanobacteria *Synechococcus elongatus* PCC 7942 was taken from log-phase growth and inoculated into fresh BG-11 buffered at pH 8.0 with Tris Ethylenediaminetetraacetic acid (TES). Similarly, the wild-type *Pseudomonas putida* was inoculated into fresh Luria Broth (LB) medium buffered with Tris/Tris HCl at pH 7.0. The bioassay set-up was performed with a

similar concept as done by Smith et al. (2016)<sup>108</sup> with some modifications. The assay was done with Corning Costar 24-well plates. The total volume of liquid loaded in each well was 2500  $\mu\text{L}$ . The biochar filtrate was loaded into each well to achieve a DOC (dissolved organic carbon) concentration ranging from 0 ppm-300 ppm; the biochar filtrate (0-1000  $\mu\text{L}$ ) was mixed with milli-Q water (0-1000  $\mu\text{L}$ ) so that the combined volume did not exceed 1000  $\mu\text{L}$ . To bring the total volume up to 2500  $\mu\text{L}$ , 1500  $\mu\text{L}$  of the PCC 7942 / *P. putida* in BG-11/LB buffered medium was added to each well. If the desired DOC concentration was not able to be obtained due to the low DOC concentration, the well was left empty. The blank wells consisted of just 1500  $\mu\text{L}$  of BG-11/LB buffered medium without the cells. The set-up of the plates is shown below in Table 17. The plates inoculated with *P. putida* were incubated at 37°C and the plates inoculated with PCC 7942 were incubated at room temperature under actinic light intensity of about 20  $\mu\text{mol}/\text{m}^2/\text{s}$ .

The assay was done using the filtrates from RBC and P400 biochars. The growth of the cells was monitored by measuring the optical density using a BioTek Synergy HT multimode microplate reader at 730 nm at day 0, day 0.5, day 1, day 2, day 3, day 4, and day 5 for the *P. putida* assays. Note that this optical density is a measurement of cell scattering. 730 nm was preferred to 600 nm as longer wavelengths have less interference issues<sup>116</sup>. For that purpose, in this project, OD730 was used to reduce absorbance signals from the biochar filtrates. For the PCC 7942, the optical density was measured at 730nm every 2 days from day 0 to day 16. Before each measurement, if evaporation occurred, milli-Q water was added to replenish wells to the initial liquid level. Cells from wells were mixed by pipetting and photographs of the multi-well plates were also taken prior to each measurement. Each plate assay was done in duplicate (n=2).

**Table 17: Set-up of bioassay multi-well plates. The first three rows show the DOC concentrations (mg/L) from the biochar filtrates from low to high concentration (right to left). Row A represents the filtrates from the non-ozonized biochar treatments. Row B represents the filtrates from the dry-ozonized biochar and row C represents the filtrates from the wet-ozonized biochar filtrates. The wells labeled “0 ppm DOC” are the controls with no DOC and the wells labeled “Blank” are contain the growth medium without cells.**

	1	2	3	4	5	6
A	1500µL cells + 300 ppm (non-ozonized)	1500µL cells + 150 ppm (non-ozonized)	1500µL cells + 75 ppm (non-ozonized)	1500µL cells + 25 ppm (non-ozonized)	1500µL cells + 10 ppm (non-ozonized)	1500µL cells + 2 ppm (non-ozonized)
B	1500µL cells + 300 ppm (dry-ozonized)	1500µL cells + 150 ppm (dry-ozonized)	1500µL cells + 75 ppm (dry-ozonized)	1500µL cells + 25 ppm (dry-ozonized)	1500µL cells + 10 ppm (dry-ozonized)	1500µL cells + 2 ppm (dry-ozonized)
C	1500µL cells + 300 ppm (wet-ozonized)	1500µL cells + 150 ppm (wet-ozonized)	1500µL cells + 75 ppm (wet-ozonized)	1500µL cells + 25 ppm (wet-ozonized)	1500µL cells + 10 ppm (wet-ozonized)	1500µL cells + 2 ppm (wet-ozonized)
D			<u>Blank</u> No cells 1500 µL LB/BG11 + 1000 µL milli-Q	<u>Blank</u> No cells 1500 µL LB/BG11 + 1000 µL milli-Q	<u>0 ppm DOC</u> 1000µL milli-Q + 1500µL cells	<u>0 ppm DOC</u> 1000µL milli-Q + 1500µL cells

As a background control, the OD730 that was measured for each plate on day 0 was used. That is, OD730 measured on day 0 for each well, served as the blank for that well for the entire time of the growth assay. For that matter, the OD730 at day 0 was subtracted from the OD730

values of the same plate at day 2, 4, 6, 8, 10, 12, 14, and 16. The purpose of that was to just monitor the OD730 due to the growth of cells and not the scattering that may be due to biochar DOC particles or other interferences.

Another background control was performed to see if biochar filtrate varied over time; an assay was also performed using just the filtrates at the different DOC concentrations without bacterial cells (Figure D1). The purpose for that is because the biochar filtrates also display a wide range of absorbance that may change over time. These plates were observed over the period of the growth assay, and their OD730 were also recorded to see if any change occurred in filtrates when bacterial cells were absent. Each control plate assay was done in duplicate (n=2). The OD730 recorded for these controls did not vary over the time of the study.

### **Determination of the anions released by biochar using ion chromatography**

To determine the effect of biochar ozonization on nutrient content, the concentrations of several anions (nitrate, phosphate, sulfate, and chloride) were measured from the filtrate of ozonized biochars and the filtrate of the non-ozonized biochars. A Dionex 5000 Ion chromatography instrument packed with AG23/AS23 column of 0.4 x 250 mm was used for anion separation. 4.5 mM Na<sub>2</sub>CO<sub>3</sub>/0.8 mM NaHCO<sub>3</sub> solutions were used as mobile phase eluents. The samples were loaded on a Dionex AS 40 autosampler. The signals were detected with a conductivity detector. The data collection time of the ion chromatography was set to 30 minutes. A Thermo Scientific Dionex 7 Anion standard solution (Thermo Fisher 057590) was used to quantify the anions. For this analysis, the filtrate was collected from the 2<sup>nd</sup> wash (25mL wash) of the 1.5 g biochar. Each sample type was measured in triplicate (n=3). A standard acetic acid ACS grade was also used as a reference.

## **Identification of potential bacterial inhibitory compounds by GC-MS (at Oak Ridge National Lab)**

The presence of potential inhibitory compounds was tested for in the filtrate of the ozonized biochars (P400 90W-F, RBC 90D-F) and the non-ozonized biochar (P400 UN-F, RBC UN-F). This analysis was performed at Oak Ridge National Laboratory using GC-MS.

## **RESULTS AND DISCUSSION**

### **Dissolved organic carbon released from of ozonization of P300, P400, P500 and RBC**

The dissolved organic carbon (DOC) concentration of the biochar filtrates was measured before and after ozonization. The pristine pine biochars (P300, P400, P500) showed less DOC in their filtrate as the pyrolysis temperature increased; the pine 300 contained a total of 2.80 mg DOC/g biochar  $\pm 0.18$ , the pine 400 contained 1.96 mg DOC/g biochar  $\pm 0.31$  and the pine 500 contained 1.40 mg DOC/g biochar  $\pm 0.19$  (Figure 20). The lower temperature biochars with a more acidic pH (Figure 9) may be more water soluble, which may explain the release of more water-soluble fragments (i.e., DOC) than the higher temperature biochars that exhibit more hydrophobic characteristics <sup>117</sup>.

The ozone treated biochars had significantly more DOC in their filtrate. The wet ozonized P300 had six times more DOC materials compared to the non-ozonized P300 (Figure 20). The wet ozonized P400 released the highest DOC amount among the pine biochars with a value of 23.49 mg DOC/g biochar  $\pm 1.70$ , which was twelve times more DOC than the non-ozonized pine 400 (Figure 20). Wet-ozone treatment of P500 also generated some DOC, but only increased by a factor of 2 to 3. The dry-ozonized rogue biochar released the most DOC material (34.49 mg DOC/g biochar  $\pm 1.00$ ).

The effect of the generated DOC materials was tested on the growth of *Pseudomonas putida* and cyanobacteria *Synechococcus elongatus* PCC 7942.

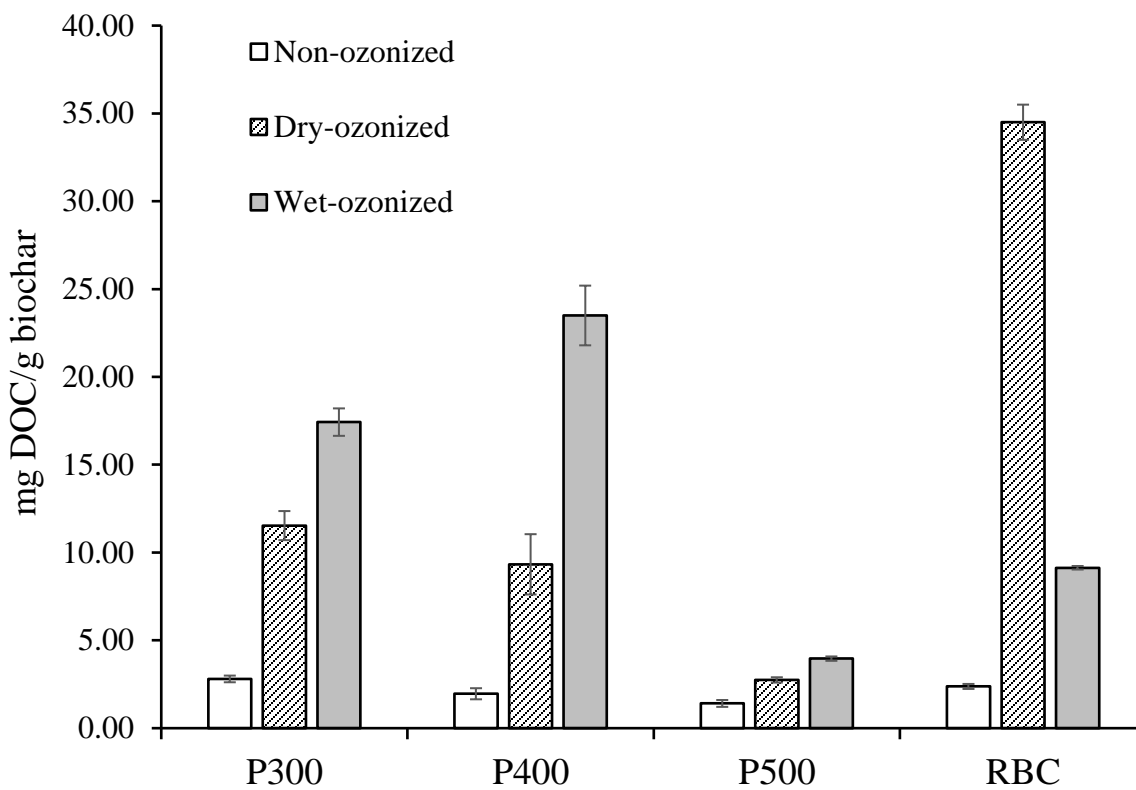


**Figure 20:** Total dissolved organic carbon measured in the filtrates of pine 300 (P300), pine 400 (P400), pine 500 (P500) and rogue biochar before and after wet/dry ozonization. The DOC amounts reported are in mg DOC/g biochar. The error bars denote the error of the average of 3 replicates measurements (n=3).

### Toxicity Assay: effect of DOC of biochar filtrates on *P. putida*

The filtrates from pine 400 biochar and rogue biochar were used for the toxicity assay as they generated the highest amount of DOC materials upon ozone treatment. In addition, the pine

400 wet ozonized biochar showed great efficiency at solubilizing phosphate from hydroxyapatite material<sup>33</sup> and the dry ozonized rogue biochar showed a high cation exchange capacity<sup>15</sup>.

Before these biochars can be considered for application into the soil, it is important to know how they would affect soil microbes.

The growth assay of *P. putida* incubation with the P400 biochar filtrate showed that the *P. putida* growth was not inhibited at any of the tested DOC concentrations of ozonized P400 filtrate and non-ozonized P400 filtrate (Figure 21). The photograph of the multi-well plates of the *P. putida* incubation with the P400 filtrates showed that there was cell growth, as seen by the turbidity of the liquid cells in each well (Figure 21). The optical density (OD730) measurements of the cells supported these observations (Figure 21B). Note that the OD730 data reported were all calculated by subtracting the scattering caused by the biochar filtrates and other particles. The OD730 from the *P. putida* incubated with the filtrates from P400 (non-ozonized, wet-ozonized, and dry-ozonized) at DOC concentrations 2-25 ppm were somewhat similar to that of the 0-ppm control. The *P. putida* incubation with the filtrates from the wet-ozonized pine 400 at high DOC concentrations also had comparable OD730 measurements to that of the control 0 ppm (Figure 21 B). The filtrate from the non-ozonized P400 did not have enough DOC, therefore that assay was limited at low DOC concentrations. The OD730 of the *P. putida* growth was also recorded daily for up to five days when incubated with non-ozonized, wet-ozonized, and dry-ozonized pine 400 biochar filtrates. The data showed that even at high DOC concentrations, the growth rate of *P. putida* was not inhibited (Figure D2, Figure D3, Figure D4).

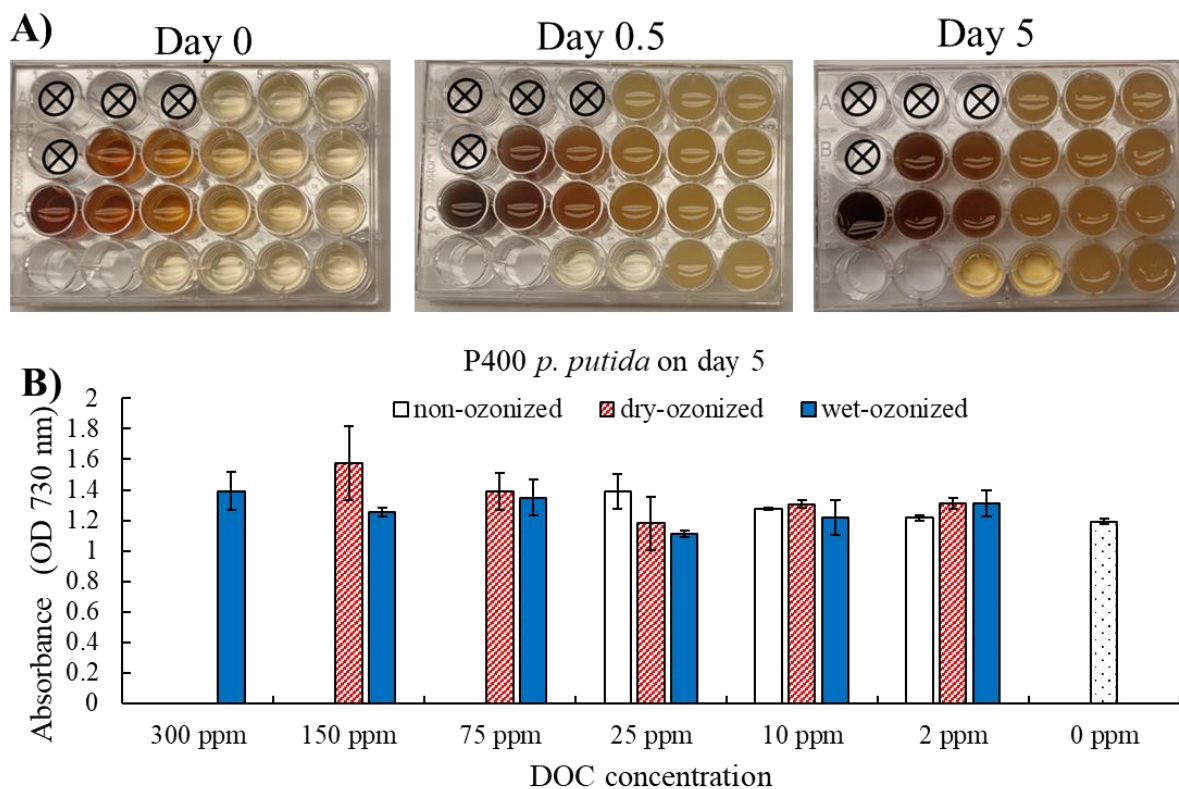


**Figure 21:** Growth of *P. putida* in incubation with filtrates from wet-ozonized, dry-ozonized, and non-ozonized pine 400 biochar at different DOC concentrations. A) Photographs of multi-well plate with P400 biochar filtrates inoculated with *P. putida* on day 0, day 0.5 and day 5 of the growth assay. The photographs shown are one of the two replicates. The set-up of the plate is shown in Table 17. B) Optical density (OD730) of *P. putida* after 5 days of incubation with P400 biochar filtrates. The error bars on the graphs represent the standard deviation of the 2 plate replicates (n=2).

The toxicity assay conducted with the filtrates from rogue biochar (RBC) also showed that *P. putida* grew at all the different DOC concentrations tested (Figure 22A). The optical density measurements confirmed these observations (Figure 22B). The RBC UN-F and RBC 90W-F did not have any effect on the growth rate of *P. putida* at the concentrations tested (Figure 22, Figure D5, Figure D6). The *P. putida* incubation with the filtrate from the dry-ozonized rogue biochar at DOC concentrations of 2 ppm and 10 ppm had similar growth to that

of the non-ozonized and wet-ozonized rogue biochar as shown by the OD730 data on day 5 (Figure 22B). At higher DOC concentrations from the dry-ozonized rogue biochar, the growth of *P. putida* was slightly stimulated; at 300 ppm DOC and 150 ppm DOC, the calculated OD730 was  $2.03 \pm 0.34$  and  $2.07 \pm 0.05$ , respectively compared to the control 0 ppm that had an OD730 of  $1.48 \pm 0.23$  (Figure 22B). The OD730 recorded daily also showed that *P. putida* grew slightly better with the dry-ozonized RBC filtrate at high DOC concentrations compared to lower DOC concentrations (Figure D7).

Low temperature-pyrolysis-produced biochars such as P400 have greater amounts of microbial inhibitory compounds, such as polycyclic aromatic hydrocarbons (PAH's), furans, volatile organic compounds, etc.<sup>106, 108</sup>. We expected the growth of *P. putida* to be inhibited by the filtrate from P400, but that was not the case. This may be because *P. putida* is capable of degrading several aromatic compounds that may be toxic to other microorganisms<sup>118</sup>.

Overall, the growth of the soil bacterium *P. putida* was not inhibited by the filtrates from the wet-ozonized pine 400 and the dry-ozonized rogue biochar. At high DOC concentrations (300 ppm), these filtrates may have some slight stimulatory effect to the growth of *P. putida*, which may be due to *P. putida* ability to degrade several aromatic compounds<sup>118</sup>.

### **Toxicity Assay: effect of DOC of biochar filtrates on cyanobacteria *Synechococcus elongatus* PCC 7942**

The effect of ozonized biochar water extractable organic carbon was tested on the growth of cyanobacteria *Synechococcus elongatus* PCC 7942 (7942). The 7942 was able to grow when incubated with filtrates from non-ozonized, wet-ozonized, and dry-ozonized pine 400 (Figure 23). At a DOC concentration of 25 ppm, the filtrate from the non-ozonized P400 (OD730  $0.72 \pm 0.05$ ) and dry-ozonized P400 (OD730  $0.77 \pm 0.02$ ) had no major effect on the growth of 7942 as

their OD730 was similar to that of the 0-ppm control ( $OD_{730} 0.72 \pm 0.11$ ) as recorded on day 16 (Figure 23).

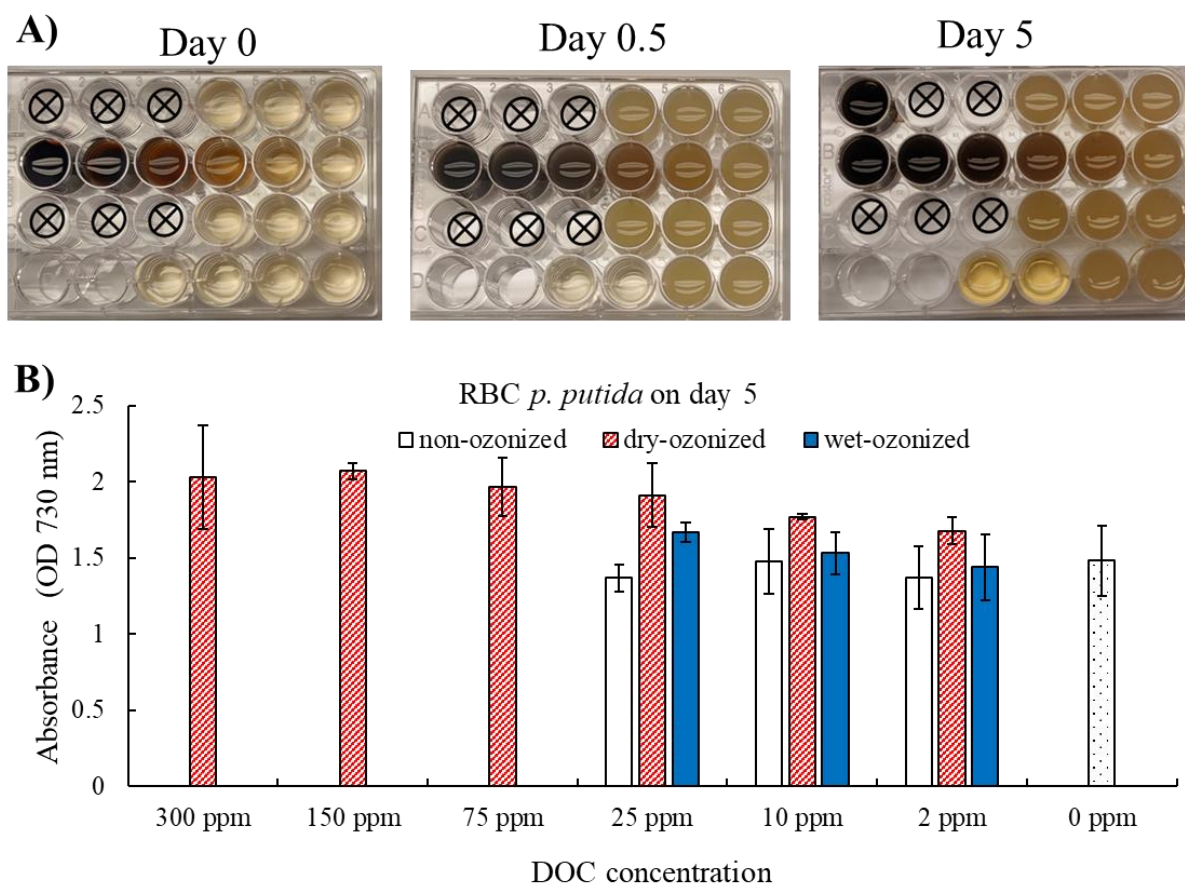


**Figure 22:** Growth of *P. putida* in incubation with filtrates from wet-ozonized, dry-ozonized, and non-ozonized rogue biochar at different DOC concentrations. A) Photographs of multi-well plate with RBC biochar filtrates inoculated with *P. putida* on day 0, day 0.5 and day 5 of the growth assay. The photographs shown are one of the two replicates. The set-up of the plate is shown in Table 17. B) Optical density ( $OD_{730}$ ) of *P. putida* after 5 days of incubation with RBC biochar filtrates. The error bars on the graphs represent the standard deviation of the 2 plate replicates ( $n=2$ ). Note: At day 5, the *P. putida* inoculated in the well with 300ppm of the dry-ozonized RBC filtrate had too much growth, therefore the content of the well was split in two wells and their  $OD_{730}$  measurements were added.

The 25-ppm DOC from the wet-ozonized P400, on the other hand, slightly stimulated the growth of 7942 with an OD730 of  $1.06 \pm 0.12$  on day 16, which was greater than the control 0 ppm (Figure 23). P400 90W-F stimulated the growth of P400 also at 75ppm DOC. However, at higher DOC concentrations (150 ppm and 300 ppm), P400 90W-F inhibited the growth of 7942 (Figure 23). The DOC extracted from the dry-ozonized P400 biochar had no major effect on the growth of 7942 at the concentrations tested (2-150 ppm DOC) (Figure 23). The growth rate was also recorded and showed that the P400 non-ozonized biochar filtrate inhibited the growth rate of 7942: from day 10 to day 14 the OD730 of 7942 incubated with non-ozonized P400 filtrate (25 ppm) was slightly less than the control 0 ppm (Figure D8). It's not until day 16 that the OD730 of the 7942 incubated with non-ozonized P400 filtrate (25 ppm) caught up to the OD730 of the 7942 incubated with the control at 0 ppm DOC (Figure D8). The 7942 incubated with the filtrate from the dry-ozonized pine 400 at 25 ppm DOC grew at the same rate as the 0-ppm control (Figure D9). 7942 incubated with the wet-ozonized P400 filtrate at 25 ppm also grew at the same rate as the 0 ppm up until day 10, then grew slightly better than the control (Figure D10). These observations indicated that at 25 ppm DOC, the non-ozonized P400 filtrate had a slight inhibition on the growth of 7942 compared to the dry and wet-ozonized P400 filtrate. It is possible that:

- 1) Some inhibitory compounds generally present in pine 400 biochar<sup>108</sup> may have been reduced upon ozonization of biochar
- 2) Ozonization of biochar have caused the release of more nutrients which may have benefited the growth of 7942

The effect of the DOC extracted from the rogue biochar was also tested. On day 16, the PCC 7942 incubated with the dry-ozonized rogue biochar filtrate at 2-25 ppm had higher OD730 reading than when 7942 was incubated with the filtrate from the wet-ozonized RBC at 2-25 ppm

and the non-ozonized RBC at 2-25 ppm (Figure 24). This indicates that at these DOC concentrations, cells grow better when incubated with the dry-ozonized rogue biochar filtrate

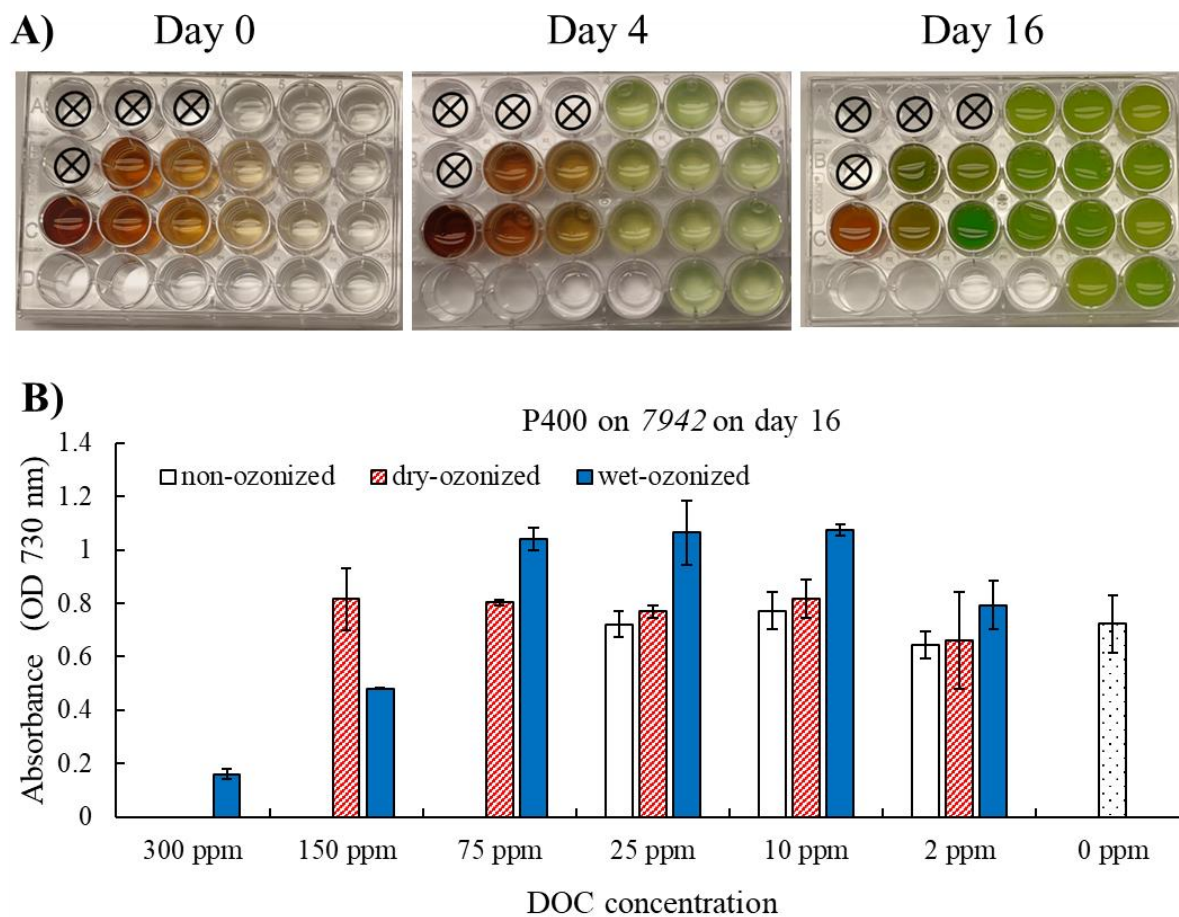


**Figure 23:** Growth of *Synechococcus elongatus* PCC 7942 (7942) in incubation with filtrates from wet-ozonized, dry-ozonized, and non-ozonized pine 400 (P400) biochar at different DOC concentrations. A) Photographs of multi-well plate with P400 biochar filtrates inoculated with 7942 on day 0, day 4 and day 16 of the growth assay. The photographs shown are one of the two replicates. The set-up of the plate is shown in Table 17. B) Optical density (OD<sub>730</sub>) of 7942 after 16 days of incubation with P400 biochar filtrates. The error bars on the graphs represent the standard deviation of the 2 plate replicates (n=2).

than with the non-ozonized rogue biochar filtrate. It's possible that dry-ozonization reduces the presence of inhibitory compounds that may be present in RBC. It's also possible that dry-ozonization caused the release of more nutrients in the filtrate of RBC. At higher concentrations (150-300 ppm), the dry-ozonized RBC filtrate inhibited the growth of 7942 (Figure 24).

Furthermore, we observed that the growth rate of 7942 was slowed by RBC UN-F (at 2-25 ppm DOC) until day 14 (Figure D11). The growth rate of 7942 was also slowed when incubated with the dry-ozonized RBC filtrate at 75 ppm for 12 days, then picked back up on day 14-16 (Figure D12). At high DOC concentrations (150-300 ppm), the dry-ozonized RBC filtrate significantly inhibited the growth rate of 7942; 7942 was still growing, but at a much slower rate than when it was incubated with the control 0 ppm DOC (Figure D12). The filtrate from the wet-ozonized RBC had a similar effect on the growth pattern of 7942 as the non-ozonized RBC; at 2-25 ppm DOC they had a slower growth than the 0-ppm control for the first 14 days (Figure D13).

The filtrate from the dry-ozonized rogue biochar (RBC 90D-F) at 300 ppm DOC was much less inhibitory to the growth of PCC 7942 than the filtrate from wet-ozonized P400 biochar at 300 ppm DOC (Figure 23, Figure 24, Figure D10, Figure D12). The rogue biochar being made at higher temperatures (700°C) may have had less inhibitory compounds to start with, compared to the pine 400 made at lower temperatures (400°C). The filtrate from dry ozonized rogue biochar at low DOC concentrations (2-25 ppm) appeared to slightly stimulate the growth of cyanobacteria PCC 7942, and have no inhibitory effect on *P. putida* at high concentrations. In addition, the dry-ozonized rogue biochar was recently characterized by our lab to be able retain and exchange cations 7-9 time more than the non-ozonized control <sup>15</sup>. These characteristics make the ozonized rogue biochar a great potential candidate for soil amendment purposes.

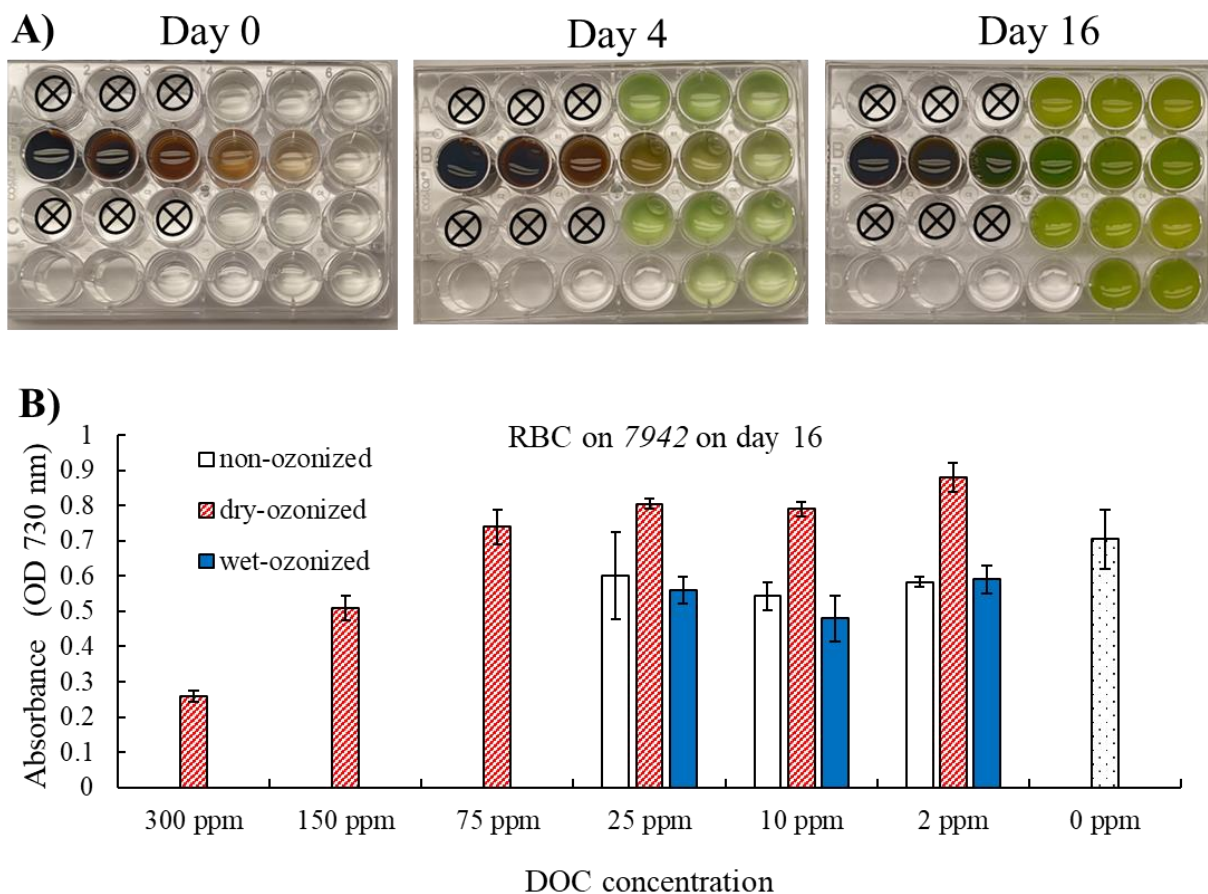


**Figure 24:** Growth of *Synechococcus elongatus* PCC 7942 (7942) in incubation with filtrates from wet-ozonized, dry-ozonized, and non-ozonized rogue biochar (RBC) at different DOC concentrations. A) Photographs of multi-well plate with RBC biochar filtrates inoculated with 7942 on day 0, day 4 and day 16 of the growth assay. The photographs shown are one of the two replicates. The set-up of the plate is shown in Table 17. B) Optical density (OD<sub>730</sub>) of 7942 after 16 days of incubation with RBC filtrates. The error bars on the graphs represent the standard deviation of the 2 plate replicates (n=2).

### Determination of the anions released by biochar using ion chromatography

In the literature, studies have shown that some biochars may contain nutrients, such as nitrate, phosphorus, ammonium that are released over time when the biochar is introduced to the soil<sup>87,88</sup>. Earlier, we hypothesized that the stimulatory effect seen in the incubation of the

bacteria with the ozonized biochar filtrates may be because of some nutrients that are released following ozonization. In this section, we tested the presence of several anions in the filtrate of biochar before and after ozonization.

We found that the filtrate from the dry-ozonized rogue biochar contained larger amounts of phosphate (32.80 mg/L  $\pm$ 0.26) and nitrate (22.75 mg/L  $\pm$ 0.20), compared to the filtrate from the wet-ozonized pine 400, where the levels were undetectable (Table 18). The release of nitrate and phosphate from the dry-ozonized rogue biochar were certainly caused by ozone treatment, given that the non-ozonized RBC only contained a small amount of phosphate (4.92 mg/L  $\pm$ 0.60) and an undetectable amount of nitrate (Table 18). Ozone treatment of rogue biochar made it more polar and water soluble, as shown by the acidic pH of the ozonized biochar in Figure 9. This may have facilitated the release of nutrients. It is possible that the extra phosphate in the filtrate of the dry-ozonized RBC favored the growth of the *P. putida* and *S. elongatus* PCC 7942 (at low DOC concentration) compared to the non-ozonized RBC. Nitrate and phosphate are important nutrients in the soil; another potential benefit of ozonized rogue biochar would be to deliver more of these nutrients in the soil upon biochar application.

Another observation made by the ion chromatography (IC) analysis was that dry ozone treatment of rogue biochar significantly decreased the amount of chloride in the filtrate (Table 2). The IC conductivity signal of the filtrates is shown in Figure D14 A. Wet-ozonized P400 filtrate showed the presence of two compounds (IC elution peaks “a” and “b”) that were not present in the non-ozonized pine 400. The exact identities of these compounds are unknown, but we suspect them to be small carboxylated molecules produced by the cleavage of biochar olefinic groups by ozone. Literature showed that under certain conditions ozone can degrade humic acids into small organic acids like formic acid, oxalic acid, acetic acid, etc<sup>102, 103</sup>. Here,

we suspect that wet ozonization of pine 400, generated some amount of these organic acids; signal “a” could be monocarboxylated organic anion like acetate <sup>104</sup>; this was previously supported as it has similar retention time with standard acetic acid (Figure D14 B).

Another hypothesis made earlier is that ozonization may reduce the amount of inhibitory compounds. Therefore, analyzing the presence of inhibitory compounds in the filtrate of biochar before and after ozonization is important.

**Table 18: Concentration of phosphate, chloride, nitrate, and sulfate concentrations in the filtrate of the non-ozonized pine 400 (P400 UN), wet-ozonized pine 400 (P400 90W), non-ozonized rogue biochar (RBC UN) and dry-ozonized rogue biochar (RBC 90D). The filtrate was obtained from the 2<sup>nd</sup> wash (25-mL) of 1.5 g biochar. The values shown are averages of 3 replicates (n=3). The conductivity signals by IC are shown in Figure D14.**

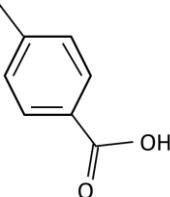
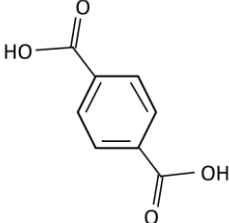
	Phosphate (mg/L)	Chloride (mg/L)	Nitrate (mg/L)	Sulfate (mg/L)
P400 UN	0	0.05 ±0.03	0	0
P400 90W	0	0.10 ±0.03	0	0
RBC UN	4.92 ±0.60	12.76 ±0.07	0	27.60 ±0.56
RBC 90D	32.80 ±0.26	4.22 ±0.32	22.75 ±0.20	22.92 ±0.76

### **Identification of bacterial inhibitory compounds by GC-MS (at Oak Ridge National Lab)**

(Note: samples were sent to Oak Ridge National Lab for analysis).

The filtrates extracted from the non-ozonized P400, wet-ozonized P400, non-ozonized RBC and dry-ozonized RBC were analyzed by GC-MS to see if they exhibited the presence of potential inhibitory compounds. Smith et al (2013) found that the toxicity of biochar water soluble organic compounds (WSOC) on algal growth was mainly caused by the presence of negatively charged groups and that these inhibitory compounds are likely to contain a carboxyl group<sup>119</sup>; these toxic compounds were particularly prevalent in pinewood-derived biochar and could originate from the degradation of lignin<sup>119</sup>. P-toluic acid was detected in non-ozonized pine 400 biochar filtrate but was not detected in wet-ozonized P400; p-toluic acid was not detected in non-ozonized rogue biochar and dry-ozonized rogue biochar filtrate (Table 19). Additionally, terephthalic acid was also detected in non-ozonized P400 filtrate but was only present in trace amounts in wet-ozonized P400 filtrate. It is possible that the effect of ozonization degraded those potential inhibitory compounds<sup>120, 121</sup>, which in turn may have helped reduce the inhibitory effect of pine 400 filtrate. Additionally, ozone has been used to degrade PAH's<sup>122</sup>. Even though we did not test for PAH's in P400, if it was present, its amount could have been reduced during the ozonization of biochar. We did not detect the presence of any major inhibitory compounds in rogue biochar before ozonization and after ozonization; these characteristics further support the application of ozonized rogue biochar as a soil amendment.

**Table 19: Detection of potential bacterial inhibitory compounds (p-toluic acid and terephthalic acid) in the filtrate of non-ozonized pine 400 (P400 UN), wet-ozonized pine 400 (P400 90W), non-ozonized rogue biochar (RBC UN) and dry-ozonized rogue biochar (RBC 90D). The detection of these compounds was done at Oak Ridge National Laboratory using GC-MS. The GC-MS spectra of the samples are shown in Figure D15 and Figure D16.**

	P-toluic acid 	Terephthalic acid 
P400 UN	(+++) detected	(+++) detected
P400 90W	(-) not detected	(+) trace amount detected
RBC UN	(-) not detected	(-) not detected
RBC 90W	(-) not detected	(-) not detected

## CONCLUSION

We previously showed that ozonization can significantly improve the CEC of biochar <sup>15</sup>. A high CEC biochar would have a greater nutrient retention capability, which is an important feature for its use as a soil amendment. Here, we conducted a toxicity assay of the filtrates from ozonized biochars on a soil bacterium (*P. putida*) and a freshwater bacterium (*S. elongatus* PCC 7942). We found that the water-soluble organic compounds from the ozone treated pine 400

biochar did not have any inhibitory effect on *P. putida*. Similarly, the filtrate from the high CEC rogue biochar<sup>15</sup> did not show any inhibitory effect on *P. putida*. On the contrary, *P. putida* slightly grew better with the filtrate from the dry-ozonized rogue biochar at high DOC concentrations.

The toxicity assay performed on the freshwater cyanobacteria *S. elongatus* PCC 7942 had different results. At low DOC concentrations (10-75 ppm), the growth of 7942 was slightly improved by wet-ozonized P400 filtrate and the dry-ozonized RBC filtrate; but at higher DOC concentration (150-300 ppm) they inhibited the growth of 7942. Additionally, we found that at a similar DOC concentration of 25 ppm, the non-ozonized P400 filtrate inhibited the growth rate of PCC 7942, but the wet-ozonized P400 filtrate did not. Furthermore, we found the presence of potential inhibitory compounds p-toluic acid and terephthalic acid in non-ozonized P400 filtrate, but only trace amounts in wet-ozonized P400 filtrate. Ozonization may have degraded these potential inhibitory compounds. Finally, we found that ozonization increased the release of phosphate and nitrate from rogue biochar, which may have provided extra nutrients for the growth of the bacteria. While many studies showed the efficiency of biochar in improving microbial life via biochar-microbe interactions<sup>123</sup>, others have shown that in the short term, biochar pores may not be a preferred habitat for microbes<sup>124</sup>. Given that the filtrate collected from ozonized biochar had no inhibitory effect on soil bacteria *P. putida*, a future and interesting study would be the use of ozonized biochar as an inoculum carrier and see how easily bacteria populate the ozonized biochar.

## CHAPTER VI

### SURVIVABILITY AND COMPETITION STUDY OF WILD-TYPE AND GENETICALLY ENGINEERED CYANOBACTERIA

#### PREFACE

Part of the content of this chapter has been published in 2020 in Applied Biosafety. Full citation of the manuscript is provided below. Reported here, is a modified version of the published work reprinted with permission from publisher. Permission is provided in Appendix F.

Sacko, O.; Barnes, C. L.; Greene, L. H.; Lee, J. W., Survivability of Wild-Type and Genetically Engineered *Thermosynechococcus elongatus* BP1 with Different Temperature Conditions.

*Applied Biosafety* **2020**, 25 (2), 104-117.

#### INTRODUCTION

Biofuels has gained particular interests as an alternative renewable energy source<sup>42, 125, 126</sup>. In the US, biofuels represented about 17% of the renewable energy sources consumption in 2020<sup>126</sup>. Biofuels are classified into generations. First generation biofuels are extracted from plants such corn, sugarcane. Its main limitation is that it produces the bioenergy from plants that are also consumable as foods and this generation of biofuels have an impact on greenhouse gas emission. The second-generation biofuels are better in that it uses nonfood feedstocks such as biomass wastes products; one of its limitations is that it would need lot of arable land, thus an indirect competition with the growth of food crops. Biofuels from algae/cyanobacteria fall in the 3<sup>rd</sup> generation since the algae do not need land to grow, there is no competition with arable land

<sup>42, 125</sup>. The limitation of the latter is that it is not as competitive in terms of energy yield when compared to fossil fuels for example. For that reason, a fourth-generation biofuels involving the bioengineering of these algae/cyanobacteria for increased productivity in addition to carbon negative effect <sup>43, 125</sup>. In addition, bioengineering of cyanobacteria can photo-autotrophically produce high value byproducts such as high alcohols <sup>43, 127</sup>. While the use of genetically engineered cyanobacteria is promising, there is a major concern about its biosafety, thus making the public opinion reserved to its use. That calls for rigorous risk assessments on the use of genetically engineered microorganisms, design of systems with great security, evidence of the benefits of these GE microorganisms and a clear communication to the public about its potential risks <sup>128</sup>. The contamination of the environment with the genetically modified organisms can pose a major biosafety and biodiversity concern. To limit such occurrence, there has been a development of biosafety-guarded mechanisms. Active containment is an efficient genetic engineering technique that uses “kill switches” such as toxin/antitoxin pairs to selectively kill the GE organisms if they were to break containment <sup>47</sup>. The use of such technique would need the “suicidal genes” to have a very tight induced promoter with low leakage for a great efficiency. Passive containment on the other hand, creates a disruption in the cell to have the latter dependent on a particular compound, not found in large quantities in natural environments; for example, this method was used to make some cyanobacteria highly dependent on very high CO<sub>2</sub> concentrations <sup>129</sup>. Therefore, if the latter breaks containment its exposure to an environment deprived of the chemicals it needs will cause it to not be able to grow <sup>129</sup>. The limitation of the passive containment mechanism is that the genetically engineered cells with the disrupted genes can pick up DNA in the environment and regain the ability to not require high amount of a particular chemical in order to grow <sup>129</sup>. Therefore, for a more efficient passive containment

mechanism, the genes participating in horizontal gene transfer can also be disrupted<sup>129</sup>.

Extremophilic bacteria are microorganisms that are able to grow in extreme environmental conditions such as high temperature, high salt concentration etc. The growth of these microorganisms thrives at these uncommon environmental conditions without needing a gene alteration. In this project, we proposed the use of the natural dependence of a microorganism to a particular environmental condition; here, we proposed the use of the thermophilic cyanobacteria *T. elongatus* BP1 that was shown to have an optimum growth at 57°C<sup>48</sup>. Being unable to grow at temperatures below 30°C<sup>48</sup>, we hypothesized that the thermophilic nature of *T. elongatus* BP1 can be used as a biosafety guarded mechanism for genetically engineered *T. elongatus* BP1 if the latter was to break containment. Given that the study involved the use of genetically engineered cyanobacteria, safety measures had to be taken and the closest to a natural environment that was able to be used for the study was the greenhouse of Old Dominion University in Norfolk Virginia. The first biosafety assessment tested the growth and survivability of GE *T. elongatus* BP1 and wild-type *T. elongatus* BP1 under greenhouse conditions in different seasons. The second biosafety assessment consisted in a competition study between GE cyanobacteria and wild-type cyanobacteria to see how the growth of other cyanobacteria is affected by the presence of GE cyanobacteria.

## **MATERIALS AND METHODS**

### **Strains of cyanobacteria and their growth conditions**

*T. elongatus* BP1 (BA000039.2) was used in this project and served as the thermophilic strain. In the lab they are grown at 45 °C under constant light source (30 μE m<sup>-2</sup> s<sup>-1</sup>) and a humidity of 50-60% RH in a Percival Environmental chamber (I66LLVLXC9). *Synechocystis*

PCC6803 is a mesophilic cyanobacteria that was grown as 25 °C on a shaking incubator. Another mesophilic cyanobacterium used in the project is *Synechococcus elongatus* PCC 7942. All the strains of wild-type cyanobacteria were grown in BG-11 liquid medium.

### **Genetic Transformation of *T. elongatus* BP1 and *Synechocystis* PCC 6803**

Wild-type *T. elongatus* BP1 was grown in liquid BG-11 media until reaching a log phase growth. The absorbance (optical density, OD at  $\lambda=730\text{nm}$ ) was then measured using a BioTek Synergy HT multimode microplate reader. The cells were then concentrated by centrifugation and resuspended in milli-Q water for a theoretical OD at  $\lambda=730\text{nm}$  of 20 (obtained by calculation) transformed with YFP-ST-R-Lipase-Tet (shown in Figure 25) vector by electroporation. 400  $\mu\text{L}$  of the concentrated cells were then mixed with 1  $\mu\text{g}$  of DNA (here, YFP-ST-R-Lipase-Tet) and electroporated at 5 kV/cm, 25  $\mu\text{F}$  and 200  $\Omega$  using a BioRad PowerPac. The cells were then transferred to 5mL of warm BG-11<sub>0</sub>SA medium, incubated for 1 day in the Percival chamber and plated on BG-11<sub>0</sub>SA agar plates with 10  $\mu\text{g}/\text{mL}$  of tetracycline antibiotic. Note that BG-11<sub>0</sub>SA is a modified BG-11 medium where potassium nitrate, was replaced with ammonium sulfate for the source of nitrogen<sup>130, 131</sup>. Nitrate is an inducer to nirA promoter gene which was used in the cassette (Figure 25). Integrative transformants colonies were then verified by PCR and inoculated in BG-11 liquid medium with tetracycline antibiotic. The *T. elongatus* BP1 transformed with YFP-ST-R-Lipase-Tet is an integrative transformant introduced in the genome at position 363134-363135; the transformant is referred to as BP1-BY20. Similarly, using the same construct (YFP-ST-R-Lipase-Tet) a transformation was performed on the *Synechocystis* PCC 6803. Given that the constructs did not have the recombination sites homologous to the *Synechocystis* PCC 6803, we did not expect integration into the genome of the *Synechocystis* PCC 6803. The following transformant was referred to as 6803-YFP.

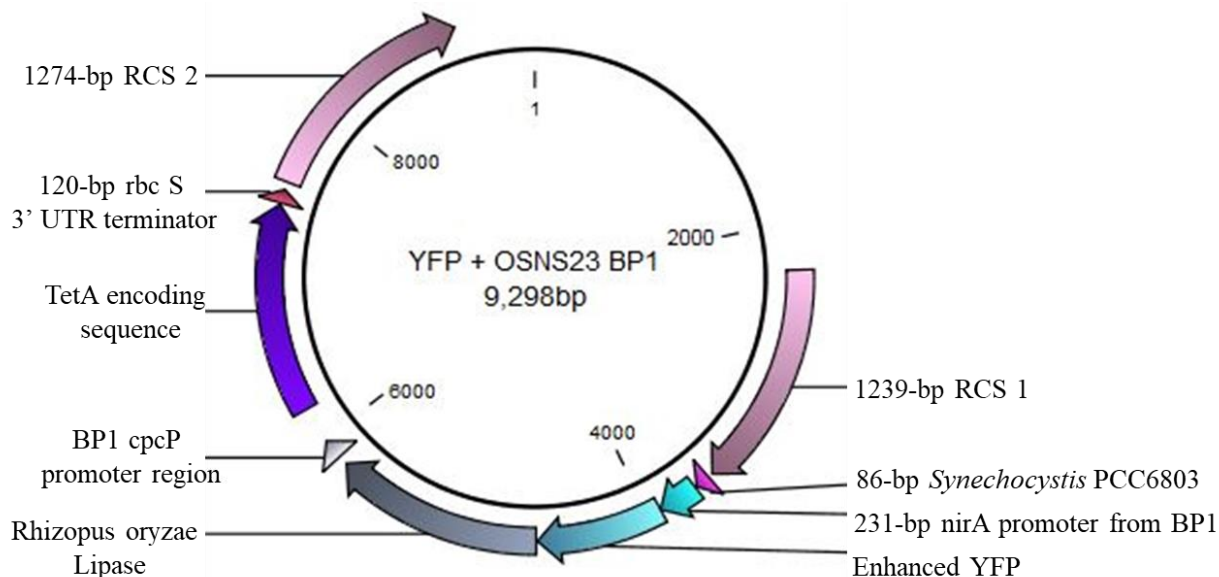


**Figure 25:** Gene map of the YFP-ST-R-Lipase construct visualized with CLC bio software. The DNA construct includes an upstream (1239 bp) and downstream (1274 bp) recombination sites, *Synechocystis* PCC 6803 nirA inducible promoter (86 bp), *T. elongatus* BP1 nirA inducible promoter (231 bp), yellow fluorescent protein molecular tag (717 bp), *Rhizopus oryzae* lipase gene (1176 bp), *T. elongatus* BP1 cpcP continuous promoter (116 bp), *Thermus thermophilus* PslpA continuous promoter (199 bp) and tetracycline resistance gene (1200 bp). The designer construct is within the pUC-SP vector containing the ampicillin resistance gene (861 bp).

### Growth study of wild-type and GE *T. elongatus* BP1, and *Synechocystis* PCC6803

Fresh cultures of wild-type *T. elongatus* BP1, wild-type *Synechocystis* PCC 6803 and GE *T. elongatus* BP1 (BP1-BY20) made for the assays in the greenhouse and incubators in the laboratory. The cell cultures were prepared in triplicate at 5E6 cells/mL and 1E7 cells/mL in BG-11 liquid medium. The liquid cultures were incubated in greenhouse or laboratory conditions for a 28-day period and the optical density at 730 nm was measured weekly. In the incubators the light source was constant, and the temperature was controlled; Percival environmental chamber was used as the incubator for the wild-type and GE *T. elongatus* BP1-BY20 and IKA KS 4000i

control incubator at 25 °C for the *Synechocystis* PCC 6803. Greenhouse conditions are more similar to a natural environment, in that there is a dark/light cycle and varied temperatures; the study was done from March 4<sup>th</sup> to April 1<sup>st</sup>, 2019, for the cool temperature and from July 1<sup>st</sup> to July 29<sup>th</sup>, 2019 for the warm temperatures. The temperature of the greenhouse was monitored using the digital temperature sensor connected to the LinkConn 1000 v 4.0 software and recorded every day at 12pm.

### **Survivability test of wild-type *T. elongatus* BP1, GE *T. elongatus* BP1-BY20 and wild-type *Synechocystis* PCC6803**

The viability of the GE *T. elongatus* BP1-BY20 cells exposed to the greenhouse conditions was tested. For the survivability assays, 0.5mL of each liquid culture was inoculated into 2.5mL of fresh liquid BG-11 culture in wells of a 24-well Costar plate in duplicate. The plates were then incubated in the Percival incubator at 45 °C under constant lighting for up to 3 weeks to see if they are able to grow; each week the plates were photographed and the optical density at 730 nm was measured. As a control, the survivability assay was also done for wild-type *T. elongatus* BP1 and wild-type *Synechocystis* PCC6803. To further quantify the viable cells, the colony forming units of the GE *T. elongatus* BP1-BY20 were measured; a quantified amount of each liquid culture was plated on BG-11 agar plates with and without tetracycline antibiotic and incubated in the Percival incubator at 45 °C. As a control the viability was also tested for the wild-type *T. elongatus* BP1.

### **Competition study between wild-type and genetically engineered cyanobacteria**

The species of cyanobacteria used in this portion were the GE *Synechocystis* PCC 6803 YFP-ST-R-Lipase or 6803-YFP initially verified as a plasmid transformant, wild-type *Synechocystis* PCC 6803 (6803), wild-type *Synechococcus elongatus* PCC 7942, GE *T.*

*elongatus* BP1 with YFP-R-Lipase construct (BY20) verified as integrative transformant and wild-type *T. elongatus* BP1. The GE cyanobacteria possess the yellow fluorescence protein but due to the low expression of the genes the latter was not able to be distinguished from the wild type by fluorescence microscopy. Due that shortcoming, the competition study was conducted using cell counting by microscopy.

#### *GE BY20 VS wild-type BP1 VS wild-type Synechocystis PCC 6803*

GE *T. elongatus* BP1 BY20 (or GE BY20) and wild-type *T. elongatus* BP1 are rod-shape cyanobacteria and can therefore be distinguished from the wild-type 6803 by microscopy. A co-culture consisting of GE. *T. elongatus* BY20 and WT 6803 was prepared with an initial starting concentration of 5E6 cells/mL where the wild-type 6803 has a slight initial advantage (60%) versus the GE BY20 (40%). Similarly, the wild-type *T. elongatus* BP1 was also co-cultured with the wild-type 6803. The co-cultures were done in triplicates. As a control, the wild-type BP1, wild-type 6803 and GE BY20 were also inoculated individually, at 5E6 cells/mL. The control liquid culture flasks were made in duplicate flasks. All the flasks were incubated in the greenhouse of Old Dominion University during wintertime, where temperature and lighting conditions varied; temperature varied from 16-26 °C and the maximum measured value of light intensity was 41.64  $\mu\text{E}/\text{m}^2/\text{s}$ . Every week for up to four weeks, the cell counting was performed on each flask in duplicate at two different dilution factors and percentage of each cell type species in the co-culture was calculated.

In order to further test the thermophilic properties of *T. elongatus* BP1 as a biosafety guarded mechanism, here a separate co-culture was done in parallel with GE *T. elongatus* BP1 BY20 (40%) and wild-type *T. elongatus* BP1 (60%). The co-culture flasks were done in triplicate and the control flasks of BY20 only and WT BP1 only were done in duplicate. Given their

similar shape under microscopy, the cells were plated on BG-11 agar with tetracycline (10µg/mL) in order to distinguish the wild-type from the GE BY20; samples from the co-cultures as well as the controls were plated with and without antibiotic after one day and four weeks of incubation in the greenhouse. Each flask was plated on agar in triplicate. At this time of year, the greenhouse temperatures varied from 16-26 °C and the maximum measured value of light intensity was 41.64 µE/m<sup>2</sup>/s.

*GE Synechocystis PCC 6803 VS wild-type Synechocystis PCC 6803 vs wild-type*

*Synechococcus elongatus PCC 7942*

GE 6803-YFP and wild-type 6803 are both round-shape mesophilic cyanobacteria. Wild-type *Synechococcus elongatus* PCC 7942 is a rod-shape mesophilic cyanobacteria and can therefore be distinguished from the wild-type 6803 and the GE 6803-YFP by microscopy. The assay was set up in a similar manner as described previously except that here the co-culture was prepared with GE 6803-YFP and wild-type 7942. The other co-culture involved wild-type 6803 and wild-type 7942. In addition to being incubated in the greenhouse during winter season (16-26°C and max light value 41.64 µE/m<sup>2</sup>/s), here a separate study was also conducted in laboratory conditions. Under laboratory conditions, the flasks were incubated at room temperature and the light source was constant at 10 µE/m<sup>2</sup>/s.

## **RESULTS AND DISCUSSION**

### **Growth and survivability of wild-type and GE *T. elongatus* BP1**

The temperature observed in the greenhouse from March 4th, 2019 to April 1st, 2019 were 15.44 °C to 25.30 °C (Figure 26), thus serving as cool temperatures; in contrast the study

conducted in the greenhouse from July 1<sup>st</sup>, 2019 to July 29<sup>th</sup>, 2019 showed warm temperatures (31.42°C to 36.27 °C) as shown on Figure 26. Also, the daylength was significantly longer (about 14hrs) during the study conducted at warm temperatures compared to the study conducted in the cool season (about 12 hrs) as shown in Table E1.

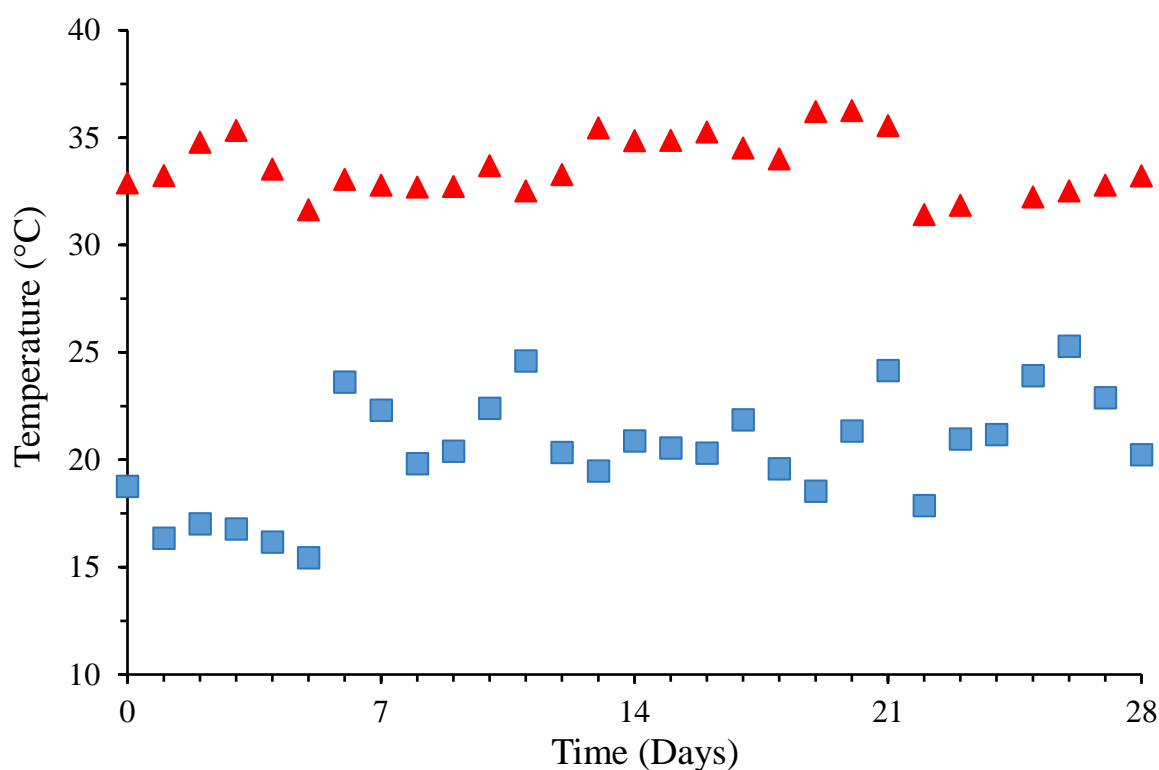


**Figure 26:** The greenhouse temperatures as recorded for the growth study during a period with cool temperatures ranging from 15.44 °C to 25.30 °C and warm temperatures ranging from 31.42°C to 36.27 °C. The cool temperatures are represented with the squares (■) and the warm temperatures are represented with the triangles (▲). The temperatures were recorded daily at noon (12:00pm) during the duration of the study. The timeframes when the temperatures were recorded were March 4<sup>th</sup>, 2019, to April 1<sup>st</sup>, 2019 (for the cool temperatures) and July 1<sup>st</sup>, 2019 to July 29<sup>th</sup>, 2019 (for the warm temperatures).

The growth of the wild-type *T. elongatus* BP1 and GE *T. elongatus* BP1-BY20 liquid cultures were monitored weekly by measuring the absorbance at 730 nm ( $O.D._{730}$ ); during cool temperatures in the greenhouse there was an overall steady decrease in the average  $O.D._{730}$  over the 28-day period for the wild-type and GE *T. elongatus* BP1-BY20 cultures in greenhouse conditions (Figure 27). In contrast, the control liquid cultures were incubated in the Percival incubator at 45 °C showed growth over the 4-week period. This showed that neither the wild-type *T. elongatus* BP1 nor the GE *T. elongatus* BP1-BY20 cells can grow in cool temperatures ranging from 15.44 °C to 25.30 °C.

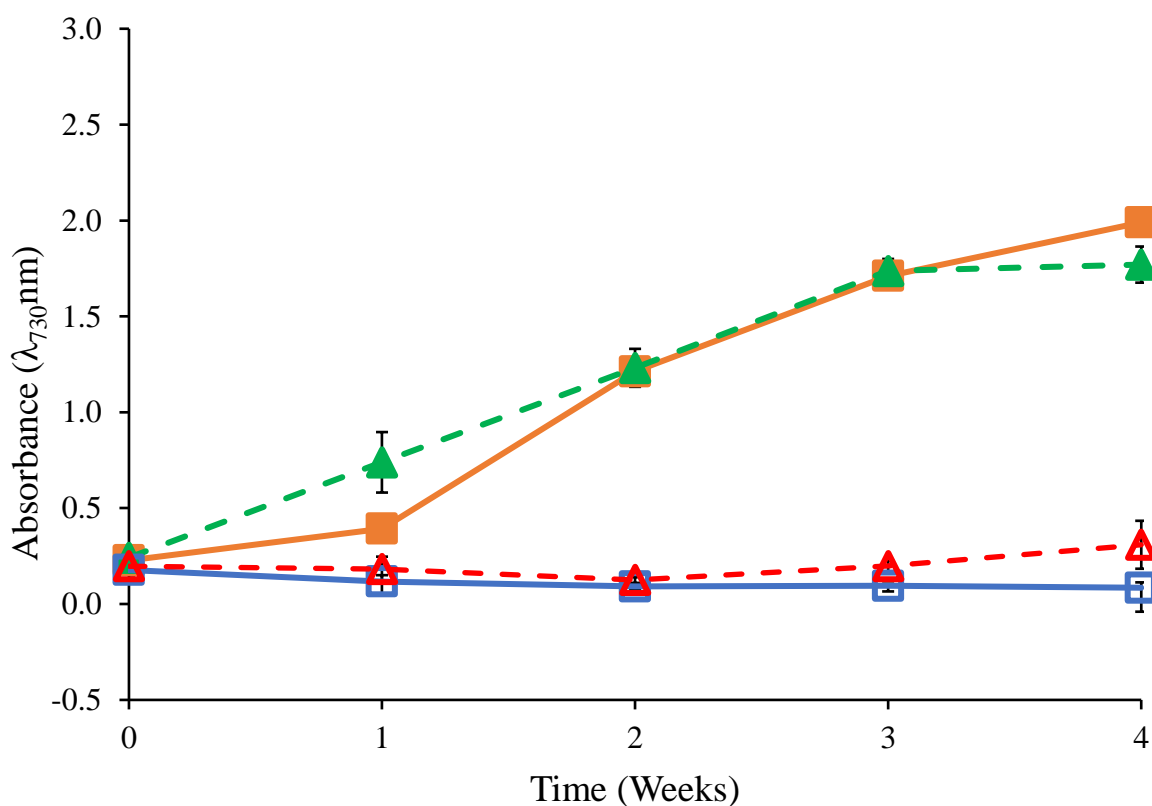


**Figure 27:** Optical Density of wild-type and GE *T. elongatus* BP1 (BP1-BY20) cultures at  $1 \times 10^7$  cells/mL during cool temperatures (15.44 °C to 25.30 °C) monitored weekly during a 4-week period in the greenhouse. Control cultures were grown in the Percival environmental chamber

(~42.2°C). The results shown here are liquid culture absorbance measurements at 730 nm in duplicates for each replicate (n=6). The graph is displayed as follows: (■) is wild-type *T. elongatus* BP1 in Percival, (□) is wild-type *T. elongatus* BP1 in greenhouse, (▲) is the GE *T. elongatus* BP1-BY20 in Percival, and (△) is the GE *T. elongatus* BP1-BY20 in greenhouse. Wild-type *T. elongatus* BP1 = solid lines, BP1-BY20 = dashed lines, closed symbols = control set and open symbols = greenhouse set.

The survivability study with the BP1-BY20 showed that the liquid cultures that were previously exposed to the greenhouse conditions for 1 week were able to recuperate upon returning to the Percival (45°C) conditions (Figure 28, Figure 29). The wild-type *T. elongatus* BP1 used in that set was also able to grow back after one week of exposure to the greenhouse conditions (Figure 28, Figure 29). After 2 weeks of the greenhouse treatment, the neither the wild-type nor the GE BP1-BY20 cells were able to grow back, possibly indicating complete death of the cells (Figure 28, Figure 29). Surprisingly, the BP1-BY20 that had an initial lower cell density ( $5 \times 10^6$  cells/mL) was not able to recuperate even after 1 week of greenhouse exposure (data not shown). This observation indicated that the survivability of the cells is also dependent on the initial concentration of the cell liquid cultures. This is also consistent with a previous study on the effects of initial cell density on cyanobacterial growth and proliferation.<sup>132</sup>

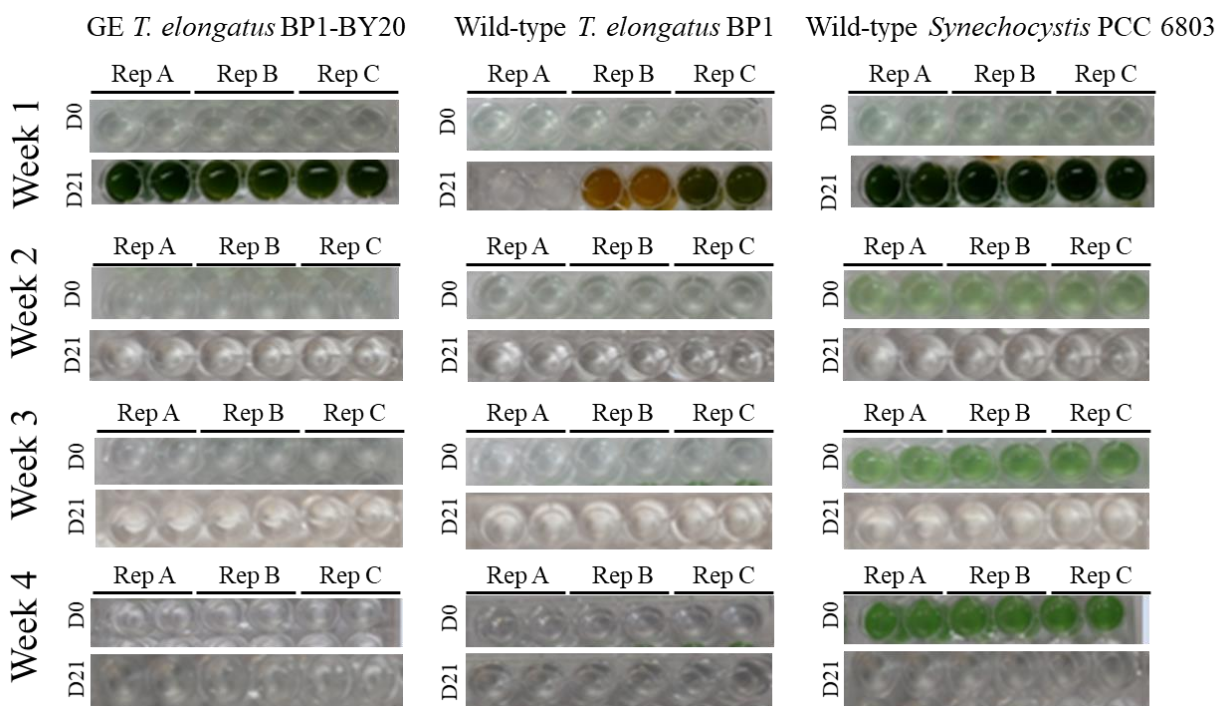


**Figure 28:** Survivability assay for wild-type *T. elongatus* BP1, wild-type *Synechocystis* PCC 6803 and GE *T. elongatus* BP1-BY20 cultures at  $1 \times 10^7$  cells/mL during cool temperatures (15.44 °C to 25.30 °C) in the greenhouse. A sample of each replicate was inoculated in fresh BG-11 media after 1, 2, 3 and 4 weeks in greenhouse in duplicates and placed in the Percival environmental chamber (~42.2 °C) for 21 days. The pictures of the multi-well plates were taken on day 0 and after 21 days in the Percival environmental chamber (~42.2 °C).

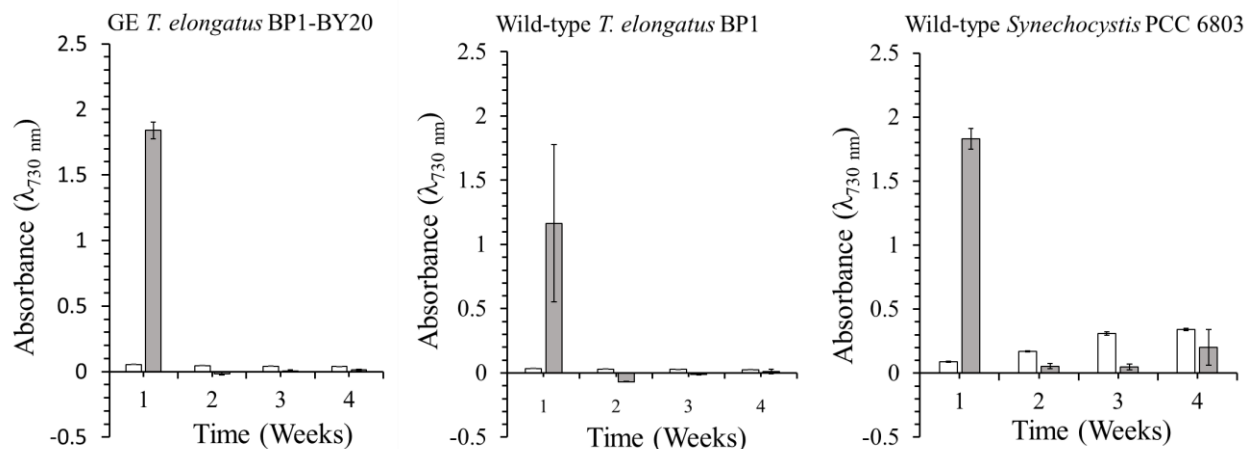


**Figure 29:** Optical density ( $\lambda=730$  nm) of survivability assay for wild-type *T. elongatus* BP1, wild-type *Synechocystis* PCC6803 and GE *T. elongatus* BP1-BY20 cultures at  $1 \times 10^7$  cells/mL during cool temperatures ( $15.44$  °C to  $25.30$  °C) in greenhouse conditions. A sample of culture after 1, 2, 3 and 4 weeks in greenhouse was inoculated in fresh BG-11 media and placed in the Percival environmental chamber ( $\sim 42.2$  °C) for 3 weeks. The growth was monitored by measuring the optical density ( $\lambda=730$  nm) weekly. The results are shown as the mean value of duplicate measurements of each replicate culture ( $n=6$ ). The error bars denote the standard deviation ( $n=6$ ). The graph is displayed as follows: white bar (□) = OD<sub>730</sub> before placed in Percival chamber and grey bar (■) = OD<sub>730</sub> after 21 days in Percival chamber.

To test the viability of the GE *T. elongatus* BP1-BY20 cells, samples were plated on BG-11 agar. As expected, the GE *T. elongatus* BP1-BY20 sample that was previously exposed to the greenhouse conditions for 28 days did not develop any colony-forming units on the BG-11 agar plates under the Percival ( $45^\circ\text{C}$ ) temperature and lighting conditions, whether the initial cell concentration was high ( $1 \times 10^7$  cells/mL) or low ( $5 \times 10^6$  cells/mL) as shown in Figure 30.

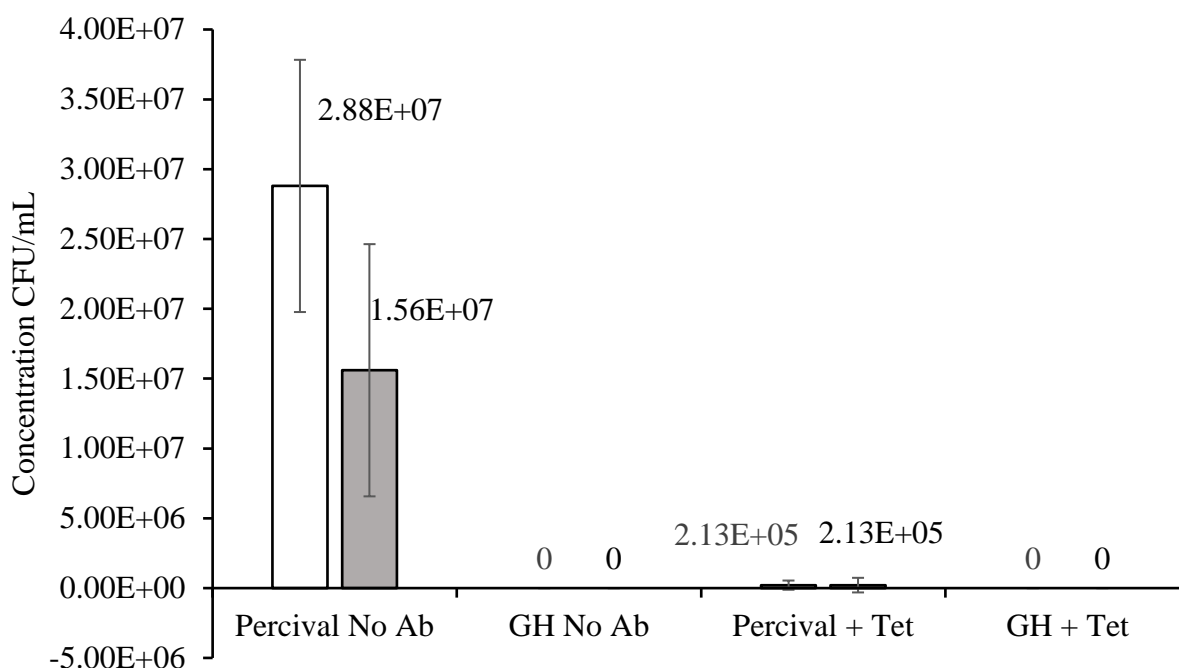


**Figure 30:** Colony-forming units (CFU) for the GE *T. elongatus* BP1-BY20 cultures during cool temperatures (15.44 °C to 25.30 °C) in greenhouse conditions (GH) and its associated control set for cultures incubated in the Percival incubator at 45 °C in (Percival). A sample from the liquid cultures was plated on BG-11 agar plates with tetracycline antibiotic (Tet) and without antibiotic (No Ab) after 1 and 28 days and placed in the Percival chamber (45 °C) for 2 weeks. The colonies were counted, and the dilution factor was applied to obtain the CFU of each flask. The results are shown as the mean value of duplicate measurements of each replicate culture (n=6). The error bars denote the standard deviation (n=6). The graph is displayed as follows: white bar (□) = at  $5 \times 10^6$  cells/mL and grey bar (■) =  $1 \times 10^7$  cells/mL.

On the other hand, the control set associated with the GE BP1-BY20 that was incubated in the Percival environmental chamber at 45°C for 28 days showed growth in O.D. <sub>730nm</sub> measurements, as expected, after 1 week, 2 weeks, 3 weeks, and 4 weeks under the Percival (45 °C) temperature and lighting conditions (data not shown). The control set also showed colony-forming units on the control BG-11 agar plates as well as the tetracycline-containing BG-11 agar plates; however, the BP1-BY20 CFU number decreased on the tetracycline plate which may be

due to an instability of the construct in the cyanobacteria (Figure 30).

The growth, survivability and viability quantification of the cells was also conducted in the greenhouse during a warmer season (from July 1<sup>st</sup> to July 29<sup>th</sup>, 2019). During that timeframe, the greenhouse temperature ranged from 31.42°C to 36.27°C as seen in Figure 2. The wild-type and GE *T. elongatus* BP1-BY20 were not actively growing as indicated by the O.D.<sub>730nm</sub> data in Figure 31. In order to test the presence of viable cells, the survivability test was conducted and showed that the 1, 2, and 3-week greenhouse incubated liquid cultures of GE *T. elongatus* BP1-BY20 were able to recuperate when inoculated in fresh BG-11 medium and incubated in the Percival chamber (45 °C) under constant lighting (Figure 32, Figure 33).

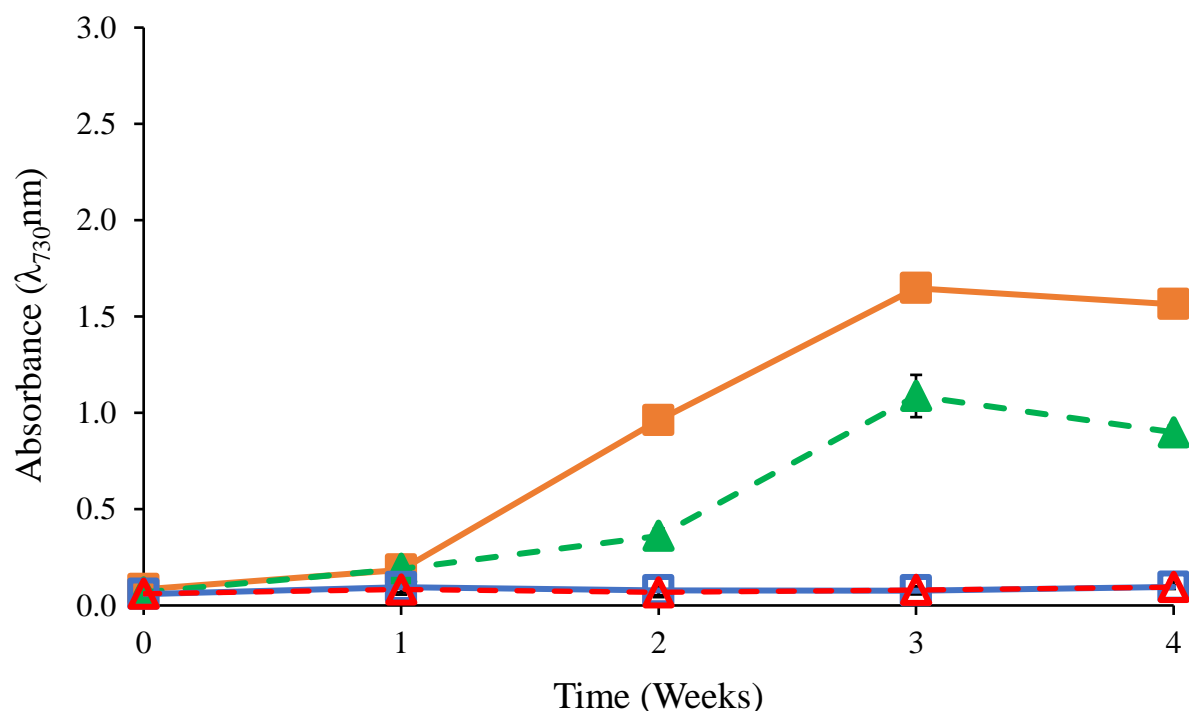


**Figure 31:** Optical Density of wild-type and GE *T. elongatus* BP1 (BP1- BY20) cultures at  $1 \times 10^7$  cells/mL during warm temperatures (31.42°C to 36.27°C) monitored weekly during a 4-week period in the greenhouse. Control cultures were grown in Percival environmental chamber

(~42.2°C) in Percival incubator. The results shown here are liquid culture absorbance measurements at 730 nm in duplicates for each replicate (n=6). The graph is displayed as follows: (■) is wild-type *T. elongatus* BP1 in Percival, (□) is wild-type *T. elongatus* BP1 in Greenhouse, (▲) is the GE *T. elongatus* BP1- BY20 in Percival, and (△) is the GE *T. elongatus* BP1- BY20 in Greenhouse. Wild-type *T. elongatus* BP1 = solid lines, BP1- BY20= dashed lines, closed symbols = control set and open symbols = greenhouse set.

In order to quantify the number of viable cells over time, the cell liquid cultures were plated on BG-11 Agar plates and the colony-forming units were measured after returning to the Percival (45°C) temperature and lighting conditions. The GE *T. elongatus* BP1-BY20 sample that was previously exposed to the greenhouse conditions for 28 days (4 weeks) showed a small number of colony-forming units (Figure 34). Based on the liquid culture volume plated on BG-11 agar plates, the number of viable cells in the GE *T. elongatus* BP1-BY20 sample that was previously exposed to the greenhouse conditions for 28 days was determined to be  $5.78 \times 10^5$  and  $2.34 \times 10^5$  viable cells/ml as calculated from the number of colonies observed on the control BG-11 agar plates and on the tetracycline BG-11 agar plates, respectively. This result indicates that only about 2 to 5 % of the initial cell population ( $1 \times 10^7$  cells/mL) remained viable after the 28 days of greenhouse exposure. In addition, the low population of viable cells may explain why the multi-well survivability assay did not show recuperation for the BP1-BY20 sample that had been exposed to greenhouse condition for 4 weeks of (Figure 31, Figure 32). The low-density cell liquid cultures (initial concentration of  $5 \times 10^6$  cells/mL) didn't have any viable cell after 28 days in the greenhouse (Figure 34), thus further supporting that the initial cells density has an influence on the cells' survivability.

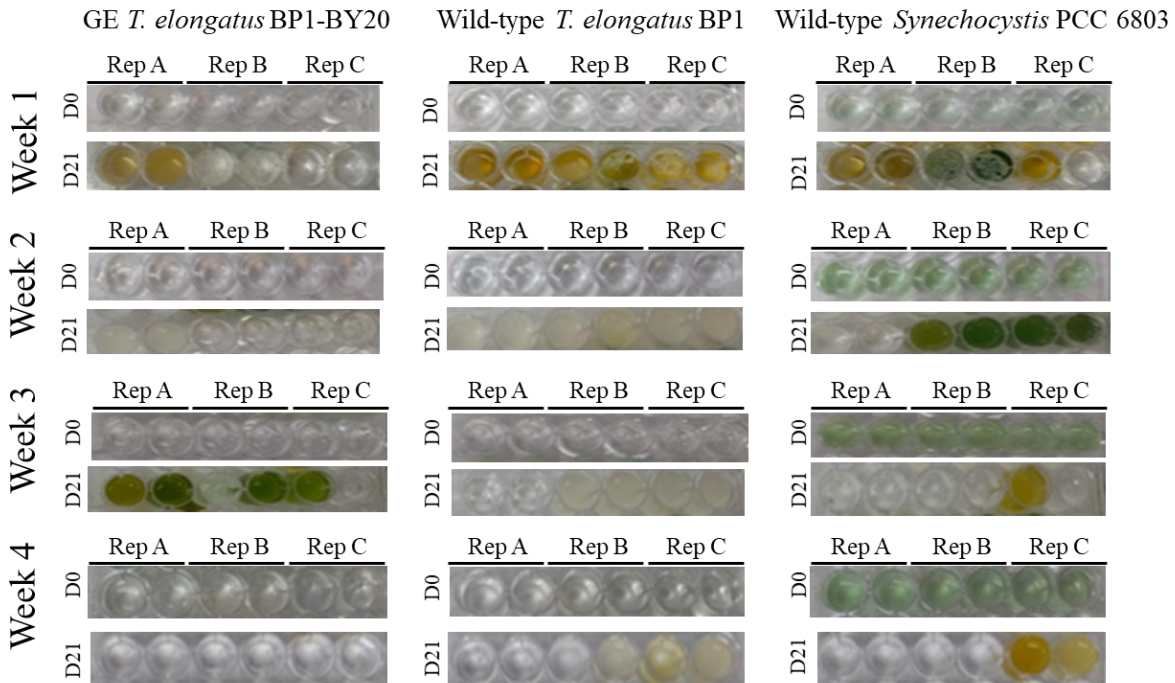


**Figure 32:** Survivability assay for wild-type *T. elongatus* BP1, wild-type *Synechocystis* PCC 6803 and GE *T. elongatus* BP1- BY20 cultures at  $1 \times 10^7$  cells/mL during warm temperatures (31.42 °C to 36.27 °C) in the greenhouse. A sample of each replicate was inoculated in fresh BG-11 media after 1, 2, 3 and 4 weeks in greenhouse in duplicates and placed in the Percival environmental chamber (~42.2 °C) for 21 days. The pictures of the multi-well plates were taken on day 0 and after 21 days in the Percival environmental chamber (45 °C).

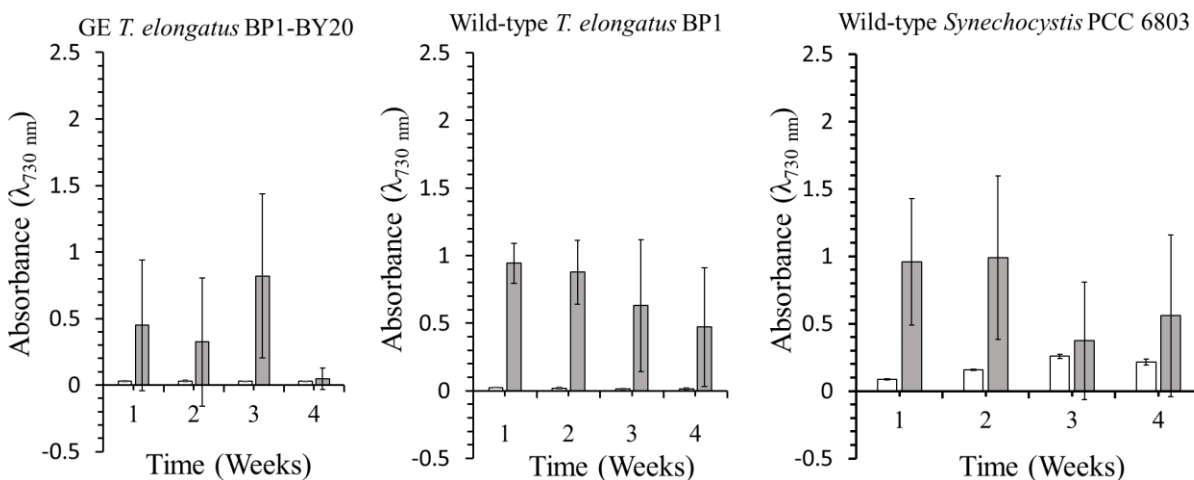


**Figure 33:** Optical density ( $\lambda=730$  nm) of survivability assay for wild-type *T. elongatus* BP1, wild-type *Synechocystis* PCC6803 and GE *T. elongatus* BP1- BY20 cultures at  $1 \times 10^7$  cells/mL during warm temperatures ( $31.42$  °C to  $36.27$  °C) in greenhouse conditions. A sample of culture after 1, 2, 3 and 4 weeks in greenhouse was inoculated in fresh BG-11 media and placed in the Percival environmental chamber ( $45$  °C) for 21 days. The growth was monitored by measuring the optical density ( $\lambda=730$  nm) weekly. The results are shown as the mean value of duplicate measurements of each replicate culture ( $n=6$ ). The error bars denote the standard deviation ( $n=6$ ). The graph is displayed as follows: white bar (□) = OD<sub>730</sub> before placed in Percival chamber and grey bar (■) = OD<sub>730</sub> after 21 days in Percival chamber.

The growth study, survivability multi-well plates and BG-11 agar plate results suggest that the genetic transformation of wild-type *T. elongatus* BP1 with the YFP-ST-R-Lipase-Tet construct does not influence the cells overall viability; both the wild-type and the GE *T. elongatus* BP1-BY20 cells cannot live in cool temperatures (here  $15.44$  °C to  $25.30$  °C). This data also supports the initial finding of Yamaoka *et al* in that *T. elongatus* BP1 actively grows at temperature ranging from  $40$  to  $57$  °C.<sup>48</sup> During warmer greenhouse temperatures ( $31.42$ °C to  $36.27$  °C) the wild-type and GE *T. elongatus* BP1-BY20 are unable to actively grow however some cells remain alive for up to 4 weeks. In order to ensure a total death of the cells, in the event of an escape of the GE cyanobacteria, other methods may deem necessary.

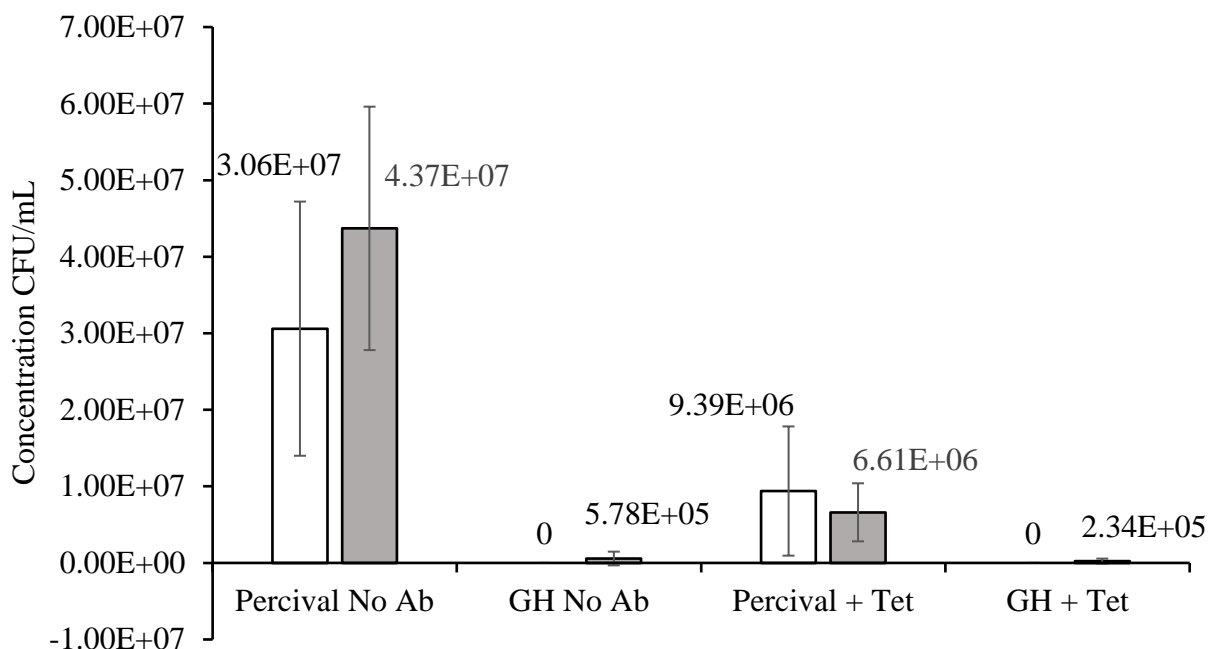


**Figure 34:** Colony-forming units (CFU) for the GE *T. elongatus* BP1-BY20 cultures during warm temperatures (31.42 °C to 36.27 °C) in greenhouse conditions in (GH) and its associated control set for cultures incubated in the Percival incubator at 45 °C in (Percival). A sample from the liquid cultures was plated on BG-11 agar plates with tetracycline antibiotic (Tet) and without antibiotic (No Ab) after 1 and 28 days and placed in the Percival environmental chamber (45 °C) for 2 weeks. The colonies were counted, and the diluted factor was applied to obtain the CFU of each flask. The results are shown as the mean value of duplicate measurements of each replicate culture (n=6). The error bars denote the standard deviation (n=6). The graph is displayed as follows: white bar (□) = at  $5 \times 10^6$  cells/mL and grey bar (■) =  $1 \times 10^7$  cells/mL.

### Competition study between GE cyanobacteria and wild-type cyanobacteria

The previous study showed the growth of the GE cyanobacteria *T. elongatus* BP1 at different temperatures. Bacteria being microorganisms living in communities, their growth may be affected by the growth of other microorganisms already present. In order to know how the growth of GE cyanobacteria is affected in presence of other cyanobacteria species, the competition study was conducted. The objective was to mimic a potential “escape” of the GE cyanobacteria into a wild-type cyanobacteria population and see if the latter would outcompete,

coexist and or be outgrown by the wild-type.

The first competition study conducted involved the GE *T. elongatus* BP1 BY20 used previously, the wild-type *T. elongatus* BP1 and the wild-type *Synechocystis* PCC 6803. In order to further test the thermophilic properties of *T. elongatus* BP1 as a biosafety guarded mechanism, the following competition study was only conducted in the greenhouse during the cool season.

We hypothesized that the GE *T. elongatus* BP1 BY20 has no competitive advantage compared to the thermophilic wild-type *T. elongatus* BP1 or other mesophilic cyanobacteria. In this study, the cocultures and controls were incubated in the greenhouse of Old Dominion University, from the 31<sup>st</sup> of January 2019 to the 28<sup>th</sup> of February 2019. The data showed that the GE *T. elongatus* BP1 BY20 was able to maintain its ratio with wild-type 6803 for up to two weeks (Figure 35 A).

After two weeks, the GE BP1 BY20 was outgrown by the wild-type 6803; the relative percentage of GE BP1 BY20 dropped from 34.5% (on week 2), to 3.9% (on week 3), and then to 1.8% (on week 4) as shown in Figure 35 A.

The wild-type *T. elongatus* BP1 also showed a similar pattern as shown in Figure 35 B; the WT BP1 cells introduced to the WT 6803 cells population were not able to coexist during the cool season in the greenhouse and lost ground to WT 6803 after 3-4 weeks of incubation (Figure 35 B). In addition, the rates at which the BY20 and the WT BP1 are being outgrown by the WT 6803 are similar. That implies that genetically altering *T. elongatus* BP1 to BY20 did not affect the competitiveness of the cells. The presence of GE *T. elongatus* BY20 neither inhibited nor stimulated the growth of wild-type 6803. The control set, where the cells were not co-cultured,

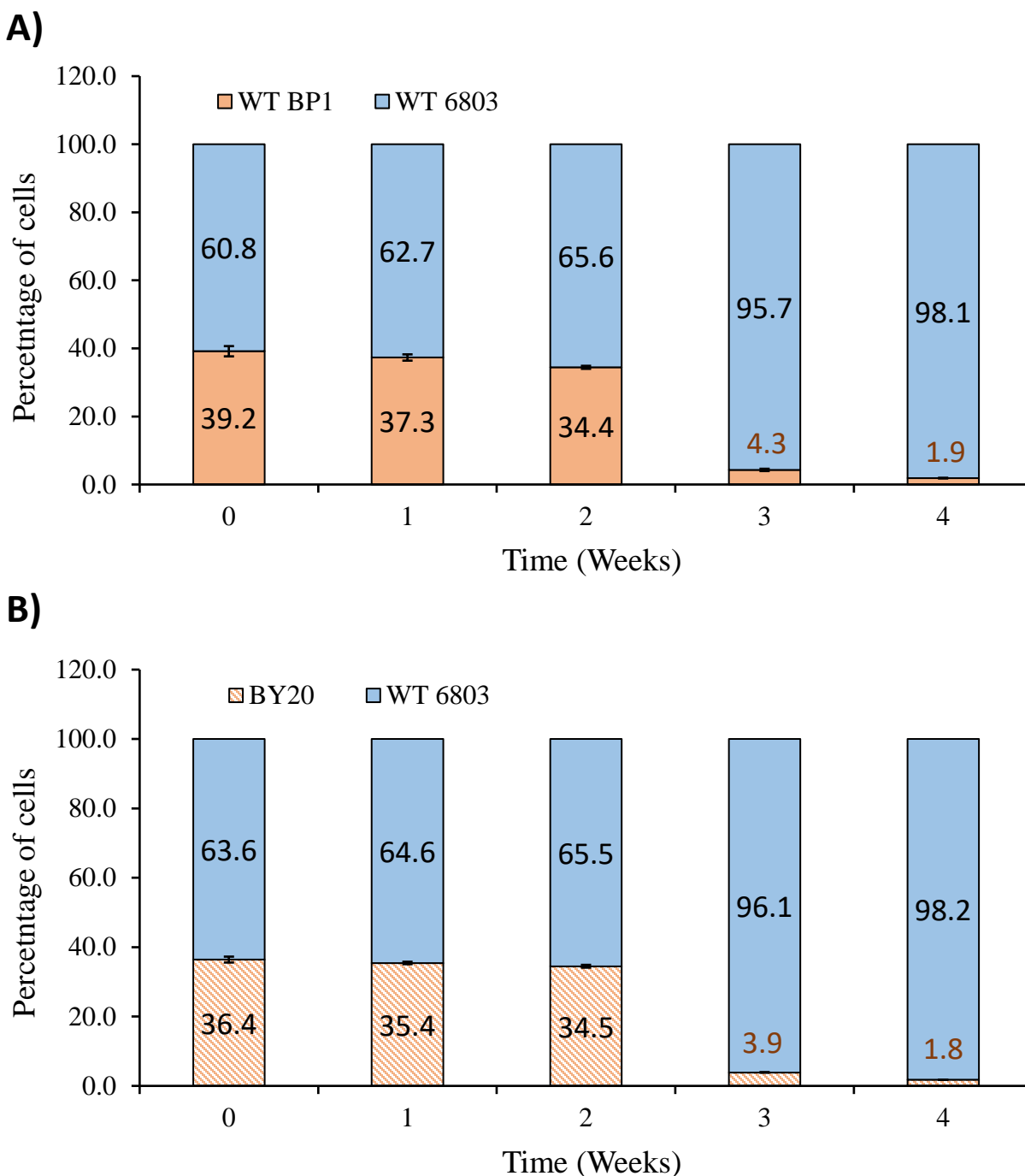


**Figure 35:** The relative percentage of cells in the coculture over a 4-week incubation in the greenhouse during the cool season (16-26°C) between the GE *T. elongatus* BP1 BY20 (BY20) and WT *Synechocystis* PCC 6803 in A and WT *T. elongatus* BP1 (WT BP1) and WT *Synechocystis* PCC 6803 in B. The error bars denote the standard deviation of the percentage cells in three liquid cultures, each counted twice (total n=6).

as expected, showed that the BY20 and the WT BP1 did not grow in the greenhouse during the cool season (Figure E1); WT 6803 on the other hand showed a gradual growth over the course of the 4-week greenhouse incubation going from  $2.6 \times 10^6$  cells/mL ( $\pm 7.6 \times 10^5$  cells/mL) on day 1, to  $5.0 \times 10^7$  cells/mL ( $\pm 4.8 \times 10^6$  cells/mL) on week 4 (Figure E1).

A co-culture of WT *T. elongatus* BP1 and GE *T. elongatus* BP1 BY20 was also incubated in the greenhouse at cool temperatures (16°C-26°C). The plating of the co-culture with and without tetracycline indicated that after 4 weeks of greenhouse incubation, there were no viable GE BY20 or WT BP1 (Table E2). That data also supports the previous findings, in that 4 weeks of incubation in cool greenhouse temperatures results in total death of WT and GE *T. elongatus* BP1.

The study conducted here supports the previous finding reported in the growth and survivability of GE and *T. elongatus* BP1 BY20. The thermophilic nature of *T. elongatus* BP1 may be used as a biosafety guarded mechanism during the cool season. During cool seasons (16°C-26°C), in the event of a potential escape of GE *T. elongatus* BP1 into a mesophile population of cyanobacteria, the GE *T. elongatus* BP1 being unable to grow at these temperatures is quickly outgrown by the mesophilic cyanobacteria.

The testing of competitive advantage of cyanobacteria exposed to a more natural environment is very important. In fact, the mimic of a potential escape from a bioreactor would result in an exposure to natural conditions. In a similar approach, a second competition study was conducted between the GE *Synechocystis* PCC 6803-YFP, the wild-type *Synechocystis* PCC 6803 and the wild-type *Synechococcus elongatus* PCC 7942 in the greenhouse during the cool season. In this study, the cocultures and controls were incubated in the greenhouse of Old Dominion University, from the from the 28<sup>th</sup> of January 2019 to the 25<sup>th</sup> of February 2019. All

these strains being mesophiles, we did not expect the cells to die, therefore we could monitor the cell relative percentage in the co-culture over the course of the study. In addition, a similar set was simultaneously conducted under laboratory conditions (room temperatures and constant lighting conditions) to serve as a control. The data showed that under cool greenhouse conditions (16-26°C), the 6803-YFP represented about 39.2% in the co-culture on day 1 (week 0) and gradually increased to 45.1% on week 4 (Figure 36). Even though this is very negligible decline in WT 7942 percentage, this indicates that 6803-YFP grows slightly better when co-cultured with WT 7942 under cool conditions; but 4 weeks is not enough for 7942 to lose ground to 6803-YFP. In the co-culture involving the wild-type 6803 and the wild-type 7942, we observed a similar pattern; the wild-type 6803 started at 41.4% on day 1 (week 0) and steadily increased to 58.4% on week 4 (Figure 36). Here, surprisingly, the wild-type 6803, unlike the 6803-YFP, dominated the co-culture after a 4-week incubation period. In Figure E2, the control liquid cultures where the cells were incubated individually showed that all cell types were able to grow in the greenhouse during the cool season. The WT 6803 did not grow at a faster rate compared to the WT 7942 or the 6803-YFP when incubated individually (Figure E2). Therefore, that supports that the WT 6803 has a competitive advantage to the WT 7942 when incubated in the greenhouse during cool temperatures.

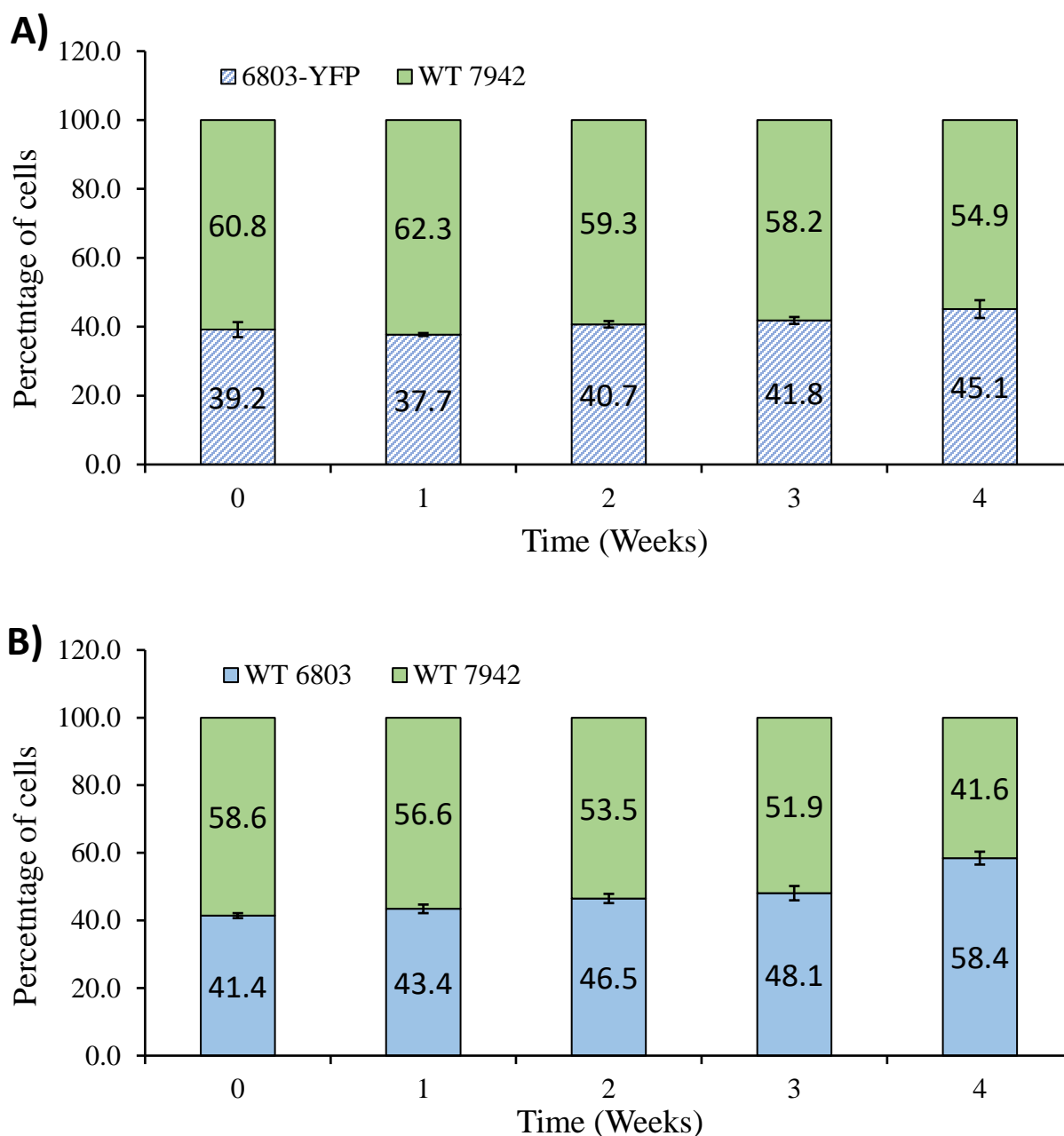


**Figure 36:** The relative percentage of cells in the coculture over a 4-week incubation in the greenhouse during the cool season (16-26°C) between the GE *Synechocystis* PCC 6803-YFP (6803-YFP) and WT *Synechococcus elongatus* PCC 7942 (WT 7942) in A; WT *Synechocystis* PCC 6803 (WT 6803) and WT *Synechococcus elongatus* PCC 7942 (WT 7942) in B. The error bars denote the standard deviation of the percentage cells in three liquid cultures, each counted twice (total n=6).

The control set that was conducted under laboratory conditions showed that when incubated at room temperature, the 6803-YFP maintains its ratio over the 4-week incubation period in the co-culture with WT 7942; 6803-YFP represented 41% and 40.5% of the coculture with wild-type 7942 on day 1 and week 4, respectively (Figure 37 A). Similarly, the WT 6803 when co-cultured with WT 7942, also maintained its percentage over time; the WT 6803 represented 39.3% and 40.3% of the total coculture cell population on day 1 and week 4, respectively (Figure 37 B). The control set showed that all cell species were able to grow under laboratory conditions (Figure E3).

Under laboratory conditions, when not subject to cold temperature stressors, the GE 6803-YFP and WT 7942 are able to coexist. Similarly, under the same conditions, the WT 6803 and the WT 7942 are also able to coexist as they grow at the same rate and neither species showed a competitive advantage to the other.

While these competition studies are based on cell counting method where both live and dead cells are taken into account, the data strongly supports that cool greenhouse temperatures provide a competitive advantage to wild-type and GE *Synechocystis* PCC 6803 compared to *Synechococcus elongatus* 7942. It is important to test the direct evolution of the GE cyanobacteria in a mixed population of other bacteria. Additionally, further enhancing of the expression of the selectable markers (here, the yellow fluorescent protein) would deem very necessary to achieve a fast screening if such competition study is conducted.

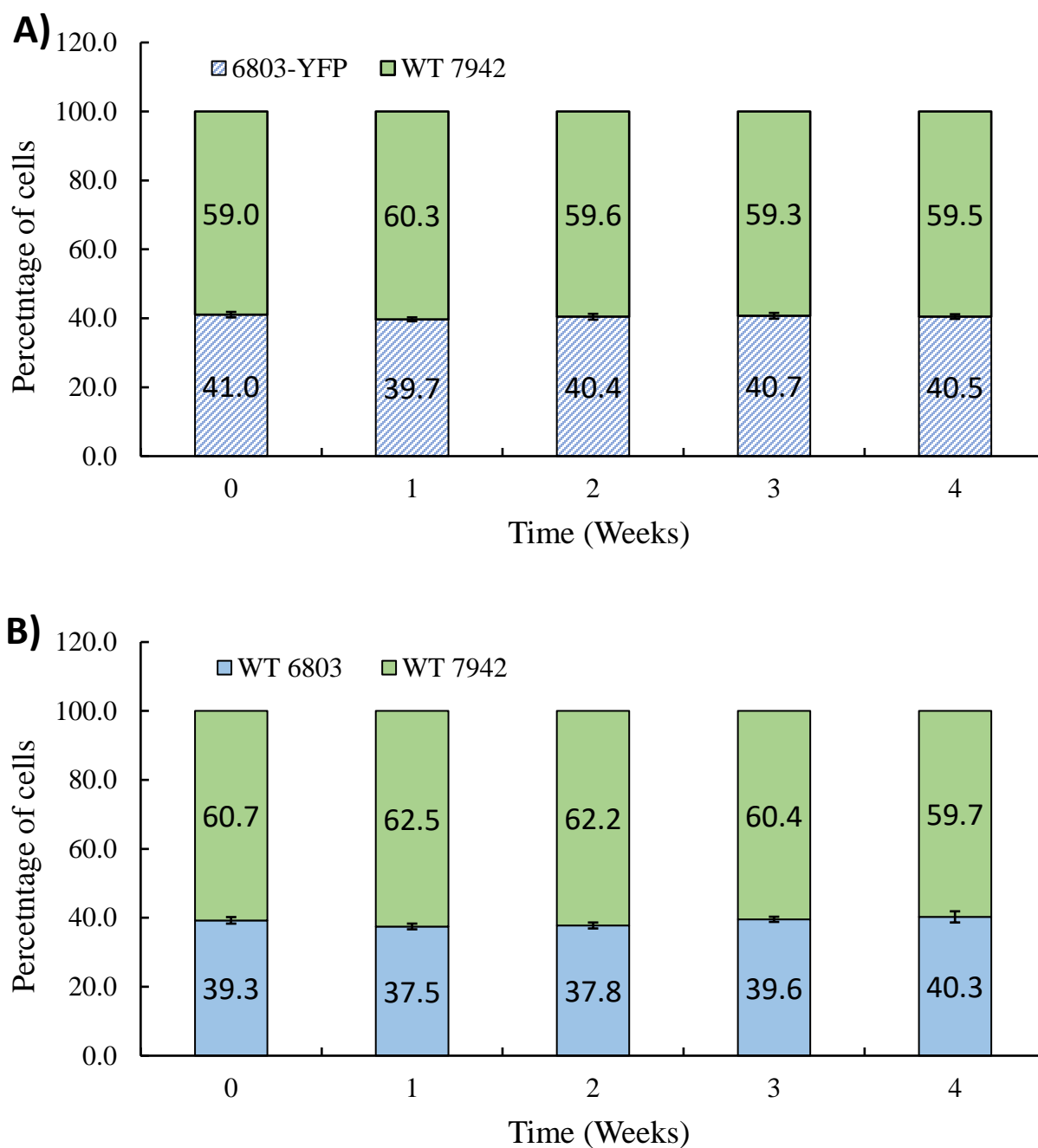


**Figure 37:** The relative percentage of cells in the coculture over a 4-week incubation at room temperatures between the GE *Synechocystis* PCC 6803-YFP (6803-YFP) and WT *Synechococcus elongatus* PCC 7942 (WT 7942) in A; WT *Synechocystis* PCC 6803 (WT 6803) and WT *Synechococcus elongatus* PCC 7942 (WT 7942) in B. The error bars denote the standard deviation of the percentage cells in three liquid cultures, each counted twice (total n=6).

## CONCLUSION

The experimental results from the multi-well survivability assay suggest that upon being genetically modified with the designer DNA construct YFP-ST-R-Lipase-Tet (Figures 1) the viability of the GE *T. elongatus* BP1 was not impacted. GE *T. elongatus* BP1 BY20 had a similar growth pattern to that of the wild-type *T. elongatus* BP1 at both cool temperatures (15.44 °C to 25.30 °C) and warm temperatures (31.42 °C to 36.27 °C). Another experiment (data not shown) was conducted in April when the greenhouse temperatures were moderate (24.5 °C to 31.5 °C) using GE *T. elongatus* BP1-BY20. The results were similar to that of the warm temperatures study, in that the GE *T. elongatus* BP1-BY20 and wild-type *T. elongatus* BP1 were not actively growing but remained viable after 1, 2, 3 and 4 weeks under the greenhouse conditions. While the results may be empirical evidence for the total death or partial death of GE *T. elongatus* BP1, the thermophilic nature of *T. elongatus* BP1 may be considered to serve as a biosafety guarded mechanism in cool seasons.

The competition study showed that during the cool season, the WT 6803 and GE 6803-YFP had a competitive advantage over the wild-type 7942. This was not observed when the study was conducted at room temperatures. Furthermore, we also found that the co-culturing of GE *T. elongatus* BP1 BY20 with WT 6803 resulted in a total death of BY20. Thus, indicating that the even in the presence of other bacteria, the thermophilic nature of *T. elongatus* BP1 may be used as a biosafety guarded mechanism.

## CHAPTER VII

### CONCLUSIONS AND DIRECTIONS FOR FUTURE WORK

#### CONCLUSIONS

Biochar post-production surface oxygenation was used to improve some key characteristics of biochar. Ozonized pine 400 and its filtrate were able to solubilize phosphate from insoluble phosphate rock material without the need of any additional acid; the effect of biochar ozonization under wet conditions improved the solubilization of efficiency of pine 400 by more than 100 times. The proposed mechanisms of solubilizations were the proton effect, the anion exchange, and the cation effect by metal complexation.

A comparative study on the effect of ozonization on biochar made at different temperatures showed that wet ozonization was more efficient at increasing the CEC of low temperature biochars (P300, P400 and P500) but showed no effect on high temperature rogue biochar. On the other hand, via dry-ozonization of rogue biochar a breakthrough CEC of  $152.08 \text{ cmol/kg} \pm 4.06$  was reached, which is almost 10 times more than the non-ozonized rogue biochar.

Wet-ozonization of pine 400 biochar and dry-ozonization of rogue biochar were also shown to increase the CEC of their filtrate/wash. Ozonization of biochar led to an installment of -COOH groups on biochar as a result of the cleavage. Smaller fragments with structures similar to humic-like materials were released but the major components in the DOC are suspected to be smaller organic acids. Filtrates from wet-ozonized pine 400 and dry ozonized rogue were able to solubilize phosphate at DOC concentrations as low as 10 ppm. The small organic acids generated by ozonization may be the main actors in solubilizing phosphate.

The toxicity study conducted with ozonized biochar filtrate on the growth of soil bacteria

*Pseudomonas putida* showed that filtrates from wet-ozonized pine 400 and dry-ozonized rogue biochar do not have any inhibitory effect on *P. putida*. On the contrary, *P. putida* grew better when it was incubated with the filtrate from the dry-ozonized rogue biochar at high DOC concentrations. However, high DOC concentrations from RBC 90D-F and P400 90W-F inhibited the growth of cyanobacteria *Synechococcus elongatus* PCC 7942. Further tests showed the presence of some potential inhibitory compounds (terephthalic acid and p-toluic acid) in the filtrate of non-ozonized pine 400 (P400 UN-F); these compounds were greatly reduced upon wet-ozonization of pine 400. Nutrient detection tests also showed that dry-ozonization of rogue biochar increased the release of nitrate and phosphate in its filtrate, a property that may be desirable for soil application.

The biosafety feature of thermophilic cyanobacteria *T. elongatus* BP1 was tested by conducting a growth study in the greenhouse at Old Dominion University. Here, we found that during the cool season the thermophilic nature of GE *T. elongatus* BP1-BY20 and wild-type *T. elongatus* BP1 may be used as a biosafety guarded mechanism. In warmer seasons, even though wild-type and GE *T. elongatus* BP1 BY20 did not actively grow, some cells remained alive for the entire period of the study; thus, indicating that the thermophilic nature of *T. elongatus* BP1 may not provide containment to GE *T. elongatus* BP1 during warmer seasons. The competition study mimicking a possible spill of GE-BY20 into a wild-type cyanobacteria population showed that in the cool season, the growth of mesophilic wild-type *Synechocystis* PCC 6803 was not affected by the presence of GE BP1-BY20 and wildtype BP1; the *T. elongatus* BP1 was quickly outgrown and showed no living cell at the end of the study. This study further supported the use of the thermophilic nature of *T. elongatus* BP1 as a biosafety guarded mechanism during cool seasons.

## **DIRECTIONS FOR FUTURE WORK**

The CEC of biochar has been highly investigated in the field. Most biochars have a net negative charge on their surface <sup>1, 133, 134</sup> which makes the CEC a more pronounced feature of the biochar. The soil also presents some anions, and it is as important to prevent the leaching of those anions. The development of biochar with anion exchange capacity (AEC) should therefore be investigated. We recently did some preliminary work and we showed that the effect of ozonization increased the adsorptive properties of pine 500 and rogue biochar for anionic Congo red dye; ozonized P500 adsorbed two-plus (2x) times more Congo red compared to the non-ozonized P500; the ozonized rogue biochar on the other hand adsorbed ten-plus (10x) times more Congo red dyes compared to the control rogue biochar <sup>135</sup>. The effect of ozonization is therefore not only a tool to increase CEC but may also increase the AEC of some biochars. More investigation is needed into the effect of biochar on AEC. Furthermore, understanding the effect of ozonization of biochar on AEC would help better understanding the mechanism of this innovative ozonization technology.

There is an interest in the field to use biochar as an inoculum carrier for microorganisms. While many studies showed the efficiency of biochar in improving microbial life via biochar-microbe interactions <sup>123</sup> others have shown that in the short-term biochar pores may not be a preferred habitat for microbes <sup>124</sup>. A future and interesting study would be the use of ozonized biochar as an inoculum carrier. Some ozonized biochars were shown here to have beneficial effects to the growth of certain bacteria.

The thermophilic property of *T. elongatus* BP1 being used as a biosafety guarded mechanism may confer some biosafety in the event the latter was to escape to the environment. However, as noted in the survivability study during the warm season in the greenhouse the cells

were not entirely dead after 4 weeks. This brings a considerable limitation on the use of the thermophilic nature of *T. elongatus* BP1 during summer seasons. In order to circumvent that, one possibility is to make the GE *T. elongatus* BP1 more vulnerable to low temperatures. Their optimum temperature being 57°C<sup>48</sup>, they can still maintain cell activity at 30°C<sup>48</sup> as discussed and shown in the survivability study. An interesting future direction would be to disrupt some low-temperature inducible genes that regulate the expression of the heat shock proteins to improve the biosafety mechanism due to the thermophilic nature of BP1. For example, in the *Synechocystis* PCC 6803, the *crhR* gene involved in RNA helicase was shown to regulate the expression of some heat shock genes<sup>136</sup>. A mutation of that gene resulted in the 6803 not being able to tolerate drops in temperatures as the production of heat shock proteins such as *groEL2* and *groESL* decreased<sup>136</sup>. Therefore, disrupting the heat shock genes of the *T. elongatus* BP1 that enable it to tolerate downward shift in temperatures would provide a tighter temperature range.

The GE *T. elongatus* BP1 was shown to be able to transfer DNA to *E. coli*<sup>131</sup>. This phenomenon poses a biosafety risk because if the GE *T. elongatus* BP1 was to escape, it could give DNA with biofuels producing genes and antibiotic resistance to wild-type *E. coli* in the environment and pose a risk to animals and humans<sup>131, 137</sup>. However, another direction to look into is the contamination of the bioreactors with wild-type microorganisms that can easily be found in the environment. If the GE *T. elongatus* BP1 can transfer DNA material to *E. coli* it is important to conduct a competition study between some *e. coli* strains and the GE *T. elongatus* BP1. Even though *e. coli* typically does not grow at high temperatures of *T. elongatus* BP1, it is important to test if horizontal gene transfer can occur and transfer genes for heat shock proteins

from *T. elongatus* BP1 to *E. coli* strains. If so, then it is also important to know if the resulting *E. coli* would coexist, outgrow or be outgrown by the GE *T. elongatus* BP1.

## REFERENCES

1. Lehmann, J.; Joseph, S., *Biochar for Environmental Management : Science and Technology*. Earthscan: London ; Sterling, VA, 2009.
2. Aghababaei, A.; Ncibi, M. C.; Sillanpää, M., Optimized Removal of Oxytetracycline and Cadmium from Contaminated Waters Using Chemically-Activated and Pyrolyzed Biochars from Forest and Wood-Processing Residues. *Bioresour. Technol.* **2017**, *239*, 28-36.
3. Jang, H. M.; Kan, E., Engineered Biochar from Agricultural Waste for Removal of Tetracycline in Water. *Bioresour. Technol.* **2019**, *284*, 437-447.
4. Gunarathne, V.; Ashiq, A.; Ramanayaka, S.; Wijekoon, P.; Vithanage, M., Biochar from Municipal Solid Waste for Resource Recovery and Pollution Remediation. *Environ. Chem. Lett.* **2019**, *17* (3), 1225-1235.
5. Cho, D.-W.; Kwon, G.; Yoon, K.; Tsang, Y. F.; Ok, Y. S.; Kwon, E. E.; Song, H., Simultaneous Production of Syngas and Magnetic Biochar Via Pyrolysis of Paper Mill Sludge Using Co<sub>2</sub> as Reaction Medium. *Energy Convers. Manag.* **2017**, *145*, 1-9.
6. Yoon, K.; Cho, D.-W.; Tsang, Y. F.; Tsang, D. C.; Kwon, E. E.; Song, H., Synthesis of Functionalised Biochar Using Red Mud, Lignin, and Carbon Dioxide as Raw Materials. *Chem. Eng. J.* **2019**, *361*, 1597-1604.
7. Allen, C. D.; Breshears, D. D.; McDowell, N. G., On Underestimation of Global Vulnerability to Tree Mortality and Forest Die-Off from Hotter Drought in the Anthropocene. *Ecosphere* **2015**, *6* (8), 1-55.
8. Novotny, E. H.; Maia, C. M. B. d. F.; Carvalho, M. T. d. M.; Madari, B. E., Biochar: Pyrogenic Carbon for Agricultural Use-a Critical Review. *Revista Brasileira de Ciência do Solo* **2015**, *39* (2), 321-344.
9. Li, L.; Rowbotham, J. S.; Greenwell, C. H.; Dyer, P. W., *An Introduction to Pyrolysis and Catalytic Pyrolysis: Versatile Techniques for Biomass Conversion*. Elsevier: 2013.
10. Safdari, M.-S.; Amini, E.; Weise, D. R.; Fletcher, T. H., Heating Rate and Temperature Effects on Pyrolysis Products from Live Wildland Fuels. *Fuel (Lond.)* **2019**, *242*, 295-304.
11. Wang, Y.; Duan, D.; Liu, Y.; Ruan, R.; Fu, G.; Dai, L.; Zhou, Y.; Yu, Z.; Wu, Q.; Zeng, Z., Properties and Pyrolysis Behavior of Moso Bamboo Sawdust after Microwave-Assisted Acid Pretreatment. *J. Anal. Appl. Pyrolysis* **2018**, *129*, 86-92.
12. Wang, H.; Wang, X.; Cui, Y.; Xue, Z.; Ba, Y., Slow Pyrolysis Polygeneration of Bamboo (*Phyllostachys Pubescens*): Product Yield Prediction and Biochar Formation Mechanism. *Bioresour. Technol.* **2018**, *263*, 444-449.
13. Read, P., This Gift of Nature Is the Best Way to Save Us from Climate Catastrophe. *The Guardian* **2009**, 27.
14. Pandit, N. R.; Mulder, J.; Hale, S. E.; Martinsen, V.; Schmidt, H. P.; Cornelissen, G., Biochar Improves Maize Growth by Alleviation of Nutrient Stress in a Moderately Acidic Low-Input Nepalese Soil. *Sci. Total Environ.* **2018**, *625*, 1380-1389.
15. Kharel, G.; Sacko, O.; Feng, X.; Morris, J. R.; Phillips, C. L.; Trippe, K.; Kumar, S.; Lee, J. W., Biochar Surface Oxygenation by Ozonization for Super High Cation Exchange Capacity. *ACS Sustain. Chem. Eng.* **2019**, *7* (19), 16410-16418.
16. Liang, B.; Lehmann, J.; Solomon, D.; Kinyangi, J.; Grossman, J.; O'Neill, B.; Skjemstad, J. O.; Thies, J.; Luizão, F. J.; Petersen, J.; Neves, E. G., Black Carbon Increases Cation Exchange Capacity in Soils. *Soil Science Society of America Journal* **2006**, *70* (5), 1719-1730.

17. Chen, Y.; Zhang, X.; Chen, W.; Yang, H.; Chen, H., The Structure Evolution of Biochar from Biomass Pyrolysis and Its Correlation with Gas Pollutant Adsorption Performance. *Bioresour. Technol.* **2017**, *246*, 101-109.
18. Xiao, F.; Bedane, A. H.; Zhao, J. X.; Mann, M. D.; Pignatello, J. J., Thermal Air Oxidation Changes Surface and Adsorptive Properties of Black Carbon (Char/Biochar). *Sci. Total Environ.* **2018**, *618*, 276-283.
19. Wu, J.; Wang, T.; Zhang, Y.; Pan, W.-P., The Distribution of Pb (Ii)/Cd (Ii) Adsorption Mechanisms on Biochars from Aqueous Solution: Considering the Increased Oxygen Functional Groups by Hcl Treatment. *Bioresour. Technol.* **2019**, *291*, 121859.
20. Zhang, H.; Yue, X.; Li, F.; Xiao, R.; Zhang, Y.; Gu, D., Preparation of Rice Straw-Derived Biochar for Efficient Cadmium Removal by Modification of Oxygen-Containing Functional Groups. *Sci. Total Environ.* **2018**, *631*, 795-802.
21. Huff, M. D.; Lee, J. W., Biochar-Surface Oxygenation with Hydrogen Peroxide. *Journal of environmental management* **2016**, *165*, 17-21.
22. Peng, H.; Gao, P.; Chu, G.; Pan, B.; Peng, J.; Xing, B., Enhanced Adsorption of Cu (Ii) and Cd (Ii) by Phosphoric Acid-Modified Biochars. *Environ. Pollut.* **2017**, *229*, 846-853.
23. Fan, Q.; Sun, J.; Chu, L.; Cui, L.; Quan, G.; Yan, J.; Hussain, Q.; Iqbal, M., Effects of Chemical Oxidation on Surface Oxygen-Containing Functional Groups and Adsorption Behavior of Biochar. *Chemosphere* **2018**, *207*, 33-40.
24. Huff, M. D.; Marshall, S.; Saeed, H. A.; Lee, J. W., Surface Oxygenation of Biochar through Ozonization for Dramatically Enhancing Cation Exchange Capacity. *Bioresour. Bioprocess.* **2018**, *5* (1), 1-9.
25. Lee, J. W. Ozonized Biochar Compositions and Methods of Making and Using the Same. U.S. Patent 10,071,335. Sep 13, 2018.
26. Suliman, W.; Harsh, J. B.; Abu-Lail, N. I.; Fortuna, A.-M.; Dallmeyer, I.; Garcia-Pérez, M., The Role of Biochar Porosity and Surface Functionality in Augmenting Hydrologic Properties of a Sandy Soil. *Sci. Total Environ.* **2017**, *574*, 139-147.
27. Rutherford, P. M.; Dudas, M. J.; Samek, R. A., Environmental Impacts of Phosphogypsum. *Sci. Total Environ.* **1994**, *149* (1-2), 1-38.
28. Potiriadis, C.; Koukoulidou, V.; Seferlis, S.; Kehagia, K., Assessment of the Occupational Exposure at a Fertiliser Industry in the Northern Part of Greece. *Radiation Protection Dosimetry* **2011**, *144* (1-4), 668-671.
29. Wu, H. J.; Gao, L. M.; Yuan, Z. W.; Wang, S., Life Cycle Assessment of Phosphorus Use Efficiency in Crop Production System of Three Crops in Chaohu Watershed, China. *J. Clean. Prod.* **2016**, *139*, 1298-1307.
30. da Silva, G. A.; Kulay, L. A., Environmental Performance Comparison of Wet and Thermal Routes for Phosphate Fertilizer Production Using Lca - a Brazilian Experience. *J. Clean. Prod.* **2005**, *13* (13-14), 1321-1325.
31. Glaser, B.; Lehmann, J.; Zech, W., Ameliorating Physical and Chemical Properties of Highly Weathered Soils in the Tropics with Charcoal – a Review. *Biol. Fertil. Soils* **2002**, *35* (4), 219-230.
32. Guo, M., The 3r Principles for Applying Biochar to Improve Soil Health. *Soil syst.* **2020**, *4* (1), 9.
33. Sacko, O.; Whiteman, R.; Kharel, G.; Kumar, S.; Lee, J. W., Sustainable Chemistry: Solubilization of Phosphorus from Insoluble Phosphate Material Hydroxyapatite with Ozonized Biochar. *ACS Sustain. Chem. Eng.* **2020**, *8* (18), 7068-7077.

34. Stevenson, F. J., *Humus Chemistry: Genesis, Composition, Reactions*. John Wiley & Sons: New York, 1994.
35. Guilayn, F.; Benbrahim, M.; Rouez, M.; Crest, M.; Patureau, D.; Jimenez, J., Humic-Like Substances Extracted from Different Digestates: First Trials of Lettuce Biostimulation in Hydroponic Culture. *Waste Manag* **2020**, *104*, 239-245.
36. Calvo, P.; Nelson, L.; Kloepper, J. W., Agricultural Uses of Plant Biostimulants. *Plant and Soil* **2014**, *383* (1), 3-41.
37. Román, J. R.; Roncero-Ramos, B.; Chamizo, S.; Rodríguez-Caballero, E.; Cantón, Y., Restoring Soil Functions by Means of Cyanobacteria Inoculation: Importance of Soil Conditions and Species Selection. *Land Degrad. Dev.* **2018**, *29* (9), 3184-3193.
38. Büdel, B., Ecology and Diversity of Rock-Inhabiting Cyanobacteria in Tropical Regions. *Eur. J. Phycol.* **1999**, *34* (4), 361-370.
39. Quintana, N.; Van der Kooy, F.; Van de Rhee, M. D.; Voshol, G. P.; Verpoorte, R., Renewable Energy from Cyanobacteria: Energy Production Optimization by Metabolic Pathway Engineering. *Applied microbiology and biotechnology* **2011**, *91* (3), 471-490.
40. Yu, J.; Liberton, M.; Cliften, P. F.; Head, R. D.; Jacobs, J. M.; Smith, R. D.; Koppenaal, D. W.; Brand, J. J.; Pakrasi, H. B., *Synechococcus Elongatus* UTEX 2973, a Fast Growing Cyanobacterial Chassis for Biosynthesis Using Light and CO<sub>2</sub>. *Sci. Rep.* **2015**, *5* (1), 1-10.
41. Ahmad, A. L.; Yasin, N. H. M.; Derek, C. J. C.; Lim, J. K., Microalgae as a Sustainable Energy Source for Biodiesel Production: A Review. *Renewable Sustainable Energy Rev.* **2011**, *15* (1), 584-593.
42. Gressel, J., Transgenics Are Imperative for Biofuel Crops. *Plant Sci.* **2008**, *174* (3), 246-263.
43. Lee, J. W., Synthetic Biology for Photobiological Production of Butanol and Related Higher Alcohols from Carbon Dioxide and Water. In *Advanced Biofuels and Bioproducts*, Springer: New York, 2013; pp 447-521.
44. Lee, J. W., Synthetic Biology: A New Opportunity in the Field of Plant Biochemistry & Physiology. *J. Plant Biochem. Physiol.* **2013**, *1* (1).
45. Chaves, J. E.; Rueda-Romero, P.; Kirst, H.; Melis, A., Engineering Isoprene Synthase Expression and Activity in Cyanobacteria. *ACS Synth. Biol.* **2017**, *6* (12), 2281-2292.
46. Mandell, D. J.; Lajoie, M. J.; Mee, M. T.; Takeuchi, R.; Kuznetsov, G.; Norville, J. E.; Gregg, C. J.; Stoddard, B. L.; Church, G. M., Biocontainment of Genetically Modified Organisms by Synthetic Protein Design. *Nature* **2015**, *518* (7537), 55-60.
47. Zhou, Y.; Sun, T.; Chen, Z.; Song, X.; Chen, L.; Zhang, W., Development of a New Biocontainment Strategy in Model Cyanobacterium *Synechococcus* Strains. *ACS Synth Biol* **2019**, *8* (11), 2576-2584.
48. Yamaoka, T.; Satoh, K.; Katoh, S., Photosynthetic Activities of a Thermophilic Blue-Green Alga. *Plant and Cell Physiology* **1978**, *19* (6), 943-954.
49. Asimov, I., *Asimov on Chemistry*. Doubleday Books: Garden City, N.Y., 1974.
50. Lindsay, W. L., *Chemical Equilibria in Soils*. John Wiley and Sons Ltd: New York, 1979.
51. Li, H.; Huang, G.; Meng, Q.; Ma, L.; Yuan, L.; Wang, F.; Zhang, W.; Cui, Z.; Shen, J.; Chen, X., Integrated Soil and Plant Phosphorus Management for Crop and Environment in China. A Review. *Plant Soil* **2011**, *349* (1), 157-167.
52. Bai, Z.; Li, H.; Yang, X.; Zhou, B.; Shi, X.; Wang, B.; Li, D.; Shen, J.; Chen, Q.; Qin, W., The Critical Soil P Levels for Crop Yield, Soil Fertility and Environmental Safety in Different Soil Types. *Plant Soil* **2013**, *372* (1), 27-37.

53. Vance, C. P.; Uhde-Stone, C.; Allan, D. L., Phosphorus Acquisition and Use: Critical Adaptations by Plants for Securing a Nonrenewable Resource. *New phytologist* **2003**, *157* (3), 423-447.
54. Moore Jr, P.; Miller, D. *Decreasing Phosphorus Solubility in Poultry Litter with Aluminum, Calcium, and Iron Amendments*; 0047-2425; Wiley Online Library: 1994.
55. Cordell, D.; Drangert, J. O.; White, S., The Story of Phosphorus: Global Food Security and Food for Thought. *Global Environmental Change-Human and Policy Dimensions* **2009**, *19* (2), 292-305.
56. Cordell, D.; White, S., Peak Phosphorus: Clarifying the Key Issues of a Vigorous Debate About Long-Term Phosphorus Security. *Sustainability* **2011**, *3* (10), 2027-2049.
57. Cordell, D.; White, S., Tracking Phosphorus Security: Indicators of Phosphorus Vulnerability in the Global Food System. *Food Secur.* **2015**, *7* (2), 337-350.
58. Jasinski, S. M. Phosphate Rock <https://pubs.usgs.gov/periodicals/mcs2020/mcs2020-phosphate.pdf> (accessed Mar 25, 2020).
59. Carpenter, S. R., Phosphorus Control Is Critical to Mitigating Eutrophication. *Proc. Natl. Acad. Sci. U. S. A.* **2008**, *105* (32), 11039-11040.
60. Rippey, J. F. M.; Nelson, P. V., Cation Exchange Capacity and Base Saturation Variation among Alberta, Canada, Moss Peats. *Hortscience* **2007**, *42* (2), 349-352.
61. Huff, M. D.; Lee, J. W., Biochar-Surface Oxygenation with Hydrogen Peroxide. *Journal of Environmental Management* **2016**, *165*, 17-21.
62. Arami-Niya, A.; Abnisa, F.; Sahfeeyan, M. S.; Daud, W. W.; Sahu, J. N., Optimization of Synthesis and Characterization of Palm Shell-Based Bio-Char as a by-Product of Bio-Oil Production Process. *BioResources* **2012**, *7* (1), 0246-0264.
63. Zhu, Y. N.; Zhang, X. H.; Chen, Y. D.; Xie, Q. L.; Lan, J. K.; Qian, M. F.; He, N., A Comparative Study on the Dissolution and Solubility of Hydroxylapatite and Fluorapatite at 25 Degrees C and 45 Degrees C. *Chemical Geology* **2009**, *268* (1-2), 89-96.
64. Imam, D. M.; Moussa, S. I.; Attallah, M. F., Sorption Behavior of Some Radionuclides Using Prepared Adsorbent of Hydroxyapatite from Biomass Waste Material. *J. Radioanal. Nucl. Chem.* **2019**, *319* (3), 997-1012.
65. Aslan, N.; Ozcayan, G., Adsorptive Removal of Lead-210 Using Hydroxyapatite Nanopowders Prepared from Phosphogypsum Waste. *J. Radioanal. Nucl. Chem.* **2019**, *319* (3), 1023-1028.
66. Pignatello, J. J., Uchimiya, M., Abiven, S., Schmidt, M.W.I., Evolution of Biochar Properties in Soil. in: *Lehmann, J., Joseph, S. (Eds.), Biochar for Environmental Management: Science, Technology and Implementation. Earthscan, London ; Sterling, VA, pp. 195–233. 2015.*
67. Kavitha, B.; Reddy, P. V. L.; Kim, B.; Lee, S. S.; Pandey, S. K.; Kim, K. H., Benefits and Limitations of Biochar Amendment in Agricultural Soils: A Review. *Journal of Environmental Management* **2018**, *227*, 146-154.
68. Katterer, T.; Roobroeck, D.; Andren, O.; Kimutai, G.; Karlton, E.; Kirchmann, H.; Nyberg, G.; Vanlauwe, B.; de Nowina, K. R., Biochar Addition Persistently Increased Soil Fertility and Yields in Maize-Soybean Rotations over 10 Years in Sub-Humid Regions of Kenya. *Field Crops Res.* **2019**, *235*, 18-26.
69. Spokas, K. A.; Cantrell, K. B.; Novak, J. M.; Archer, D. W.; Ippolito, J. A.; Collins, H. P.; Boateng, A. A.; Lima, I. M.; Lamb, M. C.; McAloon, A. J.; Lentz, R. D.; Nichols, K. A., Biochar: A Synthesis of Its Agronomic Impact Beyond Carbon Sequestration. *J Environ Qual* **2012**, *41* (4), 973-89.

70. Xu, R.-k.; Zhao, A.-z.; Yuan, J.-h.; Jiang, J., Ph Buffering Capacity of Acid Soils from Tropical and Subtropical Regions of China as Influenced by Incorporation of Crop Straw Biochars. *Journal of Soils and Sediments* **2012**, *12* (4), 494-502.
71. Lee, J. W.; Hawkins, B.; Kidder, M. K.; Evans, B. R.; Buchanan, A. C.; Day, D., Characterization of Biochars Produced from Peanut Hulls and Pine Wood with Different Pyrolysis Conditions. *Bioresour. Bioprocess.* **2016**, *3* (1), 15.
72. Lee, J. W.; Hawkins, B.; Day, D. M.; Reicosky, D. C., Sustainability: The Capacity of Smokeless Biomass Pyrolysis for Energy Production, Global Carbon Capture and Sequestration. *Energy Environ. Sci.* **2010**, *3* (11), 1695-1705.
73. Liu, X.; Mao, P. N.; Li, L. H.; Ma, J., Impact of Biochar Application on Yield-Scaled Greenhouse Gas Intensity: A Meta-Analysis. *Sci. Total Environ.* **2019**, *656*, 969-976.
74. Aller, D. M.; Archontoulis, S. V.; Zhang, W. D.; Sawadgo, W.; Laird, D. A.; Moore, K., Long Term Biochar Effects on Corn Yield, Soil Quality and Profitability in the Us Midwest. *Field Crops Res.* **2018**, *227*, 30-40.
75. Lee, J. W.; Hawkins, B.; Kidder, M. K.; Evans, B. R.; Buchanan, A.; Day, D., Characterization of Biochars Produced from Peanut Hulls and Pine Wood with Different Pyrolysis Conditions. *Bioresour. Bioprocess.* **2016**, *3* (1), 1-10.
76. Li, H.; Dong, X.; da Silva, E. B.; de Oliveira, L. M.; Chen, Y.; Ma, L. Q., Mechanisms of Metal Sorption by Biochars: Biochar Characteristics and Modifications. *Chemosphere* **2017**, *178*, 466-478.
77. Wang, Z.; Liu, G.; Zheng, H.; Li, F.; Ngo, H. H.; Guo, W.; Liu, C.; Chen, L.; Xing, B., Investigating the Mechanisms of Biochar's Removal of Lead from Solution. *Bioresour. Technol.* **2015**, *177*, 308-317.
78. Adenson, M. O.; Murillo, J. D.; Kelley, M.; Biernacki, J. J.; Bagley, C. P., Slow Pyrolysis Kinetics of Two Herbaceous Feedstock: Effect of Milling, Source, and Heating Rate. *Industrial & Engineering Chemistry Research* **2018**, *57* (11), 3821-3832.
79. Cen, K.; Chen, D.; Wang, J.; Cai, Y.; Wang, L., Effects of Water Washing and Torrefaction Pretreatments on Corn Stalk Pyrolysis: Combined Study Using Tg-Ftir and a Fixed Bed Reactor. *Energy & Fuels* **2016**, *30* (12), 10627-10634.
80. Deng, L.; Zhang, T.; Che, D., Effect of Water Washing on Fuel Properties, Pyrolysis and Combustion Characteristics, and Ash Fusibility of Biomass. *Fuel Processing Technology* **2013**, *106*, 712-720.
81. Jin, H.; Hanif, M. U.; Capareda, S.; Chang, Z.; Huang, H.; Ai, Y., Copper(II) Removal Potential from Aqueous Solution by Pyrolysis Biochar Derived from Anaerobically Digested Algae-Dairy-Manure and Effect of Koh Activation. *J. Environ. Chem. Eng.* **2016**, *4* (1), 365-372.
82. Winter, M. Webelements. <https://www.webelements.com> (accessed May 2021).
83. von Gunten, U., Ozonation of Drinking Water: Part I. Oxidation Kinetics and Product Formation. *Water Research* **2003**, *37* (7), 1443-1467.
84. Valdes, H.; Sanchez-Polo, M.; Rivera-Utrilla, J.; Zaror, C. A., Effect of Ozone Treatment on Surface Properties of Activated Carbon. *Langmuir* **2002**, *18* (6), 2111-2116.
85. Lee, J. W. Ozonized Biochar: Phosphorus Sustainability and Sand Soilization. U.S. Patent Application No. 16/104,892. Jan 3, 2019.
86. Suliman, W.; Harsh, J. B.; Abu-Lail, N. I.; Fortuna, A.-M.; Dallmeyer, I.; Garcia-Perez, M., Modification of Biochar Surface by Air Oxidation: Role of Pyrolysis Temperature. *Biomass and Bioenergy* **2016**, *85*, 1-11.

87. Mukherjee, A.; Zimmerman, A. R., Organic Carbon and Nutrient Release from a Range of Laboratory-Produced Biochars and Biochar–Soil Mixtures. *Geoderma* **2013**, *193*, 122-130.
88. Glaser, B.; Lehr, V.-I., Biochar Effects on Phosphorus Availability in Agricultural Soils: A Meta-Analysis. *Sci. Rep.* **2019**, *9* (1), 1-9.
89. Vitousek, P. M.; Porder, S.; Houlton, B. Z.; Chadwick, O. A., Terrestrial Phosphorus Limitation: Mechanisms, Implications, and Nitrogen–Phosphorus Interactions. *Ecological applications* **2010**, *20* (1), 5-15.
90. Thung, M., Phosphorus: A Limiting Nutrient in Bean (*Phaseolus Vulgaris* L.) Production in Latin America and Field Screening for Efficiency and Response. In *Genetic Aspects of Plant Mineral Nutrition*, Springer: 1990; pp 501-521.
91. Schachtman, D. P.; Reid, R. J.; Ayling, S. M., Phosphorus Uptake by Plants: From Soil to Cell. *Plant physiology* **1998**, *116* (2), 447-453.
92. Alori, E. T.; Glick, B. R.; Babalola, O. O., Microbial Phosphorus Solubilization and Its Potential for Use in Sustainable Agriculture. *Front. Microbiol.* **2017**, *8*, 971.
93. P, K.; M, P.; S, M.; C, S.; Bose, J., Applying Both Biochar and Phosphobacteria Enhances *Vigna Mungo* L. Growth and Yield in Acid Soils by Increasing Soil Ph, Moisture Content, Microbial Growth and P Availability. *Agric. Ecosyst. Environ.* **2021**, *308*, 107258.
94. Yao, Y.; Gao, B.; Zhang, M.; Inyang, M.; Zimmerman, A. R., Effect of Biochar Amendment on Sorption and Leaching of Nitrate, Ammonium, and Phosphate in a Sandy Soil. *Chemosphere* **2012**, *89* (11), 1467-1471.
95. Zheng, H.; Wang, Z.; Deng, X.; Herbert, S.; Xing, B., Impacts of Adding Biochar on Nitrogen Retention and Bioavailability in Agricultural Soil. *Geoderma* **2013**, *206*, 32-39.
96. Abbas, T.; Rizwan, M.; Ali, S.; Zia-ur-Rehman, M.; Farooq Qayyum, M.; Abbas, F.; Hannan, F.; Rinklebe, J.; Sik Ok, Y., Effect of Biochar on Cadmium Bioavailability and Uptake in Wheat (*Triticum Aestivum* L.) Grown in a Soil with Aged Contamination. *Ecotoxicol. Environ. Saf.* **2017**, *140*, 37-47.
97. Genesio, L.; Miglietta, F.; Lugato, E.; Baronti, S.; Pieri, M.; Vaccari, F., Surface Albedo Following Biochar Application in Durum Wheat. *Environ. Res. Lett.* **2012**, *7* (1), 014025.
98. Kim, J.-I.; Buckau, G.; Li, G.; Duschner, H.; Psarros, N., Characterization of Humic and Fulvic Acids from Gorleben Groundwater. *Fresenius J Anal Chem* **1990**, *338* (3), 245-252.
99. Khil'ko, S.; Kovtun, A.; Rybachenko, V., Potentiometric Titration of Humic Acids. *Solid Fuel Chem.* **2011**, *45* (5), 337-348.
100. Yang, S.; Zhang, Z.; Cong, L.; Wang, X.; Shi, S., Effect of Fulvic Acid on the Phosphorus Availability in Acid Soil. *Journal of soil science and plant nutrition* **2013**, *13* (3), 526-533.
101. Kurková, M.; Klika, Z.; Kliková, C.; Havel, J., Humic Acids from Oxidized Coals: I. Elemental Composition, Titration Curves, Heavy Metals in Ha Samples, Nuclear Magnetic Resonance Spectra of Has and Infrared Spectroscopy. *Chemosphere* **2004**, *54* (8), 1237-1245.
102. Kusakabe, K.; Aso, S.; Hayashi, J.-I.; Isomura, K.; Morooka, S., Decomposition of Humic Acid and Reduction of Trihalomethane Formation Potential in Water by Ozone with U.V. Irradiation. *Water Res.* **1990**, *24* (6), 781-785.
103. Takahashi, N.; Nakai, T.; Satoh, Y.; Katoh, Y., Ozonolysis of Humic Acid and Its Effect on Decoloration and Biodegradability. *Ozone: Science & Engineering* **1995**, *17* (5), 511-525.
104. Scientific, T., Thermo Scientific Dionex Ionpac As23 Anion-Exchange Column. Scientific, T. F., Ed. 2013.

105. de Oliveira Mendes, G.; Murta, H. M.; Valadares, R. V.; da Silveira, W. B.; da Silva, I. R.; Costa, M. D., Oxalic Acid Is More Efficient Than Sulfuric Acid for Rock Phosphate Solubilization. *Miner. Eng.* **2020**, *155*, 106458.
106. Lyu, H.; He, Y.; Tang, J.; Hecker, M.; Liu, Q.; Jones, P. D.; Codling, G.; Giesy, J. P., Effect of Pyrolysis Temperature on Potential Toxicity of Biochar If Applied to the Environment. *Environ. Pollut.* **2016**, *218*, 1-7.
107. Hale, S. E.; Lehmann, J.; Rutherford, D.; Zimmerman, A. R.; Bachmann, R. T.; Shitumbanuma, V.; O'Toole, A.; Sundqvist, K. L.; Arp, H. P. H.; Cornelissen, G., Quantifying the Total and Bioavailable Polycyclic Aromatic Hydrocarbons and Dioxins in Biochars. *Environ. Sci. Technol.* **2012**, *46* (5), 2830-2838.
108. Smith, C. R.; Hatcher, P. G.; Kumar, S.; Lee, J. W., Investigation into the Sources of Biochar Water-Soluble Organic Compounds and Their Potential Toxicity on Aquatic Microorganisms. *ACS Sustain. Chem. Eng.* **2016**, *4* (5), 2550-2558.
109. Silby, M. W.; Winstanley, C.; Godfrey, S. A. C.; Levy, S. B.; Jackson, R. W., Pseudomonas Genomes: Diverse and Adaptable. *FEMS Microbiology Reviews* **2011**, *35* (4), 652-680.
110. Mercado-Blanco, J.; Bakker, P. A., Interactions between Plants and Beneficial Pseudomonas Spp.: Exploiting Bacterial Traits for Crop Protection. *Antonie Van Leeuwenhoek* **2007**, *92* (4), 367-89.
111. Tu, C.; Wei, J.; Guan, F.; Liu, Y.; Sun, Y.; Luo, Y., Biochar and Bacteria Inoculated Biochar Enhanced Cd and Cu Immobilization and Enzymatic Activity in a Polluted Soil. *Environ. Int.* **2020**, *137*, 105576.
112. Wei, M.; Liu, X.; He, Y.; Xu, X.; Wu, Z.; Yu, K.; Zheng, X., Biochar Inoculated with Pseudomonas Putida Improves Grape (Vitis Vinifera L.) Fruit Quality and Alters Bacterial Diversity. *Rhizosphere* **2020**, *16*, 100261.
113. Głodowska, M.; Schwinghamer, T.; Husk, B.; Smith, D., Biochar Based Inoculants Improve Soybean Growth and Nodulation. *Agric. sci.* **2017**, *8* (9), 1048-1064.
114. Egamberdieva, D.; Hua, M.; Reckling, M.; Wirth, S.; Bellingrath-Kimura, S. D., Potential Effects of Biochar-Based Microbial Inoculants in Agriculture. *Environ. Sustain.* **2018**, *1* (1), 19-24.
115. Zhong, W.; Zhang, Y.; Wu, Z.; Yang, R.; Chen, X.; Yang, J.; Zhu, L., Health Risk Assessment of Heavy Metals in Freshwater Fish in the Central and Eastern North China. *Ecotoxicol. Environ. Saf.* **2018**, *157*, 343-349.
116. Hecht, A.; Endy, D.; Salit, M.; Munson, M. S., When Wavelengths Collide: Bias in Cell Abundance Measurements Due to Expressed Fluorescent Proteins. *ACS Synth. Biol.* **2016**, *5* (9), 1024-1027.
117. Xiao, X.; Chen, B.; Zhu, L., Transformation, Morphology, and Dissolution of Silicon and Carbon in Rice Straw-Derived Biochars under Different Pyrolytic Temperatures. *Environ. Sci. Technol.* **2014**, *48* (6), 3411-3419.
118. Nogales, J.; García, J. L.; Díaz, E., Degradation of Aromatic Compounds in Pseudomonas: A Systems Biology View. In *Aerobic Utilization of Hydrocarbons, Oils and Lipids*, Rojo, F., Ed. Springer International Publishing: Cham, 2017; pp 1-49.
119. Smith, C. R.; Sleighter, R. L.; Hatcher, P. G.; Lee, J. W., Molecular Characterization of Inhibiting Biochar Water-Extractable Substances Using Electrospray Ionization Fourier Transform Ion Cyclotron Resonance Mass Spectrometry. *Environ. Sci. Technol.* **2013**, *47* (23), 13294-13302.

120. Chandrasekara Pillai, K.; Kwon, T. O.; Moon, I. S., Degradation of Wastewater from Terephthalic Acid Manufacturing Process by Ozonation Catalyzed with Fe<sup>2+</sup>, H<sub>2</sub>O<sub>2</sub> and UV Light: Direct Versus Indirect Ozonation Reactions. *Appl. Catal. B* **2009**, *91* (1), 319-328.
121. Zang, X.-J.; Tong, S.-P.; Ma, C.-A., Kinetic and Mechanism of Ozonation of Terephthalic Acid. *Huan jing ke xue= Huanjing kexue* **2009**, *30* (6), 1658-1662.
122. O'Mahony, M. M.; Dobson, A. D. W.; Barnes, J. D.; Singleton, I., The Use of Ozone in the Remediation of Polycyclic Aromatic Hydrocarbon Contaminated Soil. *Chemosphere* **2006**, *63* (2), 307-314.
123. Zhu, X.; Chen, B.; Zhu, L.; Xing, B., Effects and Mechanisms of Biochar-Microbe Interactions in Soil Improvement and Pollution Remediation: A Review. *Environ. Pollut.* **2017**, *227*, 98-115.
124. Quilliam, R. S.; Glanville, H. C.; Wade, S. C.; Jones, D. L., Life in the 'Charosphere' – Does Biochar in Agricultural Soil Provide a Significant Habitat for Microorganisms? *Soil Biology and Biochemistry* **2013**, *65*, 287-293.
125. Zahra, Z.; Choo, D. H.; Lee, H.; Parveen, A., Cyanobacteria: Review of Current Potentials and Applications. *Environments* **2020**, *7* (2), 13.
126. U.S. Energy Facts Explained - Consumption and Production - U.S. Energy Information Administration (Eia). <https://www.eia.gov/energyexplained/us-energy-facts/> (accessed July 28th 2021).
127. Lan, E. I.; Liao, J. C., Metabolic Engineering of Cyanobacteria for 1-Butanol Production from Carbon Dioxide. *Metab. Eng.* **2011**, *13* (4), 353-363.
128. Varela Villarreal, J.; Burgués, C.; Rösch, C., Acceptability of Genetically Engineered Algae Biofuels in Europe: Opinions of Experts and Stakeholders. *Biotechnol. Biofuels* **2020**, *13*, 1-21.
129. Clark, R. L.; Gordon, G. C.; Bennett, N. R.; Lyu, H.; Root, T. W.; Pfleger, B. F., High-Co<sub>2</sub> Requirement as a Mechanism for the Containment of Genetically Modified Cyanobacteria. *ACS Synth. Biol.* **2018**, *7* (2), 384-391.
130. Suzuki, I.; Sugiyama, T.; Omata, T., Regulation by Cyanate of the Genes Involved in Carbon and Nitrogen Assimilation in the Cyanobacterium *Synechococcus* Sp Strain Pcc 7942. *Journal of Bacteriology* **1996**, *178* (9), 2688-2694.
131. Nguyen, T. H.; Barnes, C. L.; Agola, J. P.; Sherazi, S.; Greene, L. H.; Lee, J. W., Demonstration of Horizontal Gene Transfer from Genetically Engineered *Thermosynechococcus* *Elongatus* Bp1 to Wild-Type *E. Coli* Dh5alpha. *Gene* **2019**, *704*, 49-58.
132. Dunn, R. a. M., K. , The Effects of Initial Cell Density on the Growth and Proliferation of the Potentially Toxic Cyanobacterium *Microcystis Aeruginosa*. *J. Environ. Prot. (Irvine Calif.)* **2016**, *7*, 1210-1220.
133. Beesley, L.; Moreno-Jiménez, E.; Gomez-Eyles, J. L.; Harris, E.; Robinson, B.; Sizmur, T., A Review of Biochars' Potential Role in the Remediation, Revegetation and Restoration of Contaminated Soils. *Environ. Pollut.* **2011**, *159* (12), 3269-3282.
134. Lehmann, J.; Rillig, M. C.; Thies, J.; Masiello, C. A.; Hockaday, W. C.; Crowley, D., Biochar Effects on Soil Biota—a Review. *Soil biology and biochemistry* **2011**, *43* (9), 1812-1836.
135. Wood, C.; Sacko, O., Investigation into the Effect of Ozonation on Biochar as a Function of Pyrolysis Temperature and Its Applications in Dye Removal. In *Undergraduate Research Symposium*, Old Dominion University, 2021.
136. Prakash, J. S.; Krishna, P. S.; Sirisha, K.; Kanasaki, Y.; Suzuki, I.; Shivaji, S.; Murata, N., An Rna Helicase, Crhr, Regulates the Low-Temperature-Inducible Expression of Heat-Shock

Genes Groes, Groel1 and Groel2 in *Synechocystis* Sp. Pcc 6803. *Microbiology* **2010**, *156* (2), 442-451.

137. Gyles, C.; Boerlin, P., Horizontally Transferred Genetic Elements and Their Role in Pathogenesis of Bacterial Disease. *Vet. Pathol.* **2014**, *51* (2), 328-340.

138. S., T. Sunrise and Sunset Times in Norfolk. <https://www.timeanddate.com/sun/usa/norfolk>. (accessed October 2019).

## APPENDIX A

## SUPPORTING INFORMATION CHAPTER II

**Table A1: Adsorption of calcium ( $\text{Ca}^{2+}$ ) by non-ozonized and dry-ozonized pine 400 biochar. The adsorbed calcium in percentage, mg  $\text{Ca}^{2+}$ /g biochar.**

	Non-ozone treated biochar	Dry-ozone treated biochar
% calcium removed	99.56 ( $\pm 0.24$ )	98.66 ( $\pm 0.49$ )
mg $\text{Ca}^{2+}$ /g of biochar	3.53 ( $\pm 0.02$ )	3.56 ( $\pm 0.01$ )

## APPENDIX B

## SUPPORTING INFORMATION CHAPTER III

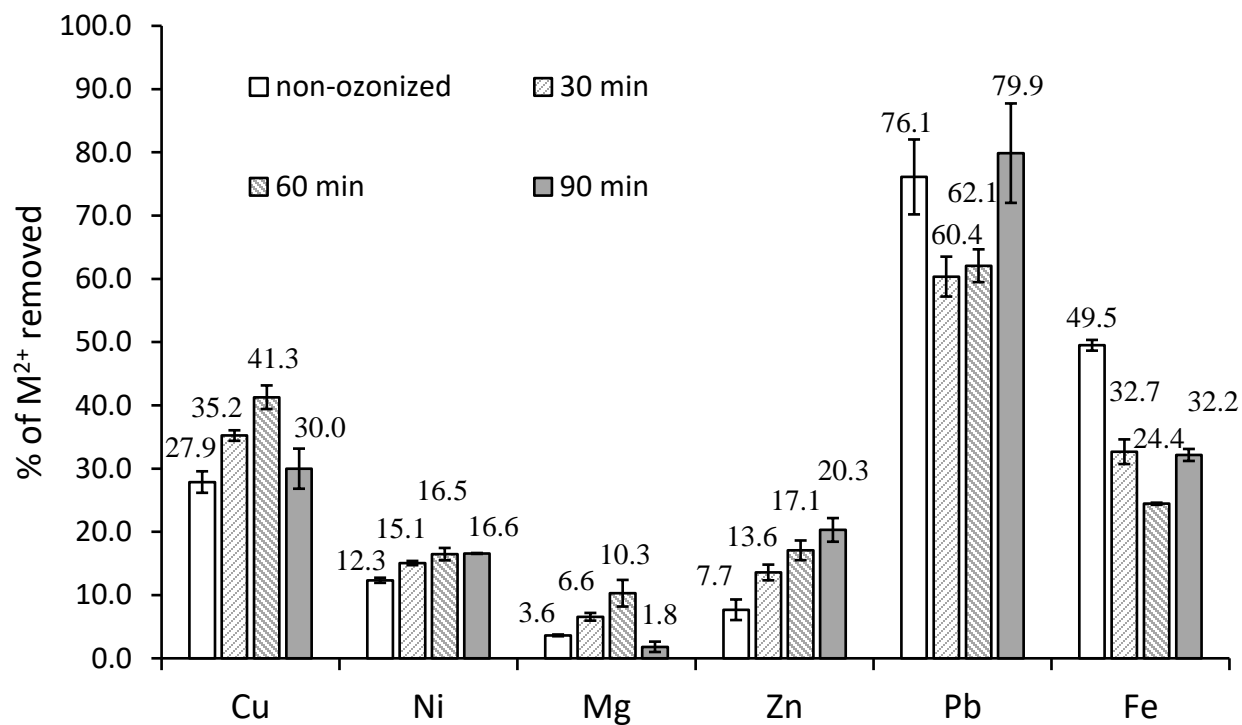


**Figure B1:** Percent removal of  $\text{Cu}^{2+}$ ,  $\text{Ni}^{2+}$ ,  $\text{Mg}^{2+}$ ,  $\text{Zn}^{2+}$ ,  $\text{Pb}^{2+}$  and  $\text{Fe}^{2+}$  from pine 400 non-ozonized biochar control, 30 min dry-ozonized, 60min dry-ozonized and 90min dry-ozonized. The error bars denote standard deviation for 3 replicates ( $n=3$ ).

**Table B1: Ionic radius of divalent cations  $\text{Cu}^{2+}$ ,  $\text{Ni}^{2+}$ ,  $\text{Mg}^{2+}$ ,  $\text{Zn}^{2+}$ ,  $\text{Pb}^{2+}$  and  $\text{Fe}^{2+}$  in picometer. The electronegativity (EN) constant of the elements is also presented. The data in this table was retrieved from WebElements <sup>82</sup>.**

	4-coordinate	6-coordinate	8-coordinate
Lead (II) (EN 2.33)	N/A	133 pm (octahedral)	143 pm
Iron (II) (EN 1.83)	77 pm (tetrahedral) 78 pm (square planar)	75 pm (octahedral) 92 pm (octahedral high spin)	106 pm
Zinc (II) (EN 1.65)	74 pm (tetrahedral)	88 pm (octahedral)	104 pm
Copper (II) (EN 1.90)	71 pm (tetrahedral) 71 pm (square planar)	87 pm (octahedral)	N/A
Magnesium (II) (EN 1.31)	71 pm (tetrahedral)	86 pm (octahedral)	103 pm
Nickel (II) (EN 1.91)	69 pm (tetrahedral) 63 pm (square planar)	83 pm (octahedral)	N/A

## APPENDIX C

## SUPPORTING INFORMATION CHAPTER IV

**Table C1: DOC concentration from the 1<sup>st</sup> 10-mL, 2<sup>nd</sup> 25-mL wash and 3<sup>rd</sup> 300-mL wash collected from biochar (mg/mL) and the total DOC extracted from biochar in mg DOC/g biochar. The error bars denote standard deviation of 3 replicates (n=3).**

	mg DOC/mL 1 <sup>st</sup> wash (2 <sup>nd</sup> wash) [3 <sup>rd</sup> wash]	Total DOC extracted DOC (mg DOC/g biochar)
P400 UN	1 <sup>st</sup> wash 0.055 ± 0.010 2 <sup>nd</sup> wash (0.018 ± 0.008) 3 <sup>rd</sup> wash [0.006 ± 0.001]	1.96 ± 0.32
P400 90D	1 <sup>st</sup> wash 0.490 ± 0.027 2 <sup>nd</sup> wash (0.132 ± 0.014) 3 <sup>rd</sup> wash [0.019 ± 0.008]	9.33 ± 1.72
P400 90W	1 <sup>st</sup> wash 2.363 ± 0.036 2 <sup>nd</sup> wash (0.262 ± 0.020) 3 <sup>rd</sup> wash [0.017 ± 0.008]	23.50 ± 1.70
RBC UN	1 <sup>st</sup> wash 0.093 ± 0.001 2 <sup>nd</sup> wash (0.033 ± 0.001) 3 <sup>rd</sup> wash [0.006 ± 0.001]	2.38 ± 0.14
RBC 90D	1 <sup>st</sup> wash 3.227 ± 0.075 2 <sup>nd</sup> wash (0.399 ± 0.015) 3 <sup>rd</sup> wash [0.032 ± 0.004]	34.50 ± 1.00
RBC 90W	1 <sup>st</sup> wash 0.116 ± 0.004 2 <sup>nd</sup> wash (0.0497 ± 0.0001) 3 <sup>rd</sup> wash [0.0376 ± 0.0005]	9.13 ± 0.10

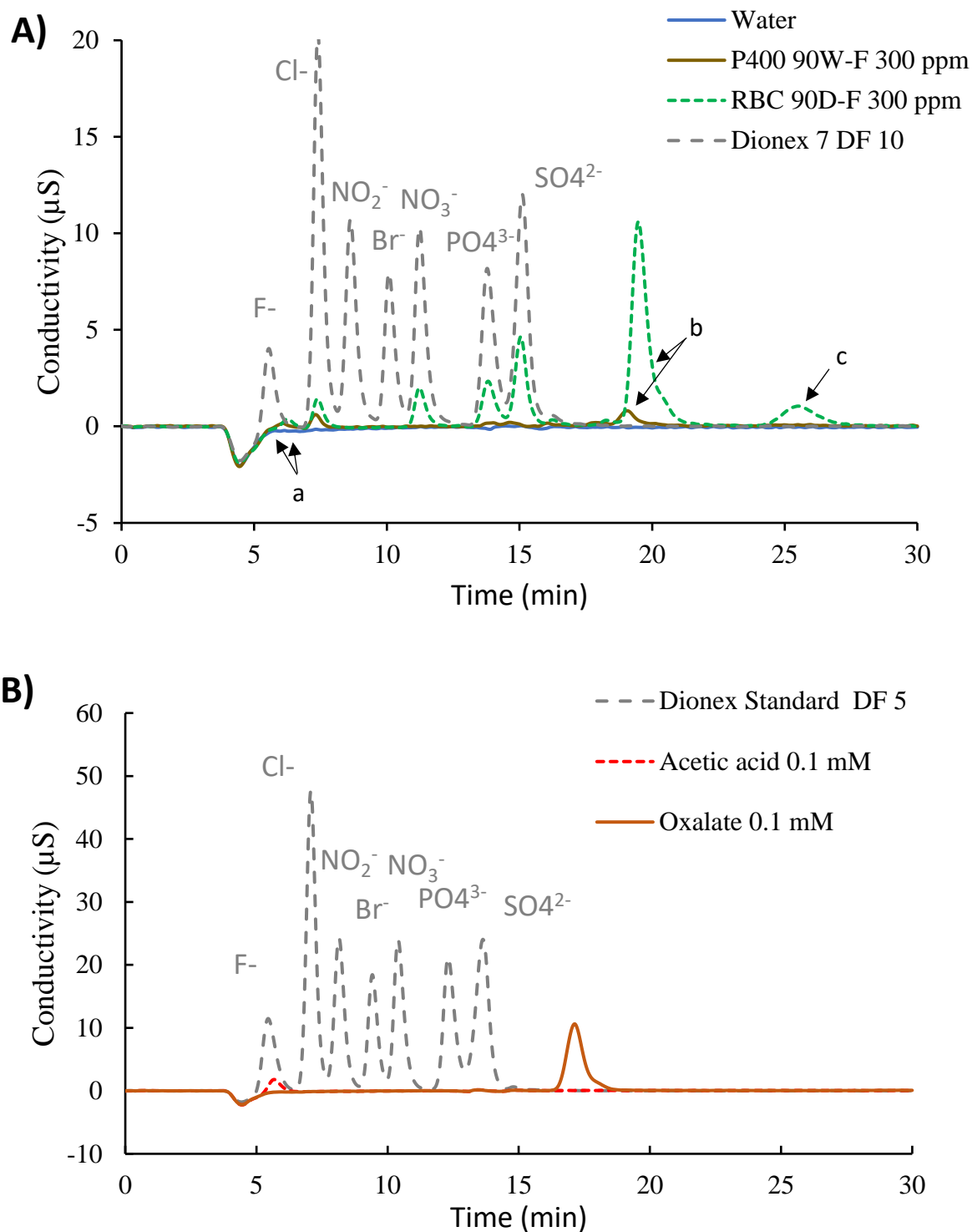


**Figure C1:** Conductivity signals of anions from the filtrate of the wet-ozonized pine 400 (P400 90W-F) biochar and the filtrate from the dry-ozonized rogue biochar (RBC 90D-F) at a DOC concentration of 300 ppm in A) and conductivity signals of standard acetate and oxalate in B). The standard Dionex seven (fluoride, chloride, nitrite, bromide, nitrate, phosphate, and sulfate) signals are also shown as a reference.

**Table C2: Solubilized phosphate from hydroxyapatite incubation with the filtrate from RBC 90D and P400 90W at different DOC concentrations and pH conditions. The values reported are averages of 3 replicates (n=3).**

	Solubilized phosphate (mg/L)				
	Day 0	Day 2	Day 4	Day 6	Day 8
milli-Q	4.4 ± 1.7	4.8 ± 1.4	4.4 ± 0.9	4.4 ± 0.5	3.8 ± 0.8
RBC 90D 10 ppm	5.6 ± 0.7	7.4 ± 0.9	8.0 ± 0.8	8.3 ± 1.1	7.5 ± 0.1
RBC 90D 75 ppm	24.7 ± 1.0	35.6 ± 0.9	34.8 ± 2.7	35.9 ± 1.8	33 ± 2.9
RBC 90D 300 ppm	86.8 ± 2.0	143.6 ± 3.0	150.2 ± 6.6	145.6 ± 2.8	115.1 ± 3.5
RBC 90D 600 ppm	182.8 ± 6.1	310.9 ± 1.0	326.3 ± 3.7	339.6 ± 8.5	301.4 ± 11.6
P400 90W 10 ppm	6.1 ± 1.6	7.7 ± 0.7	7.5 ± 2.0	8.2 ± 0.9	7.6 ± 1.3
P400 90W 75 ppm	34.9 ± 2.0	45.9 ± 2.7	47.0 ± 2.0	44.0 ± 0.4	40 ± 2.4
P400 90W 300 ppm	143.3 ± 4.8	183 ± 12.4	192.6 ± 4.5	190.2 ± 11.2	184.9 ± 5.0
P400 90W 600 ppm	260.9 ± 7.7	355.8 ± 8.3	380.7 ± 5.7	396.8 ± 28.8	387.2 ± 22.5
milli-Q pH 7	2.3 ± 0.7	NQ	1.0 ± 0.5	1.0 ± 0.4	1.0 ± 0.3
RBC 90D 10 ppm pH 7	2.0 ± 1.0	6.6 ± 1.6	3.6 ± 0	3.9 ± 1.2	4.0 ± 1.0
RBC 90D 75 ppm pH 7	3.9 ± 0.8	5.6 ± 1.5	5.9 ± 0.6	5.1 ± 0.2	5.2 ± 0.3
RBC 90D 300 ppm pH 7	2.1 ± 1.1	3.6 ± 1.6	3.0 ± 0.7	4.6 ± 0.7	2.5 ± 0.4
RBC 90D 600 ppm pH 7	1.1 ± 0.3	3.3 ± 0.3	NQ	NQ	NQ
P400 90W 10 ppm pH 7	1.8 ± 0.2	2.1 ± 0.9	2.5 ± 0.4	3.2 ± 0.7	1.7 ± 0.6
P400 90W 75 ppm pH 7	3.1 ± 0.2	6.7 ± 0.7	4.6 ± 0.3	6.4 ± 0.4	6.0 ± 0.6
P400 90W 300 ppm pH 7	5.4 ± 0.3	7.3 ± 0.5	10.1 ± 1.9	8.1 ± 0.6	6.3 ± 1.2
P400 90W 600 ppm pH 7	5.8 ± 2.1	6.5 ± 0.8	9.2 ± 0.9	6.9 ± 0.6	7.5 ± 0.7

**Table C3: Solubilized phosphorus (mg P/L) from hydroxyapatite incubation with filtrate from RBC 90D and P400 90W at different DOC concentrations and pH conditions. The values reported were converted from the solubilized phosphate ( $\text{HPO}_4^{2-}$ ) measured by ion chromatography as reported in Table C2. Values are averages of 3 replicates (n=3)  $\pm$ SD.**

	Solubilized phosphorus (mg P/L)				
	Day 0	Day 2	Day 4	Day 6	Day 8
milli-Q water	1.4 $\pm$ 0.5	1.5 $\pm$ 0.5	1.4 $\pm$ 0.3	1.4 $\pm$ 0.2	1.2 $\pm$ 0.3
RBC 90D 10 ppm	1.8 $\pm$ 0.2	2.4 $\pm$ 0.3	2.6 $\pm$ 0.3	2.7 $\pm$ 0.4	2.4 $\pm$ 0
RBC 90D 75 ppm	8.0 $\pm$ 0.3	11.5 $\pm$ 0.3	11.2 $\pm$ 0.9	11.6 $\pm$ 0.6	10.7 $\pm$ 0.9
RBC 90D 300 ppm	28.0 $\pm$ 0.6	46.3 $\pm$ 1.0	48.5 $\pm$ 2.1	47.0 $\pm$ 0.9	37.1 $\pm$ 1.1
RBC 90D 600 ppm	59.0 $\pm$ 2.0	100.3 $\pm$ 0.3	105.3 $\pm$ 1.2	109.6 $\pm$ 2.7	97.3 $\pm$ 3.7
P400 90W 10 ppm	2.0 $\pm$ 0.5	2.5 $\pm$ 0.2	2.4 $\pm$ 0.6	2.6 $\pm$ 0.3	2.5 $\pm$ 0.4
P400 90W 75 ppm	11.3 $\pm$ 0.6	14.8 $\pm$ 0.9	15.2 $\pm$ 0.6	14.2 $\pm$ 0.1	12.9 $\pm$ 0.8
P400 90W 300 ppm	46.2 $\pm$ 1.5	59.1 $\pm$ 4.0	62.2 $\pm$ 1.5	61.4 $\pm$ 3.6	59.7 $\pm$ 1.6
P400 90W 600 ppm	84.2 $\pm$ 2.5	114.8 $\pm$ 2.7	122.9 $\pm$ 1.8	128.1 $\pm$ 9.3	125.0 $\pm$ 7.3
milli-Q water pH 7	0.7 $\pm$ 0.2	NQ	0.3 $\pm$ 0.2	0.3 $\pm$ 0.1	0.3 $\pm$ 0.1
RBC 90D 10 ppm pH 7	0.6 $\pm$ 0.3	2.1 $\pm$ 0.5	1.2 $\pm$ 0	1.3 $\pm$ 0.4	1.3 $\pm$ 0.3
RBC 90D 75 ppm pH 7	1.3 $\pm$ 0.3	1.8 $\pm$ 0.5	1.9 $\pm$ 0.2	1.6 $\pm$ 0.1	1.7 $\pm$ 0.1
RBC 90D 300 ppm pH 7	0.7 $\pm$ 0.4	1.2 $\pm$ 0.5	1.0 $\pm$ 0.2	1.5 $\pm$ 0.2	0.8 $\pm$ 0.1
RBC 90D 600 ppm pH 7	0.4 $\pm$ 0.1	1.1 $\pm$ 0.1	NQ	NQ	NQ
P400 90W 10 ppm pH 7	0.6 $\pm$ 0.1	0.7 $\pm$ 0.3	0.8 $\pm$ 0.1	1.0 $\pm$ 0.2	0.5 $\pm$ 0.2
P400 90W 75 ppm pH 7	1.0 $\pm$ 0.1	2.2 $\pm$ 0.2	1.5 $\pm$ 0.1	2.1 $\pm$ 0.1	1.9 $\pm$ 0.2
P400 90W 300 ppm pH 7	1.7 $\pm$ 0.1	2.4 $\pm$ 0.2	3.3 $\pm$ 0.6	2.6 $\pm$ 0.2	2.0 $\pm$ 0.4
P400 90W 600 ppm pH 7	1.9 $\pm$ 0.7	2.1 $\pm$ 0.3	3.0 $\pm$ 0.3	2.2 $\pm$ 0.2	2.4 $\pm$ 0.2

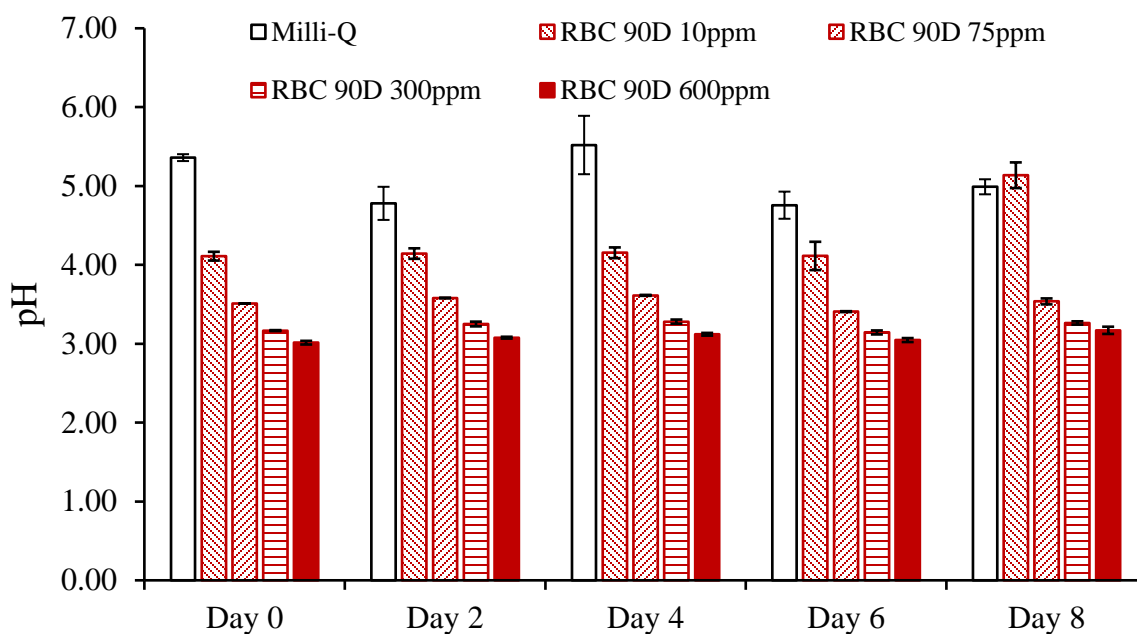


**Figure C2:** pH measurements of the filtrates from the dry-ozonized rogue biochar (RBC 90D) at different DOC concentrations (10, 75, 300 and 600 ppm), used as the no-hydroxyapatite control. The error bars denote standard deviation of 3 replicates (n=3).

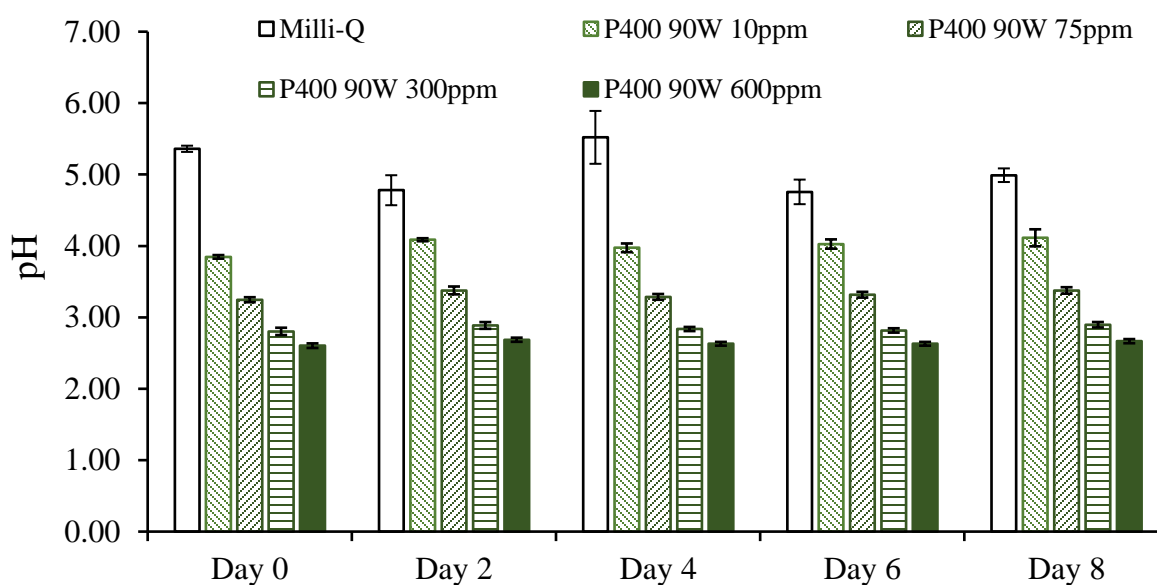


**Figure C3:** pH measurements of the filtrates from the wet-ozonized pine 400 biochar (P400 90W) at different DOC concentrations (10, 75, 300 and 600 ppm), used as the no-hydroxyapatite control. The error bars denote standard deviation of 3 replicates (n=3).

**Table C4: pH measurements of the filtrates from the RBC 90D and P400 90W (no hydroxyapatite) at different DOC concentrations measured from day 0 to day 8 of the hydroxyapatite assay experiment.**

	Day 0	Day 2	Day 4	Day 6	Day 8
Milli-Q	5.36 ± 0.04	4.78 ± 0.21	5.52 ± 0.37	4.76 ± 0.17	4.99 ± 0.10
P400 90W 10ppm	3.85 ± 0.03	4.09 ± 0.02	3.97 ± 0.06	4.03 ± 0.07	4.11 ± 0.12
P400 90W 75ppm	3.25 ± 0.04	3.38 ± 0.06	3.29 ± 0.04	3.32 ± 0.04	3.38 ± 0.05
P400 90W 300ppm	2.80 ± 0.05	2.89 ± 0.05	2.84 ± 0.03	2.82 ± 0.03	2.90 ± 0.04
P400 90W 600ppm	2.60 ± 0.03	2.69 ± 0.03	2.63 ± 0.03	2.63 ± 0.03	2.67 ± 0.03
RBC 90D 10ppm	4.11 ± 0.06	4.14 ± 0.07	4.15 ± 0.07	4.11 ± 0.18	5.14 ± 0.16
RBC 90D 75ppm	3.51 ± 0	3.58 ± 0	3.61 ± 0.01	3.41 ± 0.01	3.54 ± 0.04
RBC 90D 300ppm	3.17 ± 0.01	3.25 ± 0.03	3.28 ± 0.03	3.14 ± 0.03	3.26 ± 0.02
RBC 90D 600ppm	3.01 ± 0.02	3.08 ± 0.01	3.12 ± 0.02	3.05 ± 0.03	3.17 ± 0.05
Milli-Q pH 7	7.04 ± 0.07	6.89 ± 0.07	6.76 ± 0.09	6.77 ± 0.19	6.75 ± 0.21
P400 90W 10ppm pH 7	6.28 ± 0.01	6.86 ± 0.09	6.79 ± 0.10	6.97 ± 0.14	7.07 ± 0.11
P400 90W 75ppm pH 7	6.13 ± 0.01	6.62 ± 0.05	6.47 ± 0.06	7.05 ± 0.07	7.27 ± 0.01
P400 90W 300ppm pH 7	6.30 ± 0.02	6.67 ± 0.05	6.48 ± 0.03	7.19 ± 0.17	7.47 ± 0.02
P400 90W 600ppm pH 7	6.32 ± 0.03	6.59 ± 0.05	6.45 ± 0.02	7.30 ± 0.03	7.55 ± 0.06
RBC 90D 10ppm pH 7	6.59 ± 0.05	6.76 ± 0.22	6.88 ± 0.25	6.84 ± 0.27	6.85 ± 0.21
RBC 90D 75ppm pH 7	6.32 ± 0.03	6.63 ± 0.12	6.79 ± 0.10	6.76 ± 0.09	7.05 ± 0.07
RBC 90D 300ppm pH 7	6.69 ± 0.03	6.60 ± 0.01	6.78 ± 0.01	6.80 ± 0.03	6.87 ± 0.03
RBC 90D 600ppm pH 7	6.64 ± 0	6.65 ± 0.04	6.79 ± 0.03	6.90 ± 0.06	7.34 ± 0.14

**Table C5: mol ratio of solubilized calcium and phosphorus from the hydroxyapatite incubation assay samples collected on day 8. To obtain the mol ratio, the masses of the solubilized phosphorus and calcium obtained from the ICP-MS were converted to mol. Note that the Ca:P mol ratio in pure solid hydroxyapatite is 1.67.**

	Ca:P mol ratio	
	pH unchanged	pH neutralized
P400 90W-F 10 ppm	1.210	0.601
P400 90W-F 75 ppm	1.308	1.035
P400 90W-F 300 ppm	1.109	0.771
P400 90W-F 600 ppm	1.049	0.534
RBC 90D-F 10 ppm	0.937	0.875
RBC 90D-F 75 ppm	0.927	1.188
RBC 90D-F 300 ppm	0.798	0.865
RBC 90D-F 600 ppm	0.494	0.145
water	1.427	

**Table C6: Measured concentrations (in mg/L) of some elements from the obtained from ICP-MS from the solubilization assay on day 8 of incubation of the filtrates from wet ozonized P400 (P400 90W) and dry-ozonized RBC biochar (RBC 90D) at DOC concentration of 600ppm (mg/L). Note: The ICP-MS was run by our collaborator McAlister Council-Troche in Virginia Tech, Blacksburg VA.**

	P400 90W				RBC 90D			
	No HA	with HA	at pH 7 no HA	at pH 7 with HA	No HA	with HA	at pH 7 no HA	at pH 7 with HA
<sup>24</sup> Mg	2.534	2.244	2.400	2.219	20.608	15.935	20.710	20.170
<sup>39</sup> K	10.866	9.823	10.368	9.758	57.239	52.329	56.938	56.320
<sup>55</sup> Mn	0.125	0.033	0.117	0.036	3.194	1.102	3.175	2.414
<sup>56</sup> Fe	1.054	0.154	0.980	0.911	6.086	0.355	6.088	5.731
<sup>63</sup> Cu	0.077	0.014	0.071	0.069	0.561	0.059	0.550	0.545
<sup>66</sup> Zn	0.479	0.029	0.416	0.092	0.597	0.075	0.580	0.346
<sup>75</sup> As	0.002	0.002	0.001	0.002	1.142	1.098	1.143	1.146
<sup>95</sup> Mo	0.040	0.022	0.039	0.039	0.003	0.002	0.004	0.003
<sup>31</sup> P	0.783	98.915	0.464	4.792	18.987	98.759	18.903	20.526
<sup>44</sup> Ca	23.133	156.385	22.810	25.800	36.638	87.626	37.153	37.458

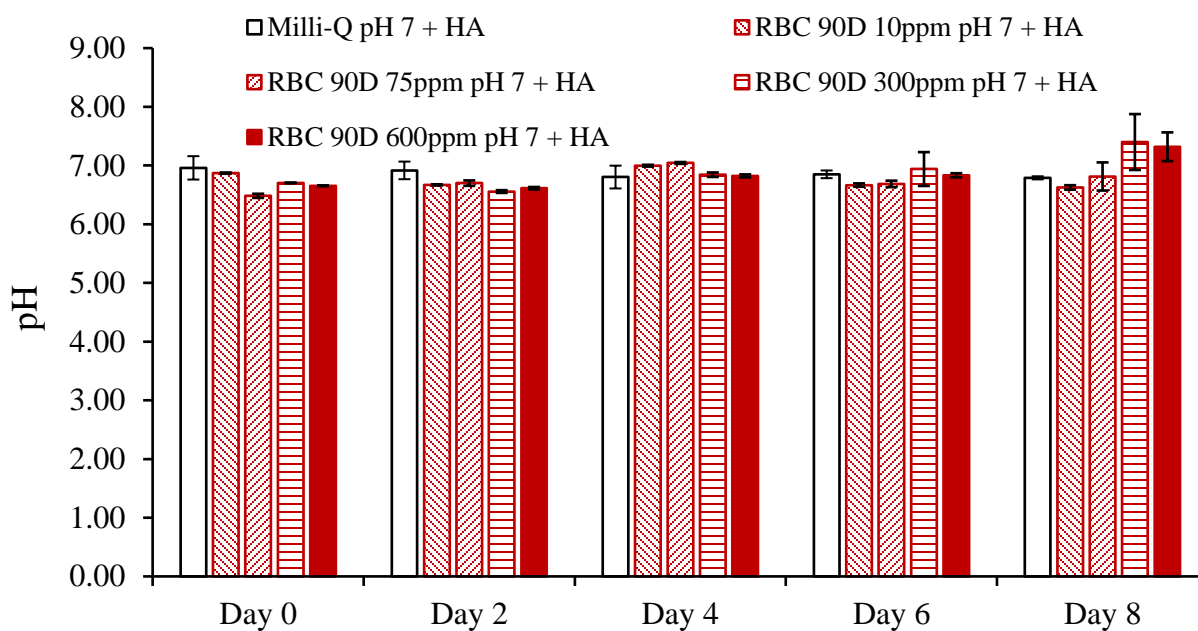


**Figure C4:** pH measurements of the filtrates from RBC 90D at neutralized pH at different DOC concentrations incubated with hydroxyapatite at day 0, 2, 4, 6 and 8. The data shown are the average of 3 replicates (n=3) for the water control (□), the 10 ppm DOC (▨), the 75 ppm DOC (▩), the 300 ppm DOC (▧) and the 600 ppm DOC (■).

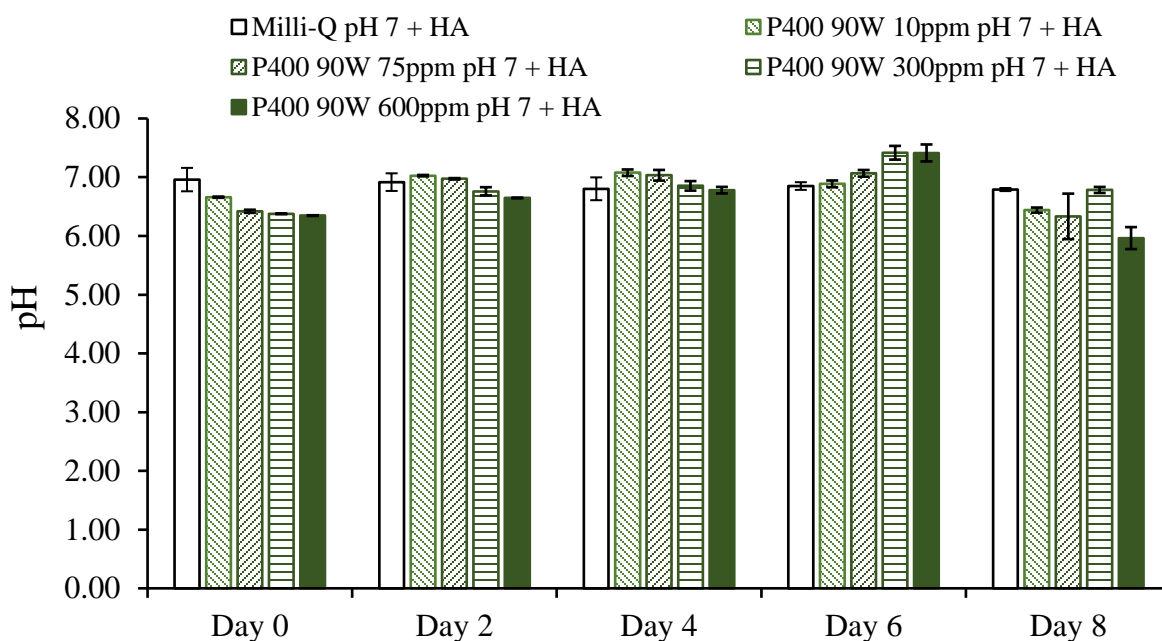


**Figure C5:** pH measurements of the filtrates from P400 90W at neutralized pH and different DOC concentrations incubated with hydroxyapatite at day 0, 2, 4, 6 and 8. The data shown are the average of 3 replicates (n=3) for the water control (□), the 10 ppm DOC (▨), the 75 ppm DOC (▩), the 300 ppm DOC (▧) and the 600 ppm DOC (■).

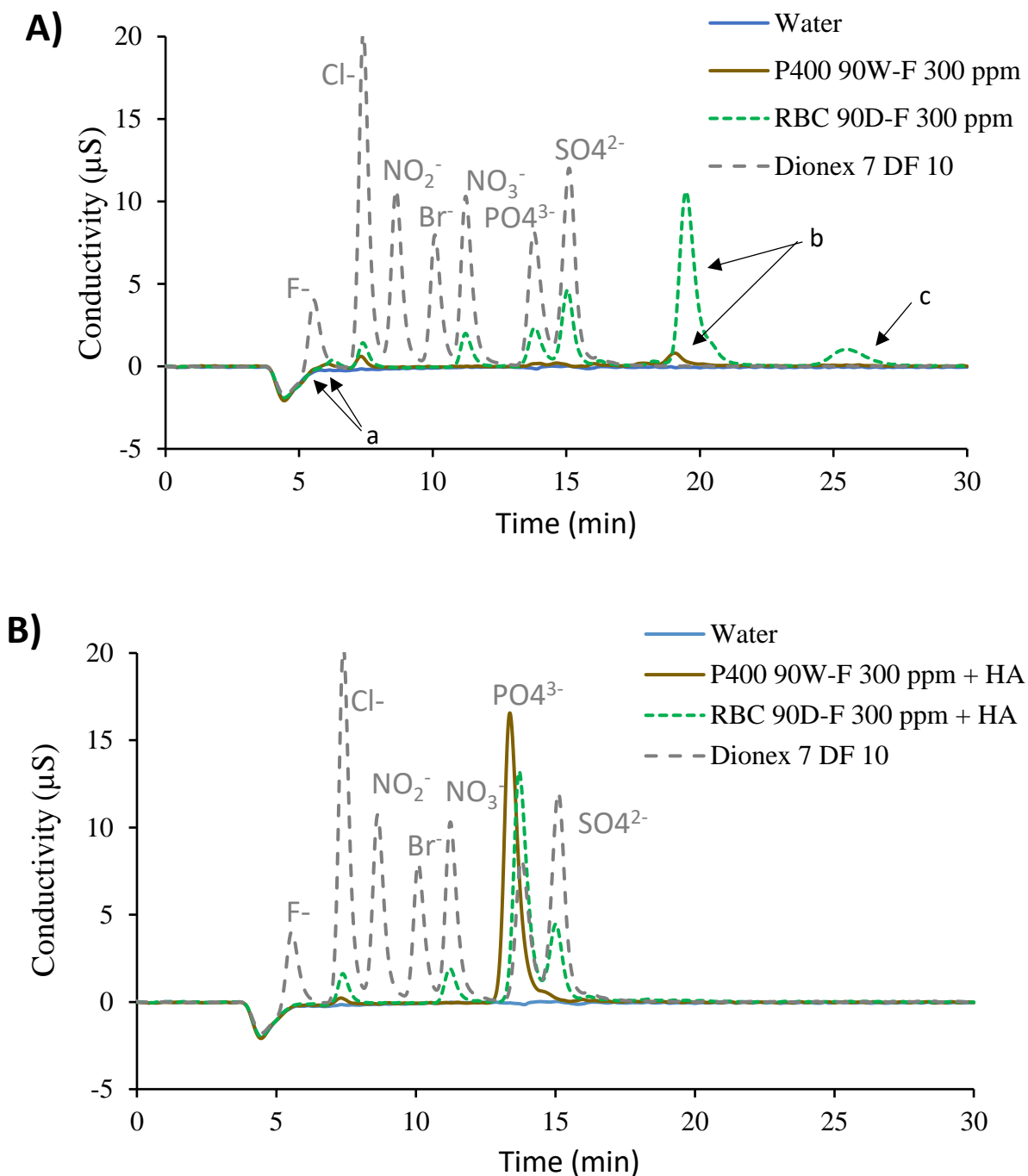


**Figure C6:** Conductivity signals of anions from the filtrate of the wet-ozonized pine 400 (P400 90W) biochar and the filtrate from the dry-ozonized rogue biochar (RBC 90D) at a DOC concentration of 300 ppm from the hydroxyapatite incubation assay on day 8. In A) the samples without HA; in B) the samples with HA. The standard Dionex seven (fluoride, chloride, nitrite, bromide, nitrate, phosphate, and sulfate) signals are also shown as a reference.

## APPENDIX D

## SUPPORTING INFORMATION CHAPTER V

A)

	1	2	3	4	5	6
A	UN 300ppm	UN 150ppm	UN 75ppm	UN 25ppm	UN 10ppm	UN 2ppm
B	90D 300ppm	90D 150ppm	90D 75ppm	90D 25ppm	90D 10ppm	90D 2ppm
C	90W 300ppm	90W 150ppm	90W 75ppm	90W 25ppm	90W 10ppm	90W 2ppm
D	empty	empty	empty	empty	empty	empty

B)

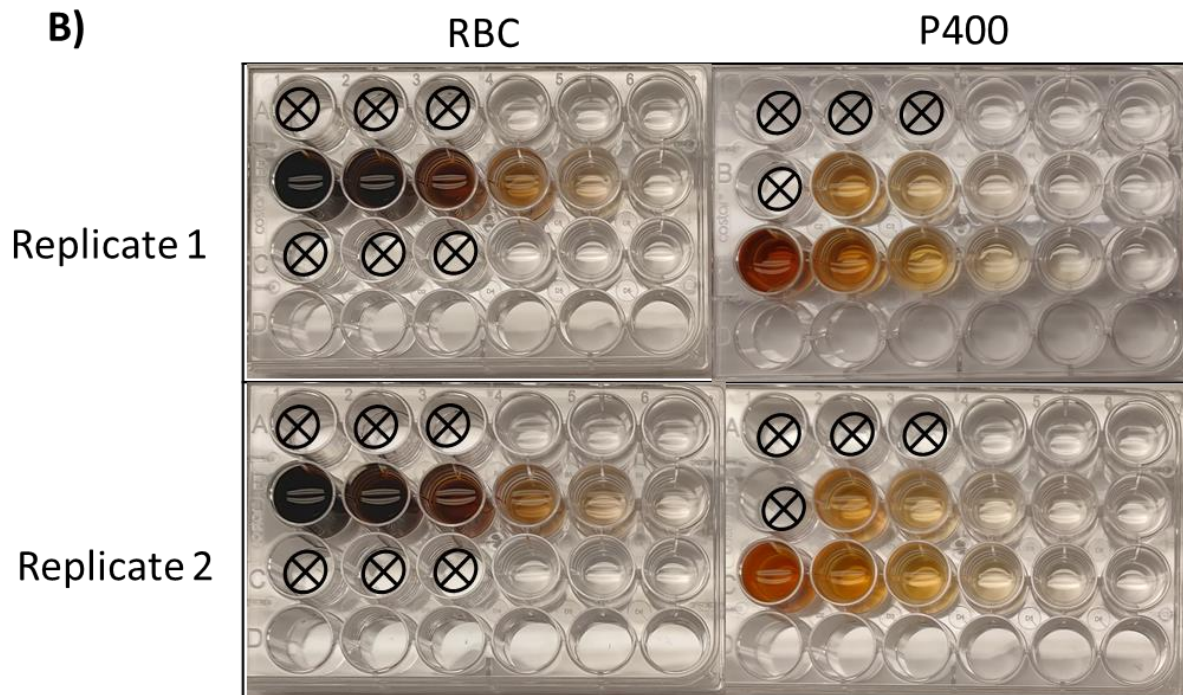


**Figure D1:** Photographs of the filtrates used as a control for the biochar filtrate toxicity assay. The layout of the multi-well plate is shown in A) where the first row represents the non-ozonized biochar filtrates, the second row represents the dry-ozonized biochar filtrates, and the third row represents the wet-ozonized biochar filtrates. The DOC concentration ranges from 2 ppm to 300 ppm going from right to left. The photographs of the two replicates multi-well plates are shown in B) for the filtrates from the rogue biochar (RBC) and pine 400 biochar (P400). Wells shown with the cross are the wells where the DOC extracted from the biochar was too low to reach the desired DOC concentration in the well.

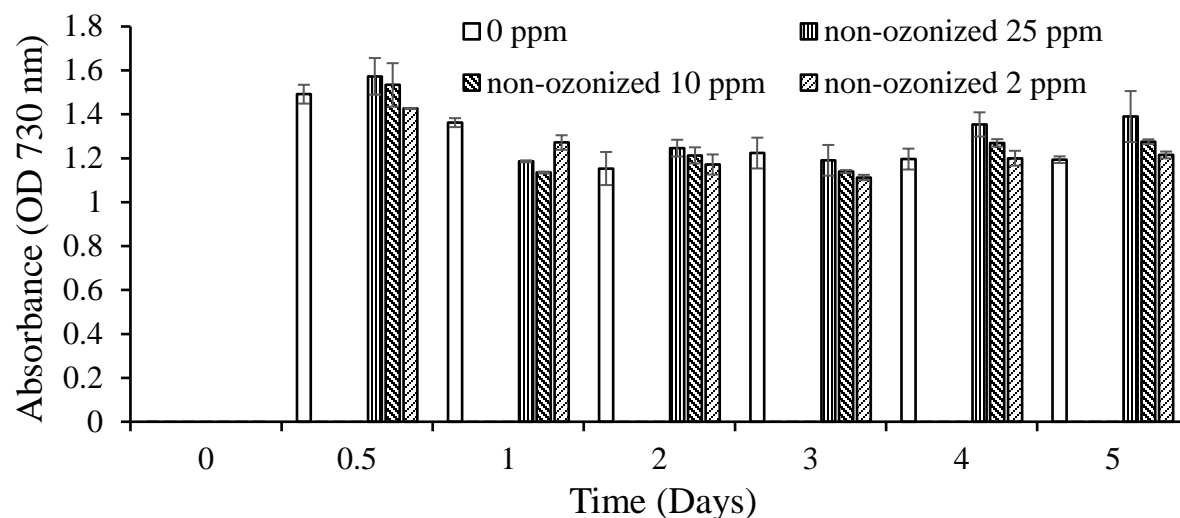


**Figure D2:** Optical density (OD<sub>730</sub>) of the growth of *P. putida* in incubation with filtrates from non-ozonized pine 400 biochar at different DOC concentrations. The OD<sub>730</sub> was measured every day for up to 5 days. The error bars on the graphs represent the standard deviation of the 2 plate replicates (n=2).

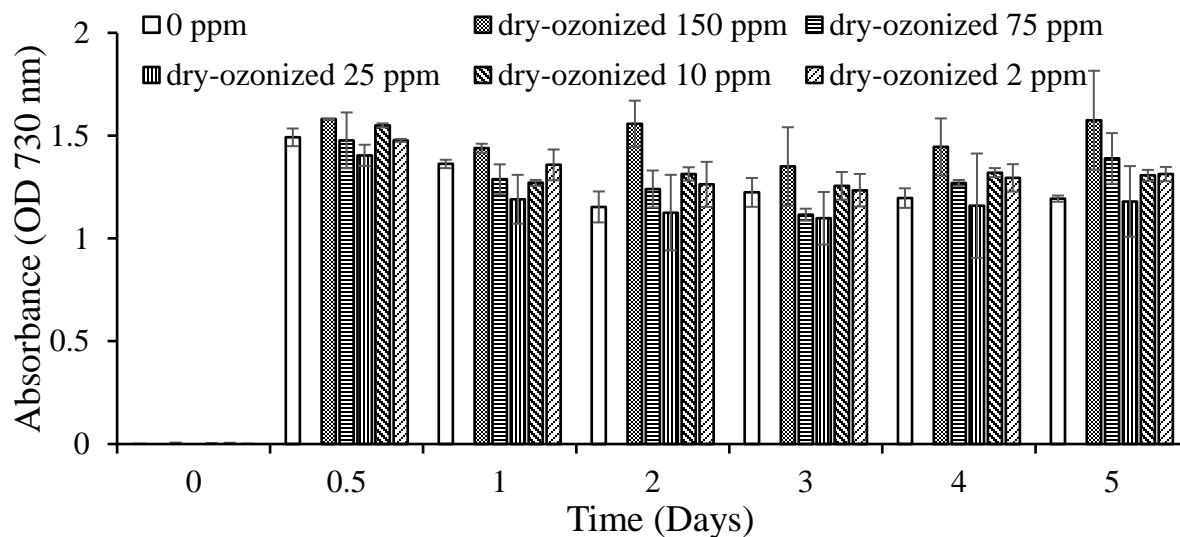


**Figure D3:** Optical density (OD<sub>730</sub>) of the growth of *P. putida* in incubation with filtrates from dry-ozonized pine 400 biochar at different DOC concentrations. The OD<sub>730</sub> was measured every day for up to 5 days. The error bars on the graphs represent the standard deviation of the 2 plate replicates (n=2).

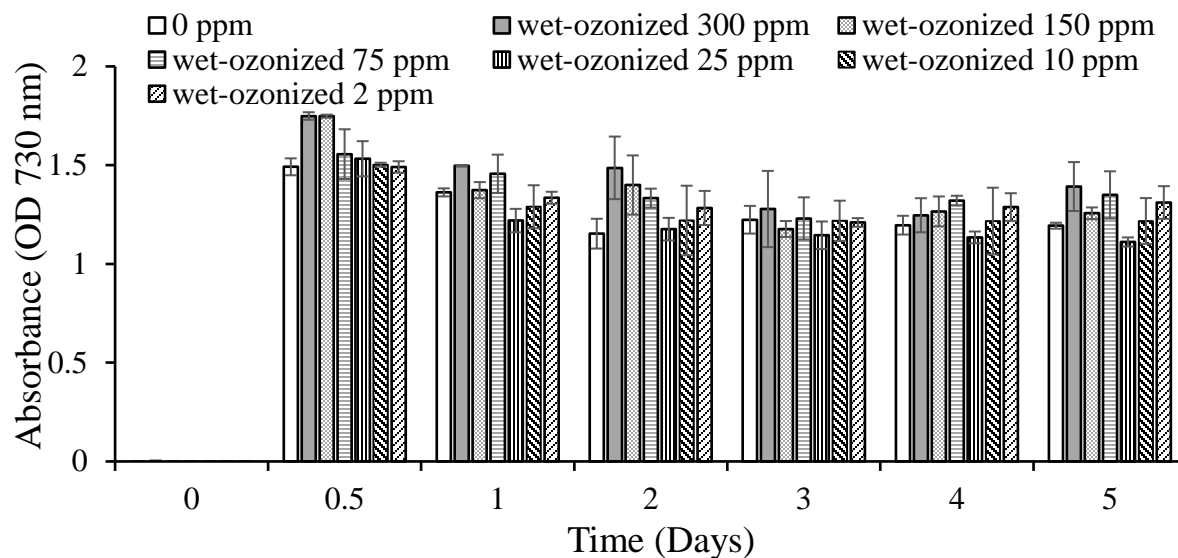


**Figure D4:** Optical density (OD730) of the growth of *P. putida* in incubation with filtrates from wet-ozonized pine 400 biochar at different DOC concentrations. The OD730 was measured every day for up to 5 days. The error bars on the graphs represent the standard deviation of the 2 plate replicates (n=2).

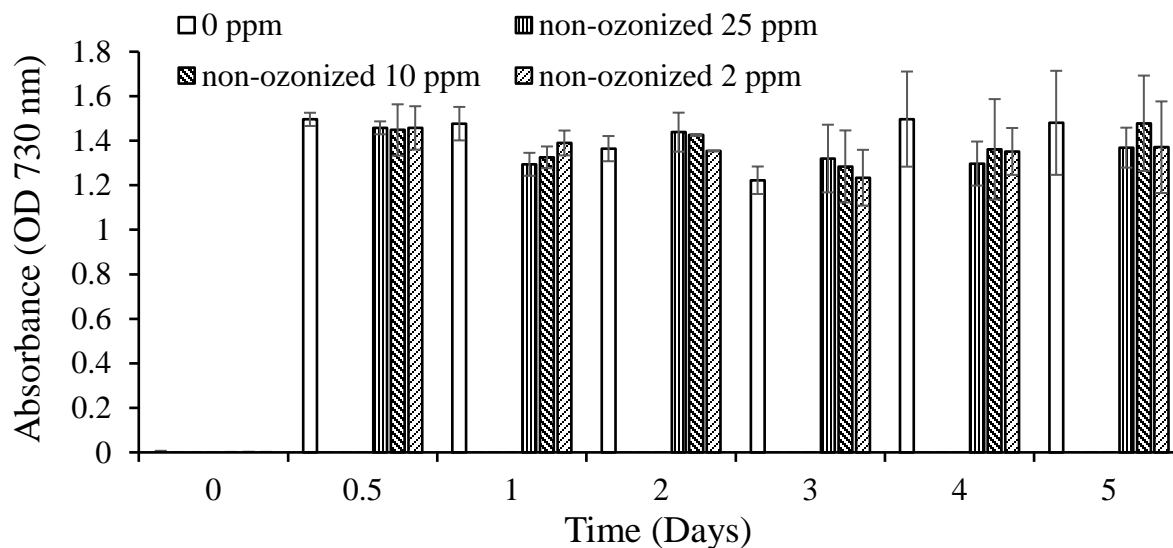


**Figure D5:** Optical density (OD730) of the growth of *P. putida* in incubation with filtrates from non-ozonized rogue biochar (RBC) at different DOC concentrations. The OD730 was measured every day for up to 5 days. The error bars on the graphs represent the standard deviation of the 2 plate replicates (n=2).

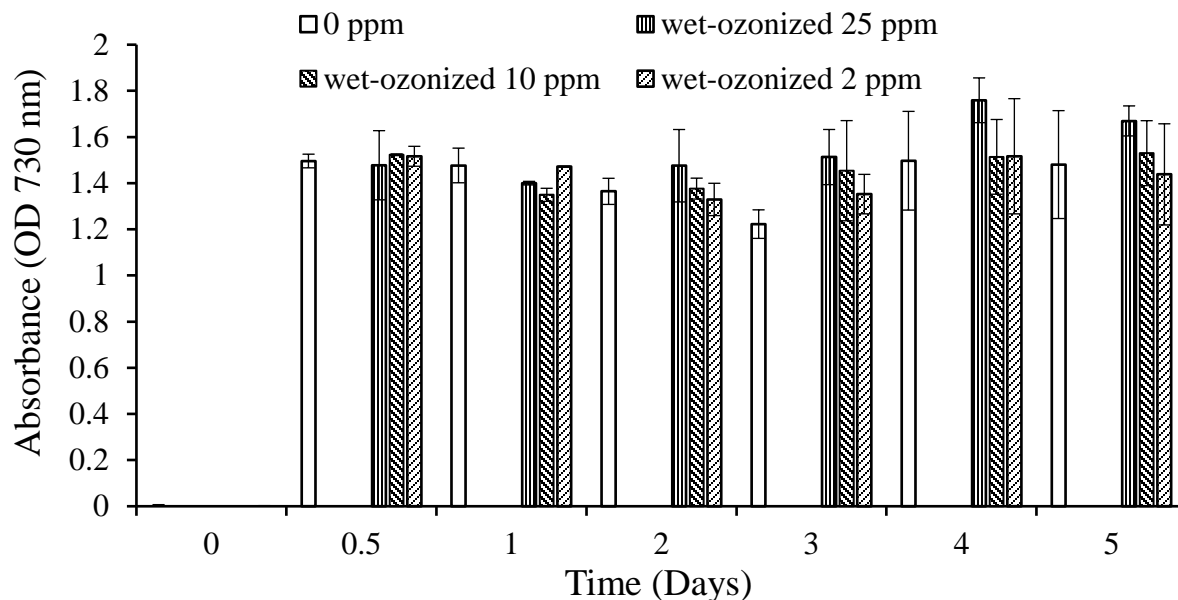


**Figure D6:** Optical density (OD<sub>730</sub>) of the growth of *P. putida* in incubation with filtrates from wet-ozonized rogue biochar (RBC) at different DOC concentrations. The OD<sub>730</sub> was measured every day for up to 5 days. The error bars on the graphs represent the standard deviation of the 2 plate replicates (n=2).

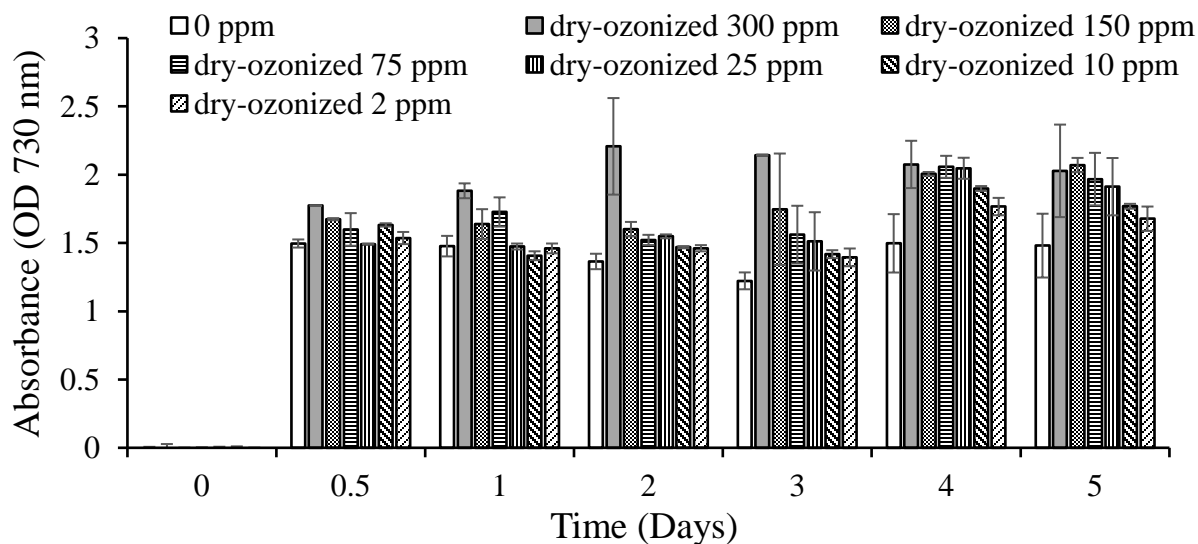


**Figure D7:** Optical density (OD<sub>730</sub>) of the growth of *P. putida* in incubation with filtrates from dry-ozonized rogue biochar (RBC) at different DOC concentrations. The OD<sub>730</sub> was measured every day for up to 5 days. The error bars on the graphs represent the standard deviation of the 2 plate replicates (n=2).

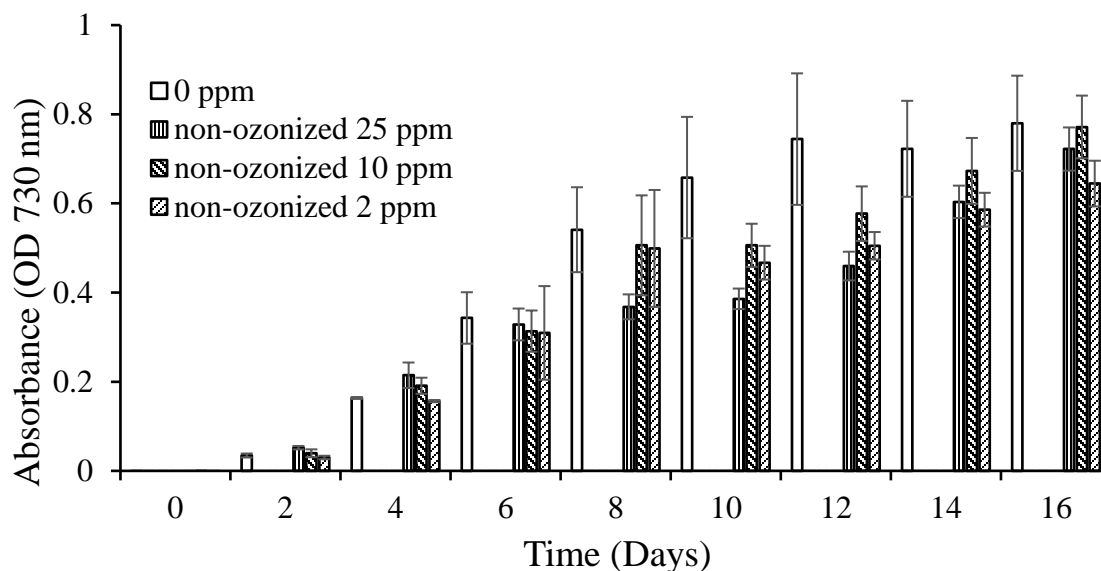


**Figure D8:** Optical density (OD730) of the growth of *Synechococcus elongatus* PCC 7942 (7942) in incubation with filtrates from non-ozonized pine 400 biochar at different DOC concentrations. The OD730 was measured every other day for up to 16 days. The error bars on the graphs represent the standard deviation of the 2 plate replicates (n=2).

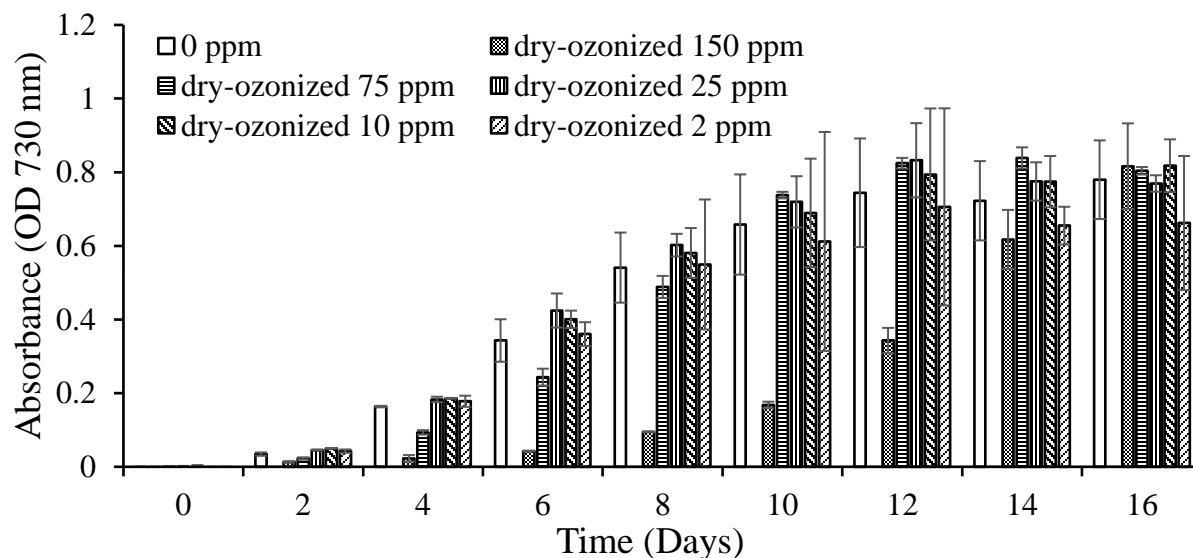


**Figure D9:** Optical density (OD730) of the growth of *Synechococcus elongatus* PCC 7942 (7942) in incubation with filtrates from dry-ozonized pine 400 biochar at different DOC concentrations. The OD730 was measured every other day for up to 16 days. The error bars on the graphs represent the standard deviation of the 2 plate replicates (n=2).

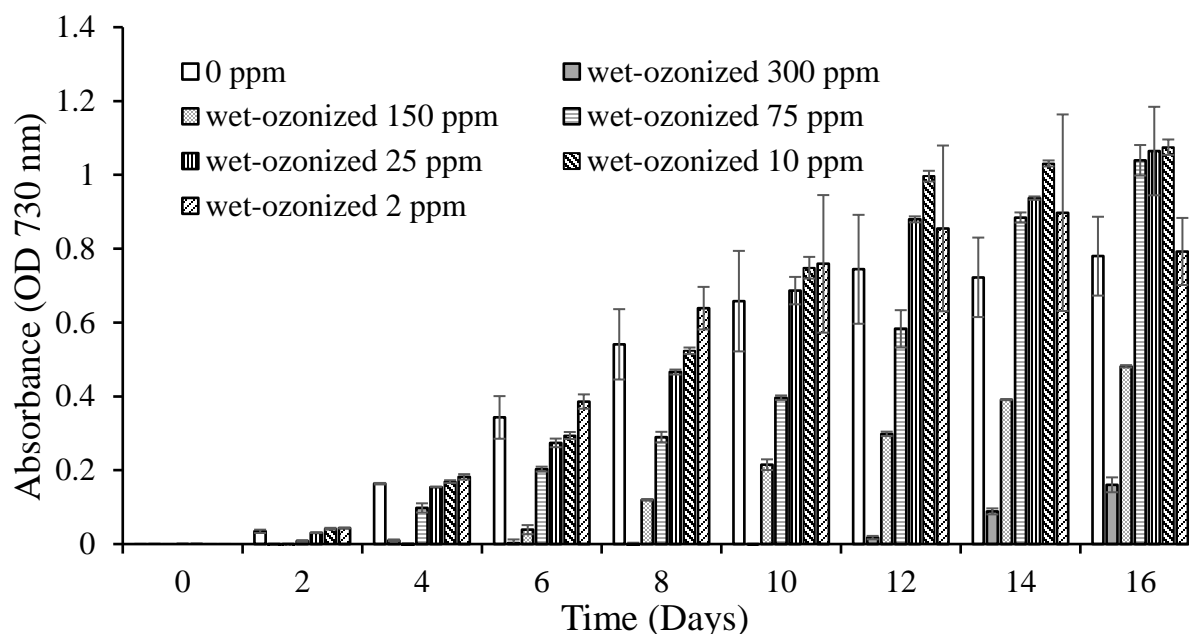


**Figure D10:** Optical density (OD<sub>730</sub>) of the growth of *Synechococcus elongatus* PCC 7942 (7942) in incubation with filtrates from wet-ozonized pine 400 biochar at different DOC concentrations. The OD<sub>730</sub> was measured every other day for up to 16 days. The error bars on the graphs represent the standard deviation of the 2 plate replicates (n=2).

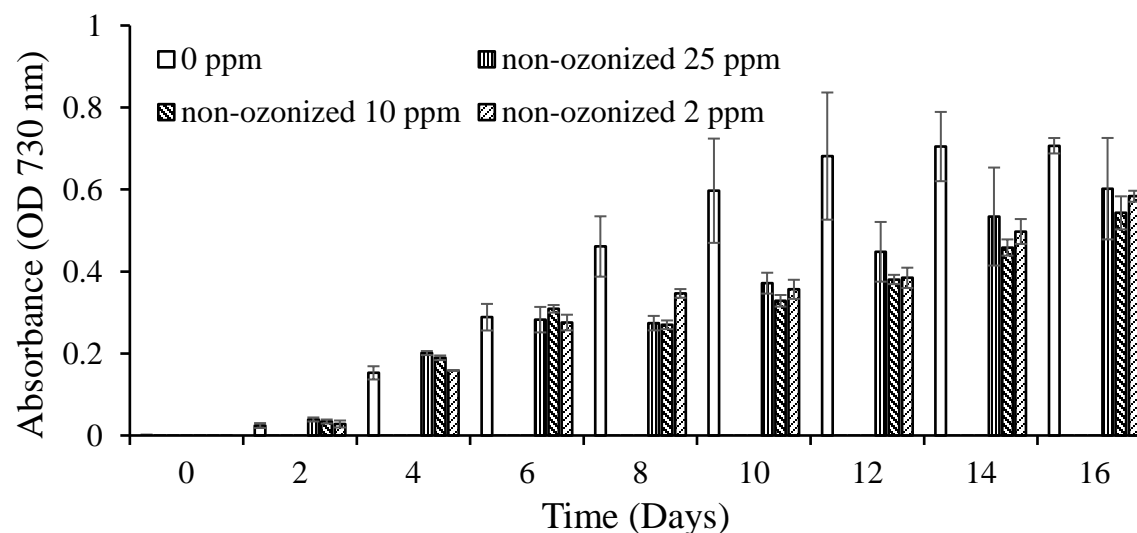


**Figure D11:** Optical density (OD<sub>730</sub>) of the growth of *Synechococcus elongatus* PCC 7942 (7942) in incubation with filtrates from non-ozonized rogue biochar (RBC) at different DOC concentrations. The OD<sub>730</sub> was measured every other day for up to 16 days. The error bars on the graphs represent the standard deviation of the 2 plate replicates (n=2).

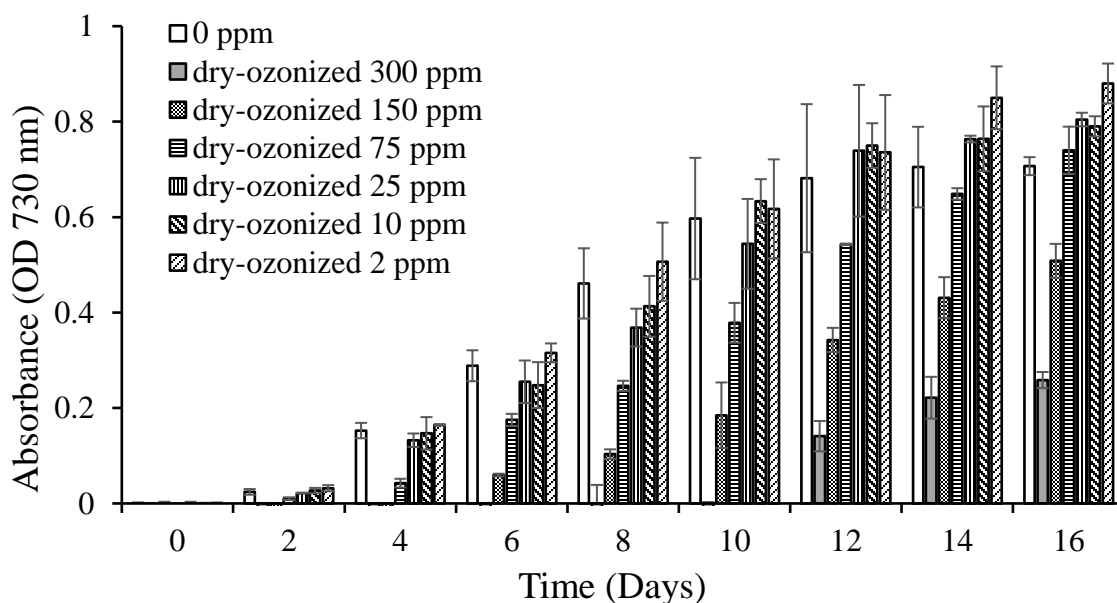


**Figure D12:** Optical density (OD730) of the growth of *Synechococcus elongatus* PCC 7942 (7942) in incubation with filtrates from dry-ozonized rogue biochar (RBC) at different DOC concentrations. The OD730 was measured every other day for up to 16 days. The error bars on the graphs represent the standard deviation of the 2 plate replicates (n=2).

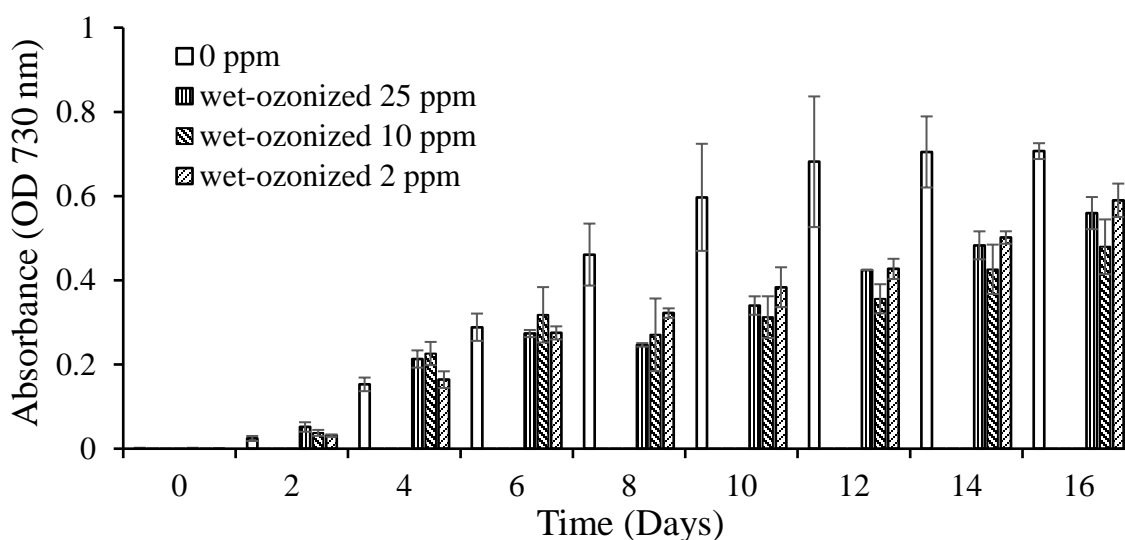


**Figure D13:** Optical density (OD730) of the growth of *Synechococcus elongatus* PCC 7942 (7942) in incubation with filtrates from wet-ozonized rogue biochar (RBC) at different DOC concentrations. The OD730 was measured every other day for up to 16 days. The error bars on the graphs represent the standard deviation of the 2 plate replicates (n=2).

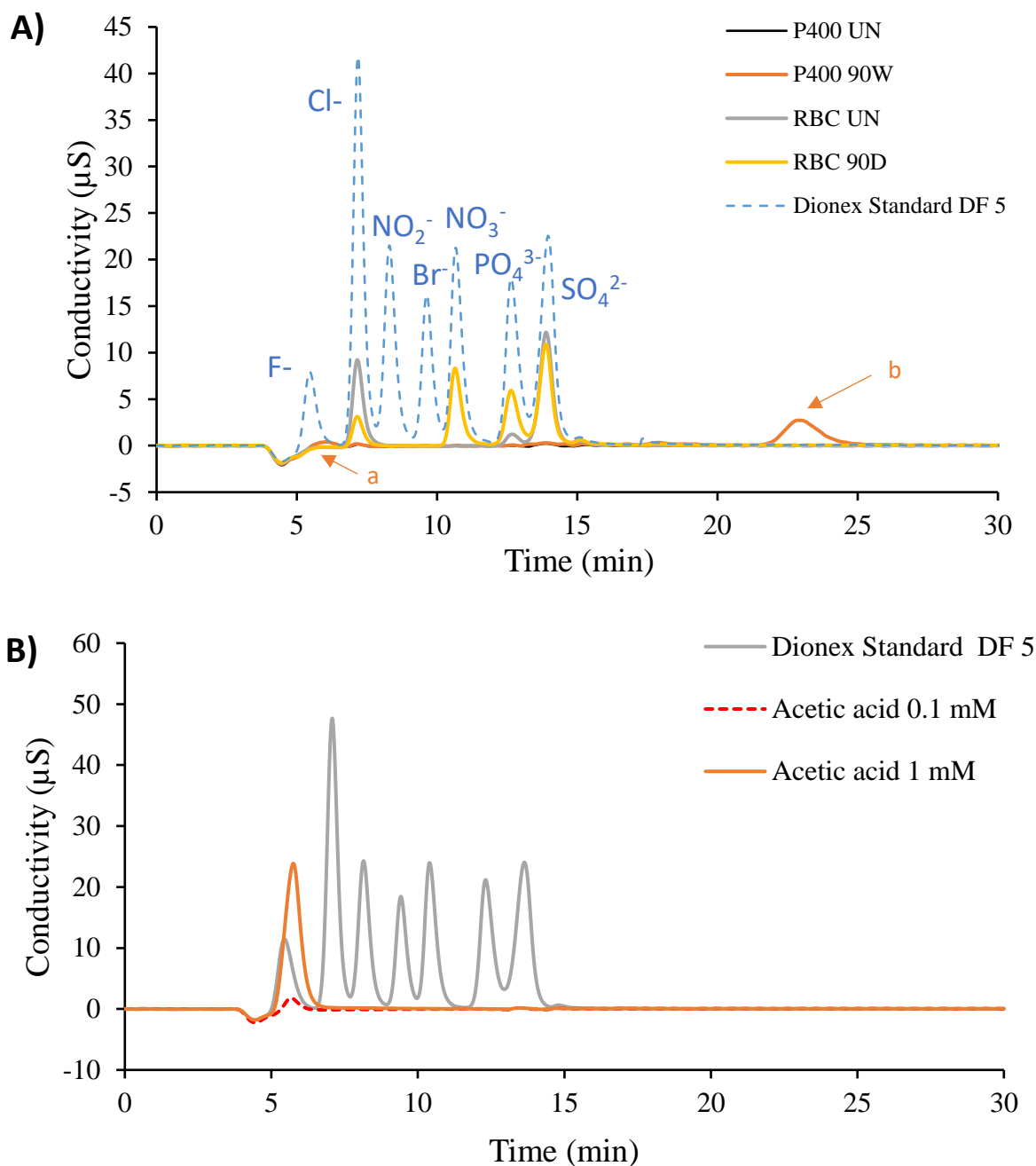


**Figure D14:** Conductivity signals of anions from pine 400 and rogue biochar (before and after ozonization) compared with standard acetic acid. In A) Conductivity signals of anions from the filtrate of the non-ozonized pine 400 biochar (P400 UN), wet-ozonized pine 400 biochar (P400 90W), non-ozonized rogue biochar (RBC UN) and dry-ozonized rogue biochar (RBC 90D). The signal shown at the “a” and “b” were generated by wet-ozonization of P400. In B) Conductivity signals of standard acetic acid. The standard Dionex seven (fluoride, chloride, nitrite, bromide, nitrate, phosphate, and sulfate) signals are also shown as a reference.

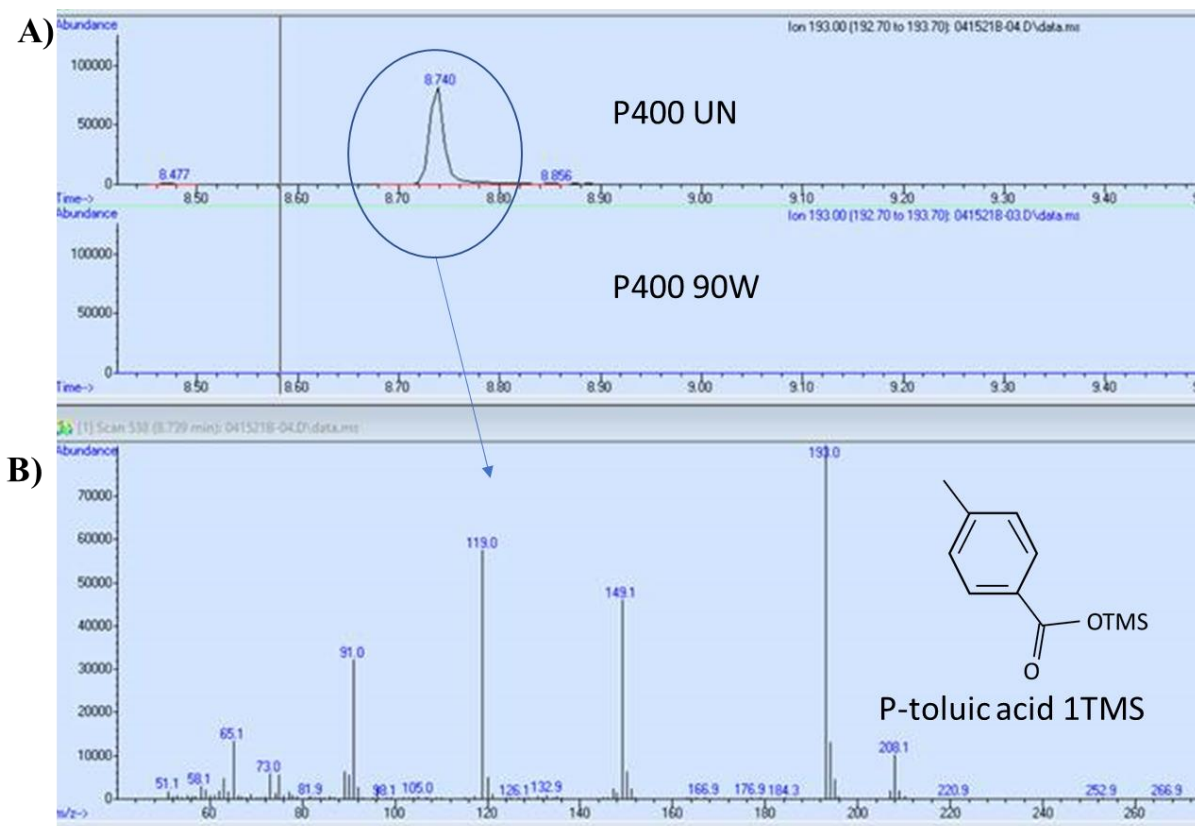


**Figure D15:** GC-MS spectra of p-toluic acid in pine 400 biochar filtrate. In A; GC spectra of the filtrate from non-ozonized pine 400 (P400 UN) on the top graph and wet-ozonized pine 400 (P400 90W) on the bottom graph. The mass spectra of the signal detected in P400 UN (circled) is shown in B. In B, mass spectra of compound (p-toluic acid 1TMS or trimethylsilyl) detected in the GC spectra of P400 UN.

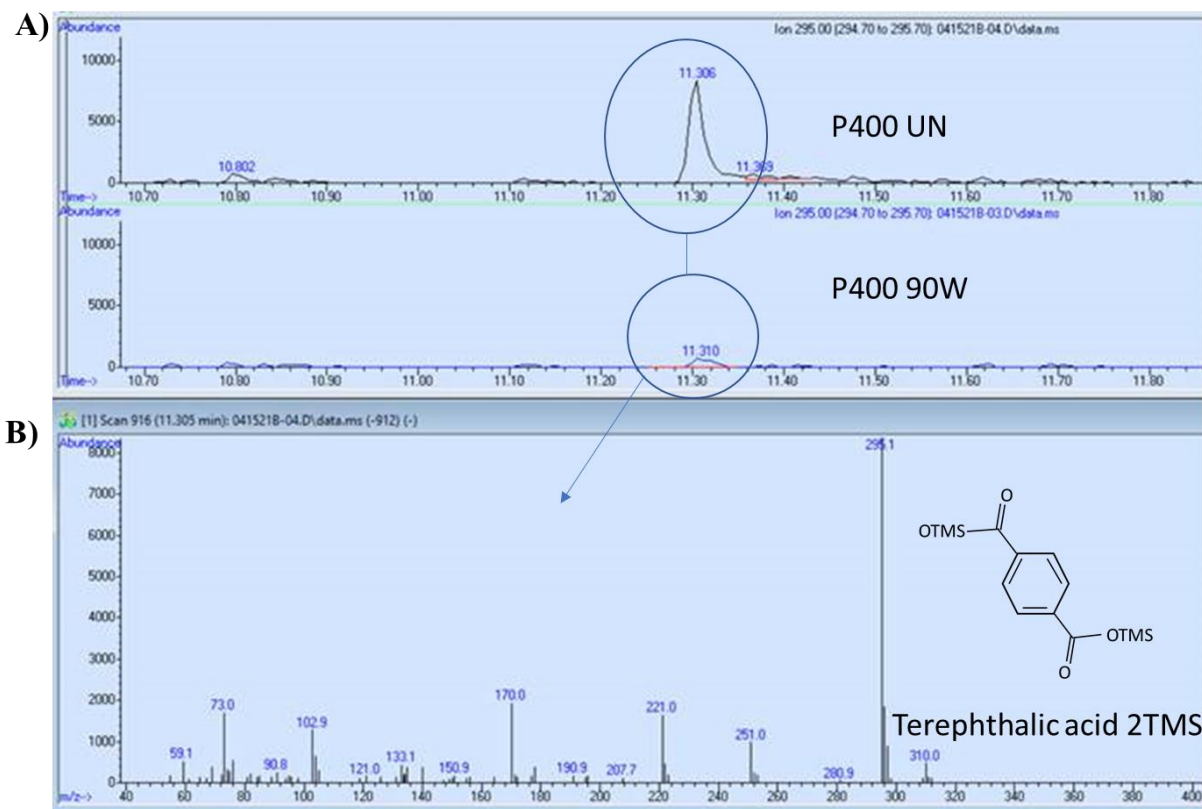


**Figure D16:** GC-MS spectra of terephthalic acid in pine 400 biochar filtrate. In A; GC spectra of the filtrate from non-ozonized pine 400 (P400 UN) on the top graph and wet-ozonized pine 400 (P400 90W) on the bottom graph. The mass spectra of the signal detected in P400 UN and P400 90W (circled) is shown in B. In B, mass spectra of compound (terephthalic acid 2TMS or trimethylsilyl) detected in the GC spectra of P400 UN and P400 90W.

**APPENDIX E**  
**SUPPORTING INFORMATION CHAPTER VI**

**Table E1: Daylength in Norfolk, Virginia during the cool season and warm season of the growth study. The day length was retrieved from Time and Date website.<sup>138</sup>**

	March 4th to April 1st, 2019	July 1 <sup>st</sup> to July 29 <sup>th</sup> , 2019
Day length (hrs: min:sec)	From 11:29:58 To 12:35:58	From 14:38:40 To 14:06:32

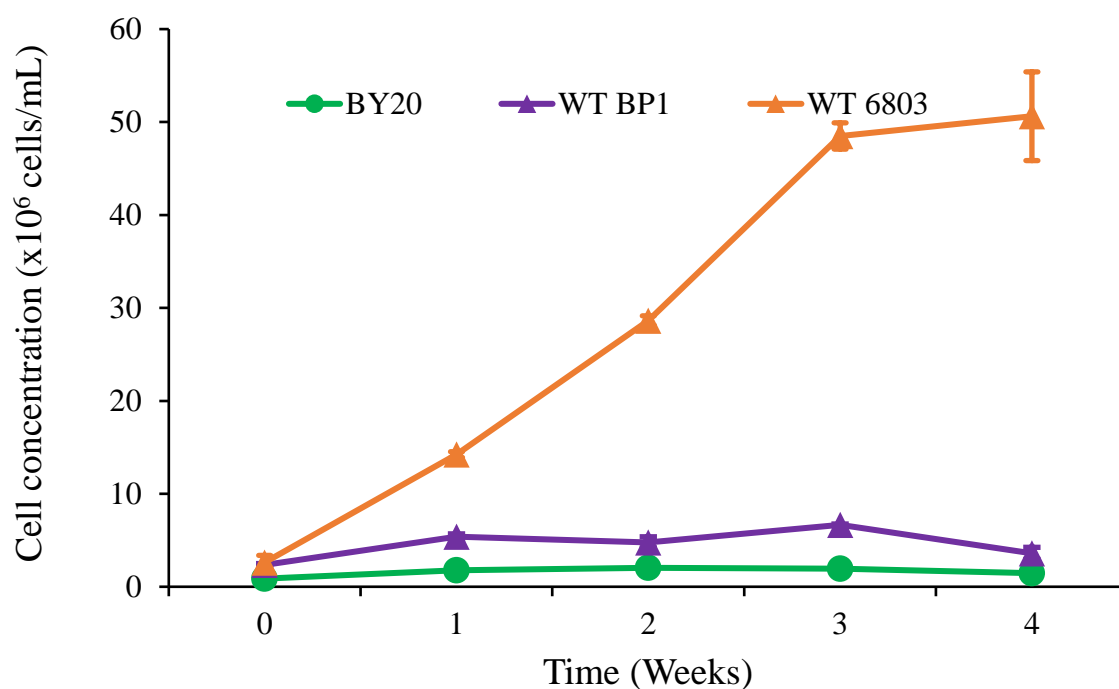


**Figure E1:** Weekly growth of GE *T. elongatus* BP1 BY20 (BY20), WT *T. elongatus* BP1 (WT BP1) and WT *Synechocystis* PCC 6803, used as control for the competition study conducted in the greenhouse during the cool season (16-26°C). The error bars denote the standard deviation of the cell concentration in two liquid culture flasks, each counted twice (total n=4).

**Table E2: Colony forming units from flask liquid cultures of GE *T. elongatus* BP1 BY20 (n=2), wild-type *T. elongatus* BP1 (n=2) and co-cultures GE *T. elongatus* BP1 BY20 + wild-type *T. elongatus* BP1 (n=3). Each flask was plated in triplicate, the CFU reported are averages from 6-9 plates.**

	BY20		WT BP1	BY20 + WT BP1	
	Control BG-11	BG-11 Tet10	Control BG-11	Control BG-11	BG-11 Tet10
Day 1	1.4E6 (±5E5) CFU/mL	9.6E5 (±2E5) CFU/mL	2.6E6 (±9E5) CFU/mL	1.8E6 (±8E5) CFU/mL	2.4E5 (±1E5) CFU/mL
Week 4	0 CFU/mL	0 CFU/mL	0 CFU/mL	0 CFU/mL	0 CFU/mL

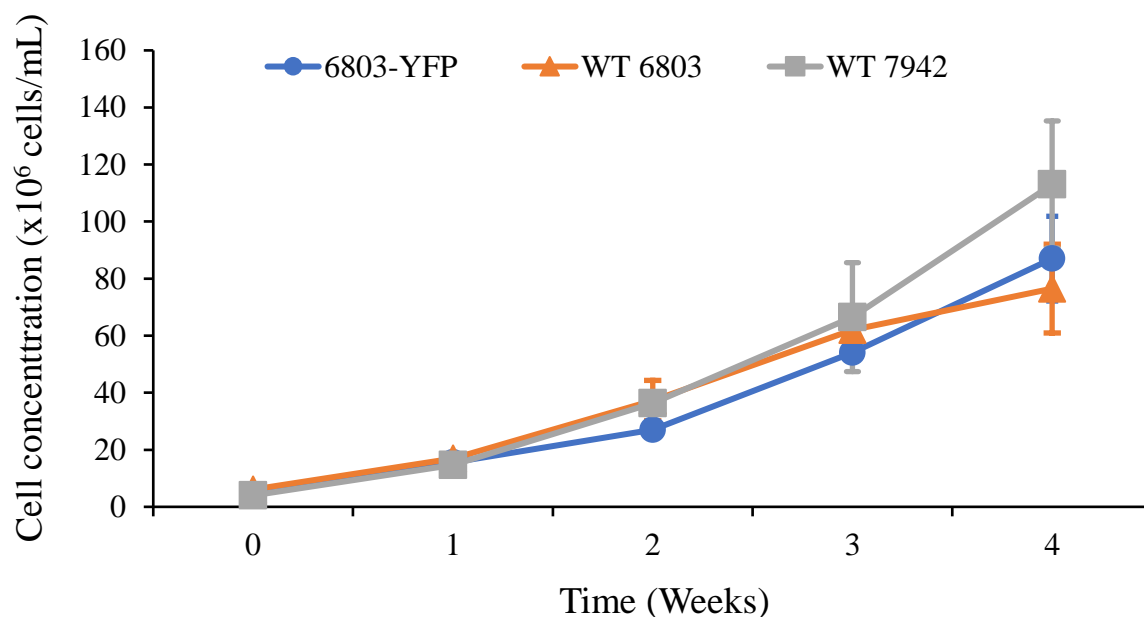


**Figure E2: Weekly growth of GE *Synechocystis* PCC 6803-YFP (6803-YFP) and WT *Synechococcus elongatus* PCC 7942 (WT 7942) and WT *Synechocystis* PCC 6803 (WT 6803), used as control for the competition study conducted in the greenhouse during the cool season (16-26°C). The error bars denote the standard deviation of the cell concentration in two liquid culture flasks, each counted twice (total n=4).**

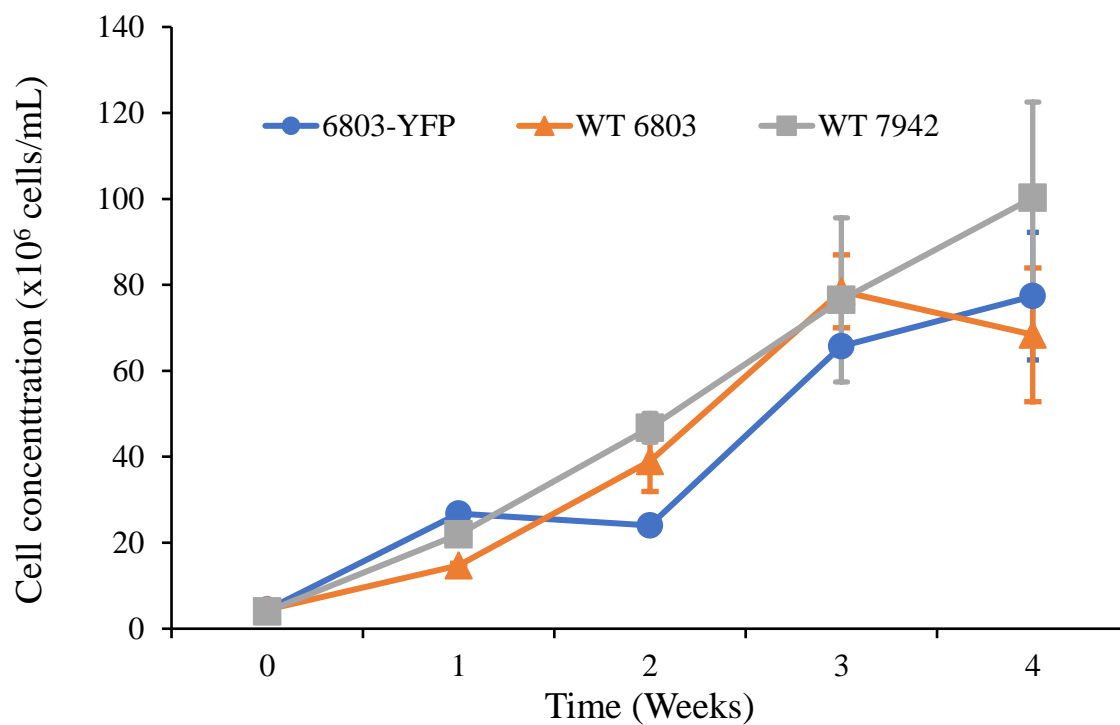


**Figure E3:** Weekly growth of GE *Synechocystis* PCC 6803-YFP (6803-YFP) and WT *Synechococcus elongatus* PCC 7942 (WT 7942) and WT *Synechocystis* PCC 6803 (WT 6803), used as control for the competition study conducted at room temperatures. The error bars denote the standard deviation of the cell concentration in two liquid culture flasks, each counted twice (total n=4).

**APPENDIX F****RIGHTS AND PERMISSIONS****Permission for the reproduction of Figure 1**

JOHN WILEY AND SONS LICENSE

TERMS AND CONDITIONS

Mar 31, 2021

This Agreement between Chemistry and Biochemistry, Old Dominion University -- Oumar Sacko ("You") and John Wiley and Sons ("John Wiley and Sons") consists of your license details and the terms and conditions provided by John Wiley and Sons and Copyright Clearance Center.

License Number 5039221441206

License date Mar 31, 2021

Licensed Content

Publisher John Wiley and Sons

Licensed Content

Publication Wiley Books

Licensed Content

Title Humus Chemistry: Genesis, Composition, Reactions, 2nd Edition

Licensed Content

Author F. J. Stevenson

Licensed Content

Date Aug 1, 1994

Licensed Content

Pages 1

Type of use Dissertation/Thesis

Requestor type University/Academic

Format Print and electronic

Portion Figure/table

Number of

figures/tables 1

Will you be

translating? No

Title

OPTIMIZATION OF BIOCHAR VIA OZONIZATION AND ITS VARIOUS APPLICATIONS  
FOR SUSTAINABILITY AND BIOSAFETY OF GENETICALLY ENGINEERED  
CYANOBACTERIA

Institution name Old Dominion University

Expected

presentation date May 2021

Portions Diagram of Humic Acid

Requestor Location

Chemistry and Biochemistry, Old Dominion University

NORFOLK, VA

United States

Attn: Chemistry and Biochemistry, Old Dominion University

Publisher Tax ID EU826007151

Total 0.00 USD

**Permission for the published Manuscript used in Chapter II**[Home](#)[Help](#)[Live Chat](#)[Oumar Sacko](#) ▾**Sustainable Chemistry: Solubilization of Phosphorus from Insoluble Phosphate Material Hydroxyapatite with Ozonized Biochar****Author:** Oumar Sacko, Rachel Whiteman, Gyanendra Kharel, et al**Publication:** ACS Sustainable Chemistry & Engineering**Publisher:** American Chemical Society**Date:** May 1, 2020*Copyright © 2020, American Chemical Society***PERMISSION/LICENSE IS GRANTED FOR YOUR ORDER AT NO CHARGE**

This type of permission/license, instead of the standard Terms and Conditions, is sent to you because no fee is being charged for your order. Please note the following:

- Permission is granted for your request in both print and electronic formats, and translations.
- If figures and/or tables were requested, they may be adapted or used in part.
- Please print this page for your records and send a copy of it to your publisher/graduate school.
- Appropriate credit for the requested material should be given as follows: "Reprinted (adapted) with permission from {COMPLETE REFERENCE CITATION}. Copyright {YEAR} American Chemical Society." Insert appropriate information in place of the capitalized words.
- One-time permission is granted only for the use specified in your RightsLink request. No additional uses are granted (such as derivative works or other editions). For any uses, please submit a new request.

If credit is given to another source for the material you requested from RightsLink, permission must be obtained from that source.

[BACK](#)[CLOSE WINDOW](#)

## Permission for Manuscript used in Chapter III



RightsLink®



Home



Help



Email Support



Oumar Sacko ▾

### Biochar Surface Oxygenation by Ozonization for Super High Cation Exchange Capacity



**Author:** Gyanendra Kharel, Oumar Sacko, Xu Feng, et al

**Publication:** ACS Sustainable Chemistry & Engineering

**Publisher:** American Chemical Society

**Date:** Oct 1, 2019

*Copyright © 2019, American Chemical Society*

#### PERMISSION/LICENSE IS GRANTED FOR YOUR ORDER AT NO CHARGE

This type of permission/license, instead of the standard Terms & Conditions, is sent to you because no fee is being charged for your order. Please note the following:

- Permission is granted for your request in both print and electronic formats, and translations.
- If figures and/or tables were requested, they may be adapted or used in part.
- Please print this page for your records and send a copy of it to your publisher/graduate school.
- Appropriate credit for the requested material should be given as follows: "Reprinted (adapted) with permission from (COMPLETE REFERENCE CITATION). Copyright (YEAR) American Chemical Society." Insert appropriate information in place of the capitalized words.
- One-time permission is granted only for the use specified in your request. No additional uses are granted (such as derivative works or other editions). For any other uses, please submit a new request.

**BACK**

**CLOSE WINDOW**

## Permission for Manuscript used in Chapter VI



RightsLink®

 Home

 Help

 Email Support

 Oumar Sacko ▾

### Survivability of Wild-Type and Genetically Engineered *Thermosynechococcus elongatus* BP1 with Different Temperature Conditions



Author: Oumar Sacko, Cherrelle L. Barnes, Lesley H. Greene, et al

Publication: Applied Biosafety

Publisher: SAGE Publications

Date: 06/01/2020

*Copyright © 2020, © SAGE Publications*

#### Gratis Reuse

If you are a SAGE journal author requesting permission to reuse material from your journal article, please note you may be able to reuse your content without requiring permission from SAGE. Please review SAGE's author re-use and archiving policies at <https://us.sagepub.com/en-us/nam/journal-author-archiving-policies-and-re-use> for more information.

If your request does not fall within SAGE's reuse guidelines, please proceed with submitting your request by selecting one of the other reuse categories that describes your use. Please note, a fee may be charged for reuse of content requiring permission. Please submit a ticket through the [SAGE Permissions Portal](#) if you have questions.

**BACK**

**CLOSE WINDOW**

## VITA

### Oumar Sacko

Department of Chemistry and Biochemistry, Old Dominion University, Norfolk, VA 23529

---

### Education

#### OLD DOMINION UNIVERSITY

*Norfolk, VA*

- Ph.D. in Chemistry and Biochemistry *Summer 2021*
- Master of Science in Chemistry and Biochemistry *May 2020*

#### JAMES MADISON UNIVERSITY

*Harrisonburg, VA*

- Bachelor of Science in Biology *May 2014*

### Publications and Awards

#### Selected Publications

Sacko, O., Whiteman, R., Kharel, G., Kumar, S., & Lee, J. W. (2020). Sustainable Chemistry: Solubilization of Phosphorus from Insoluble Phosphate Material Hydroxyapatite with Ozonized Biochar. *ACS Sustainable Chemistry & Engineering*, 8(18), 7068-7077.

Kharel, G., Sacko, O., Feng, X., Morris, J. R., Phillips, C. L., Trippe, K., Kumar, S., & Lee, J. W. (2019). Biochar surface oxygenation by ozonation for super high cation exchange capacity. *ACS Sustainable Chemistry & Engineering*, 7(19), 16410-16418.

Sacko, O., Barnes, C. L., Greene, L. H., & Lee, J. W. (2020). Survivability of Wild-Type and Genetically Engineered *Thermosynechococcus elongatus* BP1 with Different Temperature Conditions. *Applied Biosafety*, 25(2), 104-117.

#### Awards, Honors

- Outstanding Teaching Assistant Award, Chemistry and Biochemistry *ODU, 2020*
- Bruner Award, Chemistry Section, Virginia Academy of Science Conference *Spring 2018*
- Phi Beta Kappa *2014*
- Golden Key International Honour Society *2013*